UNIVERSITÉ PARIS 1
PANTHÉON SORBONNE

UNIVERSITÉ PARIS 1 PANTHÉON-SORBONNE
École Doctorale D'Économie (ED465)
Centre d'Économie de la Sorbonne (CES)

THÈSE
Pour l'obtention du titre de Docteur en Sciences Économiques

Présentée et soutenue publiquement le 27 août 2025

Pol Cosentino

Making Cities: Transport, Sorting, and Welfare

Sous la direction de

Clément Bosquet	Professeur, Université Paris 1 Panthéon-Sorbonne

Membres du jury

Présidente

Camille Hémet	Professeure, Université Paris 1 Panthéon-Sorbonne, PSE

Rapporteurs

Pierre-Philippe Combes	Directeur de recherche, CNRS, Sciences Po
Stephan Heblich	Full Professor, University of Toronto

Examinateurs

Sara Bagagli	Assistant Professor, LSE
Gabriel Loumeau	Assistant Professor, VU Amsterdam

To my parents, who taught me the value of hard work.

Remerciements

Je tiens à exprimer toute ma gratitude à mon directeur de thèse, Clément, pour son accompagnement précieux tout au long de cette aventure. Son humour et sa bonne humeur ont su alléger la pression propre au doctorat. Merci de m'avoir accordé autant (parfois trop) de flexibilité, et d'avoir su me dire quand m'arrêter et aller droit au but (même si, allez Paris !). Au delà de ça, merci de m'avoir initié au monde de la recherche à travers mon premier stage. J'ai énormément appris à tes côtés durant ces cinq dernières années. Bien que l'aventure de la thèse touche à sa fin, notre co-écriture fera en sorte que nos chemins (de fer) ne se séparent pas pour autant !

I would like to express my sincere thanks to Pierre-Philippe Combes and Stephan Heblich for agreeing to review my PhD thesis. Your feedback has been invaluable and will greatly enhance my papers. I also thank Sara Bagagli and Gabriel Loumeau for accepting to be examiners on my PhD thesis jury, and Clara Santamaria for being part of my PhD thesis committee. All your comments have greatly benefited my thesis and enriched my thoughts as a young researcher. I would like to extend my special thanks to Camille Hémet, who on two occasions guided my research by discussing my research papers. I also wish to thank Laurent Gobillon and Miren Lafourcade for their numerous comments and for inviting me to the RUES, which were great moments during my PhD. Miren, je me réjouis de commencer ce post-doc avec toi et Gabrielle à la rentrée, et de travailler ensemble sur des projets passionnants !

Je remercie chaleureusement toute l'équipe des axes éco inter et éco du dev : Léa, Rémi, Laurine, Josselin, Lisa, Julieta, Clément G., Ariell, Morgane et Nouhoum. Vous avez contribué à mon profond épanouissement durant ces années. J'ai passé de supers moments dans vos bureaux respectifs, que ce soit pour des discussions scientifiques ou des échanges du quotidien. Merci à toutes et à tous pour cette ambiance si chaleureuse et stimulante. Une pensée particulière aux doctorants des bureaux 314 et 316 qui ont partagé ce parcours avec moi, et plus spécialement à Afifi, Nada, Farida, Yasmine et Robert. Sans oublier Mila et Victoria (je te passe le flambeau en septembre !) qui ont apporté un vent de fraîcheur bienvenu lors de ma troisième année de thèse. Merci Olivier pour ta gentillesse, nos conversations toujours enrichissantes en économie urbaine, et pour m'avoir accompagné à Amsterdam (j'ai passé de supers moments !). Merci Hannes pour ta sympathie et ta bonne humeur (tu es toujours le bienvenu en Bretagne !). Je tiens à remercier tout particulièrement Camille et Stephen, qui en plus d'être de supers amis, m'ont accompagné tout au long de mon parcours académique, depuis mon premier stage jusqu'au doctorat.

Enfin, merci Pascale de m'avoir ouvert les portes du bureau R3-68 et d'avoir été ma première co-autrice pour l'écriture d'un quatrième chapitre qui, malheureusement, ne figurera pas dans cette thèse.

Je tiens également à exprimer ma profonde gratitude envers Fabien Moizeau et Étienne Dagorn qui, lors de ma première année de licence à l'Université de Rennes, m'ont donné le goût et l'envie de poursuivre dans le monde académique. Mon intérêt pour l'économie urbaine n'est pas un fruit du hasard, mais bien lié au fait que mes sources d'inspiration, Fabien et Clément, s'y sont intéressés avant moi. De ton côté, Étienne, en plus d'être un super ami, ta motivation et ton enthousiasme pour la recherche m'ont profondément marqué. Merci, je te dois beaucoup. Désormais, tu ne pourras plus m'appeler Padawan !

I would like to take this opportunity to switch to English and thank all the people who welcomed and accompanied me during my stay in the Netherlands. Special thanks to Hans, Jos, and Gabriel for welcoming me to your great lab at VU Amsterdam. I am also grateful to the PhD students and post-docs, especially Fabio, Agatha, Gigi, Thijmen, Vera, and Kieran. I had an amazing experience and I hope to come back soon! My thoughts also go to Giulia and Bea for the great dinners, parties, and concerts we shared - see you in Milan or Paris! *Grazie mille*!
Last but not least, I would like to thank my army of proofreaders: Emma, Sinead, Thijmen, Idil, Olivier, Kieran, Hannes, Vera, Camille, Juliette, Brice, Agatha, and Liam. Your invaluable work has greatly improved this thesis, even if it was an ungrateful task.

Un immense merci à mes amis bretons et parisiens qui m'ont accompagné et soutenu tout au long de cette aventure, malgré mes nombreux refus de sortir par manque de temps. Je pense particulièrement à Matiss, Ben, Maxime, Eudes, Liam, Lucas, Jeanne, Jo, Rahel, Micka, Brice, Tangi et Léna. Merci pour toutes ces soirées, ces verres partagés, ces dîners et ces concerts qui ont rythmé ces années. Merci pour les vacances en Bretagne et pour cette surprise inoubliable à Amsterdam. Vous avez rendu ces moments exceptionnels et j'espère que nous continuerons à partager ces bons moments, même si je ne peux pas vous promettre d'avoir plus de temps à l'avenir.

Enfin, j'ai une pensée particulière pour ma famille, à qui j'adresse peu de mots d'affection habituellement. Voici l'opportunité de vous remercier d'avoir été présents pour moi pendant ces longues années d'études. Les moments de coupure en Bretagne m'ont permis de respirer dans cette aventure. Aux "Tu finis quand ta thèse ?" , "T'es toujours étudiant ?", voilà, la thèse est finie, et je ne suis donc plus un étudiant. Même si vous n'avez pas tout compris, je vous remercie du fond du cœur.

Emma, les mots manquent tant tu as été importante durant mon doctorat et plus généralement au quotidien. Merci de m'avoir accompagné en conférence, et d'avoir ensoleillé ces moments. Merci pour toutes ces précieuses relectures et présentations. Merci d'avoir été à mes côtés pendant tout ce temps, et de continuer à l'être pour le futur. C'est bientôt à ton tour !

Abstract

This thesis studies characteristics making cities, namely: (i) the urban transport infrastructure, (ii) the optimal provision of public infrastructure enhancing welfare, (iii) the spatial sorting of individuals creating segregation.

The first chapter investigates how the construction of a circular transport system, such as the *Petite Ceinture* (PC), reallocates economic activity within a city. Using newly digitized data on Parisian neighborhoods and surrounding municipalities from 1801 to 1954, I show that the PC significantly influenced the spatial distribution of firms and residents during this period. I develop and calibrate a quantitative spatial model with tradable goods and non-tradable services to structurally estimate the impact of the PC on Paris' spatial equilibrium. I find that shutting down this circular railroad decreases the total population and rateable values in Paris, respectively by 10% and 10.1%, and creates a reallocation of workers and residents towards the city center. Comparing the PC railroad with a radial railroad system, I find that the latter is more efficient and results in a greater separation of workplace and residence. However, combining both infrastructures simultaneously allows for additional welfare gains. Finally, long-differences highlight the persistent effect of the PC even 50 years after its traffic decline.

The second chapter investigates how an urban transport infrastructure should be designed to maximize worker welfare while accounting for general equilibrium effects. To do so, I bridge seminal works in the quantitative urban model literature (Ahlfeldt et al., 2015; Heblich et al., 2020) with a simulated annealing algorithm used by Kreindler et al. (2024). The resulting framework accommodates several commuting modes, considers neighborhood heterogeneity, and incorporates general equilibrium effects as workers reallocate within the city in response to changes in commuting costs. I apply this framework to determine how the Parisian metro should have been planned at the beginning of the 20th century. Results suggest that the placement of strategic metro stations is driven by location centrality, productivity, and amenities. Comparative static experiments modifying the framework parameters predict different urban transport designs.

The last chapter studies whether local public goods, such as natural amenities, influence the racial sorting within a city through a market effect and an exclusion effect. First, I use a neighborhood database of the United States over the 1880-2010 period and exploit differences in natural amenities (e.g. a coastline, a lake, a river, or a hill) abundance combined with changes in anti-black attitudes. Reduced-form evidence suggests the existence of both market and exclusion effects of natural amenities influencing racial sorting. The market effect is identified by comparing neighborhoods with high natural amenities to

others, reflecting the lower affordability of blacks due to their lower average incomes. The exclusion effect is separately identified through the interaction between natural amenities and city-wide Confederate monuments, capturing variations in anti-black attitudes across cities and over time. Second, I use 2010 LODES data to get information on workplace and residence employment by race at a granular level and to quantify a heterogeneous agents quantitative spatial model on 16 of the largest CBSAs. Exploiting variations in race-specific amenities across neighborhoods, results show the existence of strong homophily preferences both for blacks and whites. Additionally, the proximity to natural amenities increases these racial preferences. Counterfactual exercises show that removing all racial preferences decreases on average the racial segregation by 11.6 percentage points.

Keywords: Location Choices, Transport Infrastructure, Quantitative Spatial Model, Optimal Urban Transport Infrastructure, Racial Segregation, Racial Sorting, Natural Amenities

Résumé

Cette thèse étudie des aspects caractérisant la ville, parmi lesquels : (i) l'infrastructure de transport urbain, (ii) la fourniture optimale d'infrastructures publiques améliorant le bien-être, ainsi que (iii) le tri spatial des individus créant la ségrégation.
Le premier chapitre étudie comment la construction d'un système de transport circulaire, tel que la Petite Ceinture (PC), ré-alloue l'activité économique au sein d'une ville. En utilisant de nouvelles données numérisées sur les quartiers parisiens et les municipalités environnantes de 1801 à 1954, je montre que la PC a significativement influencé la distribution spatiale des entreprises et des résidents pendant cette période. Je développe et calibre un modèle spatial quantitatif avec des biens échangeables et des services non échangeables pour estimer structurellement l'impact de la PC sur l'équilibre spatial de Paris. Je trouve que la fermeture de ce chemin de fer circulaire diminue la population totale et les valeurs locatives à Paris, respectivement de 10% et 10,1%, et crée une réallocation des travailleurs et des résidents vers le centre-ville. En comparant le chemin de fer de la PC avec un système de transport radial, je trouve que ce dernier est plus efficace et entraîne une plus grande séparation entre les lieux de travail et de résidence. Cependant, la combinaison des deux infrastructures simultanément permet des gains de bien-être supplémentaires. Enfin, les différences à long terme mettent en évidence l'effet persistant de la PC même 50 ans après le déclin de son trafic.
Le deuxième chapitre étudie comment une infrastructure de transport urbain devrait être conçue pour maximiser le bien-être des travailleurs tout en tenant compte des effets d'équilibre général. Pour ce faire, je fais le lien entre les travaux fondateurs de la littérature sur les modèles urbains quantitatifs (Ahlfeldt et al., 2015; Heblich et al., 2020) et un algorithme de recuit simulé utilisé par Kreindler et al. (2024). Ce cadre résultant prend en compte plusieurs modes de transport, considère l'hétérogénéité des quartiers et intègre les effets d'équilibre général lorsque les travailleurs se ré-allouent au sein de la ville en réponse aux changements des coûts de transport. J'applique ce cadre pour déterminer comment le métro parisien aurait dû être planifié au début du 20ème siècle. Les résultats suggèrent que le placement des stations de métro stratégiques est influencé par la centralité des emplacements, la productivité et les aménités. Des expériences de statique comparative modifiant les paramètres du cadre prédisent différents *designs* de métro.
Le dernier chapitre étudie si les biens publics locaux, tels que les aménités naturelles, influencent le tri racial au sein d'une ville à travers un effet de marché et un effet d'exclusion. Tout d'abord, j'utilise une base de données de quartiers des États-Unis sur la période 1880-2010 et j'exploite les différences d'abondance en aménités naturelles (par exemple,

une côte, un lac, une rivière ou une colline) combinées avec des changements d'attitudes anti-Noirs. Les résultats en forme réduite suggèrent l'existence d'effets de marché et d'exclusion des aménités naturelles influençant le tri racial. L'effet de marché est identifié en comparant les quartiers avec des aménités naturelles élevées à d'autres quartiers, reflétant la moindre accessibilité financière des Noirs en raison de leurs revenus moyens plus faibles. L'effet d'exclusion est identifié séparément par l'interaction entre les aménités naturelles et les monuments confédérés à travers la ville, capturant les variations des attitudes anti-Noirs à travers les villes et au fil du temps. Ensuite, j'utilise les données LODES de 2010 pour obtenir des informations sur l'emploi par ethnie au lieu de travail et de résidence à un niveau granulaire et pour quantifier un modèle spatial quantitatif d'agents hétérogènes sur 16 des plus grandes métropoles (CBSAs). En exploitant les variations des aménités par ethnie à travers les quartiers, les résultats montrent l'existence de fortes préférences d'homophilie à la fois pour les Noirs et les Blancs. De plus, la proximité des aménités naturelles augmente ces préférences raciales. Les exercices contrefactuels montrent que la suppression de toutes les préférences raciales diminue en moyenne la ségrégation raciale de 11,6 points de pourcentage.

Mots Clés: Choix de localisation, Infrastructure de transport, Modèle spatial quantitatif, Infrastructure de transport urbain optimale, Ségrégation raciale, Tri racial, Aménités naturelles

Contents

List of Figures

List of Tables

General introduction

Section I introduces the motivation behind this research, gives an overview of urban economics, and explains how this PhD thesis fits into this field. Section II discusses new data sources for urban economics and shows how this PhD thesis is part of this data revolution. Section III describes what makes cities unique and how this PhD thesis relates to these characteristics. Section IV provides an overview of quantitative urban models and their use in this PhD thesis.

I Cities as a Research Focus

Cities are a crucial focus for research due to their growing importance and profound impact on human life. Currently, 55% of the world's population lives in urban areas, with projections indicating that this share will rise to 68% by 2050. This trend is particularly pronounced in developing countries, where urbanization is rapidly increasing. As a result, cities reflect a collective choice as individuals concentrate in these areas for residence, economic activity, and social interaction.

Urbanization is tightly linked to economic growth and development. Empirical evidence demonstrates a strong correlation between urbanization levels and GDP per capita (Bryan et al., 2025). Cities are essential for increasing economic activity and reducing poverty, as density creates agglomeration economies, opportunities for economic mobility, and social advancement.

The importance of cities will continue to grow, shaping the living conditions of billions and defining the trajectory of human progress. As a research focus, cities provide a better understanding of urban dynamics. They are essential to help planners and policymakers design effective strategies for sustainable development, infrastructure planning, and social equity.

The Emergence of Urban Economics as an Independent Field

Urban economists focus on cities, which are inherently defined by the close proximity of economic activities, a key characteristic that creates agglomeration economies. The micro-foundations of these agglomeration economies were first introduced by Marshall (1890). While the theoretical foundations are longstanding, urban economics as a distinct field within economics is relatively new. For instance, the *Journal of Urban Economics* was

created in 1974, and it took several decades to see a significant increase in the number of urban economics papers published in top-tier economic journals (Henderson and Thisse, 2024). The field experienced a substantial surge following the 2008 Nobel Prize awarded to Krugman for his contributions to economic geography, though urban economics remains distinct as it focuses specifically on within-city activities. This distinction results in a classic division between within-city and across-city phenomena, although these research areas often overlap in practice. More recently, Jonathan Dingel has documented an increase in the total number of job market papers presenting themselves as spatial economics. With the rise of data-driven research and econometric methods, urban economists have quantified the magnitude of agglomeration economies and investigated their underlying mechanisms. Pioneering research on city size, employment density, and productivity was initiated by Ciccone and Hall (1996) and has been substantially extended over the past two decades (see Rosenthal and Strange (2004); Combes and Gobillon (2015) for a review). A meta-analysis by Ahlfeldt and Pietrostefani (2019) shows a wage elasticity with respect to population density equal to 0.04, but it hides substantial heterogeneity across different contexts.

More recently, the intersection between economic history and urban economics has gained significant momentum, as reviewed by Hanlon and Heblich (2022). This growing trend reflects both methodological advancements and new research directions in urban economics (see section II for more details). Technological progress in digitization and computing has substantially expanded the scope of historical data availability for urban economics, overcoming previous limitations that once constrained such research. A key research direction studies how past developments still shape contemporary urban structures, investigating the long-term effects of major infrastructure investments like transportation networks and sanitation systems on current urban organization and spatial segregation patterns. This historical perspective offers valuable insights into the determinants governing the equilibrium distribution of residents, workers, and land values across urban spaces.

This PhD thesis contributes to this emerging trend through three chapters in urban economics, each featuring historical research focus. The first two chapters examine the spatial distribution of economic activity within 19th century Paris and the welfare effects of public infrastructure provision. The final chapter investigates how natural amenities influence racial sorting in U.S. cities throughout the 20th century. Through these analyses, this PhD thesis expands the growing body of research on historical natural experiments in urban economics.

Theoretical Framework of Within-City Structure

The canonical monocentric model, as developed by Alonso (1964), Muth (1969), and Mills (1967) and often referred to as the AMM model, aims to understand the physical structure within a city. This theoretical framework was designed to fit the observed gradients, particularly how population density, housing prices, and land prices decline as one moves away from the city center. In the canonical Alonso-Muth-Mills model, all employment is assumed to be concentrated in a central business district (CBD). Workers face commuting costs when traveling to work, making the most attractive places to live those closest to the CBD. Consequently, workers trade off lower land prices further from the CBD with higher commuting costs. This results in land prices exhibiting a monocentric structure, with a land price peak at the CBD and a land price gradient that declines monotonically with distance from the CBD. Liotta et al. (2022) test the AMM model with a dataset containing gridded data on population densities, rents, housing sizes, and transportation in 192 worldwide cities. They find that 100% and 87% of the cities exhibit the expected negative population density and rent gradients, respectively, consistent with the AMM model. Therefore, the monocentric city model makes highly relevant predictions. However, even if it fits stylized facts, the AMM model does not accommodate all the heterogeneity in real-world data. For instance, there are stark differences in housing prices across close neighborhoods. Some parts of a city may have access to natural water and be well suited for heavy industrial use (Heblich et al., 2021), while other parts may have access to open space and scenic views, making them well suited for residential use (Lee and Lin, 2018). Other parts of a city may have good transport connections and be accessible for retail activity (You, 2021; Miyauchi et al., 2025). Within cities, we observe large differences between locations in land prices and rich patterns of land use (Duranton and Puga, 2015). Some locations are used for workplaces, while others are used for residences. Within the same city, some residential locations are prosperous (such as the 16th arrondissement in Paris), while others are poor (such as Aubervilliers at the frontier of Paris). The rise in quantitative spatial models (QSMs) over the past decade allows for the integration of these elements, addressing equilibrium responses, enabling predictions about future policies, and providing better measures of welfare (see Redding (2022) for a review). A classical distinction within QSMs is between (i) cities models (quantitative regional models) that focus on interactions between cities, and (ii) within-city models (quantitative urban models) that focus on interactions within a city. Importantly, this class of models does not impose any specific structure, such as a monocentric framework, on the city. However, it is still possible to combine a monocentric structure with the quantitative

urban model, as demonstrated by Bagagli (2023). Hence, these models are necessary to rationalize spatial equilibrium and understand the impacts of urban public policies, such as infrastructure changes on population distribution.

This PhD thesis aligns with this emerging QSM literature, as each chapter uses a different quantitative urban model (QUM) to accommodate the context but shares similarities. The tractability of these frameworks allows matching research questions with corresponding data and provides information on counterfactual spatial equilibria. In this introduction, the section IV is dedicated to describing in greater detail the advantages of these models.

II New Data, New Opportunities

The expansion of historical data offers new research perspectives by enabling additional natural experiments and uncovering previously inaccessible information. Several methodological approaches facilitate this progress in urban economic research (see Abramitzky et al. (2025) for a review). The linking of historical census data, as demonstrated by Abramitzky et al. (2021), represents a significant advancement. This methodology allows researchers to trace individuals across time, thereby enabling studies on the long-term impacts of economic shocks on occupational mobility patterns, migration decisions, and various socioeconomic outcomes. The digitization of historical maps has emerged as another crucial method for defining exposure to historical events. Researchers may employ GIS tools to manually reconstruct various urban systems, including historical transport networks between cities (Atack, 2013; Thevenin et al., 2016; Ciccarelli and Groote, 2018) and within urban areas (Brooks and Lutz, 2019; Heblich et al., 2020), as well as historical communication routes (Wang, 2025; Skoglund, 2025). Alternatively, machine learning techniques have gained prominence in this digitization process, particularly for analyzing land-use maps and building footprints (Heblich et al., 2023; Lin et al., 2023; Combes et al., 2025a,b). Combes et al. (2022) provides a comprehensive review of these machine learning applications in urban economic research. Optical Character Recognition technology has proven valuable for extracting information from extensive document archives, particularly city directories (You, 2021; Albers and Kappner, 2023; Ellen et al., 2025). This approach serves as an effective complement or alternative to traditional census data, enabling more precise geo-referencing of firms and households across multiple periods and at finer spatial resolutions. While administrative data remains the primary information source in urban economics, contemporary research increasingly incorporates alternative modern data sources. These emerging datasets provide novel insights into various dimensions of urban life. Satellite imagery, for instance, offers valuable measurements of

nighttime illumination patterns (Henderson et al., 2012; Martinez, 2022) and detailed building footprints (Harari, 2020; Henderson et al., 2021a; Gechter and Tsivanidis, 2023). Mobile phone records present another rich data source for analyzing commuting patterns, consumption behaviors, and broader mobility trends (Barwick et al., 2023; Kreindler and Miyauchi, 2023). Additionally, payment card transaction data has become instrumental in measuring spatial patterns of expenditure (Allen et al., 2020).

This PhD thesis contributes to these emerging data trends in urban economics by utilizing recently digitized historical datasets from Paris. The first and second chapters employ novel datasets comprising firm-level information from historical city directories, population and fiscal records from municipal archives, and detailed reconstructions of Paris's historical transport systems and urban footprints, all spanning the 19th century. The third chapter adopts a mixed-methods approach by integrating historical data on Confederate monument locations across the United States during the 20th century with contemporary census data and LEHD Origin-Destination Employment Statistics. By leveraging these diverse datasets, this research contributes to the growing body of literature that employs detailed historical information to identify natural experiments and improve our theoretical and empirical understanding of urban economic processes.

III What Makes Cities?

In this PhD thesis, I focus on three key characteristics among the numerous aspects that define cities. Specifically, this thesis examines: (i) the transportation infrastructure that reduces travel times and increases proximity between individuals, firms, and places; (ii) the higher well-being associated with the provision of public infrastructure; and (iii) the spatial sorting of individuals within cities, characterized by segregation and unequal access to local public goods. By analyzing these three fundamental urban characteristics, this research aims to contribute to a deeper understanding of cities and their complex dynamics.

Urban Transport Infrastructure

The emergence of cities during the 19th century and the acceleration in urbanization were accompanied by a decline in trade costs and commuting costs, urban renewal, and public infrastructure development. On the one hand, these factors may have accelerated the concentration of individuals within cities, while on the other hand, they may have mitigated the negative effects of urbanization. For example, European capitals faced urban

challenges such as sanitary crises, housing shortages due to rapid population growth, and commuting needs arising from poor transport networks at that time. The first chapter, constituting the main work of my thesis, investigates the impact of a circular railroad in Paris in 1854 on the spatial distribution of residents and firms, commuting patterns, consumption, and overall welfare. Since the initial goal was to decrease merchandise transport costs by diverting traffic away from the city center of Paris, this railroad possesses a unique feature with its circular form, making it the world's first circular transit system for passengers. To conduct my analysis, I combine several novel data sources to gather information on population, firm locations, the transport network, and rents across various locations throughout the 19th century. This allows me to provide both reduced-form and structural evidence on the effects of the circular railroad. Specifically, I construct market access measures and exploit spatial changes between 1861 and 1896 to capture changes in accessibility due to the circular railroad. Controlling for initial building share and Haussmann renovations, and employing an instrumental variable strategy to focus only on variations in commuting costs, my results indicate that an increase in market access leads to growth in population, rents, factories, and retail establishments. This suggests that the circular railroad pushed Parisian industry and residents outside the city center, ultimately decentralizing economic activities to the periphery. In line with these results, I develop and calibrate a QUM featuring (i) a tradable goods sector and (ii) a non-tradable services sector. This model helps rationalize within-city spatial equilibrium and structurally estimates the impact of the circular railroad on (i) the location choices of workers and firms, and (ii) the prices of tradable goods. Using this QUM combined with exact-hat algebra, I structurally estimate the impact of the circular railroad on Paris's spatial equilibrium. My findings reveal that shutting down the circular railroad would decrease (i) the total population by 10.0% and (ii) rateable values by 10.1%, and redistribute economic activity towards the city center. Additionally, I find sizable effects on the price of tradable goods, which would increase by 1.6% to 8.0% in neighborhoods close to the periphery. These results highlight the significant role of this circular railroad in shaping Paris's economic activities. I add to the urban transport literature by introducing a unique historical setting with a circular transport system that avoids crossing the city center, making commuting in peripheral neighborhoods more accessible for both merchandise and passengers. This contrasts with historical transit systems in cities like Berlin, Boston, Chicago, and London, which depict a radial pattern. However, modern cities have rapidly adopted circular lines. Moreover, my theoretical framework builds on the canonical urban model of Heblich et al. (2020), which models commuting choices in an open city, and integrates (i) an Armingtonian component to consider a sector of trad-

able goods (Armington, 1969) and (ii) a new economic geography component (Krugman, 1991b; Helpman et al., 1995) to consider a sector of non-tradable services. Hence, the developed QUM accommodates the dual function of the circular railroad by modeling both the trade of merchandise and passenger commuting. Additionally, I use long-differences between the populations of 1906 and 1954 to shed light on the persistent effects of the circular railroad. The starting period corresponds to the year marking the decline in the circular railroad traffic due to growing competition with the metro in Paris. Controlling for the distance to the city center to address city center outmigration, and the growth of city accessibility by metro, I find that neighborhoods within 500 meters of a train station experienced more population growth over 48 years than other neighborhoods. This analysis contributes to the persistence and path dependency literature by providing additional evidence that history plays a significant role in explaining uneven growth within a city.

The first chapter of this thesis focuses on a crucial element of cities: the proximity of individuals, achieved by lowering commuting and freight costs. It quantifies the effect of a circular railroad design on the spatial distribution of economic activities and welfare using a historical natural experiment and helps us understand the current spatial distribution of economic activity and plan future urban transport infrastructure.

Welfare and Optimal Provision of Infrastructure

Within cities, planners can implement public policies, including public infrastructure, to improve the quality of life. This provision of public goods is a further characteristic of cities. Given the wide range of options available to the planner, the interactions within the city, and the heterogeneity of locations, a key question arises: how should public infrastructure be designed? Specifically, the second chapter of this thesis examines how to design a transport system to maximize welfare. In this chapter, I develop a framework to identify the optimal design of urban transport infrastructure. The framework incorporates general equilibrium effects, which arise as workers reallocate toward different residences and workplaces within the city in response to public policy interventions, thereby influencing the land market where workers and firms compete for housing. Additionally, it accommodates multiple transport modes and accounts for neighborhood heterogeneity in terms of amenities, productivity, and housing supply. It also allows for production and residential agglomeration forces. Considering these elements is crucial to enhancing the efficiency of urban transport systems. I apply my methodology to address the following question: How should the Parisian metro have been planned at the end of the 19th century? I combine the same historical data as in the first chapter and divide

the Parisian space into a $500m \times 500m$ grid to create locations and potential metro stations. In this application, I develop and calibrate a QUM with heterogeneous workers to rationalize the within-city spatial equilibrium. I find that the strategic locations of stations are driven by amenities and productivity. In addition, the station's centrality in the network is also an important determinant in the planner's choice of metro network. This result aligns with Borusyak and Hull (2023), who emphasize that central stations are much more likely to be chosen to increase market potential. Then, I conduct several comparative experiments to assess the role of structural parameters and metro construction cost parameters, showing that the developed framework reacts to them. This work aligns with the literature on the optimal design of transport networks. Recent works have studied the provision of between-cities transport infrastructure using a trade perspective, or within-city transport infrastructure without general equilibrium effects. I contribute to this literature on optimal transport design by building on Kreindler et al. (2024) to provide a within-city framework that incorporates general equilibrium effects, as workers reallocate toward different residences and workplaces following improvements in urban transport infrastructure. This framework allows for agglomeration forces and considers several transport modes. Additionally, it enables planners to set metro construction cost parameters and the minimum number of lines to be built.

The second chapter of this thesis provides urban planners with solutions for optimal public infrastructure design. This aims to enhance the welfare of city residents by ensuring that public infrastructure is efficient and equally accessible depending on the planner objective.

Sorting and Spatial Segregation

Cities are also characterized by sorting. This can be either income sorting where there exists a strong spatial separation between rich and poor, or this can also be racial sorting with strong spatial separation between racial minorities and the rest of the population. The last chapter investigates how local public goods can shape racial sorting between blacks and whites, ultimately increasing racial segregation in the U.S. context. I consider natural amenities as local public goods since they provide leisure, anchor neighborhoods at a high income level (Lee and Lin, 2018), and individuals can cooperate to improve their quality or access. In the third chapter of this thesis, I explore two mechanisms that could explain the racial sorting created by the natural amenities: (i) a market effect reflected in higher rents, as a result of greater demand for neighborhoods close to these local public goods; (ii) an exclusionary effect arising when individuals cooperate to restrict access to local public goods within their own ethnic group (Albouy et al., 2020). I use variation

in city-wide Confederate monuments over time and across cities as a proxy for anti-black attitudes (Henderson et al., 2021b; Ferlenga, 2023) to shed light on the exclusion effect. They should capture higher racial hostility from whites toward blacks, as they represent symbols of oppression. First, I provide reduced-form evidence showing that both channels of natural amenities are at play. I find that neighborhoods that have access to natural amenities are, on average, more white compared to other neighborhoods within a city over the 1880-2010 period. In addition, neighborhoods close to natural amenities experience an increase in their white shares following an increase in citywide Confederate monuments. By doing so, I bridge the income and racial sorting literature, extending Lee and Lin (2018) by examining natural amenities' role in racial sorting beyond income, and investigating the role of racial preferences in residential choice. Unlike previous work, this paper reverses the relationship between diversity's impact on public goods, and investigates how proximity to natural amenities influences neighborhood racial composition. Second, I use a QUM of heterogeneous agents to recover race-specific amenities, and find strong and significant homophily parameters for whites and blacks, with a higher parameter for whites (Krysan and Farley, 2002; Ihlanfeldt and Scafidi, 2002), when explaining residential choices of both groups of residents. In addition, I find a positive effect of natural amenities proximity (such as coastlines, lakes, rivers, and hills) on structural amenities, and a complementarity effect with respect to racial composition. Specifically, the presence of their own racial group in a neighborhood enhances the value of access to natural amenities for both black and white residents. These results emphasize the role of racial composition in unlocking local public goods (Albouy et al., 2020). Then, I show in a counterfactual exercise that removing all racial preferences decreases, on average, racial segregation by 11.6 percentage points. Building on recent within-city spatial models, this study estimates racial preferences using contemporary data and within-city variation, while also examining how natural amenities affect these endogenous forces.

The final chapter focuses on how natural amenities shape racial sorting, aiming to provide a better understanding of long-lasting racial segregation. This is crucial since natural amenities are fixed and will continue to influence sorting within U.S. cities.

IV Quantitative Urban Model

Why?

The standard QUM has been developed by Ahlfeldt et al. (2015), drawing inspiration from trade (Eaton and Kortum, 2002) and macroeconomic literature. This framework requires a small number of structural parameters (elasticities) and allows researchers to rationalize within-city spatial equilibrium with observed features of the data. Unlike the monocentric model, it accommodates many locations that differ in productivity, amenities, land area, the supply of floor space, and transport connections within a city. These models allow researchers to make the distinction between first-nature (typically natural advantages) and second-nature geography (typically agglomeration forces). First-nature geography corresponds to exogenous natural advantages or location fundamentals, such as access to natural water or a waterfront location in a natural harbor. Second-nature geography corresponds to the location of economic agents relative to one another in geographic space. The standard QUM is characterized by three agents in the city: (i) a unique firm using commercial housing and labor to produce a final good freely traded within the city, (ii) workers who live and work, and (iii) developers providing residential and commercial housing. In each location, these agents interact together through several markets. Firms and workers match in the labor market (the standard QUM assumes full employment), but they compete with each other in the housing market. These interactions allow researchers to consider general equilibrium effects: as workers locate close to firms to avoid commuting costs, this bids up housing prices, creating dispersion forces. These general equilibrium effects are crucial for evaluating counterfactual responses from public policies (e.g., the implementation of a railroad within the city).

How?

Only a few data are required to solve a QUM since the model remains tractable. The standard way is to obtain data on residents (where workers live), employment (where workers work), housing prices by location, and commuting time between all locations. While access to this information can be relatively easy through administrative data (for example, LODES data provide commuting flows between census tracts in the U.S., and commuting time can be assessed with Google Maps Akbar (2024)), alternative methods exist in scarce data environments (typically developing countries). For example, workers' commuting flows can be estimated through phone data (Kreindler and Miyauchi, 2023;

Miyauchi et al., 2025) or surveys (Balboni et al., 2020; Franklin et al., 2024). For housing price information, it can be estimated by web-scraping real estate websites (Liotta et al., 2022). However, Sturm et al. (2023) do not observe rent and proceed differently: they use newly available satellite data on built-up areas and building heights to estimate rent data. Once armed with data and the equilibrium equations of the QUM, the unobserved characteristics of locations (wages, amenities, productivity, and the density of development) are recovered by inverting the model in order to exactly match the observed features in the data. Moreover, the distinction between natural advantages and agglomeration forces can be made by using the model's assumptions. An overidentification check can be performed by comparing observed data with the estimated characteristics of locations, using, for example, available wage or housing development data to validate the QUM's predictions.

Another property of this class of QUMs is that sufficient statistics can be computed based on measures of market access, as shown by Tsivanidis (2024), to capture general equilibrium effects. However, this can only be done when ignoring changes in housing supply, amenities, and productivity. Redding (2025) shows that predictions based on market access alone can diverge substantially from the true counterfactual changes due to these strong assumptions, and the model needs to be fully solved in order to properly assess the effect of a public policy. Since the seminal QUM of Ahlfeldt et al. (2015), a growing body of work has extended this framework, demonstrating its flexibility through various innovative applications, such as investigating transport improvements (Heblich et al., 2020; Allen and Arkolakis, 2022; Balboni et al., 2020; Severen, 2021), congestion (Herzog, 2024), consumption access (Miyauchi et al., 2025; Lee and Tan, 2024), the trade of goods (Monte et al., 2018), the sorting of heterogeneous groups of workers (Tsivanidis, 2024; Loumeau, 2024; Weiwu, 2024; Redding and Sturm, 2024; Bagagli, 2023), zoning and land use regulations (Allen et al., 2015; Parkhomenko, 2023; Chen et al., 2024), school choices (Loumeau, 2023; Pietrabissa, 2023), transport mode choices (Koster, 2024), disamenities due to transport infrastructure (Brinkman and Lin, 2022; Champalaune and Cosentino, 2025), urban revival (Owens III et al., 2020; Gechter and Tsivanidis, 2023), and telecommuting (Delventhal et al., 2022; Monte et al., 2023; Delventhal and Parkhomenko, 2024).

The three chapters of this PhD thesis use a QUM, building upon the foundational work of Ahlfeldt et al. (2015). A common feature across all chapters is the shared housing market, which is characterized by a housing supply derived from a Cobb-Douglas technology using land and machinery capital, as detailed in Combes et al. (2021). This way of modeling the housing market in order to obtain a housing elasticity with respect to rent is

commonly used in the literature. However, the chapters diverge in their specifications of workers' utility functions and firms' production functions. In the first chapter, the QUM is extended to incorporate both non-tradable services and tradable goods within a city, thereby contributing to the literature on trade of goods and consumption access. Hence, in the first chapter, a price of tradable goods and a price of non-tradable services enter into workers' utility preferences, while the other two chapters consider a price for final goods freely exchanged in the city (i.e taken as numéraire). The other chapters, on the other hand, focus on integrating two distinct groups of workers (high-skilled versus low-skilled in the second chapter, or blacks and whites in the third chapter) with non-homothetic preferences, contributing to the sorting of heterogeneous groups of workers applications. For example, the two groups of workers differ in the share of income devoted to housing. Regarding production functions, all chapters use a Cobb-Douglas specification for tradable goods. The first and second chapters, unlike the third, incorporate machinery capital alongside labor and housing to reflect 19th century production environment Heblich et al. (2020). The latter two chapters instead employ a nested labor supply with constant elasticity of substitution between worker groups (Herzog, 2024; Tsivanidis, 2024; Redding and Sturm, 2024; Weiwu, 2024; Champalaune and Cosentino, 2025), enabling the integration of different worker types within a unified production framework rather than assuming separate final goods production as in Loumeau (2024). Overall, the QUMs vary across the three chapters to align with the context specific to each research question. However, they share a similar structure, based on a class of urban models to derive generalizable conclusions.

What's New in the QUM Literature?

Dynamics

A recent advance in the QUM literature is the modeling of dynamics. These are crucial to account for dynamic agglomeration externalities (Allen and Donaldson, 2020), forward-looking location choices (Artuç et al., 2010), capital accumulation (Kleinman et al., 2023), and the evolution of wealth across space (Brunetti et al., 2025). Two key features are interesting in dynamic settings following an economic shock. First, these frameworks compute transitional dynamics and speed of convergence toward new equilibrium. By contrast, static settings fail to account for this since they solve for a steady state equilibrium. Second, distributional effects can differ along the transitional dynamics. In the presence of migration frictions, the option value of future decisions depends on the choices agents make today. Hence, the optimal location decision for an agent today

might be to stay, even if current payoffs are higher elsewhere, if the agent anticipates that future payoffs will be greater in that location. Therefore, distributional effects can differ largely between dynamic and static settings. While dynamics have been extensively studied in the macroeconomic literature, considering them within a city with many locations leads to dimensionality issues and computational challenges. Recent methods have been developed to overcome these problems and model mobility frictions. A first way to model mobility frictions is *à la* Calvo-style (Heblich et al., 2021; Takeda and Yamagishi, 2023), where workers derive the opportunity to move from an exogenous probability. The first chapter is in line with this setting and proposes an extension in the appendix of the standard QUM in dynamics by starting from the framework of Heblich et al. (2021). It incorporates workplace choices, commuting costs, and agglomeration forces. Within this extended framework, individuals are modeled as making accurate predictions about future neighborhood trajectories, firms are myopic, and developers provide housing that depreciates over two periods. Another way to consider mobility frictions is to make them a function of migration costs between locations, and the model can be solved in dynamic exact hat algebra (Caliendo et al., 2019; Warnes, 2021). However, in both settings the stickiness of migration decisions is due to calibrated mobility frictions, and this might totally influence the transitional dynamics. More recently, Greaney et al. (2024) innovates by proposing a dynamic QUM that considers consumption-saving decisions, allowing for wealth accumulation and migration decisions that are costly. This allows researchers to account for richer transition dynamics changes and spatially heterogeneous shocks and policies.

Optimal Policies

Another progress in the use of QUMs is the implementation of optimal policies (see Fajgelbaum and Gaubert (2025) for a review), particularly for transport networks. This is important because current networks are often inefficient and could be reconfigured to improve welfare. The sub-optimality of these networks can be attributed to several factors, including path dependency, where past investments constrain future developments, and the misalignment between planners' objectives and the goal of maximizing aggregate welfare. Additionally, the dynamic nature of economic fundamentals means that networks designed to be efficient at one point in time may become less efficient as conditions change. The problem of characterizing optimal transport networks is complex due to its high dimensionality and non-convexity. Transport networks consist of nodes and links, and improvements in one part can affect the entire system, making optimization

challenging. The literature explores two main types of transport investment: continuous investment in links, which focuses on the intensity of infrastructure investment, and binary investment approaches, which consider investments as discrete choices. Applications of these models, such as those by Fajgelbaum and Schaal (2020), provide conditions under which the problem can be globally convex, ensuring numerical tractability. Santamaria (2020) studies non-convex problems by incorporating market-clearing conditions as additional restrictions in the planner's problem, but this does not guarantee a globally optimal network investment. When investments are considered as binary, heuristic algorithms (Alder, 2016; Loumeau, 2023; Kreindler et al., 2024) can be used to investigate the efficiency of a transport network, but this does not guarantee a globally optimal network. The third chapter aligns with this emerging literature by using a heuristic algorithm to solve for a sub-optimal urban transport network and considering general equilibrium effects through a QUM.

The remainder of this thesis is structured as follows. Chapter 1, entitled "Circular Railroad: Evidence from the Parisian *Petite Ceinture*", studies the effect of a circular railroad implemented during the 19th century on the Parisian spatial equilibrium. Chapter 2, entitled "Optimal Urban Transport Design in a Quantitative Spatial Model", develops a framework to identify (sub)optimal metro network design, taking into account general equilibrium effects. Chapter 3, entitled "Racial Preferences and Local Public Goods", investigates the effect of local public goods on racial sorting and racial segregation. Following the three main chapters, an appendix is included to provide additional details, supplementary data, and extended analyses that support the findings presented in the respective chapters. Finally, a comprehensive summary is provided in French, offering a concise overview of the research, its key findings, and its contributions to the field.

Chapter 1

Circular railroad: Evidence from the Parisian *Petite Ceinture*

Acknowledgements

I am particularly grateful to Clément Bosquet for his guidance and support. I benefited from conversations with Prottoy Akbar, Pierre-Philippe Combes, Étienne Dagorn, Laurent Gobillon, Stephan Heblich, Camille Hémet, Hans Koster, Jean Lacroix, Miren Lafourcade, Jeffrey Lin, Gabriel Loumeau, Florian Mayneris, Ariell Reshef, Clara Santamaria, Marta Santamaria, Daniel Sturm, and Yanos Zylberberg. I thank participants of PPCR workshop, ENS Lyon Junior workshop, PSE Regional and Urban Economics seminar, AFEPOP conference, CES internal seminar, JMA conference, IEB Urban Economics workshop, YSI Economic History, UEA Summer School, CESifo workshop, Eureka seminar, Junior Migration seminar, AYEW urban workshop, and UEA 2025 conference for their valuable comments and suggestions. I would like also to thank Gael Perrot for great research assistance, Christophe Mimeur for providing data on suburban train stations, Clément Gorin for the map on Parisian buildings footprint, and researchers of the ANR SoDuCo team for sharing their data. This work has been funded by a French government subsidy managed by the Agence Nationale de la Recherche under the framework of the Investissements d'avenir programme reference ANR-17-EURE-001. I also thank ANR SINEMOB (ANR-22-CE55-0007) for financial support. Responsibility for results, opinions and errors lies with the author alone.

I Introduction

During the 19th century, European capitals faced urban challenges, including sanitary crises, inadequate road networks, poor urban transport systems, and difficulties managing rapid population growth. These issues required significant reforms to create a more balanced and harmonious urban structure across these cities. Urban planners considered two primary methods to reorganize the spatial structure of cities: zoning-based redevelopment to decrease city center density and spread out the population, and the development of urban transportation systems to facilitate commuting for workers, ultimately enhanc-

ing their well-being. Regarding the second method, most cities chose radial railroads to transport passengers efficiently between the city center and locations in the periphery. In this paper, I investigate the impact of a particular type of urban planning — the addition of a circular component to the transport system. In particular, I exploit the introduction of the *Petite Ceinture* (hereafter PC) railroad in Paris in 1854 and its impact on the spatial distribution of residents and firms, commuting patterns, consumption, and overall welfare.

Following the 1851 French coup d'état, Napoléon III ordered the construction of the PC railroad in several phases to connect existing railroad train stations due to lack of roads in the periphery and slow transportation modes at this time. Since the initial goal was to decrease merchandise transport costs by diverting traffic away from the city center of Paris, the PC possesses a unique feature with its circular form, making it the world's first circular transit system (see Figure 1.1). After the success of passenger services on the first opened line in 1854, combined with the increasing demand for commuting between peripheral neighborhoods, the PC project was quickly expanded to include intensive passenger services.[1] As a consequence, this urban project features a unique design tied to its dual function, and could have significantly influenced Paris spatial structure.

This paper studies the short-term effects of the PC railroad by examining whether it modified residential choices and firm locations, and, as a consequence, amplified city center outmigration during the 1852-1906 period. This outmigration is characterized by the relocation of the population away from the historic city center (see Figure 1.2), and could be associated with Haussmann's renovations, the new delimitations of the Paris urban area, and the reduction in passenger and freight transport costs in peripheral neighborhoods following the introduction of the PC.[2] Then, I explore whether the design of the transit system influences commuting choices and welfare by comparing a radial railroad system to the PC railroad, which represents a circular transport system. Finally, I investigate the long-term effect of the PC on Paris' spatial equilibrium 50 years after PC's traffic declined due to metro competition at the beginning of the 20th century. The PC could create a sufficient temporary shock that modifies future neighborhood pathways, and therefore, a new city spatial structure.

[1] The PC has been developed in 4 phases. The first line was the Auteuil line (see panel (a) of Figure A.11).

[2] During the Second Empire, Paris underwent extensive changes in its city planning under the direction of Georges-Eugène Haussmann. This included improvements to streets, regulations for building, parks, sewage systems, water supply networks, public facilities, and monuments. Additionally, Paris expanded by incorporating several nearby municipalities, increasing its *arrondissements* from twelve to twenty.

Figure 1.1
The *Petite Ceinture* railroad

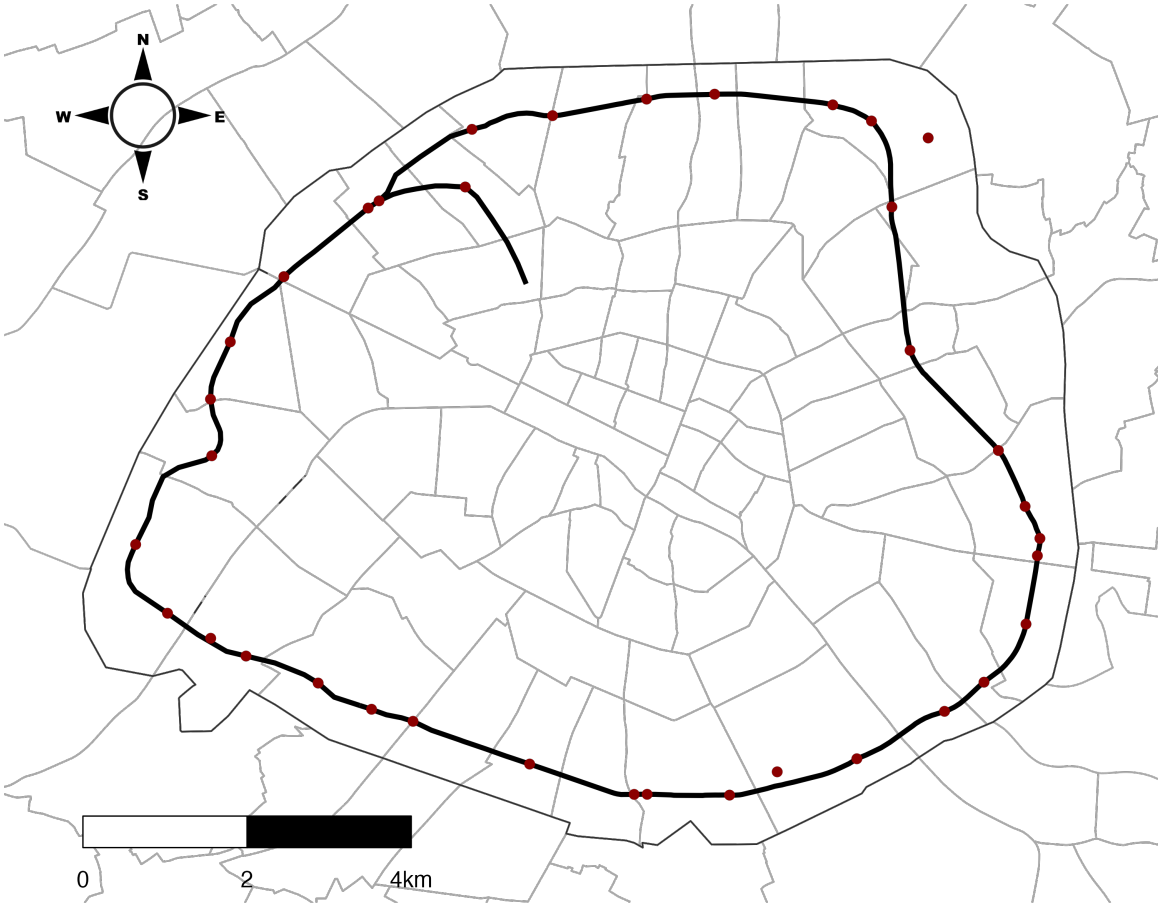

Notes: This map displays the *Petite Ceinture* network in 1900 within the 80 Parisian neighborhoods. The dark line represents the railroad and the red dots the 36 train stations. Train stations are classified as providing commercial and/or passengers services. The Paris-Bestiaux station, a merchandise train station in the northeastern part of Paris, is not directly linked to the main *Petite Ceinture* railway network. Instead, it connects through a smaller section not displayed on this map.

To conduct my analysis, I harmonize Paris's geography over time and combine several novel data sources. First, I digitized data on Parisian neighborhoods and surrounding municipalities population trends to study the dynamics of residential choices over 150 years within Paris.[3] Second, I use city directories of Paris from 1799 to 1908 to track the evolution of economic activity over time and across neighborhoods. This unique database geolocalizes firms by activity and allows me to follow firm patterns over a long period and at a small spatial scale. This rich source of micro-geographic data is yet underused in urban economics as documented by Albers and Kappner (2023). Third, I reconstructed the Parisian transport network using new data on the PC, omnibuses, tramways, and streets to calculate changes in bilateral commuting times between neighborhoods over the

[3] 1860 Paris geography is split into 20 *arrondissements*, and each *arrondissement* is divided into 4 administrative neighborhoods. There are a total of 80 neighborhoods in the Paris area.

period. Finally, I digitized neighborhood fiscal data in order to capture variations in rent levels across locations. Overall, this unique database allows me to precisely measure the evolution of economic activities of Parisian neighborhoods and suburban municipalities for a period spanning from 1801 to 1954 in order to quantitatively assess the impact of a new urban transport infrastructure.

Figure 1.2
Population trends in Paris (1801-1906): 1st-4th vs. 5th-20th *arrondissements*

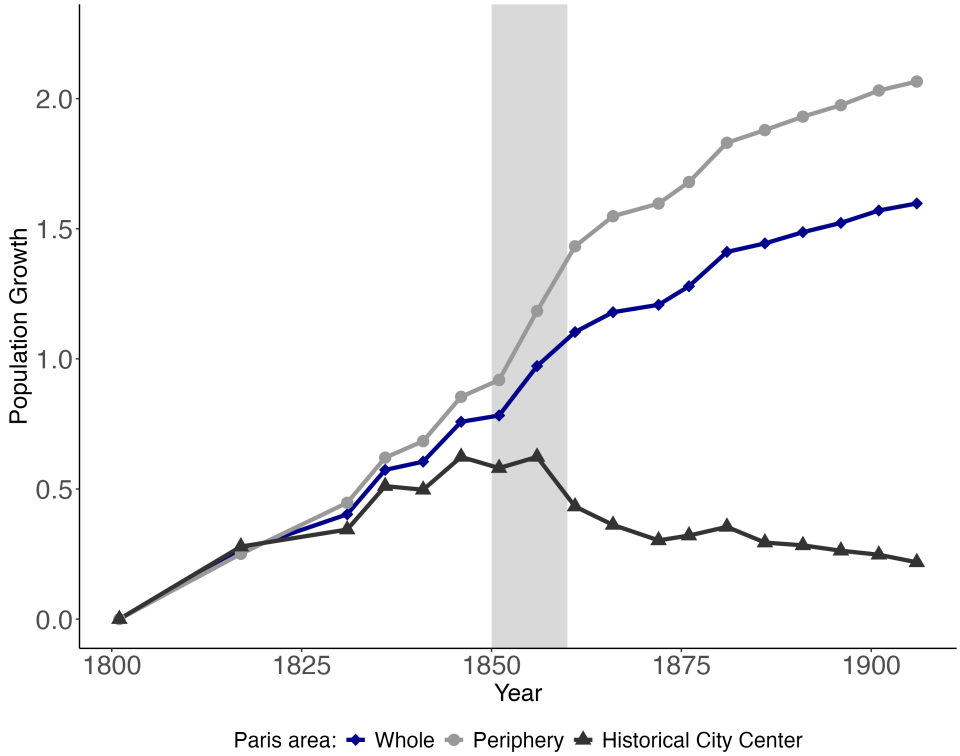

Notes: This figure displays the population evolution of Paris during the 1801-1906 period. Blue squares represent the total population, black triangles represent the historical city center including 1st-4th *arrondissements*, and light grey dots represent the old periphery including 5th-20th *arrondissements* (see Figure A.36 for boundaries). The grey area represents the 1851-1860 period, where there has been consecutively the French coup d'état of Napoléon III in 1851, the start of Haussmann renovations in 1853, and the new geographic delimitation of Paris in 1860.

The paper provides evidence of the short-term and long-term impacts of the PC on the Parisian spatial distribution of economic activity. Concerning short-term effects, I construct firm and residential market access measures and exploit spatial change between 1861 and 1896.[4] Controlling for initial building share as well as Haussmann renovations, and employing an instrumental variable strategy to exploit only variations in commuting costs, the results reveal that a 10% increase in residential market access leads to a 2.2% increase in population and a 4.7% increase in rent within a neighborhood. Additionally,

[4] For a given origin location, the firm market access is defined as the weighted sum of populations across all locations, with weights determined by the associated commuting costs. Conversely, the residential market access is defined as the weighted sum of firm across all locations, with weights determined by the associated commuting costs.

a 10% increase in firm market access results in a 3.9% increase in the number of factories and a 6.9% increase in retail establishments within a 200m×200m grid cell. Moreover, I confirm previous findings using alternative specifications and implementing a staggered differences-in-differences strategy. Testing for mechanisms, I find no effect of the commuting time reduction on street density. Therefore, the results appear to be driven mainly by reductions in commuting time, and not urbanization (i.e. development of street network and urban fabric) near PC train stations. This implies that the PC railroad has pushed the Parisian industry and residents outside the city center, ultimately creating a decentralization of economic activity in the periphery.

Motivated by these results, I develop and calibrate a quantitative spatial model with a tradable goods sector and a non-tradable services sector in order to rationalize within-city spatial equilibrium, and structurally estimate the impact of the PC on locations choices of workers and firms, and prices of tradable goods. I document a flattening relationship of estimated sector-specific wages relative to the distance to the city center over time, indicating a shift away from the monocentric city pattern. In other words, neighborhoods close to the city center become less specialized in workplaces, and employment becomes more evenly distributed across neighborhoods. Regarding structural model parameters, I estimate an amenities agglomeration forces elasticity of 0.168 (in line with Heblich et al. (2020)) using my quasi-experimental variation in commuting costs. Moreover, I estimate the housing supply elasticity by exploiting spatial and time variations in rateable values and housing units. Controlling for Haussmann renovations, I find a housing supply elasticity of 0.517, which is relatively small compared to previous estimates in the literature. This confirms that housing development during this period was driven by urban policies, and less by rent variations. Next, I use my quantitative spatial model combined with exact-hat algebra to structurally estimate the PC's impact on Paris's spatial equilibrium. In a counterfactual exercise considering open city setting, I find that shutting down the PC decreases the total population and rateable values, respectively by 10.0% and 10.1%, and creates a redistribution of the economic activity towards the city center. I also find that there are sizeable effects on the price of tradables, increasing by 1.6% to 8.0% in neighborhoods close to the periphery. This highlights the dual effects of the PC railroad on the welfare of Parisian workers, with a reduction in commuting and freight costs, allowing for greater market access, and consumption. Finally, the counterfactual exercise investigating the impact of transport design provides evidence that the radial railroad is more efficient in terms of welfare than a circular transport system such as the PC, and creates a greater separation between workplace and residence. However, combining

both transport infrastructures allows for additional welfare gains, indicating that they are complementary in reducing commuting costs.

Regarding long-term effects, I use long-differences between the populations of 1906 and 1954 to shed light on the persistence of the PC's impact. The starting period corresponds to the year marking the decline in PC traffic due to growing competition with the metro in Paris. Controlling for the distance to the city center, to address city center outmigration, and the growth of city accessibility by metro, I find that neighborhoods that were within 500 meters of a PC train station experienced 22% more population growth over 48 years than other neighborhoods. Furthermore, varying the ending year of the long differences does not change the results, and allows to rule out the threat of confounding factors during this period. This suggests that the long-term effects of PC are clearly identified. When I investigate heterogeneity based on the PC's 1901 traffic levels, I find that neighborhoods most exposed to PC passengers experienced the greatest population growth. However, I find no evidence that these neighborhoods increased their housing supply during this period.

I contribute to three strands of literature. First, this study addresses a central question in urban economics: to what extent does urban transport influence the spatial distribution of economic activity within a city? Previous work has highlighted the impact of urban transport on various aspects: income sorting (LeRoy and Sonstelie, 1983; Tsivanidis, 2024; Balboni et al., 2020; Gaigné et al., 2022), population decentralization (Baum-Snow, 2007; Garcia-López et al., 2017; Gonzalez-Navarro and Turner, 2018; Brooks and Lutz, 2019; Heblich et al., 2020), job decentralization (Baum-Snow, 2020), disamenities (Brinkman and Lin, 2022; Gendron-Carrier et al., 2022), welfare (Severen, 2021; Allen and Arkolakis, 2022). My contribution lies in exploiting a unique historical setting with a circular system of transport that avoids crossing the city center, making commuting in peripheral neighborhoods more accessible for merchandise and passengers. This stands in contrast to historical transit systems such as Berlin, Boston, Chicago, and London, which depict a radial pattern. However, cities have rapidly adopted a circular line nowadays.[5] Moreover, this paper is in line with the optimal design of transport networks. Recent works have studied the endogenous choice of transport infrastructure using a trade perspective (Balboni, 2019; Fajgelbaum and Schaal, 2020; Santamaria, 2020; Allen and Arkolakis, 2022). They provide frameworks of optimal investment for between-cities infrastructure. With

[5] Some cities such as Beijing, Shanghai, Delhi, Tokyo, Seoul, Copenhagen, Berlin, Oslo, Madrid, and London, have already or have planned to open circular lines in their transit systems.

the exception of Kreindler et al. (2024), who focus on the bus network in Jakarta, little has been done on the design effectiveness of urban transport infrastructure. In their paper, they use a travel demand model to estimate public transport preferences (directness, speed, and waiting times), and provide a set of potential optimal networks by making the assumption that commuting patterns are fixed. I contribute to this literature of optimal transport design by providing evidence that the radial design is more efficient compared to circular design for enhancing welfare, but both a circular and a radial transit system are complementary in decreasing commuting costs.

Second, this paper also relates to the debate about whether the spatial distribution of economic activity is primarily determined by first-nature factors such as natural endowments (Davis and Weinstein, 2002; Lee and Lin, 2018), or if instead, the spatial economy might be characterized by multiple steady-state equilibria where past shocks (Bleakley and Lin, 2012; Redding et al., 2011; Kline and Moretti, 2014; Ahlfeldt et al., 2015; Baerlocher et al., 2023) and expectations matter (Krugman, 1991a; Ottaviano et al., 2002; Takeda and Yamagishi, 2023).[6] I provide additional evidence that history plays a significant role in explaining uneven growth within a city by exploiting a unique setting where urban transport was shut down after intense use. This helps us in our understanding of the current spatial distribution of economic activity and in planning future urban transport infrastructure.

Finally, I also contribute to recent advances in quantitative spatial models. These models are sufficiently rich to capture the organization of economic activity within cities with low data requirements, and facilitate counterfactuals with general equilibrium effects. Since the seminal paper by Ahlfeldt et al. (2015), a growing body of work has included forward-looking migration decisions (Heblich et al., 2021; Takeda and Yamagishi, 2023; Warnes, 2021; Greaney et al., 2024); different types of workers (Tsivanidis, 2024; Weiwu, 2024; Redding and Sturm, 2024); congestion (Herzog, 2024); trade of goods (Monte et al., 2018); and consumption access (Miyauchi et al., 2025) to modelize within-city economic activities. My theoretical framework starts from the canonical urban model of Heblich et al. (2020) modelling commuting choices in an open city, and integrates an Armingtonian component to consider a sector of tradable goods (Armington, 1969), and a new economic geography component (Krugman, 1991b; Helpman et al., 1995) to consider a sector of non-tradable services. Hence, the developed quantitative urban model accommodates the dual function of the PC by modelling both the trade of merchandise and passenger

[6] See Lin and Rauch (2022) for a literature review.

commuting.[7]

The remainder of the paper is structured as follows. Section II introduces the data and discusses the historical context. Section III presents reduced-form empirical results on the impact of PC. Section IV outlines and quantifies the quantitative spatial model, and solves for unobserved characteristics rationalizing the spatial equilibrium. Section V undertakes several counterfactuals. Section VI concludes.

II Historical context and data

In this section, I first present the data that enables quantitative analysis. Next, I detail the historical context during which the PC has been constructed, as Paris experienced major urban transformations that altered population and employment dynamics in the second half of the 19th century.

II.1 Data

Geography I use neighborhoods within Paris and municipalities outside Paris as my spatial units. These are based on the 2015 geographic boundaries, with Bois-de-Vincennes and Bois-de-Boulogne being excluded.[8] After 1860, Paris's geography consists of 20 *arrondissements*, each including 4 neighborhoods, resulting in a total of 80 neighborhoods.

I create a crosswalk to harmonize the pre-1860 geography with the 2015 geography due to changes in Paris neighborhood and suburban municipality boundaries in 1860. Precisely, I use a overlapping land area method for normalization, generating weights that are then used to recalculate the pre-1860 population (as in Lee and Lin (2018)). When needed, I merge suburban municipalities to make it consistent with residential data. For example, Arcueil and Cachan are separated suburban municipalities, but they were gathered under the name of Arcueil in the 19th century (see appendix A.5.3 for more details).

Residence I digitized archives data from 1801 to 1946 of Paris neighborhoods (80) and from 1801 to 1906 for suburban municipalities (72) from *Dénombrements Statistiques* & *Annuaire Statistiques de la Ville de Paris* to look at the evolution of residential growth.

[7] In appendix A.9, I extend Ahlfeldt et al. (2015) in dynamics by starting from Heblich et al. (2021) and by adding workplace choices along with commuting cost.

[8] The Bois-de-Vincennes and Bois-de-Boulogne are two huge parks located in Paris. They provide recreational and natural spaces for residents. For comparison, Bois-de-Vincennes and Bois-de-Boulogne are respectively 2.9 times and 2.4 times larger than New York's Central Park.

The data provides me with information on population trends every 5 years from 1831 onwards.[9] Before that, I observe the population in 1801 and 1817. Moreover, some of these archives give me snapshots on the income sorting with the number of owners/managers (*patrons*), white collar workers and supervisors (*employés*) and unskilled workers (*ouvriers*) by neighborhood for 1881, 1886, 1891. The last wave presents unique features due to the availability of income sorting for suburban municipalities. More details on income segregation in supplement appendix A.1.2. Then, I use *INSEE* census to get information over 1954 population for Paris neighborhoods to study persistence effect over 50 years.

Firms I use city directories of Paris from 1799 to 1908 provided by *ANR SoDuCo* to look at the economic activity evolution across time and neighborhoods. These data geolocalize firms by activity at the street level (see Figure 1.3 for a visualization), and provide me with a proxy for neighborhood employment by activities.

Figure 1.3
Parisian city directories across time

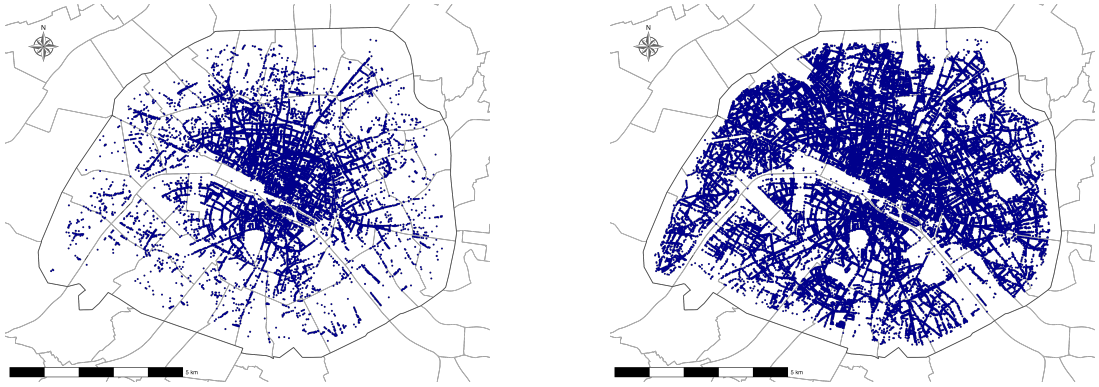

(a) City Directory 1861 **(b)** City Directory 1896

Notes: Both figures show the spatial distribution of firms in 1861 and 1896 according to the Parisian city directories.

Nevertheless, this comes with a drawback. If firms had to pay for listing in the city directory, it's possible that this could introduce selection bias. Less affluent and less attractive neighborhoods might have fewer listed firms simply because of the cost involved.

In Figure 1.4, I compare employment data at the *arrondissement* level in 1860 provided by the industrial survey with the estimated employment through city directories (see appendix A.5.2 for more details on the estimation procedure) to assess their accuracy in capturing the spatial distribution of employment. The correlation between the city directory database to the 1860 total workers by *arrondissement* is 90%. This translates that city directories are capturing a good part of the Parisian economic activity spatial

[9] With the exception of the 1871 census, which was delayed until 1872 due to the Commune.

distribution, and are able to provide a proxy for workplace employment evolution for the structural analysis.

Figure 1.4

Estimation of workers by *arrondissements* in 1860 with city directories

Notes: This figure compares the (log) predicted total number of workers through city directories with the (log) observed total number of workers by arrondissement in 1860. A weight representing the average number of workers by industry in 1872 is applied to each firm (see appendix A.5.2 for more details on the estimation procedure). The number of workers is then aggregated to the arrondissement level.

Next, I employ the R "stringdist" package to categorize firms, considering potential spelling errors resulting from Optical Character Recognition.[10]

Rents Rents are crucial for recovering location-specific productivity and amenities in the structural analysis. I collect Parisian fiscal matrices from 1855 to 1906 at the neighborhood level to get the land taxes (*contribution foncière*) to capture housing prices variations across locations, and rationalize the spatial equilibrium in 1861 and 1896.

Transport network The database on Paris transport during this period serves two objectives. First, to assess the impact of the PC on the growth of firms and residents in the reduced-form section. Second, to compute bilateral commuting times between neighborhoods, taking into account different modes of transport, in order to rationalize spatial equilibrium in Paris in the structural section. To do so, I use various sources of urban transport data in Paris to accurately describe the existing transport network during that period.

[10] Optical Character Recognition (OCR) is used to automate the digitization and extraction of textual information from printed or handwritten documents, facilitating data analysis and research.

To begin with the *Petite Ceinture*, I rely on the *Association Sauvegarde Petite Ceinture* and Open Street Map for details regarding its creation date and locations. Additionally, the *Annuaire Statistiques de la Ville de Paris* provides bilateral flows between train stations in 1895 and 1901 (see Figure A.13 in appendix).[11] This allows me to get a measure of traffic intensity by train stations. The average distance travelled by a passenger using the *Petite Ceinture* in 1901 is 5.6km.

Since tramways and omnibus were the main means of commuting alongside the PC in the 19th century, I construct their networks by combining archival maps from *Bibliothèque nationale de France* with data from the *Annuaire Statistiques de la Ville de Paris*. Both sources allow me to reconstruct station locations as well as line distances (see Figure A.15 for stations locations in 1896). The omnibus network was largely in place before 1856, with 25 lines, while tramways were introduced in 1872. In 1881, the whole network is constituted of 35 omnibus lines and 19 tramways lines.

I compute two type of bilateral travel time between all locations for 1861 and 1896 using a least cost path method. First, I create a bilateral commuting time matrix for passengers. I consider several transport modes such as omnibuses, tramways, walk, and railroad (PC and others). I consider a 5-minute waiting if there is a connection between different modes, and combine different sources to calibrate the speed of urban transport (see Table A.2 in appendix). All entries, connections, and exits of the transport network are calculated using euclidean distance. The network of multi-modal transport allows me to compute bilateral time in minutes through a least cost path Dijkstra algorithm. Second, I create a bilateral freight travel time matrix for merchandise. I consider only euclidean distance and railroad for freight transport, and a 10-minute waiting time for connection.

Lastly, regarding the metro, I use *Régie autonome des transports parisiens* (RATP) databases to construct a measure of Paris's accessibility through the metro in 1906 and 1954, crucial for controlling factors that influence residential choices within the persistence analysis.[12]

II.2 Historical context and stylized facts

City Planification Government officials, engineers, and architects in Paris during the 1840s committed to reorganizing the city's spatial structure to address five related issues

[11] Unfortunately, I lack data on the timing of these flows, preventing me from deducing commuting patterns.

[12] I complement these data with Valentine Bernasconi's work, which can be found here.

i) the displacement of the population; ii) the inadequacy of the city's road network; iii) the absence of connections between train stations; iv) the expansion and location of the Halles Centrales (central markets); v) the sanitary situation within the city center (Francke and Korevaar, 2021).[13]

These challenges were not unique to Paris and they also impacted other European capitals, especially concerning sanitary situation due to the second cholera epidemic. Therefore, it was necessary to reform historical city centers of European cities to achieve urban balance and ultimately establish a harmonized urban structure during this period. Moreover, planners started to perceive cities as a system where economic activities could efficiently commute (Papayanis and Sanconie, 1998). For Paris, two methods were considered to reorganize its spatial structure: 1) zoning-based renovations to decrease city center density and spreading out the population, and 2) the development of an urban transportation system to facilitate the commuting of workers, and ultimately enhancing their well-being.

Regarding the second method, multiple proposals from engineers aimed to innovate and establish a railroad network in Paris. The concept of a circular railroad, connecting various existing train stations of national lines, surfaced repeatedly during the 1840s due to the high costs associated with commuting. In 1845, the Kérizouet project was published, outlining an underground railroad system designed to achieve this objective. It was believed that this system could accelerate commercial transactions within Paris, while also addressing issues related to decentralization and urban expansion. This approach could improve living conditions in Paris, reduce poverty, and decrease overpopulation in the historical city center. Parisian public transport was at the center of the public debate. Figure A.6 in appendix shows an increase in the frequency of words relating to transport in Paris used in French newspapers. This could translate into an increase in demand for urban transport in Paris.

The French coup d'état of 1852 played a central role in these developments. Napoléon III issued decrees mandating the creation of the PC just eight days after his coup d'état in order to connect existing Parisian train stations for commercial purposes. Ultimately, the PC was extended to passenger services, and this urban transit project served as a means to complement the transformative Haussmann's renovations, which led low-skilled workers to move away from the city center.[14] More precisely, around 20,000 houses were

[13] I use lexicometrics to document these issues with *Gallicagram* application (Azoulay and de Courson, 2021), which allows to find the frequency of words used in French newspaper corpus between 1790 and 1900. Results are shown in appendix A.2.1 and they confirm these issues in the Parisian public debate.

[14] Georges Eugène Haussmann was the Prefect of the Seine from 1853 to 1870 and was in charge of

demolished in the historical city center between 1852 and 1870, and new construction and redevelopment drove up rents, contributing to a gentrification process (Faure and Jaillet, 2008). Consequently, the PC aimed to provide a circular means of transport in a decentralization context and where transportation modes (mainly omnibuses and walking) were poorly developed in the periphery.

The PC represents a circular line of 32 km, serving as the precursor to the metro, offering the first passenger service within the Paris intra-muros. The development of the PC can be divided into four phases, as illustrated in Figure A.11 in appendix: i) Auteuil line (1854); ii) PCRD line (1862); iii) PCRG line (1867); iv) the completion of the circle with the connection between the Auteuil line and PCRD line in 1869. This historical setting allows for the evaluation of a unique circular urban transport, which is increasingly adopted nowadays transit networks.

Parisian building footprint in the 1850s Regarding Paris before the PC, Figure 1.5 taken from the *carte d'état major* displays the building footprint during the 1850s. Note that the railroad has been added on this map a posteriori. The concentration of dark pink areas in the city center shows that the economic activity in the periphery was poorly developed before the PC arrival. It mainly consisted of agricultural land.

Population dynamics within the Greater Paris Area I use the residential data of the Greater Paris area from 1801 to 1906 in order to quantify the city center outmigration. On average, both Parisian neighborhoods and suburban municipalities experienced a population growth of 235% during the period from 1801 to 1906. However, this average growth hides heterogeneity among different locations, as illustrated graphically in Figure 1.6. Firstly, it appears that suburban municipalities exhibited a higher growth rate (247%) compared to Paris neighborhoods (224%). Secondly, within the Paris area, neighborhoods close to the city center (i.e. Notre-Dame) experienced very limited or even negative population growth, in contrast to neighborhoods situated on the periphery of the Paris boundary. This is the prevailing pattern of outmigration from the city center during this period that I am documenting in this paper. Nevertheless, suburban municipalities appear not to have experienced this decentralization effect; instead, municipalities close to Paris seem to have experienced the largest population growth.

the extensive urban changes in Paris during Napoleon III's Second Empire.

Figure 1.5
Parisian footprint in 1850 before the PC

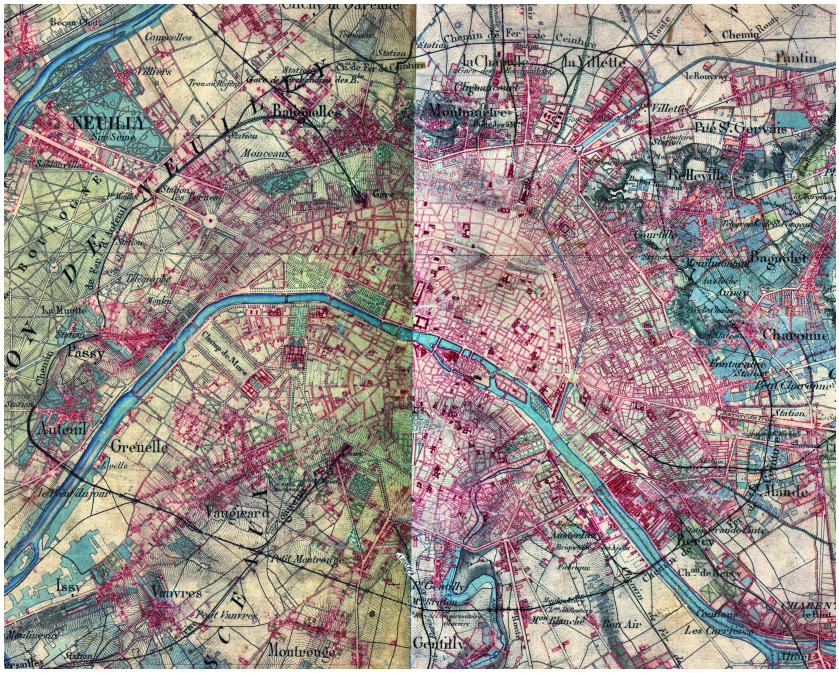

Notes: This map from the "*carte d'état major*" displays the Parisian building footprint during the 1850s. Note that the railroad has been added on this map a posteriori.

Jobs conditions and commuting patterns within the Parisian Industry I use the 1860 industrial survey in order to describe the labor conditions in Paris at this period. A total of 101,171 establishments were counted. The 1860 industrial survey also categorized these establishments into 10 industry groups. Figure A.1 shows in which *arrondissement(s)* each group of industries was clustered. They were primarily concentrated in the 3rd (11.5%), 11th (9.1%), and 2nd (7.8%) *arrondissements*.

Table 1.1 highlights the prevalence of small-scale firms in Paris with a significant majority of single-worker businesses or self-employed individuals, indicating a highly fragmented industrial landscape.

Table 1.1
Firms per size in 1860

Firms	Numbers
+10 Workers	7,492
2 − 10 Workers	31,480
Single-Worker / Self-Employed	62,199
Total Surveyed	101,171

Notes: This table decomposes the Parisian industry by firm size in 1860.

Parisian workers experienced substantial heterogeneous working and living conditions across time and positions in the 19th century. Regarding men worker daily wages, the mean was 4.20 francs, but there exists a substantial disparity. Focusing on men exclu-

Figure 1.6
Population Difference 1801-1906 in the Great Paris

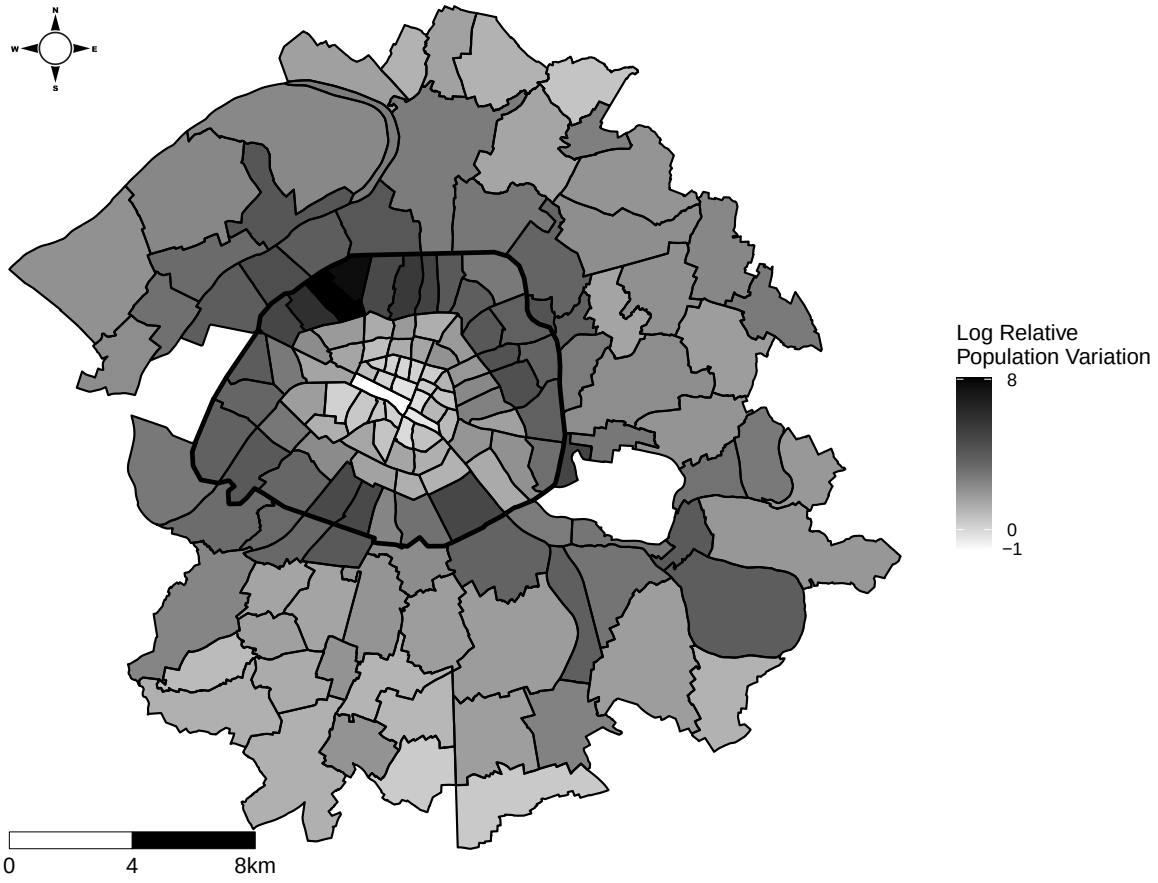

Notes: This map displays the population dynamics between 1801 and 1906 of the Greater Paris area. Neighborhoods that have experienced population decline are the following: Saint-Germain-l'Auxerrois, Halles, Saint-Merri, Notre-Dame, Sorbonne. Neighborhoods that have experienced population increase but are in the bottom two deciles, are the following: Palais-Royal, Place-Vendôme, Gaillon, Vivienne, Mail, Bonne-Nouvelle, Arts-et-Métiers, Enfants-Rouges, Archives, Sainte-Avoie, Saint-Gervais, Arsenal, Saint-Victor, Monnaie, Odéon, Saint-Germain-des-Prés, Saint-Thomas-d'Aquin, Invalides, Chaussée-d'Antin, Salpêtrière, Antony, Le Plessis-Robinson, Dugny, Stains, Villetaneuse, Bonneuil-sur-Marne, Chevilly-Larue, L'Haÿ-les-Roses, Orly, Rungis, with D2 = 1.19. Neighborhoods that have experienced population increase and are in the top two deciles, are the following: Gare, Petit-Montrouge, Plaisance, Javel, Porte-Dauphine, Ternes, Plaine de Monceaux, Batignolles, Epinettes, Grandes-Carrières, Clignancourt, Goutte-d'Or, La Chapelle, Villette, Combat, Belleville, Père-Lachaise, Asnières-sur-Seine, Clichy, Levallois-Perret, Montrouge, Neuilly-sur-Seine, Le Pré-Saint-Gervais, Saint-Ouen, Alfortville, Joinville-le-Pont, Saint-Mandé, Saint-Maur-des-Fossés, with D9 = 4.33. .

sively, 50% of workers earned less than 4 francs and daily wages could range from as low as 50 cents to as high as 20 francs as shown by Figure A.2 in appendix, indicating large heterogeneity in living conditions. As indicated by the industrial survey of 1872, mean of daily wages increases to reach 5.80 francs, and was roughly 30% higher than the closest suburban *arrondissement* Saint-Denis, and Sceaux (4.5 francs). Parisian workers were already higher paid than less populated suburban cities. Regarding job offers, the frequency of unemployment word in French newspaper corpus (see Figure A.7) indicates different waves of difficulties for Parisian workers to find a job, particularly during the 1830-1850 and 1870-1880 periods. This indicates the emergence of an excessive labor supply in the Parisian labor market in the 19th century. Another compelling observation given by the 1860 industrial survey, which emphasizes the relevance of a commuting model employed in section IV, is that a significant majority of workers in 1860 (72%) were already residing in their own accommodations and thus had to commute to reach their workplaces. Faure (2010) documents distortions between residence and workplace that began to manifest after 1860 when workers left the city center, but employment partially remained there, without the suburb being able to absorb this labor supply. Consequently, the residence-workplace relationship was already spatially disconnected. In "L'Assomoir" (1877), Emile Zola described the movement of workers as herd movements, as the majority relied on walking for their daily commute. However, it would be too simplistic to overlook other modes of transportation. Analyzing a 1890 questionnaire from the parliamentary commission studying legal working hours reform, Faure (2010) reports that some workers mentioned using trams, omnibuses, and the Petite Ceinture when asked about transportation. To investigate that, I digitized data from Martin (1894) and plot the transportation use of these 3 modes in Paris over the 1854-1890 period in Figure 1.7. The PC railroad traffic progressively increased over the period, and represented nearly 16% of the total number of trips over these 3 modes (220, 544, 751 trips) in 1890.

Figure 1.7
Transportation mode use in Paris

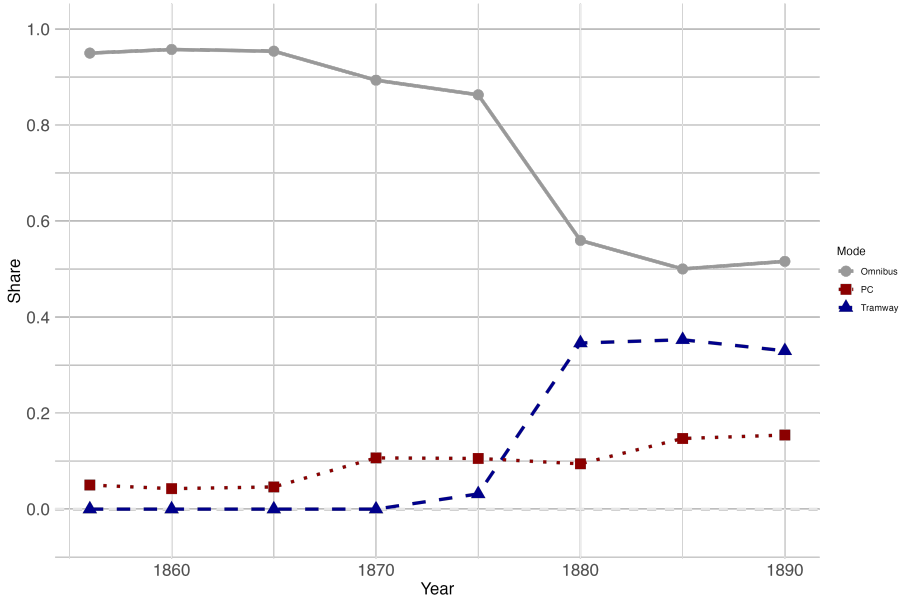

Notes: This figure displays the transport mode use in Paris over the 1854-1890 period, considering the 3 main transportation modes: trams, omnibuses, and the PC. Data are taken from Martin (1894).

III Reduced-Form Evidence

III.1 Short-term effects

The purpose of this subsection is to assess whether the PC altered the spatial distribution of economic activities during its main operational period (1854-1896).

III.1.1 Empirical Strategy

To investigate whether the *Petite Ceinture* impacted the population and firms growth in the Parisian area, I consider the following long-difference specification

$$\Delta\, Y_n = \eta_0 + \beta\, \Delta\, \mathrm{MA}_n + X_n\gamma + \epsilon_n, \tag{1.1}$$

where $\Delta\ Y_n \equiv ln\left(\frac{Y_{n,1896}}{Y_{n,1861}}\right)$ is the outcome growth in location n between 1861-1896, $\Delta\ \mathrm{MA}_n \equiv ln\left(\frac{\mathrm{MA}_{n,1896}}{\mathrm{MA}_{n,1861}}\right)$ is the (firm or residential) market access growth in location n between 1861-1896, X_n is a vector of location n characteristics controlling for Haussmann renovations and land availability in the initial period, and ϵ_n captures unobserved shocks (such as productivity or amenities) specific to location n that occurred between the two periods.

The decrease in commuting costs following PC railroad implementation should improve (i) access to jobs and consumption for workers, (ii) access to labor supply for factories, and (iii) access to buyers for retail establishments.[15] Therefore, I define two measures of market access to capture these improvements,

$$\text{FMA}_{i,t} \equiv \sum_{n} \frac{\text{Pop}_{n,t}}{d^{C}_{ni,t}},$$

$$\text{RMA}_{n,t} \equiv \sum_{i} \frac{\text{Firms}_{i,t}}{d^{C}_{ni,t}},$$

where $\text{FMA}_{i,t}$ is the firm market access in location i at time t, $\text{RMA}_{n,t}$ is the residential market access in location n at time t, $\text{Pop}_{n,t}$ is the population in n at time t, $\text{Firms}_{i,t}$ is the total number of firms in i at time t, and $d^{C}_{ni,t} \equiv e^{\nu\, t^{C}_{ni,t}}$ is the commuting costs between n and i at time t which is function of commuting time $t^{C}_{ni,t}$ and an elasticity parameter ν.[16] In this framework based on Donaldson and Hornbeck (2016), market access aims to capture changes in commuting time that are not only localized close to train stations, but also in its neighboring locations. Moreover, it can be seen as sufficient statistics to capture general equilibrium effects (Tsivanidis, 2024; Redding, 2025) when ignoring changes in housing supply, amenities and productivity. To exploit the granularity dimension of the city directories, I construct grids of 200m×200m resulting in 2,293 spatial units. Therefore, the firm market access is given by the sum of neighborhoods population in n weighted by their commuting costs to grid i. Conversely, the residential market access is given by the sum of total firm across grids i weighted by their commuting costs to neighborhood n. I calibrate ν to 0.107, and compute the commuting time between pairs n and i using least cost path method and considering PC railroad, tramways, omnibuses,

[15] I also exploit the decrease in freight costs following the implementation of the PC railroad in the additional results section III.1.3 using a NLS estimator.

[16] Commuting time between locations also depends on trams and omnibuses. This could create endogeneity issues in the measurement of the Market Access, given that the tram network was implemented in 1873, and omnibus network slightly increased. However, the Figure A.16 in the appendix compares commuting times between locations in 1896 with and without the inclusion of tram and omnibus expansion, and shows a slight increase. Out of 5,987,809 location pairs, only 16% experiences a commuting time increase of over 1%, and only 4% experiences a commuting time increase of over 10%, when the tram network is removed and omnibus keeps to initial period. Finally, the average difference in commuting time when comparing with and without tram and omnibus expansion is -0.47 min. Moreover, Figure 1.7 shows that the tramway traffic mainly absorbed the omnibus traffic. Overall, these evidence suggest that including tramways/omnibuses expansion in 1896 commuting time computation is unlikely to create endogeneity.

walking, and other railroads.[17] Figure 1.8 shows the firm market access change in Panel (a) and the residential market access change in Panel (b) between 1861 and 1896, and it suggests that the largest changes are in locations near to PC train stations.

Figure 1.8

Market access change between 1861 and 1896

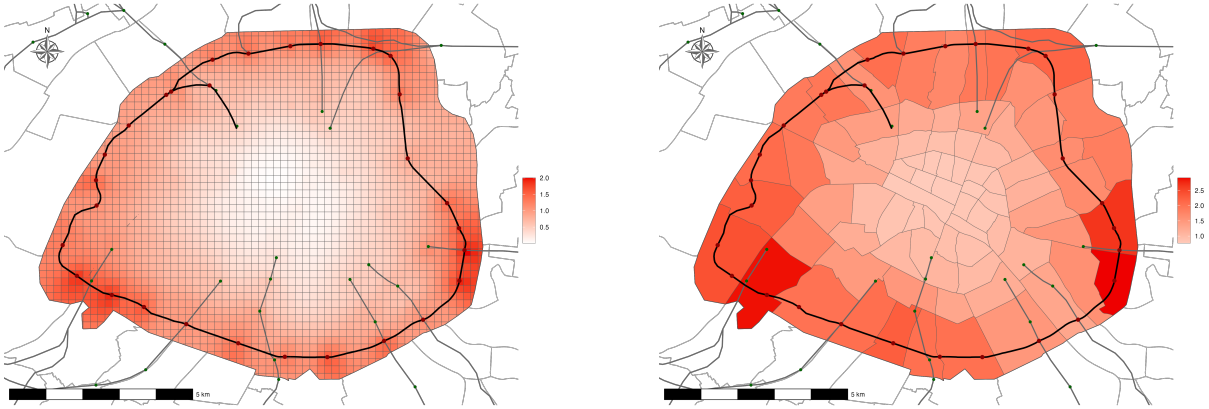

(a) Change of FMA between 1861 and 1896 **(b)** Change of RMA between 1861 and 1896

Notes: Both figures show growth in Market Access between 1861 and 1896. Panel (a) displays the firm market access growth in each 200m×200m grid cell. Panel (b) displays the residential market access growth in each Parisian neighborhood.

III.1.2 Baseline results

Residential growth The outcomes of interest are the changes in the logarithms of population between 1861 and 1896 within neighborhood n, and the changes in the logarithms of rent between 1861 and 1896 within neighborhood n. The variable of interest is the difference in residential market access logarithms between 1861 and 1896 within neighborhood n which aims to capture change in firm access across neighborhoods. Table 1.2 shows the results for population and rent outcomes. Columns (1) and (4) show the estimated coefficient associated with the residential market access change without any controls. In these baseline specifications, both estimates are positive and significant, and a 1% increase in residential market access is associated, on average, with an increase of 0.80% in population and 0.90% in rent, respectively. However, other factors could explain residential growth during this period. For example, Haussmann renovations that reshaped the urban structure mainly during this period could either displace the population by changing the housing stock or increase rent by increasing amenities (Brueckner et al., 1999). Moreover, residential growth in the periphery could be due to land availability rather than a decrease in commuting time following the implementation of the PC

[17] The value 0.107 corresponds to the product of ϵ and τ, calibrated to 5.25 and 0.0204 respectively for the structural model. For further details, see section IV. I test for alternative calibration in additional results section III.1.3

railroad. In order to correct for these endogeneity issues, I control for the total length of Haussmann renovations (mainly streets and boulevards) by neighborhood to capture changes in urban structure, and for the initial building share to capture the mechanical expansion of the population toward the periphery due to land availability.[18] Columns (2) and (5) show the results and estimates associated to change in residential market access decrease in magnitude but remain positive and significant. Columns (2) and (5) show the results and estimates associated to change in residential market access decrease in magnitude but remain positive and significant. Nevertheless, there is still an endogeneity issue due to reverse causality, as population growth also influences firm growth, which could ultimately overestimate the effect of market access on the dependent variables. An additional concern could be the Parisian expansion in 1860, which also extended the frontier of *octroi* taxation and could influence the spatial growth of firms in the periphery.[19]

To address this potential confounder and the reverse causality issue, I employ an instrumental variable strategy by setting the numerator of residential market access (the total number of firms) to its initial level (see Figure A.20 in appendix for a visualization). By doing so, I don't take into account the response of firms to population growth and the change in taxation in the periphery, and exploit only the variation in commuting costs. As a consequence, this strategy mitigates reverse causality concerns between residential and firm growth as well as the frontier expansion. Columns (3) and (6) show the estimates with the instrumental variable strategy and both magnitudes decrease but remain statistically non-different at 5% from the previously estimated coefficients. On average, a neighborhood experiencing a 1% increase in its residential market access sees its population and rent increase by 0.22% and 0.47%, respectively.

[18] It aims to capture the city center outmigration pattern depicted in Figure 1.6.

[19] The Octroi tax in France was a local tax on imported goods such as beverages, food, fuel, and building materials entering a municipality for consumption. It aimed to generate municipal revenue and could influence firm location choices, as businesses might opt to establish themselves in areas with lower or no Octroi taxes to reduce costs.

Table 1.2
Residential growth and Market Access

	Population			Rent		
	(1)	(2)	(3)	(4)	(5)	(6)
Δ RMA	0.799***	0.482***	0.221***	0.900***	0.716***	0.470*
	(0.068)	(0.101)	(0.077)	(0.129)	(0.210)	(0.271)
Controls		✓	✓		✓	✓
S.D Δ RMA	0.540	0.540	0.540	0.540	0.540	0.540
Mean Δ RMA	1.41	1.41	1.41	1.41	1.41	1.41
Observations	80	80	80	80	80	80
R^2	0.723	0.778	—	0.504	0.514	—
F-stat, Δ RMA			111.3			111.3

Notes: Each column reports estimates from a separate regression. Regressions use 80 Parisian neighborhoods. Dependent variable is the Residential Market Access growth between 1861 and 1896. From (1) to (3) the independent variable is the growth in population. From (4) to (6) the independent variable is the growth in rent. Controls are initial building share and the total length of Haussmann renovations within each neighborhood. Instrumental variable is the Residential Market Access growth between 1861 and 1896 with the numerator fixed to the initial period. Heteroskedasticity-robust standard errors are in parentheses and ***, **, * indicate significance at the 1%, 5% and 10% level, respectively.

Firms growth To investigate the effect on firm growth, the outcome is the difference in logarithms of the total number of firms between 1861 and 1896 within grid cell i, and the variable of interest is the difference in firm market access logarithms between 1861 and 1896 within grid cell i, which aims to capture changes in population access across grids.

Since city directories document the locations of firms by their respective activities, I also focus on specific firms that have an interest in locating near the PC railroad to gain market access. First, I consider factories because they represent firms that extensively use the workforce to produce goods. A reduction in commuting costs for factories might broaden their access to a larger workforce supply, thus increasing their market potential. Second, I consider firms associated with small-scale activities, such as retail establishments (e.g., wine shops, creamery stores, grocery stores). The proximity to the PC railroad would extend their market by increasing the number of potential buyers. Therefore, I also use the difference in logarithms of the total number of firms in industry g between 1861 and 1896 within grid cell i as outcome variables.

Table 1.3 shows the results for total number of firms, factories, and retails outcomes. Columns (1), (5), and (9) show the estimated coefficient associated with the firm market

access change on each outcomes without any controls.[20] In these baseline specifications, all estimates are positive and significant. On average, a 1% increase in firm market access is associated with a 2.22% increase in the total number of firms, a 0.91% increase in the total number of factories, and a 2.26% increase in the total number of retail establishments, respectively. As detailed previously in the residential growth results, other factors such as Haussmann renovations or land availability in the periphery could explain firm growth during this period. Therefore, I control for the proximity to the nearest Haussmann renovations to capture changes in urban structure and for the initial building share to capture the mechanical expansion of economic activity toward the periphery due to land availability. Columns (2), (6), and (10) show the results and estimates associated with changes in firm market access, which remain positive and significant. However, their magnitudes are divided by approximately 1.5, suggesting a strong upward bias. Controlling for a dummy variable indicating whether the grid is within the old or new Parisian border in columns (4), (8), and (12) reduces the magnitude of the coefficients, but they remain positive and significant. Then, I also proceed to the same instrumental variable strategy to correct for reverse causality issues as firm growth influences population growth, and frontier expansion could attract population in the periphery. To address these endogeneity issues, I set the numerator of firm market access (population) to the 1846 level see Figure A.20 in appendix for a visualization), which corresponds to the period before the planning and implementation of the PC railroad. As before, I exploit only the variation in commuting costs, which helps mitigate reverse causality concerns between residential and firm growth, and the expansion of Paris. Columns (4), (8), and (12) present the estimates using the instrumental variable strategy. While all magnitudes decrease, they remain statistically significant at the 5% level, except for factories, which is close to the 5% significance level. Moreover, all estimate are statistically non-different at 95% from the previously estimated coefficients. On average, within a 200m×200m grid cell, a 1% increase in firm market access increases the total number of firms, factories, and retail establishments by 0.80%, 0.39%, and 0.69%, respectively.

Nevertheless, there are factors that can be considered to further discuss this result. For instance, it is possible that because firms had to pay to appear in the directory, there could be a selection bias. Even though it represents a small fee, firms in relatively less developed and/or connected neighborhoods (i.e., in the periphery) with a small market potential may not have an incentive to pay to be listed in this directory. Firms could exist, but would

[20] Note that the number of observations varies across outcomes due to the presence of 0 in the grid cells in the initial period.

prefer not to report themselves in order to avoid paying the cost. Consequently, the PC railroad by reducing commuting costs automatically enhances the market potential of peripheral firms and firms could find it advantageous to register themselves in city directories. Therefore, the effect of PC development on the firms listed in city directories captured in Table 1.3 could be a mix of a size and signal effect.

Table 1.3
Firms growth and Market Access

	Total				Factories				Retails			
	(1)	(2)	(3)	(4)	(5)	(6)	(7)	(8)	(9)	(10)	(11)	(12)
Δ FMA	2.22***	1.48***	0.840***	0.798***	0.913***	0.620***	0.594***	0.386*	2.26***	1.35***	0.645***	0.685***
	(0.098)	(0.145)	(0.159)	(0.169)	(0.114)	(0.173)	(0.206)	(0.220)	(0.113)	(0.171)	(0.189)	(0.203)
Baseline controls		✓	✓	✓		✓	✓	✓		✓	✓	✓
Old Paris border			✓				✓				✓	
S.D Δ FMA	0.410	0.410	0.410	0.410	0.410	0.410	0.410	0.410	0.410	0.410	0.410	0.410
Mean Δ FMA	0.770	0.770	0.770	0.770	0.770	0.770	0.770	0.770	0.770	0.770	0.770	0.770
Observations	1,326	1,326	1,326	1,326	743	743	743	743	1,226	1,226	1,226	1,226
R^2	0.312	0.355	0.385	—	0.090	0.100	0.100	—	0.286	0.335	0.367	—
F-stat, Δ FMA				2,082.6				963.3				1,786.2

Notes: Each column reports estimates from a separate regression. Regressions use 200mx200m grid cells. Dependent variable is the Firm Market Access growth between 1861 and 1896. From (1) to (4) the independent variable is the growth in the total number of firms. From (5) to (8) the independent variable is the growth in the total number of factories. From (9) to (12) the independent variable is the growth in retail establishments. Baseline controls are the share of buildings in initial period and the distance to nearest Haussmann renovations. Columns (3), (7) and (11) control for a dummy indicating whether the grid cell is within the boundary of 1859 Paris. Instrumental variable is the Firm Market Access growth between 1861 and 1896 with the numerator fixed to the initial period. Heteroskedasticity-robust standard errors are in parentheses and ***, **, * indicate significance at the 1%, 5% and 10% level, respectively.

III.1.3 Additional results and robustness checks

Freight costs improvements In addition to passenger services, the PC railroad has also improved the flow of merchandise by decreasing freight travel time ($t^T_{ni,t}$) between locations. Therefore, it should have improved access to suppliers and consumers for firms selling final goods (such as retail establishments) following Redding and Venables (2004). To explore this effect of freight costs, I use the same long-difference specification as in equation (1.2) with the growth of retail as the dependent variable. I consider both supplier market access ($SMA_{i,t} \equiv \sum_n \frac{\text{Factories}_{n,t}}{d^T_{ni,t}}$) and consumer market access ($CMA_{i,t} \equiv \sum_n \frac{\text{Pop}_{n,t}}{d^C_{ni,t}}$). Both freight travel costs ($d^T_{ni,t} = e^{\kappa\, t^T_{ni,t}}$) and commuting costs ($e^{\nu\, t^C_{ni,t}}$) take an exponential form. They are functions of freight elasticity (κ) and freight time ($t^T_{ni,t}$), and commuting elasticity (ν) and commuting time ($t^C_{ni,t}$), respectively. Since I do not have a good calibration for freight time elasticity (κ), I use non-linear least squares (NLS) to estimate it. Results in appendix A.4.1 provide evidence of positive and significant effects of supplier market access and consumer market access on the growth of retail establishments. This highlights the dual function of the PC railroad in decreasing both freight and commuting costs. I also replicate the baseline specifications and find a positive and significant effect of population access on the growth of factories, as well as a positive and significant effect of total firms on population growth.

Placebos I conduct two placebo tests to check the validity of the baseline results. First, I investigate the effect of firm market access on firms that have no interest in relocating close to the PC railroad. To do so, I consider liberal profession (such as lawyer, or teacher) growth and implement the same long-difference strategy. Although these professions may benefit from better access to the population, they should value less the decline in transport costs that firms which rely heavily on labor (factories) or consumers (retail establishments). Table A.9 shows the associated coefficients for firm market access change. Baseline specification estimates a positive and significant effect on liberal progressions growth. However, the magnitude is relatively small and not statistically different from 0 using the instrumental variable strategy. Therefore, it provides evidence that the liberal professions value proximity to the population, but not the decrease in commuting time due to the PC railroad. Second, I investigate the effect of residential market access change during the 1861-1896 period on population growth during the 1831-1856 period. This exercise, which can be considered as a pre-trends test, determines whether the neighborhoods that experienced residential market access growth were already experiencing population growth before treatment. Table A.10 shows the associated coefficients for residential market access change, and once using the instrumental strategy, it becomes not statistically different from 0. Therefore, neighborhoods that experienced a reduction in commuting time following the implementation of the PC railroad were not already undergoing population growth. Consequently, these placebo tests highlight the previous results and show that only the instrumental variable strategy is credible.

Alternative specifications and calibration I consider alternative specifications and calibration to check the robustness of the results using market access measures. First, I implement a Poisson regression model to account for the large number of 200m$\times$200m grid cells without any firms, and find positive and significant effects of firm market access on the total number of firms, factories, and retail establishments (see Table A.6). Second, I test alternative calibration of the commuting time elasticity ν considering 0.07 and 0.143. Table A.7 shows the results for firm market access change, and Table A.8 shows the results for the residential mark access change.[21] All results are robust to the use of other values of travel time elasticity.

[21] The value 0.07 corresponds to the commuting time elasticity of Ahlfeldt et al. (2015), and 0.143 corresponds to the product 0.0204×7, with 7 being a higher Fréchet parameter ϵ than the baseline (5.25), based on Ahlfeldt et al. (2015).

Mechanisms To investigate whether previous results are only driven by a reduction in commuting costs and not urbanization (i.e. urban fabric or urban network) close to the PC railroad, I use digitalized data on the street network over the 19th century in order to follow the evolution of urban development at a small spatial level. I use a similar long-difference specification where the dependent variable is the total growth in the street length between 1861 and 1896 within a 200m×200m grid cell, and the variable of interest is the change in firm market access within the same period. Table A.11 presents the results, and the coefficient associated to the firm market access is negative and not statistically different from 0 in the instrumental variable specification. Moreover, the coefficient associated with the distance to the nearest Haussmann renovations is negative and precisely estimated, aligning with the idea that these urban renovations reshape and increase the density of the street network. Hence, the change in commuting time following the PC railroad implementation does not appear to have changed the street development and the spatial structure. This reinforces that decrease in commuting costs are mainly at play in the main results.

Staggered DiD strategy Since market access measurements capture non-localised transport changes, all units can be treated and this does not allow for a control group. As a consequence, it is difficult to assess whether locations that received the PC railroad were already growing before the treatment. To investigate this concern, and whether the PC railroad impacted the population and firms growth in the Parisian area taking into account staggered timing of the treatment, I rely on the estimator proposed by De Chaisemartin and d'Haultfoeuille (2024) and run Differences-in-Differences event-study specification. I consider a treatment threshold of 500m (see A.12 to see the treated units for neighborhoods and grids), and population, factories, and retails densities as outcomes over the 1831-1896 period each 5 years. I also control for Haussmann renovations, other railroads proximity, a dummy capturing area expansion in 1860, and non-parametric trends based on distance to the city center to capture city center outmigration pattern (see appendix A.4.3 for more details). Overall, event-study plots for population (Figure A.21), and firms (Figure A.22) show a positive effect of the PC railroad proximity on these outcomes. I also conduct the same placebo test and Figure A.24 suggests no treatment effect of the PC on the liberal professions.

Finally, I also investigate whether previous results are only driven by a reduction in commuting costs and not urbanization using an event-study specification where the dependent variable is the total length of streets over the 1831-1896 period. Figure A.23 shows the

event-study results and there is no effect of the PC on the street length. However, significant pre-trends indicate that spatial units receiving the PC were less developed than others, even after controlling for non-parametric trends based on the distance to city. This suggests an endogenous location of PC train stations

A potential threat would be to attribute the effect of a linear trend to the effect of the PC. To test this, I use the honestdid package developed by Rambachan and Roth (2023) to conduct pre-trends sensitivity analysis. This "honest" approach to parallel trends is based on the computation of robust confidence intervals by using pre-trends as information to restrict possible values of post-treatment trends. I use second differences (SD) approach and create the robust confidence intervals for the last two lags using deviation from a linear extrapolation of the pre-trend information. Results of pre-trends sensitivity analysis for the effects of the PC are shown in Figure A.25 of appendix. Overall, it is possible to rule out null effect the PC for factories, retails, and population event-study results when considering a linear trend.

To verify the validity and the magnitude of the residential growth effects, I perform several tests. First, I investigate whether a similar pattern holds for train stations across the entire Greater Paris railroad network by using suburban municipalities only. I control for non-parametric trends based on the distance to Paris city fringe to capture the pattern observed in Figure 1.6, and I consider a binary dummy equal to one if the municipality has or not a train station within its area. Given that the first Greater Paris railroad train stations has been implemented in 1837, the period of interest starts from 1801 in order to test existing pre-trends. Figure A.26 in appendix shows that the average treatment effect of train station implementation is positive and the magnitude is similar to the effect of the PC on Parisian neighborhoods. Second, I replicate Heblich et al. (2020) who examines the effect of railways on population growth in London during the 1801-1901 period using my baseline empirical specification. As in the Parisian context of the PC, the treatment is staggered and I use an indicator variable equal to one if a neighborhood has an overground or underground railway station. Because their sample includes neighborhoods located farther away from the city center compared to my Parisian sample, I use 20 indicator variables based on distance to the city center to control for non-parametric trends and to allow different population growth. Figure A.27 in appendix shows the event study plot using De Chaisemartin and d'Haultfoeuille (2024) estimator and results indicate a positive and significant effect of railways on population growth with a magnitude similar to previous findings in the Parisian context.

III.2 Path Dependency

The aim of this subsection is to investigate whether the construction of the PC generated a significant shock that had a long-term impact on the spatial growth within Paris. It focuses on the period between 1906 and 1954, as this marks the decline of PC usage due to the increasing prominence of Parisian metro.

III.2.1 Empirical Strategy

To investigate whether the PC created long-term effects on Paris' spatial equilibrium, I employ the following long-difference specification,

$$\Delta\ pop_{n(a)} = \theta_a + \beta\ \mathbb{1}_{n(a),1900} + X_n\ \gamma + \epsilon_{n(a)}, \tag{1.2}$$

with the dependent variable $\Delta\ pop_{n(a)} \equiv ln\ \left(\frac{pop_{1954}}{pop_{1906}}\right)_{n(a)}$ being the log of relative population change within neighborhood n of *arrondissement* a between 1906 and 1954. The variable of interest, $\mathbb{1}_{n(a),1900}$, is a binary variable indicating whether a neighborhood n within *arrondissement* a is within 500m of a PC train station in 1900, as the PC network had not evolved since. Finally, θ_a represents an *arrondissement* fixed effect, and X_n is a vector of neighborhood controls.

III.2.2 Baseline Results

Table 1.4 shows the results. The simplest specification in column (1) depicts substantial effects of PC on population growth between 1906 and 1954. On average, neighborhoods that were close to 500m of a train station of the PC had grown 49% more than others neighborhoods. Furthermore, PC train stations alone account for approximately 35.6% of the variation in neighborhood population growth. However, at this point, there is an omitted variable bias resulting from the PC's location. As they are situated on the periphery, the results could potentially reflect a pattern of outmigration from the city center, as mentioned in II.2. To address these migration patterns, I control for the log of distance to the city center of Paris, located at Notre-Dame, and the log of area in column (2). The coefficient is divided by 2 but remains statistically significant at the 1% level. On average, neighborhoods that were close to 500m of a PC train station experienced 23% more population growth, at an equal area and distance from Notre-Dame.

Nevertheless, other factors can also impact the dynamics of residential growth between 1906 and 1954, and one such factor that gained significant popularity during this time

period was the metro. To account for this commuting system, I generate a Least Cost Path (LCP) measure in 1906 and 1954, considering only the metro and walking for simplicity, between all neighborhoods. Then, I calculate the neighborhood's average LCP, which serves as a measure of the average accessibility from that location to the entire Paris area via the metro. Finally, I compute the difference between both periods to measure an average growth of accessibility. As expected, the coefficient associated to metro growth is negative in column (3). This implies that an increase in accessibility (and therefore a decrease in average LCP) is correlated with higher population growth. However, the coefficient is not statistically significant, possibly due to insufficient variation in the data. Regarding the coefficient of interest, its magnitude does not change compared to column (2) specification, and maintains statistical significance at the 1% level. This emphasizes the strong persistence effect created by the PC on the residential spatial growth dynamics. Finally, adding an *arrondissement* fixed effect, which restricts the source of variation, does not shrink drastically the magnitude in column (4), but the coefficient becomes insignificant.

From these different estimates of long-difference specifications, it seems that PC has created a temporary and sufficient shock, anchoring the neighborhoods in a population growth dynamic long after this mode of transport ceased to be used by passengers.

Table 1.4

Long-Differences (1906-1954)

	Δpop_n			
	(1)	(2)	(3)	(4)
$\mathbb{1}^{500m}_{n,1900}$	0.49***	0.23***	0.22***	0.14
	(0.08)	(0.08)	(0.07)	(0.11)
Log d2CC		0.11	0.13*	0.25**
		(0.08)	(0.08)	(0.10)
Log area		0.21***	0.20***	0.15*
		(0.06)	(0.05)	(0.08)
Metro LCP Growth			-0.25	-0.20
			(0.28)	(0.34)
Arrondissement FE	○	○	○	✓
R^2	0.356	0.661	0.666	0.765
Observations	80	80	80	80

Notes: Each column reports estimates from a separate regression. Regressions use 80 Parisian neighborhoods. Dependent variable is the log of relative population change within neighborhood between 1906 and 1954, and the independent variable is a binary dummy indicating whether a neighborhood is within 500m of a PC train stations. Regression (4) includes an *arrondissement* fixed effect. Heteroskedasticity-robust standard errors are in parentheses and ***, **, * indicate significance at the 1%, 5% and 10% level, respectively.

III.2.3 Additional results and robustness checks

Additional results To investigate heterogeneous treatment effects, I exploit variation in traffic size by train stations. By comparing train stations with substantial passenger inflows to others, it could offer insights into the mechanism behind the significant growth experienced by certain neighborhoods following the implementation of PC train stations.

Following Gechter and Tsivanidis (2023), I build a measure of exposure to 1901 traffic of the PC,

$$\text{Traffic}_{n(a),1901} \equiv \sum_{j=1}^{N^{TS}} e^{-\delta\, Dist_{nj}} \big(\text{Passengers}_{j,1901}\big),$$

with N^{TS} being the total numbers of PC train stations in 1900. The spatial decay parameter, denoted as δ, determines how localized is the traffic exposure. The baseline value is set at 1, and I vary it to perform sensitivity analysis. Finally, $Dist_{nj}$ is the distance in km between neighborhood n and train station j and $\text{Passengers}_{j,1901}$ is the sum of passengers coming from station j in 1901 (see Figure A.13 in appendix) in millions. This measure of exposure to 1901 traffic is going to be the independent variable in equation 1.2.

Table A.12 shows the results. The estimated coefficient in column (1) suggests that an increase of one standard deviation in the traffic exposure leads to 15.5 higher growth of population between 1906 and 1954. Adding the set of controls and the *arrondissement* fixed-effect does not significantly change the estimated parameter in column (2). The coefficient associated to traffic exposure suggests that one standard deviation increase in the exposure of PC traffic in 1901 leads to 12.9% higher growth of population between 1906 and 1954. Varying the spatial decay highlights that the effect is once again very localized, particularly when considering the inconsistency of the effect associated with column (3). Excluding the case when $\delta = 0.5$ meaning that the treatment of traffic exposure affects neighborhoods located far away from train stations, the estimated coefficient associated to the traffic exposure is relatively stable when increasing the spatial decay.

Robustness checks I conduct robustness checks by varying the final year of long-differences in Figure A.28, and I confirm both baseline and heterogeneity results. It suggests that the effect of PC on population growth has reached its equilibrium level, given that estimates are stable. Moreover, this rules out the possibility of attributing the PC effect to unobservable shocks during the period given the consistency of the results.

Mechanisms In order to test mechanisms explaining path dependency results, I explore whether the PC magnifies the housing supply. To do so, I compute the difference in housing stock between 1906 and 1954 by using the national housing database (*BDNB*), and I use it as a dependent variable in the long-difference specification (1.2). Results are shown in Table A.13, and after controlling for neighborhood characteristics, the estimated coefficient of PC proximity is insignificant. On average, neighborhoods that were located within 500m of PC train stations have not experienced a higher growth of housing supply. This suggests that the effect of PC on population growth is not due to a greater supply of housing.

IV Quantitative Spatial Model

In this section, I develop a within-city quantitative spatial model of commuting and trade to rationalize Paris's spatial equilibrium in 1896. The primary objective of this model is to quantitatively assess the development of urban transport infrastructure, considering commuting and freight costs. These two key features allow the model to match reduced-form and historical evidence, where the PC railroad improved the flows of goods and passengers.

Within this framework, I consider a homogeneous mass of workers living and working in an open city. In addition, they choose to work in one of two sectors of production: tradable goods and non-tradable services. An Armington model allows to determine trade within the city subject to freight costs. As a consequence, residences not only differ by rent and amenities, but also price indexes of tradable goods and non-tradable services. This structural model offers two noteworthy features. First, it provides a way to uncover unobserved location characteristics, including amenities, and wages. Second, it allows the computation of counterfactual scenarios, such as removing the *Petite Ceinture* transport network.

As detailed in the data section II, a range of data sources, including *Annuaire Statistiques* for residence employment, *Annuaire Almanach* for workplace employment by neighborhood during the same period, and Parisian fiscal data for neighborhood rents, are employed in this analysis.[22]

[22] See appendix A.5.2 for details of workplace employment inference.

IV.1 Workers

I consider a homogeneous mass of workers within an open city of $\mathbb{J}$ discrete locations, embedded within an economy $\mathbb{E}$. An individual ω derives the following indirect utility from living in neighborhood n, working in workplace i and sector j,

$$U_{nij}(\omega) = \frac{B_n w_{ij}}{d_{ni}^C (P_n^T)^{\alpha^T} (P_n^S)^{\alpha^S} Q_n^{1-\alpha^T-\alpha^S}} \; z_{nij}(\omega), \tag{1.3}$$

where B_n are the amenities in location n, w_{ij} is the wage in i and sector j, d_{ni}^C is the commuting costs between n and i locations, P_n^T and P_n^S are respectively the price indexes of tradables and non-tradable services in location n, Q_n is the rent in location n, and z_{nij} is an idiosyncratic shock following a Frechet distribution with shape parameter ϵ. Finally, α^T, α^S and $1-\alpha^T-\alpha^S$ represent respectively the shares of income that worker ω spends on tradables, non-tradable services, and housing.

Prices of tradables and non-tradable services are derived following CES preferences. First, the consumption index of tradable goods follows this form $C_n^T = \left[\sum_{i\in\mathbb{J}} (c_{ni}^T)^{\rho}\right]^{\frac{1}{\rho}}$, with c_{ni}^T the consumption of location n of the good produced in location i and ρ the elasticity of substitution between tradable goods. Using standard CES properties, the price index for tradable goods is expressed as $P_n^T = \left[\sum_{i\in\mathbb{J}} (p_{ni}^T)^{1-\sigma}\right]^{\frac{1}{1-\sigma}}$, assuming that workers in each location consume tradable goods produced in all locations at equilibrium. Second, the consumption index of non-tradable services follows this form $C_n^S = \left[\int_0^{\mathcal{M}_{iS}} (c_n^S)^{\rho}(j)dj\right]^{\frac{1}{\rho}}$, with $\mathcal{M}_{iS}$ being the mass of varieties produced in location i, and ρ the elasticity of substitution between non-tradable services. Using CES properties, the price index for non-tradable services is expressed as $P_n^S = p_n^S\Big(\mathcal{M}_{iS}\Big)^{\frac{1}{1-\sigma}}$.

Using standard properties of Frechet distribution (McFadden, 1974), the probability that a worker chooses location pairs n and i, and sector j is,

$$\lambda_{nij} = \frac{\Big(B_n w_{ij}\Big)^{\epsilon}\Big(d_{ni}^C (P_n^T)^{\alpha^T}(P_n^S)^{\alpha^S} Q_n^{1-\alpha^T-\alpha^S}\Big)^{-\epsilon}}{\sum_{j'}\sum_k\sum_l \Big(B_k w_{lj'}\Big)^{\epsilon}\Big(d_{kl}^C (P_k^T)^{\alpha^T}(P_k^S)^{\alpha^S} Q_k^{1-\alpha^T-\alpha^S}\Big)^{-\epsilon}}, \tag{1.4}$$

with k, l being all the other residences and workplaces in the city, and j' all sectors ($\{S, T\}$). Summing across workplace and sector we get the probability that a worker lives

in residence n (see equation A.2 in appendix), and summing across residence we obtain the probability that a worker is employed in workplace i working in sector j (see equation A.3 in appendix). Using the probability that a worker commutes to workplace i in sector j from residence n (equation (1.4)), and the probability that a worker lives in residence n (equation (A.2) in appendix), the conditional probability that a worker commutes to workplace i and works in sector j conditional on living in residence n can be expressed as,

$$\lambda^R_{nij|n} = \frac{\lambda_{nij}}{\lambda^R_n} = \frac{\left(w_{ij}/d^C_{ni}\right)^\epsilon}{\sum_{j'\in\{S,T\}}\sum_l \left(w_{lj}/d^C_{nl}\right)^\epsilon}. \tag{1.5}$$

Population mobility within the economy implies that expected utility is equalized across all different residence-workplace-sector choices within the economy. Using Frechet distribution properties, the expected utility is,

$$\overline{U} = \vartheta\left[\sum_{j'\in\{S,T\}}\sum_{k\in\mathbb{E}}\sum_{l\in\mathbb{E}}\left(B_k w_{lj'}\right)^\epsilon\left(d^c_{kl}(P^T_k)^{\alpha^T}(P^S_k)^{\alpha^S}Q_k^{1-\alpha^T-\alpha^S}\right)^{-\epsilon}\right]^{1/\epsilon} \tag{1.6}$$

where $\vartheta \equiv \Gamma\left(\frac{\epsilon-1}{\epsilon}\right)$, and $\Gamma(.)$ is the gamma function. Following Heblich et al. (2020), it is possible to rewrite the previous equation using the probability that a worker chooses *Paris* $\left(\frac{L_{\mathbb{J}}}{L_{\mathbb{E}}}\right)$ as a living and working place,

$$\overline{U}\left(\frac{L_{\mathbb{J}}}{L_{\mathbb{E}}}\right)^{1/\epsilon} = \vartheta\left[\sum_{j'\in\{S,T\}}\sum_{k\in\mathbb{J}}\sum_{l\in\mathbb{J}}\left(B_k w_{lj'}\right)^\epsilon\left(d^c_{kl}(P^T_k)^{\alpha^T}(P^S_k)^{\alpha^S}Q_k^{1-\alpha^T-\alpha^S}\right)^{-\epsilon}\right]^{1/\epsilon}. \tag{1.7}$$

For a given level of utility in the economy $\overline{U}$, *Paris* must offer higher levels of amenities or higher levels of wages, or lower costs of living (commuting costs, prices of tradable goods, prices of non-tradable services, rents) in order to attract workers from the economy.

IV.2 Non-tradable sector

The production of non-tradable services follows the new economic geography literature (Krugman, 1991b; Helpman et al., 1995) . Firms in location i produce non-tradable services of different varieties with a homothetic technology using labor, machinery capital and commercial housing, and under monopolistic competition. Firms must pay a fixed and a variable cost to produce a variety j. Hence, the profit of a firm producing $y_i(j)$ units of variety j is,

$$p^S_i(j)y^S_i(j) - \Gamma_i(j), \tag{1.8}$$

with $\Gamma_i(j) = \Big(F + y_i^S(j)\Big) w_{iS}^{\beta_L^S} Q_i^{\beta_H^S} r_i^{\beta_M^S}$ being the total cost function. Firm profit maximization under monopolistic competition implies that equilibrium variety prices are a constant mark-up over marginal cost,

$$p_i^S(j) = p_i^S = \Big(\frac{\sigma}{\sigma - 1}\Big) w_{iS}^{\beta_L^S} Q_i^{\beta_H^S} r_i^{\beta_M^S}, \tag{1.9}$$

and zero profits imply that the equilibrium output of each variety is the same for all varieties produced in a given location i,

$$y_i^S(j) = \overline{y}_i^S = F(\sigma - 1). \tag{1.10}$$

Using equations (1.9) and (1.10), the revenue $x_i^S(j) = p_i^S(j) y_i^S(j)$ of a variety j in location i can be written as,

$$p_i^S(j) y_i^S(j) = x_i^S(j) = \overline{x}_i^S = \sigma w_{iS}^{\beta_L^S} Q_i^{\beta_L^S} r_i^{\beta_M^S} F. \tag{1.11}$$

In addition, the common equilibrium wage bill for each variety j in location i is,

$$w_{iS} l_{iS}(j) = x_i^S \bar{l}_{iS} = \beta_L^S \overline{x}_i^S, \tag{1.12}$$

with $l_{iS}(j) = \bar{l}_{iS}$ is workplace employment for variety j in location i. Aggregating across varieties within a location i, the aggregate revenue is,

$$X_i^S = \mathcal{M}_{iS} \overline{x}_i^S, \tag{1.13}$$

and profit maximization combined with zero profits implies that labor payment, housing payment, and machinery payment are constant shares of revenue,

$$w_{iS} L_{iS} = \beta_L^S X_i^S, \quad Q_i H_{iS} = \beta_H^S X_i^S, \quad r_i M_{iS} = \beta_M^S X_i^S, \tag{1.14}$$

with X_i^S the aggregate revenue of sector S in location i, L_{iS} the labor supply of sector S in location i, H_{iS} the commercial housing of sector S in location i, M_{iS} the machinery capital of sector S in location i, w_{iS} the non-tradable service wages in location i, Q_i the rent in location i, and r_i the price of machinery capital.
Therefore, payments for commercial housing in the non-tradable services sector can be

expressed with the sector-specific workplace income,

$$Q_i H_{iT}^S = \frac{\beta_H^S}{\beta_L^S} w_{iS} L_{iS}. \tag{1.15}$$

Using aggregate revenue equation (1.13) and labor payment equation (1.14), the total of varieties of non-tradable services in a location i is,

$$\mathcal{M}_{iS} = \frac{w_{iS} L_{iS}}{\beta_L^S \overline{x}_i^S}. \tag{1.16}$$

Finally, using CES preference properties, the price index of non-tradable services in a location n can be rewritten as,

$$P_n^S = p_n^S \Big(\mathcal{M}_{iS} \Big)^{\frac{1}{(1-\sigma)}}. \tag{1.17}$$

IV.3 Tradable sector

IV.3.1 Production

The tradable sector follows an Armingtonian model. In each location, firms produce traded goods using labor, machinery capital and commercial housing with a constant return to scale Cobb-Douglas technology under perfect competition. Using firm profit maximization and zero profits condition at equilibrium, the "free on board" price of tradable goods produced in location i can be expressed as,

$$p_i^T = w_{iT}^{\beta_L^T} Q_i^{\beta_H^T} r_i^{\beta_M^T}, \tag{1.18}$$

where w_{iT} represents wages of tradable sector in location i, Q_i represents the rent in location i, and r_i the price of machinery capital in location i. In addition, it also implies that payment of housing is a constant share of labor payments (as in the non-tradable services sector),

$$Q_i H_{iT}^L = \frac{\beta_H^T}{\beta_L^T} w_{iT} L_{iT}. \tag{1.19}$$

Tradable goods shipped from a location i to a location n are subject to iceberg trade costs $d_{ni}^T \geq 1$. Hence, the cost inclusive of freight can be expressed as,

$$p_{ni}^T = d_{ni}^T p_i^T, \tag{1.20}$$

and the price index of tradable goods can be rewritten as,

$$P_n^T = \Big[\sum_{i \in \mathbb{J}} (d_{ni}^T p_i^T)^{1-\sigma} \Big]^{\frac{1}{1-\sigma}}. \tag{1.21}$$

IV.3.2 Armingtonian model of trade

Combining this Armington model with properties of CES preferences, gravity equation for bilateral trade in goods between locations n and i can be written as,

$$\pi_{ni} = \frac{\left(d_{ni}^T p_i^T\right)^{1-\sigma}}{\sum_{k \in \mathbb{J}} \left(d_{nk}^T p_k^T\right)^{1-\sigma}}, \tag{1.22}$$

where π_{ni} is the share of expenditure from location n on goods produced in location i, and $1-\sigma$ is the elasticity of substitution between the tradable goods produced by each location.

IV.4 Housing market

I assume that housing is owned by landlords. They receive payments from residential and commercial housing consumption, and they consume only consumption goods. The housing market clearing condition implies that the rateable values equal the sum of payments for residential and commercial housing,

$$\mathbb{Q}_n = Q_n H_n \tag{1.23}$$

with $\mathbb{Q}_n$ the rateable values in location n, Q_n the rent in location n, and $H_n = H_n^R + H_{nS}^L + H_{nT}^L$ the total housing demand in location n which is the sum of residential and both commercial housing demand. I follow traditional urban economics literature (Combes et al., 2021) and assume that the housing is supplied by a competitive construction sector using a Cobb-Douglas technology function of land and capital. Therefore, I obtain a constant elastic housing supply function as in Saiz (2010),

$$H_n = h Q_n^{\mu} K_n. \tag{1.24}$$

Using previous equations (1.23) and (1.24), the rateable values can be expressed as,

$$\mathbb{Q}_n = Q_n H_n = h Q_n^{1+\mu} K_n. \tag{1.25}$$

IV.5 Model Inversion

IV.5.1 Step 1: recover wages

The commuting market clearing condition can be written as follow,

$$L_{ij} = \sum_{n \in \mathbb{J}} \lambda^{R}_{nij|n} \, R_n. \tag{1.26}$$

Plugging conditional probability equation (1.5) into previous equation (1.26), the commuting market clearing condition can be expressed as,

$$L_{ij} = \sum_{n \in \mathbb{J}} \frac{\left(w_{ij}/d^{C}_{ni}\right)^{\epsilon}}{\sum_{j' \in \{S,T\}} \sum_{l} \left(w_{lj}/d^{C}_{nl}\right)^{\epsilon}} \, R_n. \tag{1.27}$$

Proposition 1 *Given the Fréchet parameter* $\{\epsilon\}$*, the observed data on sector-specific workplace employment* (L_{ij}) *and residence employment* (R_n)*, and passengers commuting costs* (d^{C}_{ni})*, there exists a unique vector of sector-specific wages (up to scale)* w_{ij} *that solve the commuters market clearing condition.*

IV.5.2 Step 2: recover prices of tradable and non-tradable

Using gravity equation (1.22), and the fact that $d^{T}_{nn} = 1$, the price index of tradable goods equation (1.21) can be rewritten as,

$$P^{T}_{n} = \left(\frac{1}{\pi_{nn}}\right)^{\frac{1}{1-\sigma}} \left(w^{\beta^{T}_{L}}_{nT} Q^{\beta^{T}_{H}}_{n} r^{\beta^{T}_{M}}_{n}\right). \tag{1.28}$$

I make the assumption that machinery capital is freely traded in the city, and normalize the price of the machinery capital $r_{i,t} = 1$ for all workplace l.[23] Hence, it is possible to recover price P^{T}_{n} by combining recovered wages of tradable goods sector w_{nT}, observed rent Q_n, domestic trade share π_{nn}, and parameters $\{\sigma, \beta^{T}_{L}, \beta^{T}_{H}, \beta^{T}_{M}\}$.
Using total varieties equation (1.16), and equilibrium variety prices equation (1.9), the

[23] According to the industrial survey of 1872, machinery capital was provided by the public authorities of Paris. They offered industrial enterprises the option to rent motorized resources. Hence, this assumption seems plausible.

price index of non-tradable services equation (1.17) can be rewritten as,

$$P_n^S = p_n^S \left(\frac{w_{nS} L_{nS}}{\beta_L^S \overline{x}_n^S} \right)^{\frac{1}{1-\sigma}}. \tag{1.29}$$

Similarly, it is possible to recover price P_n^S by combining recovered wages of non-tradable services sector w_{nS}, observed rent Q_n, the number of workers in non-tradable services sector L_{nS}, the revenue $\overline{x}_n^S$, and parameters $\{\sigma, \beta_L^S\}$.

IV.5.3 Step 3: recover amenities

Using the residential probability equation (A.2) combined with the population mobility equation (1.7), it is possible to recover (up-to-scale) amenities vector,

$$B_n = \left[\frac{\lambda_n^R \left((P_n^T)^{\alpha^T} (P_n^S)^{\alpha^S} Q_n^{1-\alpha^T-\alpha^S} \right)^{\epsilon}}{\sum_{j'} \sum_l \left(w_{lj'} / d_{nl}^C \right)^{\epsilon}} \right]^{1/\epsilon}, \tag{1.30}$$

where the denominator represents the commuter market access of the worker, and the numerator is composed of the residential choices weighted by the living cost in residence n. For a given market access and living cost, a location n with a higher number of residents implies a higher level of amenities.[24]

IV.5.4 Step 4: recover rateable values

I use the housing market clearing in order to recover rateable values,

$$\mathbb{Q}_n = Q_n H_n = Q_n \big(H_n^R + H_n^L \big), \tag{1.31}$$

with $\mathbb{Q}_n$ the rateable values in location n, Q_n the rent in location n, H_n^R the residential housing demand in location n, and H_n^L the total commercial housing demand in location n.

Static Spatial Equilibrium Definition: *Given the economic parameters calibration, and a commuting and freight costs parametrization* $\{d_{ni}^C, d_{ni}^T\}$*, a static spatial equilibrium is defined with a set of observed vectors* $\{R_n, L_{iS}, L_{iT}, Q_n\}$*, and a set of unobserved vectors*

[24] Note that any constant scalar such as $\overline{U}$ does not appear in this specification since I divide amenities vector B_n by its geometric mean.

$\{w_{iS}, w_{iT}, B_n, P_n^S, P_n^T, \mathbb{Q}_n\}$ such that: i) labor markets clear (1.27); ii) sector-specific firms markets clear (1.28), (1.29); iii) population mobility is satisfied (1.30) ; and iv) housing markets clear (1.31).

IV.6 Model Quantification

This subsection presents the calibration and estimation of structural parameters in order to rationalize observed data (see Table A.16 in appendix for an overview of model quantification).

IV.6.1 Estimation

Housing supply elasticity I estimate housing supply elasticity μ by using observed data on rateable values $\mathbb{Q}_n$ and housing units H_n in 1861 and 1896. To do so, I rewrite equation 1.24 by using rateable values equation 1.25 to get,

$$H_n = h \left(\frac{\mathbb{Q}_n}{h \, K_n} \right)^{\tilde{\mu}} K_n, \tag{1.32}$$

with $\tilde{\mu} \equiv \frac{1}{1+\mu}$. By taking the log difference between both periods of housing supply equation (1.24), I can estimate $\tilde{\mu}$ through a long-difference OLS model,

$$ln \, \widehat{H}_n = \mu_0 + \tilde{\mu} \, ln \, \widehat{\mathbb{Q}}_n + \nu_n, \tag{1.33}$$

with $\widehat{H}_n$ the change of housing stock between 1861 and 1896 in location n, μ_0 a constant, $\tilde{\mu}$ the transformed housing supply elasticity, $\widehat{\mathbb{Q}}_n$ the change of rateable values between 1861 and 1896 in location n, and ν_n an error term.

Table 1.5 shows the different estimations of transformed housing supply elasticity $\tilde{\mu}$, and the housing supply elasticity μ. Baseline specification in column (1) estimates a housing supply elasticity μ of 0.786. While the estimated elasticity is relatively low compared to the literature, this result goes in line with other factors such as Haussmann renovations influencing the housing stock. To address this concern, I control for the change in Haussmann renovations and the initial building share in column (2). The estimated housing supply elasticity parameter μ decreases in magnitude and reaches 0.511. Finally, columns (3) controls for distance to the city center and its interaction with Haussmann renovations, and the estimated housing supply elasticity remains stable. Moreover, estimates show that Haussmann renovations decreased the housing stock in neighborhoods close to the city center, and increased the housing stock in the periphery. These results align

with historical evidence, and suggest that housing supply was driven by an urban renewal policy instead of housing price. Therefore, I calibrate μ to 0.517 corresponding to the preferred specification in column (3).

Table 1.5
Housing supply elasticity ($\mu \equiv (1-\tilde{\mu})/\tilde{\mu}$)

	$\ln \widehat{H}_n$		
	(1)	(2)	(3)
$\ln \widehat{\mathbb{Q}}_n$	0.560***	0.645***	0.659***
	(0.173)	(0.103)	(0.098)
Haussmann renovations		0.089	-3.46***
		(0.063)	(1.20)
Initial building share		-2.08***	-1.42***
		(0.251)	(0.280)
Log distance to city center			0.095
			(0.134)
Haussmann renovations × Log distance to city center			0.438***
			(0.149)
μ	0.786	0.551	0.517
Observations	76	76	76
R^2	0.248	0.703	0.754

Notes: Each column reports estimates from a separate regression. Regressions use 76 Parisian neighborhoods. Dependent variable is the housing units growth between 1861 and 1896. The independent variable is the rateable values growth, and its estimated coefficient corresponds to $\tilde{\mu}$. Controls are the total length of Haussmann renovations, the initial share of buildings, and the distance to city center (Notre-Dame). Heteroskedasticity-robust standard errors are in parentheses and ***, **, * indicate significance at the 1%, 5% and 10% level, respectively.

Commuting cost Assuming a semi-elasticity functional form for passengers commuting costs ($d_{ni}^C = e^{\tau\, t_{ni}^C}$), and summing equation (1.4) across sectors, it is possible to estimate the commuting cost parameter by taking its logarithm,

$$ln(\lambda_{ni}) = \zeta_n + \delta_i - \epsilon\ \tau\ t_{ni}^C + \xi_{ni}, \tag{1.34}$$

where λ_{ni} is the commuting flows of workers between residence n and workplace i, ζ_n and δ_i are origin and destination fixed effects, t_{ni} the commuting time between location n and location i, and ξ_{ni} an error term.

Because I do not observe λ_{ni}, I make the assumption that τ is common to all transportation modes, and I use 1895 bilateral flows of passengers between train stations in order to quantify the commuting cost elasticity,

$$ln(\text{Passengers}_{od}^{PC}) = \zeta_o + \delta_d - \tau\ t_{od}^{PC} + \xi_{od}, \tag{1.35}$$

where $\text{Passengers}_{od}^{PC}$ is the number of passengers commuting from station o to d, ζ_o is an

origin station fixed-effect, δ_d is a destination station fixed-effect, t_{od}^{PC} is the commuting time between origin and destination stations, and ξ_{od} an error term. I estimate previous equation (1.35) by using OLS estimator and find an associated coefficient to the commuting cost elasticity of 0.0204. While the estimated coefficient is relatively large compared to the literature (see Ahlfeldt et al. (2015) for an example), I test for more alternative specifications in appendix A.7.2 and find similar magnitudes. To provide evidence on the fit of the semi-elasticity functional form of commuting cost, I regress both the log bilateral passengers and travel times on origin and destination stations fixed effects and plot the correlation between residuals of both regressions in Figure (1.9).

Finally, I assume a similar function form for freight commuting costs ($d_{ni}^{T} = e^{\kappa\, t_{ni}^{T}}$) and calibrate $\kappa = \frac{\tau}{3} = 0.0068$ since Monte et al. (2018) find that freight commuting is three times less costly than passengers commuting.

Figure 1.9

Commuting time and 1895 bilateral flows of passengers between PC train stations

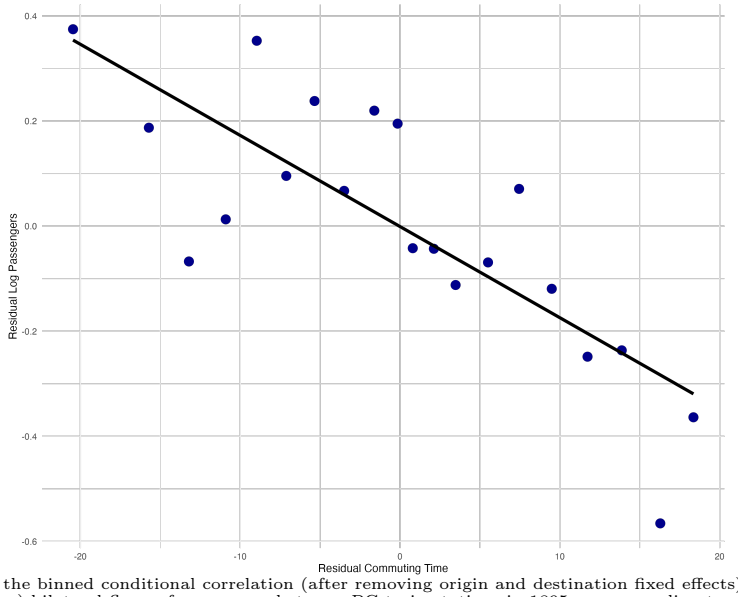

Notes: This figure displays the binned conditional correlation (after removing origin and destination fixed effects) between bilateral commuting time and the (log) bilateral flows of passengers between PC train stations in 1895, corresponding to equation 1.35.

IV.6.2 Calibration

Share of factors in the production function For the tradable goods sector, I use the same values as in Heblich et al. (2020) which focuses on the London context within the same period. First, the share of machinery capital β_M^T within the production function is calibrated to 0.2. According to the industrial survey of 1872 and *Annuaires statistiques de la ville de Paris*, the use of machinery capital in the production function of firms was common at this period. Second, the share of floorspace β_H^T used in the production function is calibrated to 0.2. Finally, using the assumption of production function under constant

return to scale, I derive the share of workers β_L^T used in the production function in the production of 0.6.

For the non-tradable services sector, I use the industrial survey of 1872 to adjust previous values. I find that the share of floorspace β_H^S in services production function is 33% higher than β_H^T, which gives 0.266. I set the share of machinery β_M^S in services production function to 0.2, and finally derive the share of labor β_L^S in services production function to 0.534.

Workers preferences I also calibrate several values based on Heblich et al. (2020) which applies for the London context. First, the Fréchet shape parameter ϵ is set to 5.25. Second, I calibrate the share of housing consumption α_H to 0.25, the share of services consumption α_S to 0.5, and the share of tradable consumption α_T to 0.25. Finally, I calibrate the parameter of elasticity of substitution σ to 4.5 which represents a standard value in the literature.

IV.7 Spatial Equilibrium

IV.7.1 Model fit and spatial distribution of fundamentals

The model's fit can be assessed through the floorspace market since I observe the total of occupied housing units by residents in 1891. Figure A.31 is a binned scatter plot comparing the model estimated floorspace demand (H_n) with the observed occupied housing units in 1891. The model on average fits the observed data very well, with the slope of the linear regression close to the 45-degree line, and a really high R-squared.

Regarding the recovered spatial equilibrium, Figure A.32(a) displays the spatial distribution of amenities in 1896, and it appears that locations with greater amenities are located in the west of Paris.

IV.7.2 Wages

The estimated sector-specific wages aim to identify the most attractive locations for workers, considering the transport network. Analysing them provides insights for the evolving spatial equilibrium of workers and the desirable workplace locations.

In Figure A.33, the relationship between sector-specific wages and distance to the city center in 1861 and 1896 shows a significant transition. In 1861, the city exhibits a more monocentric pattern where individuals tend to commute to the city center for work.

In this context, distance to the city center explains 92% of tradable sector wages variation and 97% of non-tradable sector wages variation within the city. Conversely, this relationship is less pronounced in 1896. It becomes more flattened, with distance to the city center explaining less of sector-specific wages variation across neighborhoods. This suggests a diminished attractiveness of the city center as a workplace location.

IV.8 Amenities agglomerations forces

As in Heblich et al. (2020), I allow agglomeration forces by letting amenities be function of two components: (i) exogenous residential ($b_{n,t}$) fundamental, and (ii) endogenous residential externalities,

$$B_{n,t} = b_{n,t} \left(\frac{R_{n,t}}{K_n} \right)^{\eta^R} \tag{1.36}$$

where endogenous residential externalities depend on neighborhood's own residence employment density weighted by a constant elasticity (η^R) parameter. I do not consider surrounding activities in order to model externalities due to the fact that I only observe 80 neighborhoods, and they are sufficiently large areas.[25]

Taking the logarithm and the difference between 1861 and 1896 of previous equation (1.36) delivers,

$$ln\ \widehat{B}_n = \eta_0^R + \eta^R\ ln\ \widehat{R}_n + X_n\ \gamma + ln\ \widehat{b}_n \tag{1.37}$$

where η_0^R is a common shock across Parisian neighborhoods, and η^R is the residential agglomerations forces parameter. Finally, $ln\ \widehat{b}_n$ is an idiosyncratic shock representing residual variation in unobserved amenity growth. I augment this equation by adding a vector of neighborhood characteristics X_n aiming to control for changes in unobserved amenities. Therefore, the residential agglomeration forces parameter η^R is captured through variation in residence employment and amenities across Parisian neighborhoods.

Table 1.6 presents the estimation of the previous equation. Column (1) shows the simplest specification without controls, and the estimated residential agglomeration force, η^R, is higher than typical urban economics literature values. In order to address the omitted variable bias issue, column (2) controls for the change in the length of Haussmann renovations within each neighborhood during 1861-1896, which influenced economic activity distribution and housing quality (Brueckner et al., 1999). The magnitude of η^R decreases

[25] Using the same first-difference specification and a GMM estimator, I quantify the effect of surrounding activities as in Ahlfeldt et al. (2015) and find a spatial decay parameter close to 0.5. With an exponential form, this means that after 10min travel, neighborhood density no longer matters ($1 \times e^{(-0.5 \times 10)} = 0.007$).

but remains high. A remaining challenge in estimating agglomeration forces is reverse causality, where residential choices influenced by amenities can lead to an upward bias. To mitigate this concern, I leverage the quasi-experimental variation in commuting costs to estimate the strength of amenities agglomeration forces. Specifically, I use the change in residential market access, as detailed in the reduced-form section (III), as an instrumental variable for the change in residential choices in Column (3). The estimated coefficient shows that, on average, a 1% increase in residential density leads to a 0.168% increase in amenities within a neighborhood. Finally, adding an *arrondissement* fixed-effect in columns (4) and (5) restricts the source of variation but does not diminish substantially the magnitude of the coefficient associated with η^R. Overall, the estimated residential agglomeration forces fall within the range reported by Ahlfeldt et al. (2015) and Heblich et al. (2020). Therefore, I calibrate the agglomeration forces parameter that govern the endogenous residential externalities to $\eta^R = 0.168$, corresponding to the preferred specification reported coefficient in column (3).

Table 1.6
Residential agglomeration forces within Paris (1861-1896)

	$\ln \widehat{B}_n$				
	(1)	(2)	(3)	(4)	(5)
$\ln \widehat{R}_n$	0.193***	0.178***	0.168***	0.164**	0.160**
	(0.043)	(0.042)	(0.060)	(0.070)	(0.070)
Haussmann		0.020	0.022		0.018
		(0.024)	(0.024)		(0.023)
IV			Change RMA		
Arrondissement FE				✓	✓
Observations	80	80	80	80	80
R^2	0.212	0.219	0.219	0.481	0.485
F-stat, $\ln \widehat{R}_n$			161.3		

Notes: Each column reports estimates from a separate regression. Regressions use 80 Parisian neighborhoods. Dependent variable is the growth in amenities between 1861 and 1896, and the independent variable is the growth in number of residents. Instrumental variable is the growth in Residential Market Access between 1861 and 1896. Control variable Haussmann is the total length of Haussmann renovations. Two last columns control for an arrondissement FE. Heteroskedasticity-robust standard errors are in parentheses and ***, **, * indicate significance at the 1%, 5% and 10% level, respectively.

V Counterfactuals

Now that the distribution of fundamentals rationalizing the data has been recovered, it is possible to undertake a counterfactual exercise to structurally estimate the impact of PC on the spatial distribution of economic activity during the period.

While initial spatial equilibrium is solved step by step with the model inversion method, I use exact hat algebra ($\widehat{x} = x'/x$) approach popularized by Dekle et al. (2007), combined

with an iterative algorithm to compute counterfactual equilibrium (see appendix A.6.2 for derivations of equations). The process begins with an initial distribution guess on endogenous variables and subsequently updates these distributions iteratively based on the model's equilibrium conditions until convergence is reached.[26]

V.1 Experiment I: removing the *Petite Ceinture*

V.1.1 Reallocation of workers and residents, and price variation

In this experiment, I exclude the PC network from the Paris urban transport system to assess its influence on commuting choices and price index of tradable goods. This experiment is conducted while considering a scenario with agglomeration forces, elastic housing supply, and an open city setting. Figure 1.10 shows the counterfactual results at the neighborhoods level. The y-axis represents the percentage change between the counterfactual and 1896 data for (a) workplace employment, (b) residence employment, (c) price index of tradable goods, and (d) ratio between total number of workers in service versus tradable sector, while the x-axis represents the distance to the city center of Paris. As observed, the counterfactual exercise significantly influences jobs and residential dynamics with a smooth reallocation of the economic activity within the city center. By removing the PC from the transport network while keeping other transportation modes constant, locations close to the city center experience a relatively smaller decrease in residents and workers compared to locations in the periphery. Moreover, locations in the periphery experience an increase in the price of tradable goods due to higher freight costs. Note that most locations experience a decrease in workers and residents because of the outflow of Parisian workers in the open city setting. Moreover, the ratio of the total number of workers in the service sector compared to the tradable sector increases in locations close to the city center, meaning that workers in the service sector leave relatively more than those in the tradable sector. This result aligns with the estimates from the reduced-form section (III), where retail establishments are relatively more affected by the PC railroad. Overall, this experiment highlights the role of the PC in shifting economic activities toward the periphery and improving living conditions by reducing trade costs of merchandise.

[26] See Nagy (2022) for a comprehensive presentation and illustration.

Figure 1.10
Counterfactual I

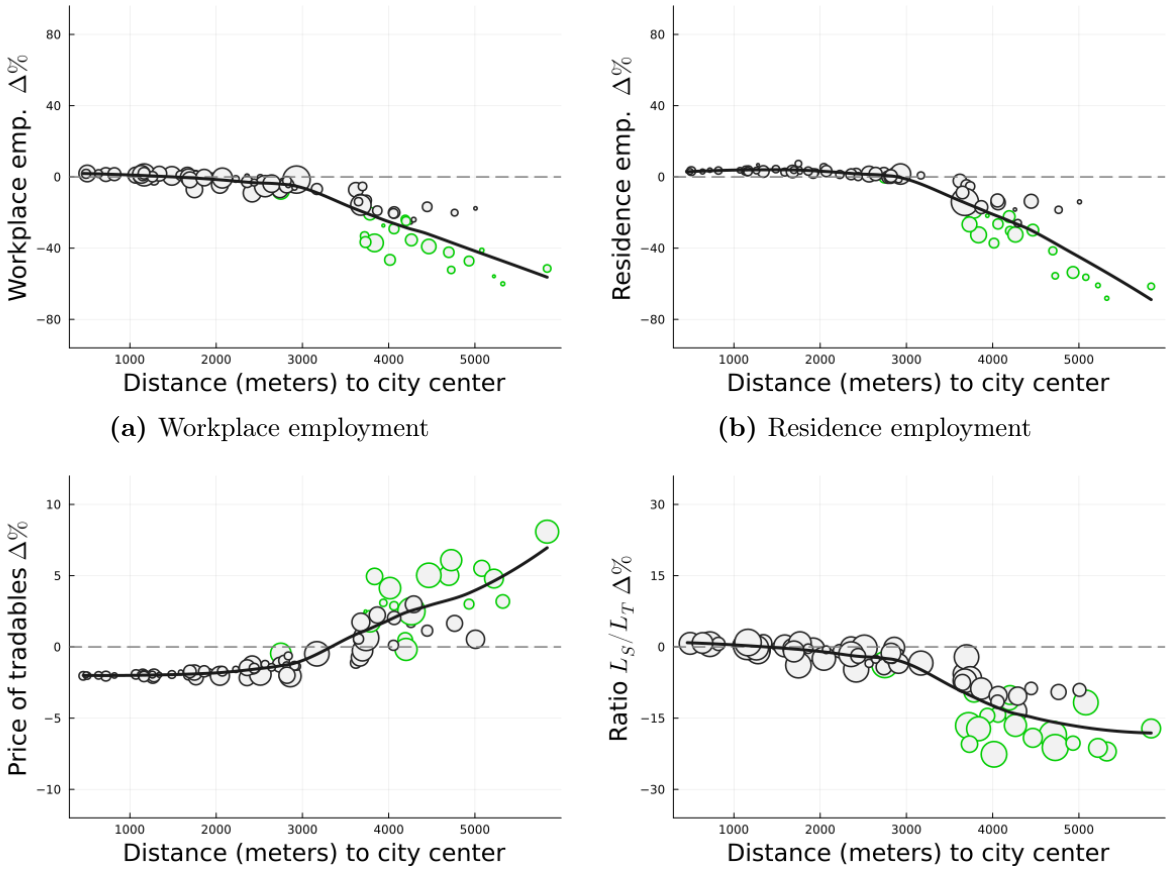

(a) Workplace employment

(b) Residence employment

(c) Tradable goods price index

(d) Ratio Service/Tradable

Notes: These figures represent the counterfactual changes regarding distance to the city center, for Panel (a) 1896 workplace employment, Panel (b) 1896 residence employment, Panel (c) price index for tradable goods, Panel (d) ratio between total number of workers in each sector. Each circle represents the percentage change between counterfactual and data of a neighborhood in 1896. Circle size reflects the observed population in initial data. Green circles represent neighborhoods that are within 600m of a train station of the *Petite Ceinture*. Black lines represent a non-linear fitted model.

V.2 Experiment II: radial railroad

While London workers benefited from the underground metro since the 1860s, Parisian workers exclusively relied on the PC for within-city commuting by railway. With the opening of the metro in 1901, PC traffic rapidly declined over time due to increased competition between both transport modes. Hence, a key question arises: would a radial railroad system, as in London, have been better for Parisian workers than the PC? The spatial equilibrium distribution of workers and residents will be impacted differently by the two transport systems, as one connects to the city center while the other does not. Despite technological constraints that might make construction unfeasible, exploring this question with a counterfactual exercise can provide some insights. To do so, I create a hypothetical radial railroad with 20 metro stations spaced on average every 1 km (similar

to the PC), consisting of 2 lines connecting the northern, southern, western, and eastern parts of Paris (see Figure 1.11 for an illustration).

Figure 1.11

An alternative network: radial railroad

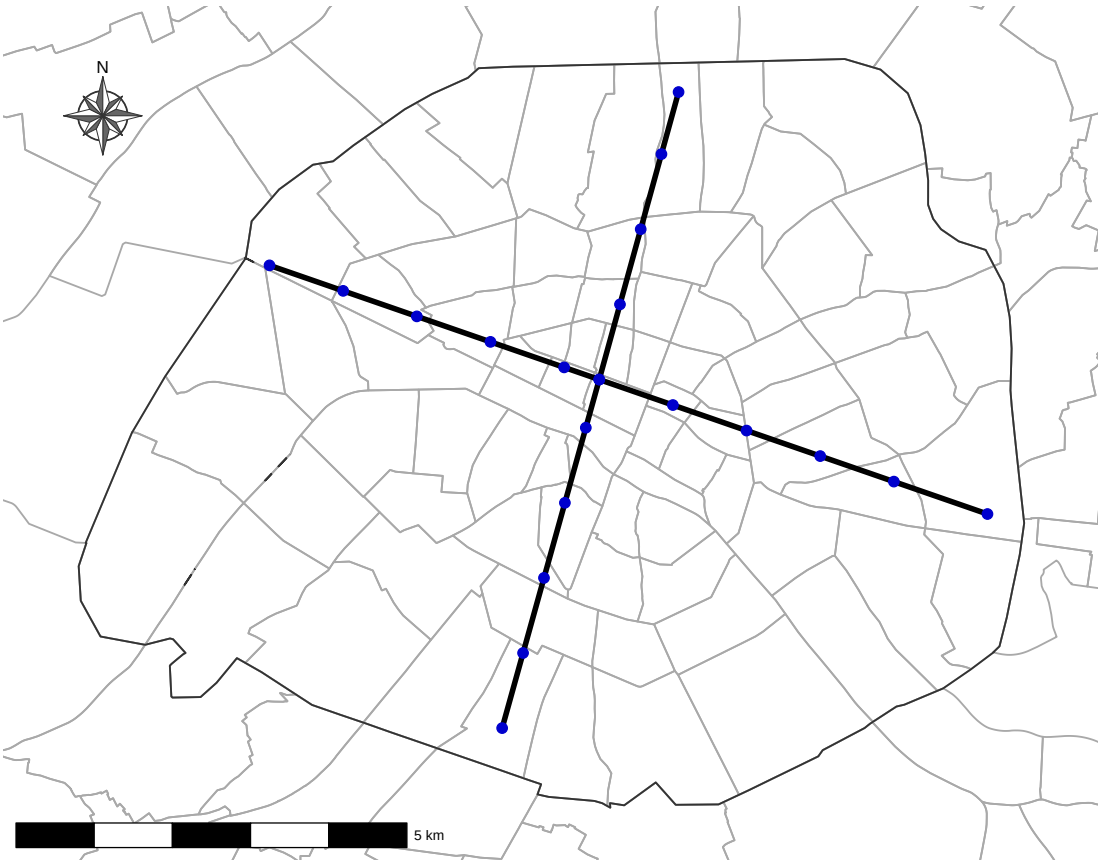

Notes: This map displays a hypothetical metro within the 80 Parisian neighborhoods. The dark line represents the metro and the blue dots 20 represent train stations.

V.2.1 Reallocation of economic activities, and price variation

In this experiment, I exclude the PC network from the Paris urban transport system and consider the radial railroad system previously presented. As before, the experiment is conducted while considering a scenario with agglomeration forces, elastic housing supply, and an open city setting. Figure 1.12 shows the counterfactual results at the neighborhoods level. The y-axis represents the percentage change between the counterfactual with the radial railroad and the counterfactual without the PC railroad, for (a) workplace employment, (b) residence employment, (c) price index of tradable goods, and (d) ratio between total number of workers in service versus tradable sector, while the x-axis represents the distance to the city center of Paris. As observed, implementing a radial railroad instead of the PC significantly affects the spatial equilibrium, with opposite effect on workers and residents reallocation with respect to distance to the city center.

On average, locations close to the city center experience a relatively higher increase in workers compared to locations in the periphery. By contrast, locations in the periphery experience a relatively higher increase in residents compared to those in the city center. Note that a small number of locations experience negative growth in residents or workers, since there is an inflow of workers from the outside economy. Moreover, this increase in total number of Parisian workers drives up the price of tradable goods in all locations. In this counterfactual, the ratio of workers in service sectors to those in tradable sectors increases in neighborhoods close to the city center, indicating a specialization of the city center in retail activities.

Figure 1.12
Counterfactual II

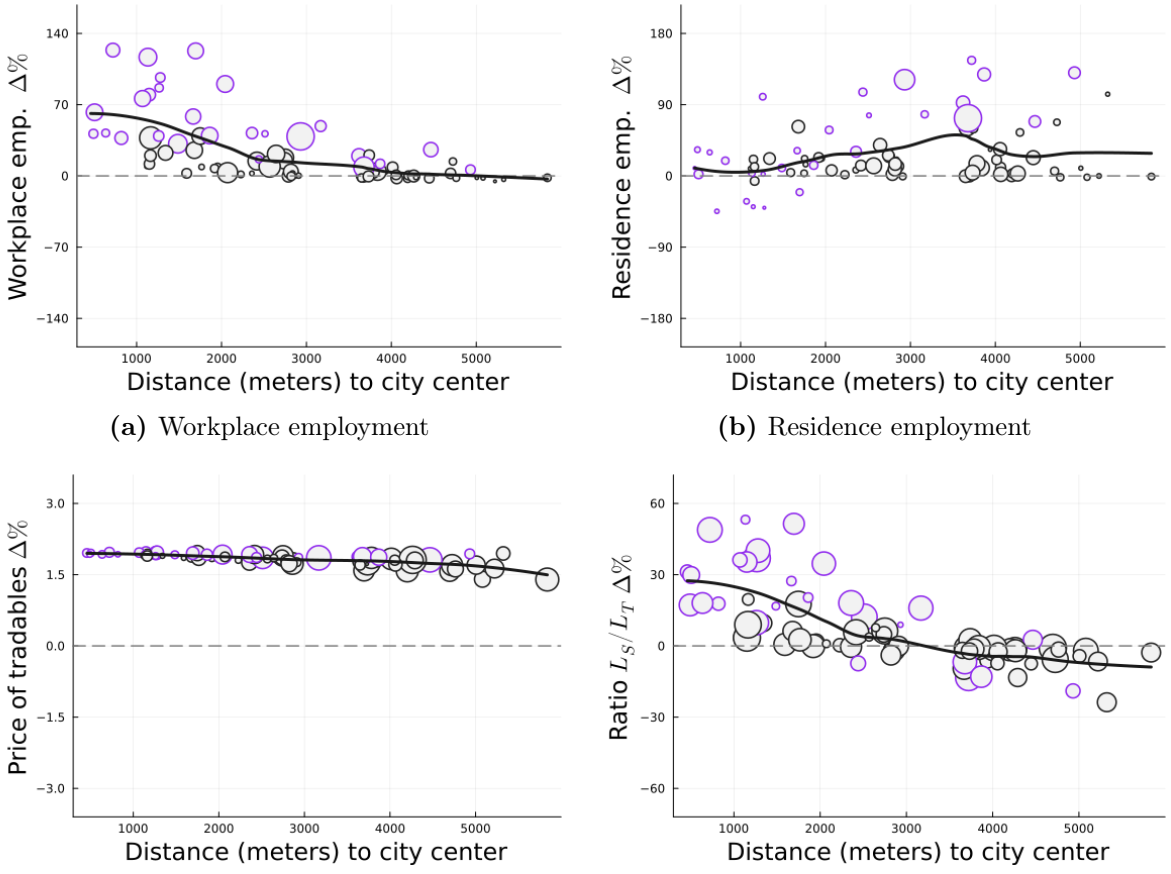

(a) Workplace employment

(b) Residence employment

(c) Tradable goods price index

(d) Ratio Service/Tradable

Notes: These figures represent the counterfactual changes regarding distance to the city center, for Panel (a) 1896 workplace employment, Panel (b) 1896 residence employment, Panel (c) price index for tradable goods, Panel (d) ratio between total number of workers in each sector. Each circle represents the percentage change between counterfactual and data of a neighborhood in 1896. Circle size reflects the observed population in initial data. Purple circles represent neighborhoods that are within 600m of a train station of the metro. Black lines represent a non-linear fitted model.

V.3 Urban transport design and aggregate implications

Previous results show that the transport design matters when explaining the uneven spatial distribution of economic activity, but are silent in terms of specialization as residence or workplace, aggregate implications on the historical city center, and welfare effects.

Specialization To investigate the effect of urban transport design on the specialization of locations, I compute the ratio of workers to residents for both counterfactual scenarios (without the PC railroad, and with a radial railroad) in open city setting, without elastic housing supply and agglomeration forces. I also compute the ratio of workers to residents for the observed 1896 data, which corresponds to the scenario with the PC railroad. Panel (a) of Figure 1.13 shows the growth of this ratio for both the radial railroad (in red) and PC railroad scenarios (in black), relative to the counterfactual without the PC railroad. It can be clearly seen that both transport designs have totally different impacts on the specialization of neighborhoods. The PC railroad has a small effect, while the radial railroad creates an increase in the ratio of workers to residents in neighborhoods close to the city center and a decrease in locations close to the periphery. Moreover, this specialization could create different commuting patterns. Panel (b) of Figure 1.13 shows the cumulative distribution of commuting distances in the initial equilibrium, and both counterfactual scenarios: without the PC railroad, and with a radial railroad. By sorting each residence-workplace pairs based on the distance and plotting the cumulative share of commuters, it aims to show how much workers commute less than each distance. In the equilibrium without the PC railroad, around 20% of workers work in their place of residence, and more than 50% of Parisian workers commute less than 1.5 km. Compared to the equilibrium without the PC railroad, both urban transport designs create disconnections between workplace and residence, but in different ways. While the PC railroad slightly decreases the share of commuters working in their place of residence and increases long-distance commuting, the radial railroad significantly decreases the share of commuters working in their place of residence and also increases long-distance commuting. Hence, urban transport design seems to have consequences on the city structure and commuting patterns, and these results are in line with Heblich et al. (2020), which documented a workplace and residence separation following railroad implementation in the London context.

Historical city center The effect of removing the PC railroad on aggregate population in the historical city center depends on whether the city setting is closed or open. Figure

Figure 1.13
Counterfactuals: specialization and commuting patterns

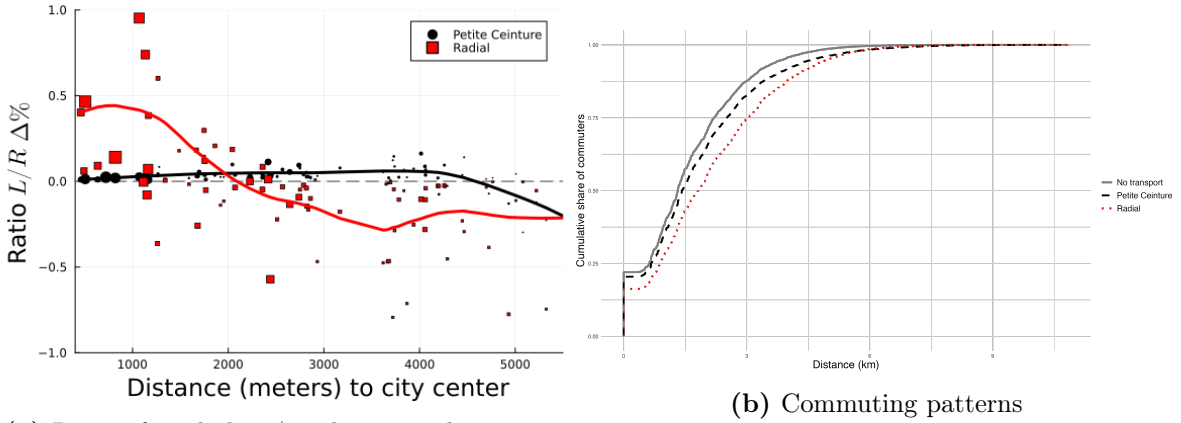

(a) Ratio of workplace/residence employment

(b) Commuting patterns

Notes: This figure displays the consequence of urban transport design on Panel (a): ratio of workplace/residence employments; Panel (b) commuting patterns. The growth of workplace/employment ratio in Panel (a) is computed through an initial scenario without the PC. Commuting patterns in Panel (b) are computed by sorting each residence-workplace pair based on the euclidean distance, and by plotting the cumulative share of commuters.

1.14 displays the counterfactual population in 1896 when removing the PC railroad, as well as the observed population trends between 1801 and 1896 (as in Figure 1.2) by historical city center and periphery. In a closed city setting illustrated in Figure 1.14(a), removing the PC railroad increases the population living in the historical city center by 15.06% corresponding to 48,137 additional residents. Therefore, the PC railroad could have accelerated the outmigration patterns from the city center depicted. However, in an open city setting illustrated in Figure 1.14(b), these effects are mitigated by the outflow of Parisian workers, resulting in an increase in the population living in the historical city center by 3.72% corresponding to 11,895 additional residents. Nevertheless, the aggregate impact of the PC railroad on residential choices (taking into account the total population level) is an increase of 1.9 percentage points.

Welfare measures The relationship between urban transport design and welfare is unclear and needs to be investigated. While the PC railroad is longer (32 km) due to its circular shape and was built at a low cost, the considered metro is shorter (18 km) but requires expropriation and underground digging. To take into account these construction costs differences, I use Henry George Theorem (George, 1879) to measure welfare effects in open city setting and consider the following economic impact factor,

$$\text{Economic Impact}_m = \frac{\sum_{n \in \mathbb{J}} (\Delta \mathbb{Q}_n)}{r} \times \frac{1}{\text{Cost}_m}, \tag{1.38}$$

Figure 1.14
Counterfactual population in Paris: 1st-4th vs. 5th-20th *arrondissements*

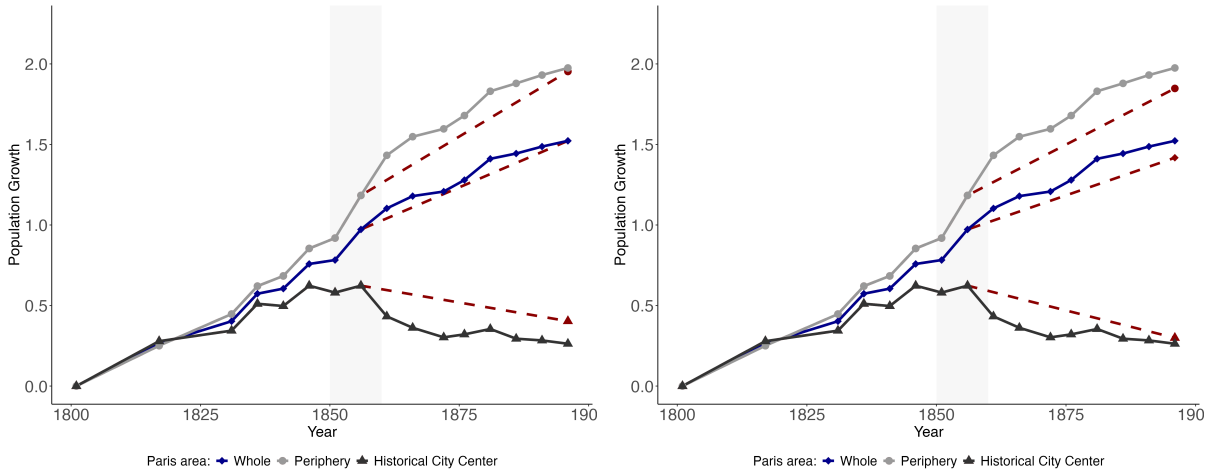

(a) Counterfactual I: closed **(b)** Counterfactual I: open

Notes: This figure displays the population evolution of Paris during the 1801-1906 period, and its counterfactual result. Panel (a) shows the counterfactual result in a closed city setting, and Panel (b) in open city setting. Blue squares represent the total population, black triangles represent the historical city center including 1st-4th *arrondissements*, and light grey dots represent the old periphery including 5th-20th *arrondissements* (see Figure A.36 for boundaries). Dashed red lines represent the counterfactual population evolution for the whole Paris, the historical city center, and the historical periphery.

where $\sum_{n\in\mathbb{J}}(\Delta\mathbb{Q}_n) \equiv \sum_{n\in\mathbb{J}}(\mathbb{Q}'_n - \mathbb{Q}_n)$ is the variation of the total rateable values within the city after the urban transport infrastructure implementation, and Cost_m the total cost of construction of the infrastructure m. Following Heblich et al. (2020), I compute the net present value of changes in rateable values considering an infinite lifetime and a discount rate r calibrated to 5%. This classical approach to value public goods using land values allows to compare directly the economic gains with the economic costs. To calibrate correctly Cost_m, I estimate PC construction costs using authorized capital per km for the company that built the *PCRG* line, and I use measures from Heblich et al. (2020) to estimate metro construction costs. Moreover, using commuting choices probability equation (1.6) and expected utility of workers equation (1.4), I rewrite the welfare change in hat expression as follow,

$$\widehat{\overline{U}} = \frac{\widehat{B}_n \; \widehat{w}_{nj} \; \widehat{\lambda}_{nnj}^{-1/\epsilon}}{(\widehat{P}_n^T)^{\alpha^T} \; (\widehat{P}_n^S)^{\alpha^S} \; \widehat{Q}_n^{1-\alpha^T-\alpha^S}}, \tag{1.39}$$

with $\widehat{\lambda}_{nnj}$ being the change in non-commuting probability in sector j. For any location n within the city, a positive (or negative) change in sector-specific wages ($\widehat{w}_{nj}$) or amenities ($\widehat{B}_n$), need to be compensated by a positive (or negative) change in living costs ($(\widehat{P}_n^T)^{\alpha^T}$, $(\widehat{P}_n^S)^{\alpha^S}$, $\widehat{Q}_n^{1-\alpha^T-\alpha^S}$) or non-commuting probability ($\widehat{\lambda}_{nnj}$) in order to expected utility con-

dition holds. Taking the geometric mean on both sides yields to,

$$\widehat{\overline{U}} = \frac{\widehat{\overline{B}}_n \, \widehat{\overline{w}}_{nj} \, \widehat{\overline{\lambda}}_{Nj}^{-1/\epsilon}}{(\widehat{\overline{P}}_n^T)^{\alpha^T} \, (\widehat{\overline{P}}_n^S)^{\alpha^S} \, \widehat{\overline{Q}}_n^{1-\alpha^T-\alpha^S}}, \tag{1.40}$$

allowing the decomposition of the average welfare change into several components.

Table 1.7 shows the aggregate change in expected utility of workers in both closed and open city settings, decomposing it into amenities, rent and the price of tradables, and shows the economic impact in open city setting. The different scenario varying the transport shape within Paris are: columns (1) and (4) no railroad; columns (2) and (5) a radial railroad system; and column (3) and (6) a radial metro complemented with the PC.

First counterfactual shows that removing the PC railroad decreases the average utility of workers by 1.82% in closed city setting, and by 1.98% in open city setting. These values suggest that removing the PC railroad creates moderate welfare losses. But this does not take into account the relatively low cost of the infrastructure. Column (4) in open city setting shows that removing the PC railroad decreases the total population and the total rateable values respectively by 10% and 10.1%. Moreover, the impact factor of 17.09 suggests that the land value gains largely outweigh the costs. Decomposing the average welfare change provides a clear understanding of the differences in welfare loss between closed and open city settings. In the closed city setting, removing the PC railroad increases commuting and freight costs, resulting in an increase in the average price of tradables and a decrease in average amenities and rent. In the open city setting, removing the PC railroad increases commuting and freight costs and leads to an outflow of Parisian workers. While rent decreases due to reduced pressure on the housing market and the price of tradables decreases due to lower demand, these benefits are offset by lower average amenities within the city due to the worker outflow. Therefore, the welfare loss is magnified in the open city setting.

Second counterfactual shows that implementing a radial railroad instead of the PC railroad increases the average utility of workers by 2.84% in closed city setting, and by 3.15% in open city setting. These values suggest that the radial railroad is more efficient in increasing worker welfare compared to the PC railroad. However, both infrastructures do not share the same construction costs, with the radial metro being significantly more costly. Column (5) shows that the radial railroad increases the total population and total rateable values by 30.7% and 34.2%, respectively. The impact factor of 23.36 is high and aligns with the findings of Heblich et al. (2020), which examined the London

railway network. Overall, this suggests that, in this Parisian context and considering the construction costs, the radial railroad system appears to be roughly 1.37 times more efficient than the PC railroad. Decomposing the average welfare change suggests no change in the price of tradables and a decrease in rent in the closed city setting. In contrast, in the open city setting, there is a strong increase in both rent and the price of tradables. This increase is due to an inflow of workers from the outside economy, creating pressure on the housing and tradables markets. However, these increases are offset by the increase in average amenities within the city.

Third counterfactual shows that implementing both urban infrastructures at the same time increases the average utility of workers by 4.39% in closed city setting, and by 4.9% in open city setting. These values suggest that implementing these infrastructures simultaneously yields additional gains. However, these gains suggest the non-linearity of the relationship between commuting costs and welfare, as they do not simply add up to the sum of the separate counterfactual welfare gains ($1.82 + 2.84 > 4.39$ in closed city setting, and $1.98 + 3.15 > 4.9$ in open city setting). Column (6) shows that implementing both urban infrastructures increases the total population and total rateable values by 42.7% and 46.9%, respectively. Here, the gains in rateable values are greater than the sum of the separate counterfactual gains, suggesting additional gains for landlords and complementarity between both infrastructures. While the impact factor of 22.11 is relatively high, it is slightly lower than the impact factor considering radial metro alone. Decomposing the average welfare change suggests a negative change in amenities, the price of tradables, and rent in the closed city setting. However, in the open city setting, there is a strong increase in the average rent due to an inflow of workers from the outside economy, along with an increase in the price of tradables. Nevertheless, this is compensated by a significant increase in amenities. This explains the striking difference in average welfare change between the closed and open city settings.

Robustness of the welfare effects with bootstrap procedure Given that the estimation of structural parameters can be subject to noise, and that calibration can be arbitrary, I implement a bootstrap procedure to evaluate the robustness of the estimated residential agglomeration forces (η^R) and the economic impact factor of the PC. For each draw, some structural parameters are randomly picked with uniform distributions.

Table 1.8 summarizes the parameters and range of random draws. First, I draw random parameters on the workers' preferences side, $\{\epsilon, \alpha_H, \alpha_T, \alpha_S\}$, based on standard values in the literature and a plausible range. Second, for the freight and commuting costs $\{\kappa, \tau\}$,

Table 1.7
Urban transport design: economic impact and complementarity evaluation

	Counterfactual Scenario					
	Closed city			Open city		
	(1) No PC	(2) Radial Metro	(3) Both	(4) No PC	(5) Radial Metro	(6) Both
Average change (Δ%)						
Workers Utility	-1.82	2.84	4.39	-1.98	3.15	4.9
Amenities	-0.41	-1.61	-1.24	-2.14	1.04	2.9
Rent	-0.74	-1.3	-0.46	-2.49	1.48	3.98
Price of Tradables	0.25	-0.0	-0.27	-0.03	0.43	0.43
Population						
Change				-252,682	700,619	976,401
Level	2,536,834	2,536,834	2,536,834	2,284,152	2,984,771	3,260,554
Rateable Value						
(million francs)				-54.39	166.19	227.7
NPV (5%)						
(million francs)				-1087.87	3323.76	4554.08
Construction Costs						
(million francs)				-63.65	142.3	205.95
Economic Impact $\left(\frac{\text{NPV}}{\text{Construction Costs}}\right)$				17.09	23.36	22.11

Notes: Each column reports a separate counterfactual result with baseline structural parameters. Columns (1) to (3) show results with a closed city setting, and columns (4) show results with an open city setting. Rateable values (RV), net present values (NPV), and construction costs are expressed in millions of francs. NPV are evaluated over an infinite lifetime, assuming 5% discount rate. Construction costs are based on authorized capital. Average change in workers utility is the growth in expected utility that a worker would derive if living/working the city. Average changes in amenities, rent, and price of tradables are the growth of in their geometric mean. Counterfactual results in RV and NPV for columns (1) and (4) are relative to the observed 1896 spatial equilibrium. Counterfactual results in RV and NPV for columns (2), (3), (5), and (6) are relative to the scenario without the PC.

the commuting costs parameter is sampled based on the range reported in Table A.17. The calibrated freight costs parameter is then derived from the draw of the commuting costs parameter and a scaling parameter varying between 2 and 5. Third, for the production side, I draw random parameters for $\{\beta_H^S, \beta_L^S, \beta_M^S, \beta_H^T, \beta_L^T, \beta_M^T\}$ based on standard values in the literature. Finally, the housing supply elasticity $\{\mu\}$ is sampled based on the range reflecting the 95% confidence interval reported in column (3) of Table 1.5.

Table 1.8
Parameters and range of random draws

Parameter	**Range**
	Workers preferences
ϵ	Uniform(3, 7)
α_H	Uniform(0.15, 0.3)
α_S	Uniform(0.3, 0.6)
α_T	$1 - \alpha_S - \alpha_H$
	Freight and Commuting costs
τ	Uniform(0.014, 0.026)
scale factor	[2, 5]
κ	(τ/scale factor)
	Production parameters
β_{L_T}	Uniform(0.5, 0.7)
β_{H_T}	Uniform(0.15, 0.25)
β_{M_T}	$1 - \beta_{L_T} - \beta_{H_T}$
β_{H_S}	$\beta_{H_T} \times 1.33$
β_{M_S}	β_{M_T}
β_{L_S}	$1 - \beta_{H_S} - \beta_{M_S}$
	Housing supply elasticity
μ	Uniform(0.175, 1.142)

After a random draw of these structural parameters, the spatial equilibrium is recalculated for each combination of $\{\epsilon, \alpha_H, \alpha_T, \alpha_S, \kappa, \tau, \beta_H^S, \beta_L^S, \beta_M^S, \beta_H^T, \beta_L^T, \beta_M^T\}$, allowing for the estimation of residential agglomeration forces parameter $\{\eta^R\}$. Then, the PC's impact factor is computed through a counterfactual experiment (removal of the PC) by using all baseline parameters and parameters randomly drawn.

I consider $10,000$ random parameter draws combined with different trade cost scaling parameter values, giving a total of $40,000$ spatial equilibrium and counterfactuals to solve. This procedure generates distributions for η^R and the PC's impact factor, enabling the assessment of their robustness. Figure 1.15 shows the distribution of both the residen-

tial agglomeration parameter in Panel (a), and the economic impact in Panel (b). Both baseline estimated values are close to the median. By doing a variance decomposition exercise, I find that the ϵ parameter governs the forces of residential agglomeration. A higher Frechet shock is associated with a lower η^R. Turning to the economic impact factor, I find that the parameters ϵ, η^R and μ explain most of its variance. (See appendix A.8 for correlation between structural parameters and both η^R and economic impact factor, and variance decomposition exercises.)

Figure 1.15
Bootstrap results

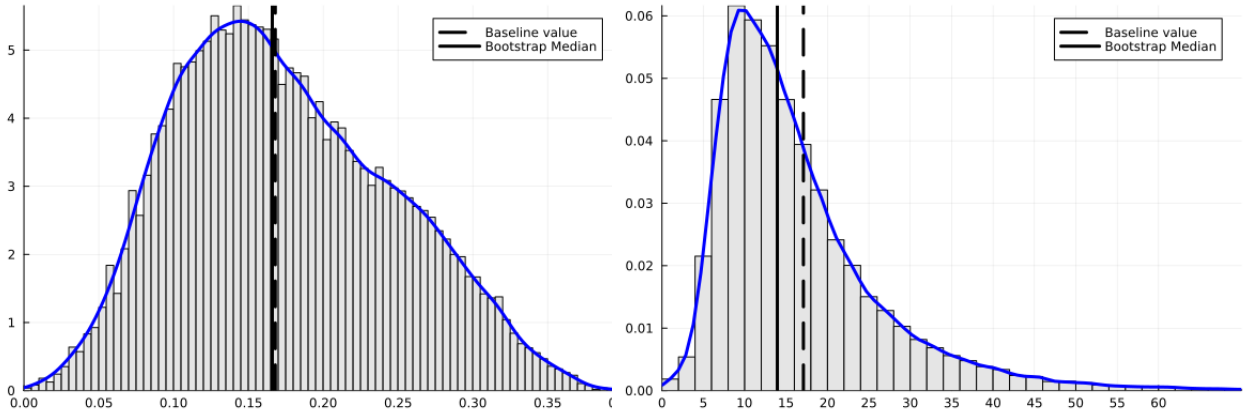

(a) Residential agglomeration forces (η^R) **(b)** Economic impact factor of the PC

Notes: These figures show the distribution of residential agglomeration forces in Panel (a), and economic impact factor of the PC removal in Panel (b), from a bootstrap procedure of 20,000 random draws of $\{\epsilon, \alpha_H, \alpha_T, \alpha_S, \kappa, \tau, \beta_H^S, \beta_L^S, \beta_M^S, \beta_H^T, \beta_L^T, \beta_M^T\}$.

Discussion The underlying assumptions for making the quantitative spatial model tractable present some limitations.

A first limitation stems from the fact that the utility of the outside economy is fixed and does not vary. However, improvements in Paris, the largest French city, could affect the entire economy as a system of cities and create divergence (Combes et al., 2025b). To make the model tractable, I assume that localized changes in transport costs should have little effect on the outside economy.

A second limitation arises because the within-city quantitative spatial model does not allow for an area extensive margin as in the monocentric model.[27] Due to data scarcity on workplace employment, I am unable to include the suburban municipalities. However, as shown in Figure A.29 (described in Appendix A.4.5), Paris experienced a smaller

[27] Within a QSM, a null workplace and residence employment ($L_i = R_n = 0$) implies null fundamentals, and no possibility to extend the city.

extensive margin compared to London. By comparing neighborhood population growth during the 1861-1901 period with respect to distance from the city center, Paris exhibited a discontinuity beyond $5,800$ meters (corresponding to the maximum distance of Paris's peripheral neighborhoods), with suburban cities growing at significantly lower rates than peripheral Parisian neighborhoods. This result highlights a potential barrier effect of the PC separating Paris from its suburbs, and slowing down area extensive margin of the city.

VI Conclusion

This paper employs a novel database of 19th-century Greater Paris to describe the dynamics of residential and job growth. It also provides evidence of the first circular railroad effect, specifically the *Petite Ceinture*, on both short-term and long-term spatial equilibrium.

First, I find substantial effects of the *Petite Ceinture* on firms and population growth. I develop and estimate a simple quantitative spatial model that incorporates tradable goods and non-tradable services to assess the aggregate impact of the *Petite Ceinture* on the economic activity. First counterfactual exercise suggests a significant impact of the *Petite Ceinture* on outmigration from the city center. In terms of welfare gains, this circular system has a relatively low effect on the rateable values compared to the radial railroad, but this is compensated by a low costs of construction. Second counterfactual exercise provides evidence that a radial metro system would have led to a separation between workplace and residence, and would have been more efficient. Nevertheless, including both types of transport systems allows for additional welfare gains measured by the rateable values.

Second, long-term differences over the period from 1906 to 1954 highlight that the *Petite Ceinture* had an impact on population growth, even though it initially experienced a decline in traffic due to competition from the metro at the beginning of the period. More precisely, neighborhoods close to *Petite Ceinture* train stations that had intense traffic experienced more population growth than other neighborhoods. These key findings on historical urban transport shed light on the long-term impact of temporary shocks. They are crucial and need to be considered in current transport planning.

Chapter 2

Optimal Urban Transport Design in a Quantitative Spatial Model

Acknowledgements

I am particularly grateful to Clément Bosquet and Clément Gorin for their guidance and support. I benefited from conversations with Pierre-Philippe Combes, Tilman Graff, Stephan Heblich and Gabriel Kreindler. I thank participants of AFET conference for their valuable comments and suggestions. Responsibility for results, opinions and errors lies with the author alone.

I Introduction

Many cities expand their public transportation systems to address the needs of commuting to work, access to urban amenities, and reduce congestion. Over the last 25 years, 80 metro projects have been implemented or extended worldwide. However, optimal design of these massive infrastructure investments is challenging due to the wide variety of spatial decisions, location heterogeneity, inter-modality, and spatial linkages between locations (Redding and Turner, 2015; Ahlfeldt et al., 2015; Heblich et al., 2020; Tsivanidis, 2024).

In this paper, I develop a framework to identify the optimal design of urban transport infrastructure. The framework incorporates general equilibrium effects, which arise as workers reallocate toward different residence and workplace within the city in response to public policy interventions, thereby influencing the land market where workers and firms compete for housing. Additionally, it accommodates multiple transport modes, and accounts for neighborhood heterogeneity in terms of amenities, productivity, and housing supply. It also allows for production and residential agglomeration forces. Taking these elements into account is crucial to enhance the efficiency of urban transport systems.

In this framework, the planner's problem involves choosing a metro network M based on an economic objective $W(M;\theta)$, that depends on structural parameters θ. Additionally, the planner's preferences are influenced by factors beyond the economic objective, such as unobserved preferences for specific characteristics of the metro network. I model this as an

idiosyncratic shock, denoted by ι_M. Therefore, the planner faces a discrete choice problem within the space of all possible metro networks. While it is impossible to derive a unique global metro network due to the high-dimensional optimization problem, a simulated annealing algorithm is used to sample (sub)optimal metro networks.

First, I provide a numerical example of a city with random distributions of fundamentals and demonstrate how to rationalize the within-city spatial equilibrium using a canonical quantitative urban model (QUM) *à la* Ahlfeldt et al. (2015), with structural parameters calibrated to the literature. Subsequently, I apply the developed framework to compute the optimal metro design in this numerical example.

Second, I apply my methodology to address the following question: How should the Parisian metro have been planned at the beginning of the 20th century? I combine several historical data and divide the Parisian space into a $500m \times 500m$ grid to create locations and potential metro stations. In this application, a calibrated quantitative urban model (QUM) with heterogeneous workers allows to recover location type-specific amenities and productivity through the rationalization of the within-city spatial equilibrium. In the baseline scenario, I define an economic objective $W(M;\theta)$ as the gains in rateable value in open city settings, following the Henry George Theorem (George, 1879).[1] Additionally, I estimate the construction cost of the metro M based on fixed costs, the number of stations, and lines.

First, the numerical example of a city with a data generating process and a canonical QUM without agglomeration forces provides generalizable results. I find that the strategic locations of stations are driven by amenities and productivity. In addition, the station's centrality in the network is also an important determinant in the planner's choice of metro network. This result goes in line with Borusyak and Hull (2023) who emphasize that central stations are much more likely to be chosen to increase market potential.

Second, I validate these findings in my historical application on Paris using the economic objective based on rateable values gains and without considering agglomeration forces. As in the numerical simulation, I find that the strategic locations of stations are driven by centrality, productivity and low-skilled amenities (since low-skilled workers constituted the main labor force at that time). Additionally, over the sampled metro networks, the average economic impact factor is approximately 9.71, aligning with the findings of

[1] In the classical approach to valuing public goods, landlords experience the welfare gains from new transport technology through changes in the value of land and buildings (George, 1879). This methodology has also been used in Heblich et al. (2020) to evaluate the metro in London.

Heblich et al. (2020). This means that the economic benefits are 9.71 times the metro construction costs. The average number of metro stations is around 55, leading to an average distance to a metro station of approximately 913 meters.[2] The average increases in total production and population within the city are 32.0% and 23.7%, respectively. Furthermore, the average decrease in total commuting time within the city is 20.4%, with significant disparities and greater improvements in locations closer to the city center.

Then, I conduct several comparative experiments to assess the role of structural parameters and metro construction cost parameters. First, I confirm the role of productivity in determining strategic metro stations by creating a counterfactual CBD. I demonstrate that the developed framework reacts to this experiment and predicts a different urban transport design which follows the productivity shock. This is reflected in a higher proportion of strategic metro stations in the new CBD. Second, I assess the role of metro construction fixed costs (such as technology acquisition) and show that these costs determine the size of the metro network, as they create incentives for planners to amortize these large investments. The higher the fixed cost, the larger the metro network. Lastly, introducing agglomeration forces to the quantitative urban model (QUM) results in strategic stations being less concentrated in the periphery and more evenly distributed. Hence, agglomeration forces prevent the convergence toward an optimal urban transport design.

Next, I consider a budget-constrained planner that tries to build a metro system in this historical context. I calibrate the total metro budget achieved at that time, and I compare an utilitarian scenario, where the planner aims to maximize the sum of utilities for both high-skilled and low-skilled workers, with an egalitarian scenario, where the planner seeks to maximize the minimum utility of both groups. I find that the utilitarian scenario predicts relatively more strategic metro stations in the west side of Paris compared to the egalitarian scenario. Hence, it tends to favor high-skilled workers more than low-skilled workers, as high-skilled amenities are relatively more prevalent in the west of Paris than low-skilled amenities.

Finally, I define an optimal urban transport design proximity index and use it to evaluate metro projects proposed during the 19th century. The results suggest that the adopted metro design by Fulgence Bienvenüe was not intended for a specific group of workers but aimed at maximizing general welfare gains, as defined by the Henry George Theorem.

[2] The total potential area consists of 367 grid cells. Each grid cell covers $0.25km^2$, resulting in a total area of $91.75km^2$. With 55 stations, each station covers approximately $1.668km^2$. Assuming a square area per station, the side length is $\sqrt{1.668km^2} \approx 1.292km$. The diagonal of this square is $1.292km \times \sqrt{2} \approx 1.826km$, so the average distance is half the diagonal: $1.826km/2 \approx 0.913km$.

However, the Alphand-Huet metro project proposed in 1876 emerged as the best candidate among other metro projects, as it would have achieved high welfare gains with relatively low construction costs. This result aligns with Fajgelbaum et al. (2023), highlighting the role of political preferences in transport investment and inefficiency.

My work relates to two strands of literature. First, I connect to recent research in quantitative spatial models by using and extending a canonical quantitative urban model (QUM) developed by Ahlfeldt et al. (2015). Since this seminal work, a large literature has emerged to study the welfare and distributional effects of transport infrastructure improvements (Heblich et al., 2020; Severen, 2021; Allen and Arkolakis, 2022; Brinkman and Lin, 2022; Bagagli, 2023; Weiwu, 2024; Tsivanidis, 2024; Cosentino, 2025), neighborhood effects (Redding and Sturm, 2024), and forward-looking migration decisions (Desmet et al., 2018; Caliendo et al., 2019; Balboni, 2019; Allen and Donaldson, 2020; Heblich et al., 2021; Kleinman et al., 2023; Takeda and Yamagishi, 2023). These models are sufficiently rich to capture the organization of economic activity within cities with low data requirements and facilitate counterfactual analyses that take into account general equilibrium effects to quantify the welfare effects of public policies. Second, this paper aligns with the literature on the optimal design of transport networks. Recent works have studied the endogenous choice of transport infrastructure using a trade perspective (Balboni, 2019; Fajgelbaum and Schaal, 2020; Santamaria, 2020; Allen and Arkolakis, 2022). These studies provide frameworks for optimal investment in inter-city infrastructure. With the exception of Kreindler et al. (2024), who focus on the bus network in Jakarta, and Cosentino (2025), who compare circular and radial transit systems in historical settings, little has been done on the design effectiveness of urban transport infrastructure. In their paper, Kreindler et al. (2024) use a travel demand model to estimate public transport preferences (such as directness, speed, and waiting times) and provide a set of potential optimal networks under the assumption that commuting patterns are fixed. I contribute to this literature on optimal transport design by building on Kreindler et al. (2024) to provide a new framework that incorporates general equilibrium effects, as workers reallocate toward different residence and workplace following improvements in urban transport infrastructure. This framework allows for agglomeration forces and considers several transport modes. Additionally, it enables planners to set metro construction cost parameters and the minimum number of lines to be built.

The remainder of the paper is structured as follows. Section II presents a canonical quantitative urban model with homogeneous workers residing in a closed city and provides a numerical example of a city. Section III introduces a simulated annealing algorithm to de-

termine an optimal urban transport infrastructure design and discusses the findings of this numerical example. Section IV introduces the application to Paris by presenting the data and discussing the historical context, outlining and quantifying the quantitative spatial model by solving the spatial equilibrium, and presenting the findings. Section V presents an index for comparing the different historical metro network projects with the results from the simulated annealing algorithm based on various scenarios. Finally, Section VI concludes.

II Canonical Quantitative Urban Model

II.1 Model set-up

II.1.1 Workers

I consider a mass of workers living and working within a city of $\mathbb{N}$ discrete locations embedded in an economy $\mathbb{M}$. Workers choose a pair of locations $\{n, i\}$, where n is the location of residence and i is the workplace. A worker o choosing the pair of locations $\{n, i\}$ derives the following indirect utility,

$$U_{ni}(o) = \frac{B_n w_i}{d_{ni} P_n^{1-\beta} Q_n^{\beta}} \epsilon_{ni}(o), \tag{2.1}$$

where B_n represents the amenities in residence n, w_i is the wage in workplace i, and $d_{ni} = e^{\kappa t_{ni}}$ is the commuting cost, which takes an exponential functional form (following Ahlfeldt et al. (2015)). P_n is the price of the final consumption good (taken as numéraire, $P_n = 1$ for all n), and Q_n is the rent paid in location n. The worker o derives an idiosyncratic shock $\epsilon_{ni}(o)$ following a Fréchet distribution. Finally, β represents the share of income that the worker spends on housing.

Using standard properties of the Fréchet distribution (McFadden, 1974), the probability that a worker chooses to live in n and work in i is given by,

$$\lambda_{ni} = \frac{L_{ni}}{R_{\mathbb{N}}} = \frac{(B_n w_i)^{\epsilon} (d_{ni} Q_n^{\beta})^{-\epsilon}}{\sum_{k \in \mathbb{N}} \sum_{l \in \mathbb{N}} (B_k w_l)^{\epsilon} (d_{kl} Q_l^{\beta})^{-\epsilon}} = \frac{\Phi_{ni}}{\sum_{k \in \mathbb{N}} \sum_{l \in \mathbb{N}} \Phi_{kl}}, \tag{2.2}$$

where L_{ni} is the number of commuters from n to i and $R_{\mathbb{N}}$ is the total number of workers in the city. As explained in Redding (2022), the probability of commuting between locations n and i depends on location characteristics, workplace characteristics, and the bilateral cost (numerator), as well as all other residence and workplace characteristics, and bilateral

commuting costs (denominator).

By summing across workplaces, I obtain the probability that a worker lives in n,

$$\lambda_n^R = \frac{R_n}{R_{\mathbb{N}}} = \frac{\sum_{i\in\mathbb{N}} \Phi_{ni}}{\sum_{k\in\mathbb{N}}\sum_{l\in\mathbb{N}} \Phi_{kl}}, \tag{2.3}$$

and by summing across residence places, I obtain the probability that a worker works in i,

$$\lambda_i^L = \frac{L_i}{R_{\mathbb{N}}} = \frac{\sum_{n\in\mathbb{N}} \Phi_{ni}}{\sum_{k\in\mathbb{N}}\sum_{l\in\mathbb{N}} \Phi_{kl}}. \tag{2.4}$$

Finally, population mobility ensures that everyone derives the same expected utility in the city,

$$\overline{U} = \delta \left[\sum_{k\in\mathbb{N}}\sum_{l\in\mathbb{N}} \Phi_{kl}\right]^{1/\epsilon}, \tag{2.5}$$

where $\delta \equiv \Gamma\left(\frac{\epsilon-1}{\epsilon}\right)$ and $\Gamma(.)$ is the gamma function.

II.1.2 Firms

The representative firm produces the final good with a Cobb-Douglas technology under constant returns to scale,

$$Y_i = A_i \left(\frac{L_i}{\alpha}\right)^{\alpha} \left(\frac{H_i^L}{1-\alpha}\right)^{1-\alpha}, \tag{2.6}$$

where A_i represents productivity in workplace i, L_i is the total labor supply in workplace i, and H_i^L is the housing used commercially in workplace i. The share of labor in the production function is α.

The first-order conditions of the firm's profit maximization with respect to labor and housing are,

$$w_i = \alpha \frac{Y_i}{L_i}, \tag{2.7}$$

$$Q_i = (1-\alpha)\frac{Y_i}{H_i^L}. \tag{2.8}$$

II.1.3 Housing

Following Combes et al. (2021), housing is produced by developers with a Cobb-Douglas technology combining land and machinery capital. Using profit maximization, the housing

supply can be written as,

$$H_i^S = k_i \, Q_i^{\frac{(1-\mu)}{\mu}}, \tag{2.9}$$

where $k_i = (1-\mu)^{\frac{(1-\mu)}{\mu}} K_i$, and $\frac{(1-\mu)}{\mu}$ is the housing supply elasticity. Since land availability K_i is assumed to be fixed, only rent variation drives the housing supply (see appendix B.2.1 for more details).

II.1.4 Markets clearing

Commuter market clearing The commuter market clearing condition implies a gravity equation, requiring that the number of workers employed at each workplace equals the total number of residents commuting there.

Using the commuting probability equation (2.2) and the residential probability equation (2.3), it is possible to write the probability that a worker commutes from n to i, conditionally on living in location n as,

$$\lambda_{ni|n}^R = \frac{\lambda_{ni}}{\lambda_n^R} = \frac{(w_i/d_{ni})^\epsilon}{\sum_{l \in N}(w_l/d_{nl})^\epsilon}. \tag{2.10}$$

Therefore, the commuter market clearing can be expressed as,

$$L_i = \sum_{n \in N} \frac{(w_i/d_{ni})^\epsilon}{\sum_{l \in N}(w_l/d_{nl})^\epsilon} R_n. \tag{2.11}$$

Housing market clearing The housing market clearing condition implies that the housing supply, H_n^S, equals the total housing demand by residents and firms at equilibrium,

$$H_n^S = H_n^R + H_n^L = \beta \, \nu_n \, \frac{R_n}{Q_n} + \frac{1-\alpha}{\alpha} \, \frac{w_n}{Q_n} \, L_n, \tag{2.12}$$

where H_n^R and H_n^L are the residential and commercial housing demand in n, respectively, and $\nu_n \equiv \sum_{i \in N} \lambda_{ni|n}^R w_i$ is the expected income from residents living in location n. The housing demand of firms in workplace i is derived from the first-order conditions equations (2.7) and (2.8).

II.1.5 General equilibrium

In a closed-city setting with an integrated housing market, and given the structural parameters $\{\alpha, \beta, \kappa, \epsilon\}$, a spatial equilibrium is defined by a set of endogenous variables $\{R_n, L_i, Q_n, w_i, \overline{U}\}$ that rationalize the spatial distribution of fundamentals $\{B_n, A_i\}$,

housing supply $\{H_n^S\}$, commuting costs $\{d_{ni}\}$, and a calibrated total population $\{R_{\mathbb{N}}\}$.

II.1.6 Model extension

Several model extensions can be made from this canonical quantitative urban model. For example, some papers have considered different types of workers (Tsivanidis, 2024; Loumeau, 2024; Weiwu, 2024; Redding and Sturm, 2024), dynamics due to mobility friction (Warnes, 2021; Takeda and Yamagishi, 2023; Greaney et al., 2024), congestion (Herzog, 2024), trade of goods (Monte et al., 2018; Cosentino, 2025), consumption access (Miyauchi et al., 2025; Cosentino, 2025), school choices (Loumeau, 2023; Pietrabissa, 2023), and transport mode choices (Koster, 2024; Champalaune and Cosentino, 2025). These extensions of the canonical QUM à la Ahlfeldt et al. (2015) are specific to the context and the research question. Although tractable, they require additional data than the usual observation of residence employment, workplace employment, commuting time and housing.

II.2 Quantitative illustration

II.2.1 City structure

To illustrate an urban spatial equilibrium from the canonical quantitative urban model developed in section II, I present a numerical example based on a data-generating process (DGP) and calibrated parameters. The city consists of locations arranged on a 16×16 grid, with each point spaced 500 meters apart. I abstract from agglomeration forces and randomly assign residential and production fundamentals (B_n and A_i), as shown in Figure 2.1. Housing supply is assumed to be uniform across locations, with $H_n = 100$. Commuting times, t_{ni}, are based on Euclidean distances and a walking speed of 5 km/h.

II.2.2 Parametrization

I calibrate the structural parameters using central values from the literature. First, the Fréchet parameter ϵ is set to 5, within the typical range of 2 to 7 reported by Severen (2021) and Ahlfeldt et al. (2015). Second, the commuting cost elasticity κ is calibrated to 0.01, consistent with the estimate in Ahlfeldt et al. (2015). Finally, I set α and β to 0.7 and 0.25, respectively, aligning with commonly used values in the literature.

Figure 2.1
Numerical example: Spatial distribution of fundamentals

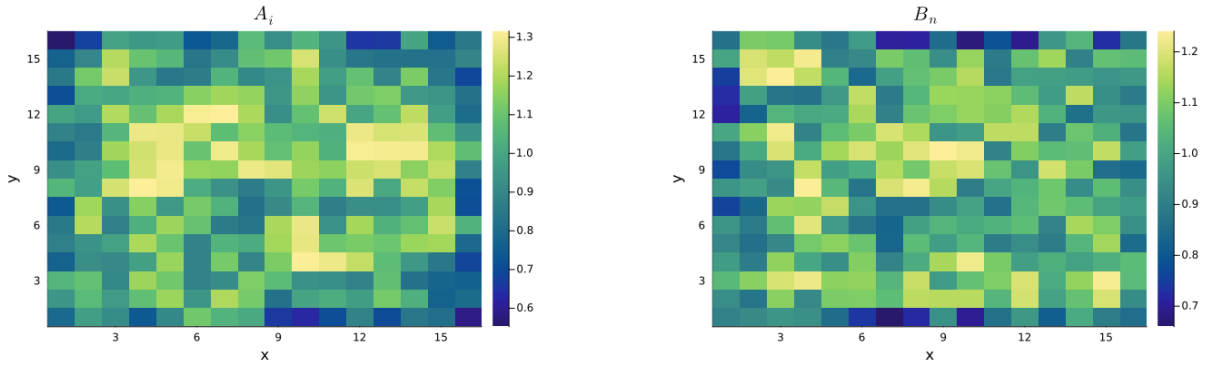

(a) Productivity **(b)** Amenities

Notes: This figure presents the distribution of fundamentals in each location following a data generating process, with Panel (a) depicting productivity and Panel (b) depicting amenities. The color intensity in each panel corresponds to the magnitude of the respective variable, with the color bar indicating the scale.

II.2.3 Initial spatial equilibrium

Figure 2.2 illustrates the initial spatial equilibrium by plotting the distribution of residence employment (R_n), workplace employment (L_i), rent (Q_n), and wage (w_i) in each location.

III Optimal Urban Transport Design

III.1 Optimization Environment

The planner chooses the metro network M consisting of L metro lines and S selected metro stations that maximizes an economic objective $W(M;\theta)$. The economic objective can take various forms (such as expected utility, total population, total rateable values, total agglomeration forces, etc.) and is context-specific.

The planner can face different constraints in the maximization process, such as network constraints (connecting the metro network to the existing network, a limit on the total number of lines, etc.) or construction constraints (metro stations cannot be implemented in some areas due to monuments, land availability, etc.).

The economic objective $W(M;\theta)$ results from a spatial equilibrium computed through a quantitative spatial model (previously developed in section II), which is a function of the metro network M and model parameters ($\theta \equiv \{\alpha, \beta, \epsilon, \mu, \kappa, A_i, B_n, H_n, R_{\mathbb{N}}\}$) capturing structural parameters and the spatial distribution of fundamentals.

Finally, the planner needs to divide the space into grid cells to create potential metro stations $\mathcal{S}$ to choose a metro network M. The more granular the space of potential

Figure 2.2
Numerical example: Initial spatial equilibrium

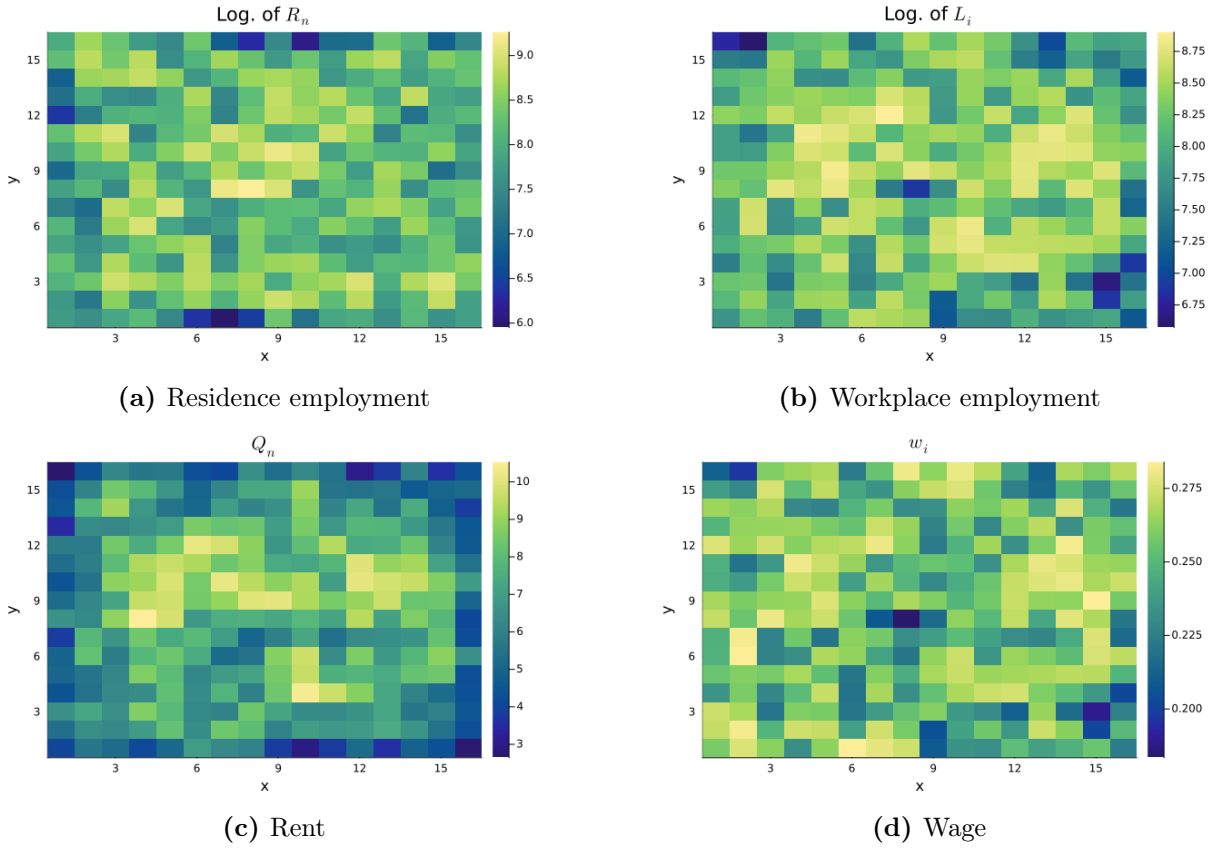

(a) Residence employment

(b) Workplace employment

(c) Rent

(d) Wage

Notes: This figure presents the initial spatial equilibrium resulting from a canonical QUM with the numerical example. Panel (a) shows the logarithm of residence employment $\log(R_n)$, illustrating the distribution of residential employment across different locations. Panel (b) depicts the logarithm of workplace employment $\log(L_i)$, showing the distribution of workplace employment. Panel (c) represents rent Q_n, indicating the spatial variation in rent levels. Panel (d) displays wages w_i, reflecting the spatial distribution of wage levels. The color intensity in each panel corresponds to the magnitude of the respective variable, with the color bar indicating the scale.

stations, the better it captures the complexity of the transport design. However, a large set of potential metro stations also implies a large solution space.

In the numerical example, I consider a planner implementing 3 metro lines without constraints on the number of stations. The planner can build a potential metro station in each location, as shown in Figure 2.3. Finally, the planner maximizes the expected utility of workers in this city, $\overline{U}$, given by equation (2.5). However, the optimization problem is discrete and high-dimensional, as highlighted by Kreindler et al. (2024), and it does not appear to have an analytical solution.

Figure 2.3
Numerical example: Potential metro stations

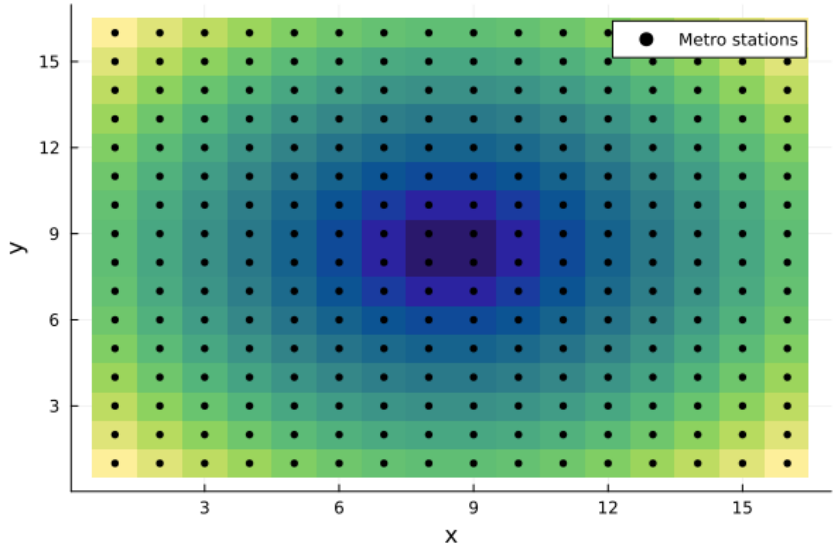

Notes: This figure shows the potential metro stations of the numerical example. Each black dot represents a potential metro station. The background color gradient is based on the distance to the city center, with darker colors indicating closer proximity to the center.

III.1.1 Planner problem

Considering the framework where the planner needs to choose a metro network M among $\mathcal{M}$, she solves,

$$\max_{M \in \mathcal{M}} W(M;\theta) + \iota_M, \tag{2.13}$$

where $W(M;\theta)$ is the economic objective (here $\overline{U}$) given the metro network M and model parameters θ, and ι_M represents an idiosyncratic shock for a network M following a Gumbel distribution with a shape parameter σ. For example, the idiosyncratic shock captures a specific planner's preference for a particular design. Hence, the probability that the network M is chosen by the planner is,

$$\pi(M;\theta) = \frac{\exp(\sigma\, W(M;\theta))}{\sum_{M' \in \mathcal{M}} \exp(\sigma\, W(M';\theta))}. \tag{2.14}$$

III.1.2 Optimization process

While the probability distribution π cannot be computed due to the high dimensionality of $\mathcal{M}$, the probability ratio of two different metro networks can be computed as follows,

$$\frac{\pi(M';\theta)}{\pi(M;\theta)} = \frac{\exp(\sigma\, W(M';\theta))}{\exp(\sigma\, W(M;\theta))}. \tag{2.15}$$

Therefore, I use a simulated annealing (SA) algorithm to explore the space of metro networks as in Kreindler et al. (2024). This algorithm is a step-by-step process. It starts with an initial metro network (randomly draw) M_k with L metro lines and S metro stations, which gives an initial economic objective $W(M_k;\theta)$. In addition, there is an "inverse temperature" parameter σ that increases over the K steps.[3] This parameter is crucial and ensures that the algorithm explores the space of networks widely.

At step k, a perturbation function Ψ creates a candidate network M' given the current network M_k. The acceptance probability of the candidate network is defined as,

$$Pr(M_{k+1} = M'|M_k) = \min\left(1, \frac{\exp(\sigma\, W(M';\theta))}{\exp(\sigma\, W(M_k;\theta))}\right). \tag{2.16}$$

Hence, the candidate network M' is always accepted if it has a greater economic objective ($W' > W_k$), and otherwise M' is accepted with a probability that increases with W' and decreases with σ.

By doing so, this Markov chain samples from the planner's distribution π, starting with low values of σ to more often accept M' and widely explore the space of metro networks, and ending with high values of σ to put more weight on the economic objective W'.

The perturbation function Ψ modifies the current metro network M based on probabilistic scenarios. For simplicity, I consider only the possibility to remove the current network and create a new one in this numerical example. After this perturbation, which gives a candidate network M', the matrix of commuting cost is updated by computing bilateral commuting time between locations, which in turn allows the computation of a candidate economic objective $W'(M';\theta)$ through the quantitative urban model.[4]

[3] For more on the "inverse temperature", I refer the reader to Kreindler et al. (2024).

[4] I use the Leontief inverse of the weighted adjacency matrix to compute commuting cost following the implementation of a metro network (Allen and Arkolakis, 2022).

III.2 Simulation results with a numerical example

Using this naive numerical example as an experiment, I sample 300 metro networks through independent runs with 150 iterations and $\sigma_K = 1,000$. Panel (a) of Figure 2.4 shows the convergence of each run over the iterations, with most stabilizing between 2% and 3% welfare gains. Over the 300 sampled metro networks, it may be more efficient for a metro line to pass through certain locations than others. In order to test whether certain metro stations are more strategic than others, I sum up the frequency of appearance of the stations across all runs. Panel (b) of Figure 2.4 displays all potential metro stations, with their size being proportional to the frequency of their appearance across all runs, providing an indication of the systematic importance of certain stations. We observe that stations in the city center are sampled more frequently than those on the periphery. This pattern is a mechanical result, as central stations inherently possess greater market potential than others. Controlling for the distance to the city center to capture centrality, as well as longitude and latitude, Panels (c) and (d) illustrate the correlation between location fundamentals and the frequency of metro stations. The results indicate that amenities and productivity are positively correlated with the frequency of metro stations. Therefore, these factors appear to be crucial in the design of optimal urban transport infrastructure.

Figure 2.4
Numerical example: Simulated annealing algorithm results

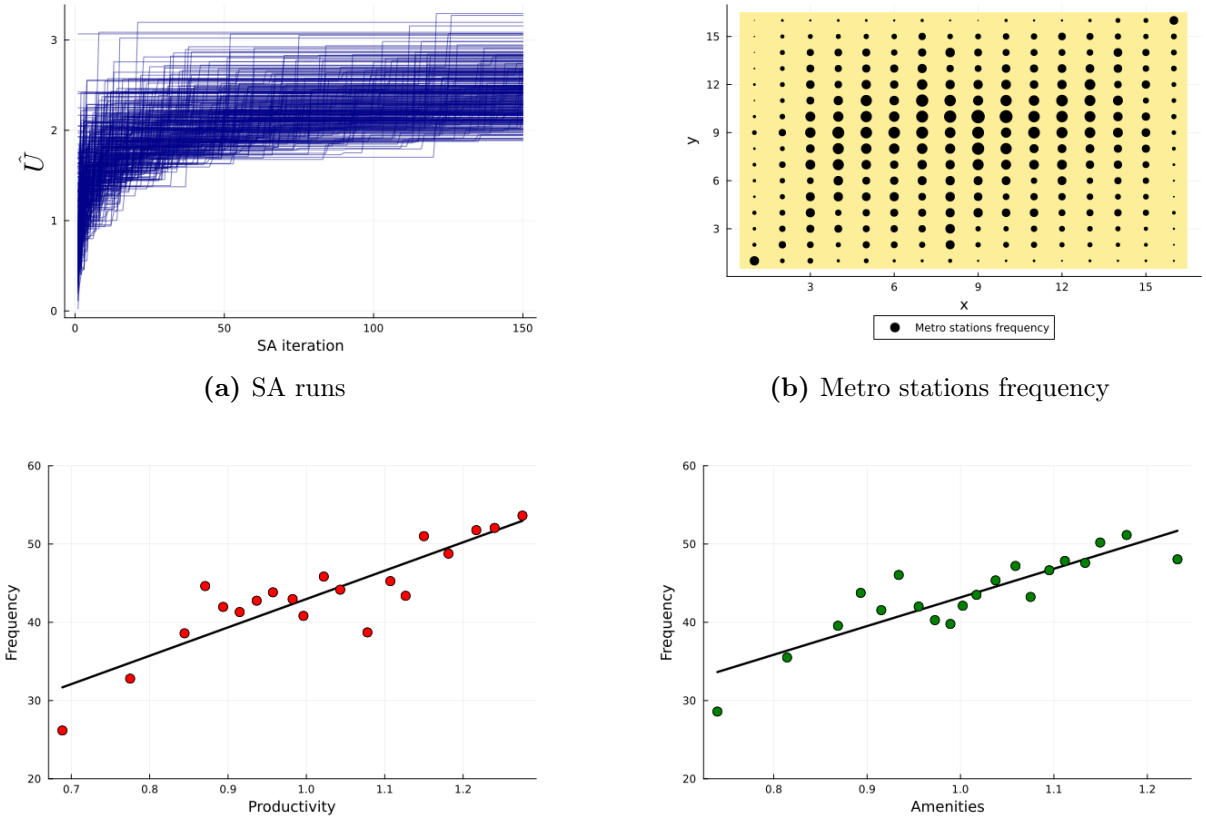

(a) SA runs

(b) Metro stations frequency

(c) Productivity and frequency

(d) Amenities and frequency

Notes: This figure presents the results of the simulated annealing algorithm in a numerical example. Panel (a) shows the results of SA runs over 150 iterations, with each line representing a single run. Panel (b) displays all potential metro stations, with their size being proportional to the frequency of their appearance across all runs. Panel (c) plots a binned correlation between metro station frequency and their associated productivity, illustrating how productivity influences station frequency. Panel (d) plots a binned correlation between metro station frequency and their associated amenities, showing the relationship between amenities and station frequency.

IV An application to historical Paris

IV.1 Context and data

In this subsection, I first present the data that enables quantitative analysis. Next, I detail the historical context during which the Parisian metro was constructed.

IV.1.1 Data

Geography I use a grid of 500 m × 500 m, made up of 450 spatial units. This granularity matters as it allows capturing more complexity in location characteristics, and therefore in urban transport design. Each spatial unit varies in terms of amenities, productivity, centrality, housing supply, and transport network. This variation allows for a better understanding of the different factors at play in explaining urban transport design.

Residence and workplace employments First, I use data from Cosentino (2025) to obtain residential information across Parisian neighborhoods in 1896. Overall, the Parisian population reached $2,536,834$ in 1896, but this aggregate figure masks significant spatial disparities. Specifically, the city center experienced a decrease in population, while most residents moved to the periphery throughout the 19th century, as documented by Cosentino (2025). I combine this residential information with occupational data provided by the 1891 census, which allows for the differentiation between high-skilled and low-skilled residents by neighborhood. Then, I proceed to distribute the population by type across the grid cells using a newly digitized urban footprint map shown in Figure 2.5. This map, consisting of around 4,600 buildings and areas, enables me to distinguish between permanent structures (such as monuments and scenic gardens) and non-permanent footprints (such as commercial and residential buildings). I supplement the footprint information with building height data from the national buildings database (BDNB), which provides the year of construction and height of each building not yet demolished. This allows me to compute the building volume within each grid cell and distribute the population of each neighborhood accordingly. Panel (a) and Panel (b) of Figure 2.6 show the spatial distribution of high-skilled and low-skilled residents, respectively. While both types of workers seem to concentrate in the city center, there is spatial sorting of high-skilled workers toward the west and low-skilled workers toward the east, aligning with the pattern described by Heblich et al. (2021) (see Figure B.2 for an illustration by showing the ratio of the high-skilled residence employment with respect to the low-skilled residence employment). Second, I use city directories of Paris from 1896 provided by *ANR SoDuCo* to obtain a proxy for neighborhood workplace employment, as in Cosentino (2025). These city directories provide detailed information on firm locations and their respective industries. To compute the number of low-skilled workers in each grid cell, I apply weights based on the worker intensity by industry of the 1872 industrial survey to transition from individual firm data to aggregate counts. For high-skilled workers, I assume that each firm is managed by an owner, who is considered a high-skilled worker. Panel (c) and Panel (d) of Figure 2.6 show the spatial distribution of high-skilled and low-skilled workers, respectively. Both are concentrated in the city center, where most economic activities took place during this period.

Figure 2.5
Parisian buildings in 1894

Notes: This figure illustrates the distribution of 4,600 buildings and areas in Paris in 1894, highlighting the urban footprint of the period. The map differentiates between permanent areas (such as monuments and gardens), depicted in dark red, and non-permanent areas (such as commercial and residential buildings), shown in light gray.

Figure 2.6
Spatial distribution of residents and workers by skilled in 1896

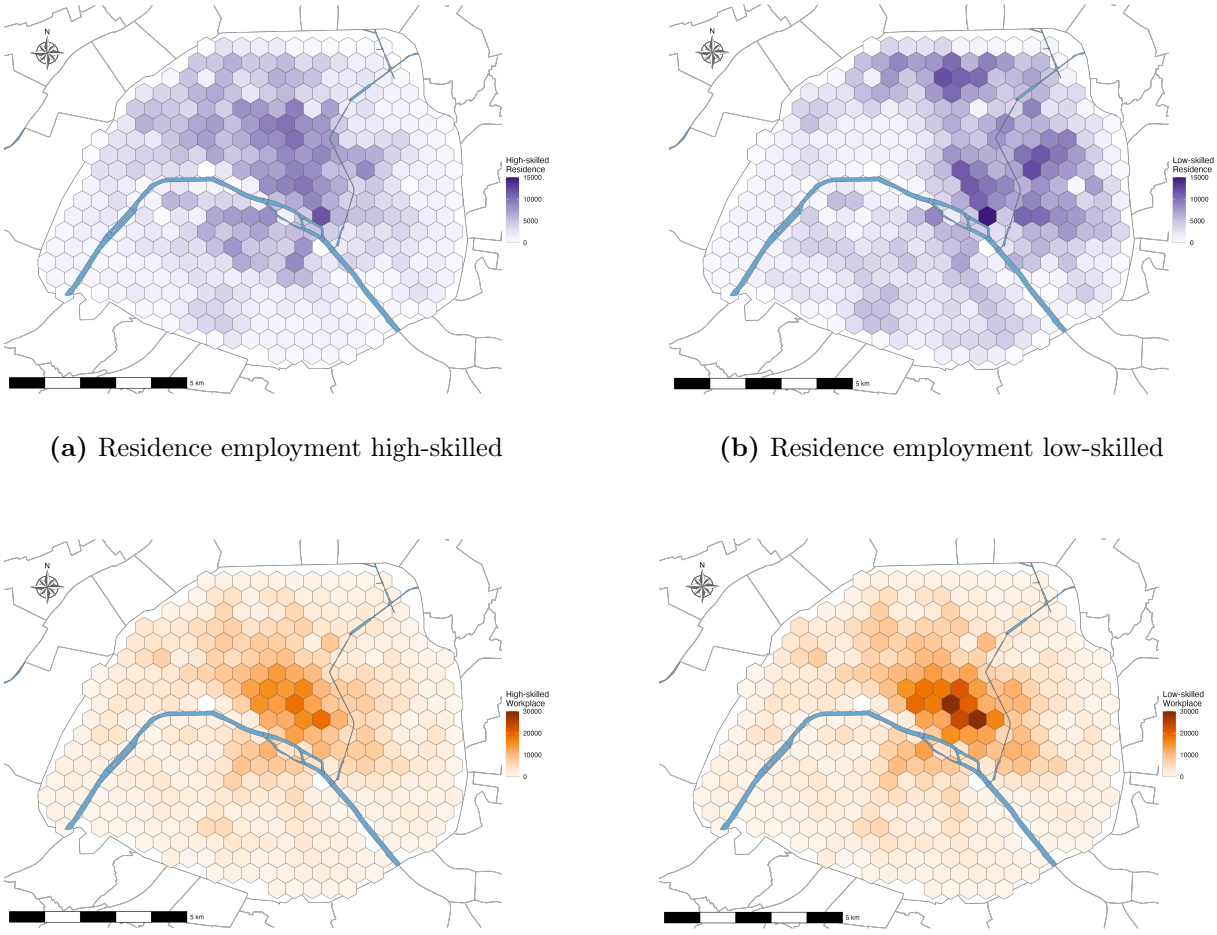

(a) Residence employment high-skilled

(b) Residence employment low-skilled

(c) Workplace employment high-skilled

(d) Workplace employment low-skilled

Notes: This figure illustrates the spatial distribution of residence and workplace employment by skill level in 1896. Panel (a) shows the residence employment for high-skilled workers, while Panel (b) depicts the residence employment for low-skilled workers. Residence employment at the grid cell level is estimated through the footprint and building heights. Panel (c) presents the workplace employment for high-skilled workers, and Panel (d) shows the workplace employment for low-skilled workers. Workplace employment at the grid cell level is estimated through city directories. The color intensity in each panel represents the density of employment, with darker shades indicating higher concentrations.

Rents Since I lack accurate and detailed data on rents, I use Paris fiscal matrices provided by the tax authorities to obtain the property taxes (*contribution foncière*) by neighborhoods. These data are crucial for recovering location-specific productivity and amenities in the structural analysis. I use the same previous building information to assign an average housing price per grid cell.

Transport network I combine several data sources in order to accurately construct the historical Parisian transport network. In 1896, workers mainly relied on three commuting modes: the *Petite Ceinture*, omnibus, and tramways. To begin with the *Petite Ceinture*, I rely on the *Association Sauvegarde Petite Ceinture* and OpenStreetMap to

obtain detailed information on train stations and railroad locations. This circular line of 32 km was the metro precursor and offered the first railroad passenger service within the Paris intra-muros. Its average speed was 20 km/h, which is similar to the metro. Finally, I construct omnibus and tramway networks by using the *Tableau des lignes de tramways* from the *Bibliothèque nationale de France*. These archival data provide information on the starting and ending stations of omnibuses and tramways, as well as connections between lines. Overall, the network consisted of 35 omnibuses and 19 tramways (see Figure B.1). According to Passalacqua (2012), the average speed of omnibuses and tramways was 9 km/h. Therefore, this transportation information provides me with a set of stations connected within a network $\Xi = \left[\xi^{\text{OT}}, \xi^{\text{PC}}\right]$, where subscripts OT and PC indicate the omnibuses as well as tramways, and the *Petite Ceinture* railroad, respectively. I assume a vector of travel time $\Omega = \left[\omega^{\text{OT}}, \omega^{\text{WA}}, \omega^{\text{PC}}\right]$, where subscripts WA indicate walking. I calibrate the walking speed to 5 km/h and consider a 5-minute waiting time γ^C if there is a connection between different modes. Overall, this rich transport network allows the computation of the commuting time $t_{ni} = t_{ni}(\Omega, \Xi, \gamma^C)$ between all locations considering different transport modes, and by using a least cost path method based on a Dijkstra algorithm. It aims to: (i) rationalize the initial spatial equilibrium in Paris, (ii) obtain a fixed network where an optimal metro will be added.

IV.1.2 Historical context: metro planning

According to Cottereau (2004), the first legal initiative to create the Parisian metro came from a deliberation of the Seine General Council on November 10, 1871. Several goals were considered, such as unifying the Seine department through a railroad network, connecting the city center of Paris, and making interconnections between major train stations.[5] This was followed by a series of metro projects with different designs and objectives, but some of these metro projects shared a common philosophy. The London metro, built in 1863, had the effect of separating work from home by creating internal migration between suburbs and the city center, as shown by Heblich et al. (2020). In contrast to London, the Parisian metro was designed to connect residences to workplaces, rather than pushing them into the suburbs.

In 1872, Léon Say proposed a metro network that would use existing railways by adding two radial metro lines within Paris to complete the *Petite Ceinture* (see Panel (a) of

[5] I do not include the major train stations in my analysis, as this would increase the computation time for commuting times between neighborhoods, and these stations are mainly intended to carry passengers from the suburbs.

Figure 2.7). In 1876, another project by Alphand-Huet suggested diverting as much traffic as possible to the old network (see Panel (b) of Figure 2.7). In 1883, a metro project that did not rely on the existing transport network was proposed (see Panel (c) of Figure 2.7). Finally, the final metro project by Fulgence Bienvenüe was adopted in 1896 (see Panel (d) of Figure 2.7). This metro was designed to be self-sufficient and to guarantee access to all residents through a wide range of connections. In addition, it had to maintain the residential-workplace ties within Paris itself.

Figure 2.7
Metro Network Projects

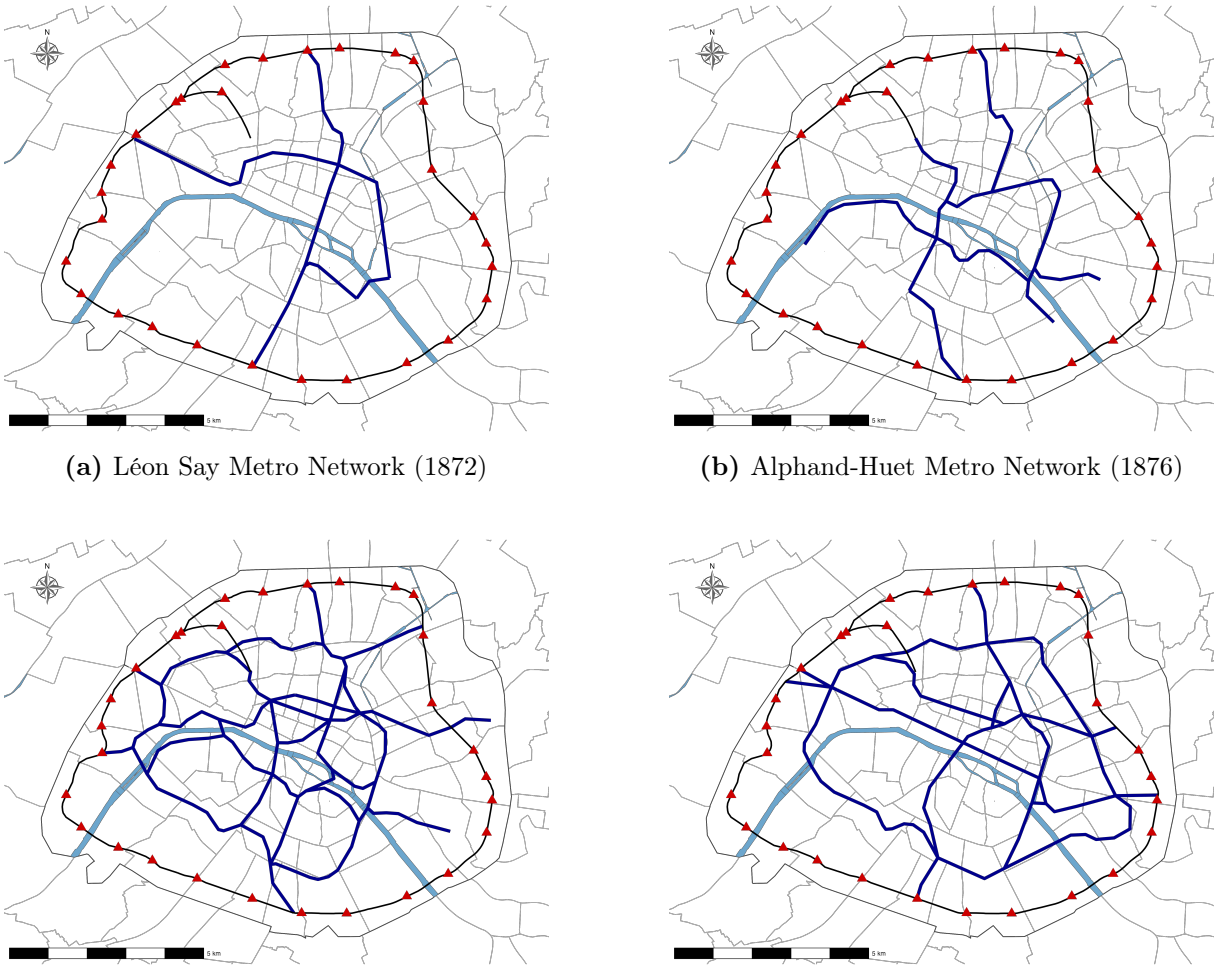

(a) Léon Say Metro Network (1872)

(b) Alphand-Huet Metro Network (1876)

(c) Council Metro Network (1883)

(d) F. Bienvenüe Metro Network (1896)

Notes: This figure illustrates various historical proposals for metro networks in Paris. Panel (a) depicts the Léon Say Metro Network proposed in 1872. Panel (b) presents the Alphand-Huet Metro Network from 1876. Panel (c) shows the Council Metro Network proposed in 1883. Panel (d) illustrates the F. Bienvenüe Metro Network from 1896, which was ultimately implemented.

IV.2 QUM extension

In this subsection, I adapt the canonical urban model developed in section II to match the historical Parisian setting and the empirical facts. I modify several components presented below: (i) worker heterogeneity with high-skilled and low-skilled workers, (ii) an open city setting, and (iii) worker substitution by considering a CES nested within the firm production function, with machinery capital.

IV.2.1 Workers heterogeneity

As shown in subsection IV.1, the occupational sorting of that time in Paris highlights the need to consider both high- and low-skilled workers. This addition allows to rationalize factors influencing spatial sorting at equilibrium. I consider a mass of workers of type g living and working within a city embedded in an economy. A worker o of type g choosing the residence-workplace pair $\{n, i\}$ derives the following indirect utility,

$$U_{ni,g}(o) = \frac{B_{n,g} w_{i,g}}{d_{ni} P_n^{1-\beta_g} Q_n^{\beta_g}} \epsilon_{ni,g}(o), \tag{2.17}$$

where only amenities ($B_{n,g}$), the wage ($w_{i,g}$), the housing share (β_g), and the idiosyncratic shock ($\epsilon_{ni,g}(o)$) differ from equation (2.1), and are type-specific. Hence, the same properties of the Fréchet distribution can be applied to recover the type-specific commuting probability $\lambda_{ni,g}$, the type-specific residential probability $\lambda^R_{n,g}$, the type-specific workplace probability $\lambda^L_{i,g}$, and the type-specific conditional commuting probability $\lambda^R_{ni|n,g}$ (see appendix B.2.2 for more details).[6]

IV.2.2 Open city setting

I consider an open city setting where workers from the outside economy are free to enter the city. This setup reflects the historical context in which the population of Paris doubled during the 19th century, as documented by Cosentino (2025). Within this open city framework, the expected utility of a worker of type g residing and working in Paris can be expressed as,

$$\overline{\mathbb{U}}_g \left(\frac{R_{\mathbb{N}_g}}{R_{\mathbb{M}_g}} \right)^{1/\epsilon_g} = \overline{U}_g, \tag{2.18}$$

[6] The extension that allows locations to have different consumption prices by relaxing the assumption of free trade is not implemented in order to maintain tractability and limit computational complexity.

with $\overline{U}_g \equiv \delta_g \left[\sum_{k\in\mathbb{N}} \sum_{l\in\mathbb{N}} \Phi_{kl,g}\right]^{1/\epsilon_g}$ the type-specific expected utility that a worker derives from living and working in Paris (which is a type-specific version of equation (2.5)), $\overline{\mathbb{U}}_g$ the type-specific expected utility in the wider economy, and $R_{\mathbb{N}_g}/R_{\mathbb{M}_g}$ the share of workers of type g living in the economy choosing a pair of locations within Paris. To satisfy the population mobility condition, a relatively higher expected utility within the city compared to the economy implies a greater proportion of workers opting for Paris, as expressed by the ratio,

$$\frac{R_{\mathbb{N}_g}}{R_{\mathbb{M}_g}} = \left(\frac{\overline{U}_g}{\overline{\mathbb{U}}_g}\right)^{\epsilon_g}. \tag{2.19}$$

IV.2.3 Firms

Additionally, I consider an extension of the firm production function by incorporating a Cobb-Douglas framework that includes machinery capital and a CES for labor supply. These two features reflect the extensive use of machinery in Parisian production during 1896 and accommodate the diverse skill levels of the workforce at that time. Therefore, the representative firm produces the final good with Cobb-Douglas technology under constant returns to scale,

$$Y_i = A_i \left(\frac{L_i}{\alpha_L}\right)^{\alpha_L} \left(\frac{H_i^L}{\alpha_F}\right)^{\alpha_F} \left(\frac{M_i}{\alpha_M}\right)^{\alpha_M}, \tag{2.20}$$

where A_i represents the productivity in workplace i, L_i is the total labor supply in workplace i, H_i^L is the housing used commercially in workplace i, and M_i is the machinery capital used in workplace i. The total labor supply is expressed as $L_i = \left(\sum_g a_{i,g} L_{i,g}^{\rho}\right)^{1/\rho}$ and takes the form of a constant elasticity of substitution (CES) function, where $a_{i,g}$ is the group-specific skill intensity and ρ is the parameter governing substitution. The shares of labor, machinery, and housing dedicated to the production function are α_L, α_M, and α_F, respectively.

The first-order conditions of the firm's profit with respect to type-specific labor, housing, and machinery are given by,

$$w_{i,g} = \alpha_L^{(1-\alpha_L)}\, a_{i,g}\, L_{i,g}^{\rho-1}\, A_i\, L_i^{\alpha_L-\rho} \left(\frac{H_i^L}{\alpha_F}\right)^{\alpha_F} \left(\frac{M_i}{\alpha_M}\right)^{\alpha_M}, \tag{2.21}$$

$$Q_i = \alpha_F^{(1-\alpha_F)}\, A_i \left(\frac{L_i}{\alpha_L}\right)^{\alpha_L} \left(H_i^L\right)^{\alpha_F-1} \left(\frac{M_i}{\alpha_M}\right)^{\alpha_M}, \tag{2.22}$$

$$r_i = \alpha_M^{(1-\alpha_M)}\, A_i \left(\frac{L_i}{\alpha_L}\right)^{\alpha_L} \left(\frac{H_i^L}{\alpha_F}\right)^{\alpha_F} \left(M_i\right)^{\alpha_M-1}. \tag{2.23}$$

IV.3 Model inversion

In contrast to the numerical example presented above, the distribution of housing supply and fundamentals (amenities by skill, as well as productivity) are not known. Therefore, the model needs to be inverted step by step in order to rationalize the spatial equilibrium with observed residence, workplace, and rent data.

IV.3.1 Wages

Using the type-specific conditional commuting probability combined with the labor market clearing condition,

$$L_{i,g} = \sum_{n \in \mathbb{N}} \frac{(w_{i,g}/d_{ni})^{\epsilon_g}}{\sum_{l \in \mathbb{N}} (w_{l,g}/d_{nl})^{\epsilon_g}} R_{n,g}, \tag{2.24}$$

there exists a unique vector of wages that solves the labor market, given a calibration of ϵ_g, the observed vectors of residence employment, workplace employment, and the commuting cost parametrization.

IV.3.2 Skill intensity

Using type-specific wages, the first-order condition of the firm equation (2.21), and the condition $a_{i,L} + a_{i,H} = 1$, the intensity in low-skilled workers $a_{i,L}$ can be recovered,

$$\frac{1 - a_{i,L}}{a_{i,L}} = \frac{w_{i,H}}{w_{i,L}} \left(\frac{L_{i,L}}{L_{i,H}} \right)^{\rho - 1}, \tag{2.25}$$

where $w_{i,H}$ is the high-skilled wage in workplace i, $w_{i,L}$ is the low-skilled wage in workplace i, $L_{i,H}$ is the total high-skilled labor employed in workplace i, and $L_{i,L}$ is the total low-skilled labor employed in workplace i.

IV.3.3 Productivity

From the zero profit condition due to free entry, and the first-order conditions of the firm's profit maximization, it is possible to express the location productivity as,

$$A_i = W_i^{\alpha_L} Q_i^{\alpha_F} r_i^{\alpha_M}, \tag{2.26}$$

which is a function of aggregate wages $W_i \equiv \left(\sum_g a_{i,g}^{\frac{1}{1-\rho}} w_{i,g}^{\frac{\rho}{\rho-1}} \right)^{\frac{\rho-1}{\rho}}$ (see appendix B.2.2 for more details), the price of machinery capital r_i, and rents Q_i. I make the assumption that

machinery capital is freely traded in the city and normalize the price of the machinery capital $r_i = 1$ for all workplaces i. Intuitively, higher costs (wages, rents) imply a higher productivity in order for the zero profit condition to hold.

IV.3.4 Amenities

Combining the residential probability equation (2.3) and expected utility equation (2.18), it is possible to derive type-specific amenities as,

$$B_{n,g} = \frac{(\lambda^R_{n,g})^{1/\epsilon_g} Q_n^{\beta_g}}{\left(\sum_{i\in\mathbb{N}} (w_{i,g}/d_{ni})^{\epsilon_g}\right)^{1/\epsilon_g}} \frac{\overline{U}_g}{\delta_g} \left(\frac{R_{\mathbb{N}_g}}{R_{\mathbb{M}_g}}\right)^{1/\epsilon_g}, \tag{2.27}$$

where amenities are considered as residuals explaining residential choices in this commuting model. Recalling that $\frac{\overline{U}}{\delta}\left(\frac{R_{\mathbb{N}}}{R_{\mathbb{M}}}\right)^{1/\epsilon}$ is a scalar, for a given residential market access (denominator), and a given rent, a higher share of workers living in location n implies higher amenities.

IV.3.5 Rateable values

Finally, the housing market clears and rateable values ($\mathbb{Q}_n$) are determined by the total housing demand by residents and firms, and rents,

$$\mathbb{Q}_n = Q_n(H^R_n + H^L_n) = \sum_g \beta_g \nu_{n,g} R_{n,g} + \frac{\alpha_F}{\alpha_L} w_{i,g} \frac{L_i^{\rho} L_{i,g}^{1-\rho}}{a_{i,g}}, \tag{2.28}$$

where H^R_n and H^L_n are the residential and commercial housing demand in n, respectively, and $\nu_{n,g} \equiv \sum_{i\in\mathbb{N}} \lambda^R_{ni|n,g} w_{i,g}$ is the type-specific expected income from residents living in location n. The housing demand of firms in workplace i is derived from the first-order conditions equations (2.21) and (2.22).

IV.3.6 Equilibrium

Spatial Equilibrium Definition: *Given the structural parameters* $\{\beta_g, \alpha_M, \alpha_F, \alpha_L, \epsilon_g, \kappa, \rho\}$, *and a commuting cost parametrization, a spatial equilibrium is defined with observed vectors* $\{L_{i,g}, R_{n,g}, d_{ni}, Q_n\}$, *and unobserved vectors* $\{w_{i,g}, a_{i,g}, A_i, B_{n,g}, \mathbb{Q}_n\}$ *such that: i) commuting market clears (2.11); ii) skill-intensity (2.25) and zero profit condition (2.26) are satisfied; iii) population mobility is satisfied (2.27); and iv) housing market clears (2.28).*

IV.4 Model Quantification and Spatial Equilibrium

IV.4.1 Parameters calibration

Internally calibrated I internally calibrate the commuting cost elasticity (κ) and the housing supply elasticity ($1 - \mu/\mu$). Using bilateral flow data from the *Petite Ceinture* railroad prior to the metro's implementation, Cosentino (2025) estimates a commuting cost elasticity of 0.0204. While this value is relatively high compared to the literature, it is robust to using alternative specifications. Then, Cosentino (2025) also estimates a housing supply elasticity of 0.517 with rateable values and housing units data. Although this value is relatively low compared to the literature, it reflects a historical context in which building construction was driven primarily by urban renewal (e.g., Haussmann renovations) rather than by rent variation.

Externally calibrated The remaining parameters are calibrated using values from the existing literature. The housing expenditure share (β_g) is set to 0.3 for low-skilled and 0.2 for high-skilled workers, reflecting the empirical observation that higher-income households spend a smaller proportion of their income on housing (Tsivanidis, 2024; Redding and Sturm, 2024; Weiwu, 2024). The Fréchet dispersion parameter (ϵ_g) is calibrated to 6 for low-skilled and 4 for high-skilled workers, following estimates in Redding and Sturm (2024), matching the fact that the poor are more sensitive to location characteristics than the rich. The production function parameters are drawn from Heblich et al. (2020), who study London during a comparable historical period: the shares are set to 0.2 for housing (α_F), 0.2 for machinery capital (α_M), and 0.6 for labor (α_L). Finally, the elasticity of substitution between skill groups (ρ) is set to 0.3, consistent with the estimates provided by Card (2009), which are largely used in the literature (e.g., Tsivanidis (2024); Herzog (2024); Redding and Sturm (2024); Weiwu (2024)).

Table 2.1
Calibration of structural parameters for heterogeneous QUM

Parameter	Description	Method	Value
	Calibrated		
α_F	Share of housing in production function	Heblich et al. (2020)	0.2
α_M	Share of machinery in production function	Heblich et al. (2020)	0.2
α_L	Share of labor in production function	CRS ($\alpha_L + \alpha_M + \alpha_F = 1$)	0.6
ρ	Elasticity of substitution between skill groups	Card (2009)	0.3
β_L	Share of housing consumption for low-skilled workers	Weiwu (2024)	0.3
β_H	Share of housing consumption for high-skilled workers	Weiwu (2024)	0.2
ϵ_L	Fréchet parameter for low-skilled workers	Redding and Sturm (2024)	6
ϵ_H	Fréchet parameter for high-skilled workers	Redding and Sturm (2024)	4
$d_{ni} = e^{\kappa\, t_{ni}}$	Commuting cost elasticity	Cosentino (2025)	$\kappa = 0.0204$
$(1-\mu)/\mu$	Housing supply elasticity	Cosentino (2025)	0.517

IV.4.2 Results from spatial equilibrium

Fundamentals Figure 2.8 shows the results of the spatial equilibrium, with spatial distributions of high-skilled amenities in Panel (a), low-skilled amenities in Panel (b), and productivity in Panel (c). Overall, these fundamentals recovered by the model are higher in the middle and west of Paris. For amenities, the pattern is consistent with the east-side story described in Heblich et al. (2021), where high-skilled workers value the west side of Paris relatively more than low-skilled workers, and sort themselves there.

Figure 2.8
Fundamentals distribution

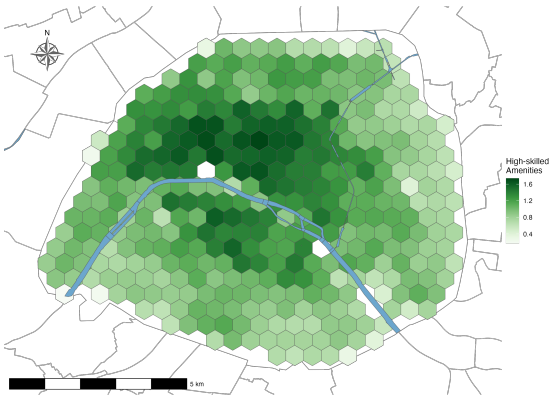

(a) High-skilled amenities

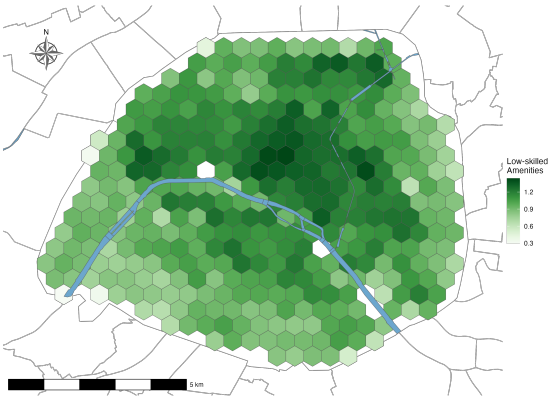

(b) Low-skilled amenities

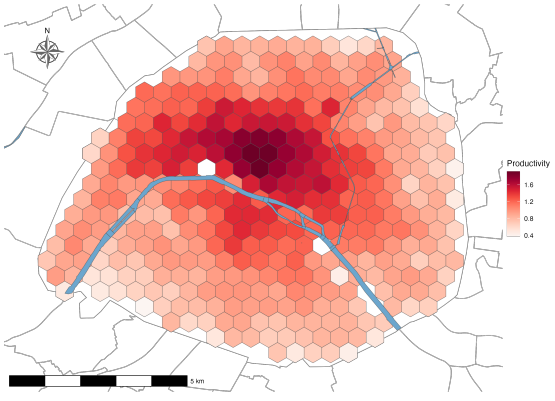

(c) Productivity

Notes: This figure illustrates the distribution of amenities and productivity fundamentals, resulting from a heterogeneous agents QUM and rationalizing within-city spatial equilibrium in 1896. Panel (a) depicts the distribution of high-skilled amenities. Panel (b) shows the distribution of low-skilled amenities. Panel (c) presents the distribution of productivity across the city. Darker shades indicate areas with higher productivity/amenities.

Commuting Regarding commuting patterns predicted by the quantitative urban model, Figure 2.9 shows the cumulative distribution of commuting with respect to distance in the initial equilibrium by skill level. By sorting each residence-workplace pair based on

Euclidean distance and plotting the cumulative share of commuters by skill level, it aims to show how many workers commute less than each distance. Based on the initial equilibrium, high-skilled workers commute more and further than low-skilled workers. More than 65% of Parisian low-skilled workers commute less than 2 km, compared to 57% for high-skilled workers.

Figure 2.9
Cumulative commuting distance distributions

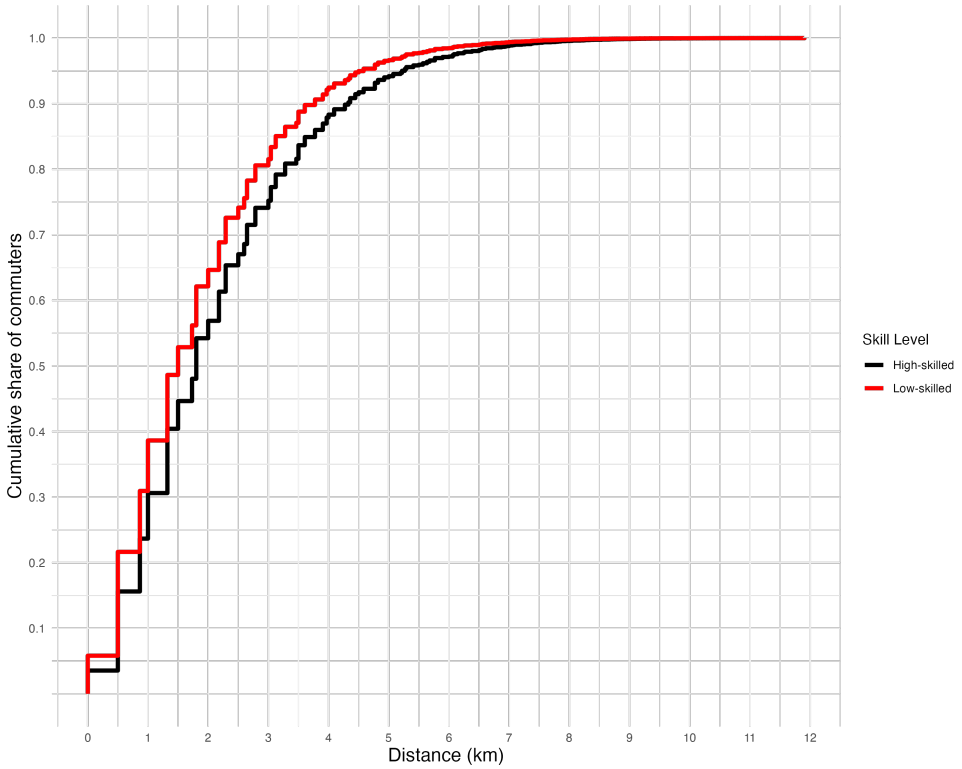

Notes: This figure shows the cumulative distribution of commuters by skill level in the initial equilibrium. Each residence-workplace pair is sorted based on Euclidean distance. The black line represents high-skilled workers, and the red line represents low-skilled workers. The x-axis indicates the distance in kilometers, and the y-axis shows the cumulative share of commuters.

IV.5 Optimal Metro Design

IV.5.1 Optimization Environment

As before, the planner chooses the metro network M consisting of L_M metro lines and S_M selected metro stations that maximizes an economic objective $W(M;\theta)$.

In this application to Paris, I consider several economic criteria W, and I constrain the starting and ending metro stations of each line to be connected with the Petite Ceinture (PC).[7] The baseline W is defined following the Henry George Theorem (George, 1879),

[7] This provides a natural way to start with existing transport infrastructure and, importantly, decreases the optimization space.

implying that public infrastructure gains are valued through the land market.

Hence, the economic impact factor W is defined as the ratio between the net present value of changes in rateable values considering an infinite lifetime, and metro construction costs,

$$W(M;\theta) \equiv \frac{\sum_{n\in\mathbb{N}} \Delta\mathbb{Q}_n(M;\theta)}{r} \times \frac{1}{\text{Cost}(M)}, \tag{2.29}$$

where $\sum_{n\in\mathbb{N}} \Delta\mathbb{Q}_n(M;\theta)$ is the total change in rateable values occurring in the city following the implementation of the metro M, r is a discount rate calibrated to 5%, and $\text{Cost}(M)$ is the cost of infrastructure M.[8]

For simplicity, I make the assumption that $\text{Cost}(M)$ is a linear function of the total number of unique stations and the total length of the metro,

$$\text{Cost}(M) = \vartheta_0 + \sum_{s\in S_M} \vartheta_1 Q_n S_{s(n)} + \sum_{l\in L_M} \vartheta_2 \mathbf{1}^{\text{Seine}} L_{c,o}, \tag{2.30}$$

where ϑ_0 is a fixed cost (representing, for example, technology acquisition), ϑ_1 is the average cost per unique metro station, and ϑ_2 is the average cost per kilometer of tunnel. $S_{s(n)}$ represents a metro station s within location n, which is part of the metro network M, and Q_n is the average rent in location n (with a geometric mean equal to 1). The latter acts as a local shifter allowing for heterogeneity in construction costs across space and captures the fact that implementing a metro station in a rich location is more costly (representing, for example, land acquisition or building destruction) than in a poor location. $L_{c,o}$ is a segment c of a given length connecting two metro stations, part of the metro network M. The subscript o indicates whether the segment is over the Seine or not, and $\mathbf{1}^{\text{Seine}}$ is a shifter capturing the fact that it is more costly to construct a metro line segment under the Seine (for example, it requires using “bored-tube" instead of “cut-and-cover" construction technology) than in other areas within Paris.

To estimate the construction cost parameters $\vartheta = \{\vartheta_0, \vartheta_1, \vartheta_2\}$, I rely on the “cut-and-cover” estimates provided by Heblich et al. (2020) and calibrate a total metro construction cost of 5,126,325 francs per kilometer. This value aligns with the findings of Cottereau (2004), which suggest a cost of approximately 5,000,000 francs per kilometer without expropriation. The total construction cost per kilometer can then be divided into a fixed cost $\vartheta_0 = 46{,}136{,}926$ francs (based on the length of the metro in the Fulgence Bienvenüe

[8] Rateable values equal the sum of prices times quantities for residential floor space and commercial floor space. I calibrate the baseline rateable value by using the per head revenue of the 1872 industrial survey.

project), a station cost $\vartheta_1 = 512{,}632.5$ francs, and a tunneling cost $\vartheta_2 = 2{,}819{,}479$ francs per kilometer (see appendix B.3.1 for more details). Finally, the shifter $\mathbf{1}^{\text{Seine}}$ is calibrated to align with the "bored-tube" estimates provided by Heblich et al. (2020).

To choose a metro network M, I divide the Parisian space into grid cells, each 500 meters apart, to construct 397 potential metro stations.[9] From the information in Figure 2.5, I remove the metro stations that lie within a permanent area (for example, a monument), ending with 367 potential metro stations $\mathcal{S}$. Then, I select all stations that are within 500 meters of the Petite Ceinture (PC) to construct the sample of potential starting/ending stations, resulting in 103 potential metro stations connected to the PC as represented in Figure 2.10. Again, the optimization problem is discrete and high-dimensional, without having an analytical solution. Consequently, I use the same simulated annealing algorithm previously developed in section III with the same optimization process. I adapt my perturbation function Ψ to my context and consider 3 probabilistic scenarios to create a candidate metro network M':

(i) Deviation: randomly selects an existing line, maintains its departure and arrival stations, and makes it pass through a randomly selected point within the grid.

(ii) Add: creates a new line by randomly picking starting/ending metro stations, or randomly selects an existing line, deletes it, and a new line is created by randomly picking starting/ending metro stations.

(iii) Remove: randomly selects an existing line and deletes it.

After this perturbation, which gives a candidate network M', the matrix of commuting cost is updated by computing bilateral commuting time between locations, taking into account fixed transport modes (omnibus, tramways, and the *Petite Ceinture*), which in turn allows the computation of a candidate economic impact factor $W'(M';\theta)$ through the quantitative urban model.

[9] This corresponds to the average length between stations of the actual Parisian metro network.

Figure 2.10
Potential metro stations

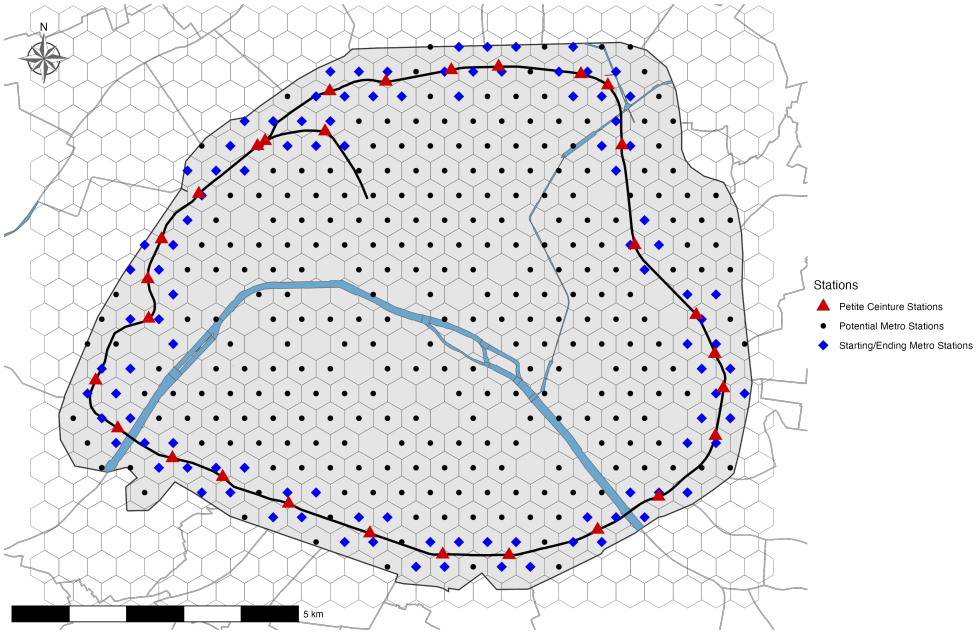

Notes: This figure shows potential metro stations. Red triangles represent *Petite Ceinture* stations, blue diamonds indicate starting/ending metro stations, black dots denote potential metro stations, and the black line represents the *Petite Ceinture* railroad.

IV.5.2 Need for speed

Since the number of steps K needs to be high in order to widely explore the space of metro networks, each iteration must be optimized to reduce computation time. Therefore, I combine R software to handle the perturbation function creating a candidate network M' and an associated commuting costs matrix, and Julia software to efficiently solve the new spatial equilibrium and welfare using exact-hat algebra (Dekle et al., 2007). To speed up the process, I use the *JuliaCall* package to create a permanent Julia session in R, while parallelizing the computation. On average, an iteration of the algorithm takes 0.05 seconds.

IV.5.3 Simulation Results

Using the vector of structural parameters θ, and calibrated metro costs ($\vartheta = \{\vartheta_0, \vartheta_1, \vartheta_2\}$), I set the number of steps K to 1,000 and consider 500 independent simulated annealing runs to sample from π. I consider a minimum number of metro lines of 2, and a maximum of 10. I set the inverse temperature parameter $\sigma_K = 30$, and gradually increase it from 1.

Convergence and examples Figure 2.11 shows the convergence of all runs. Overall, they depict a similar pattern with a progressive increase towards similar values ranging from 9 to 10. Finally, Figure 2.12 shows sampled metro networks with similar economic impact factors but different designs.

Figure 2.11
Simulated annealing algorithm convergence

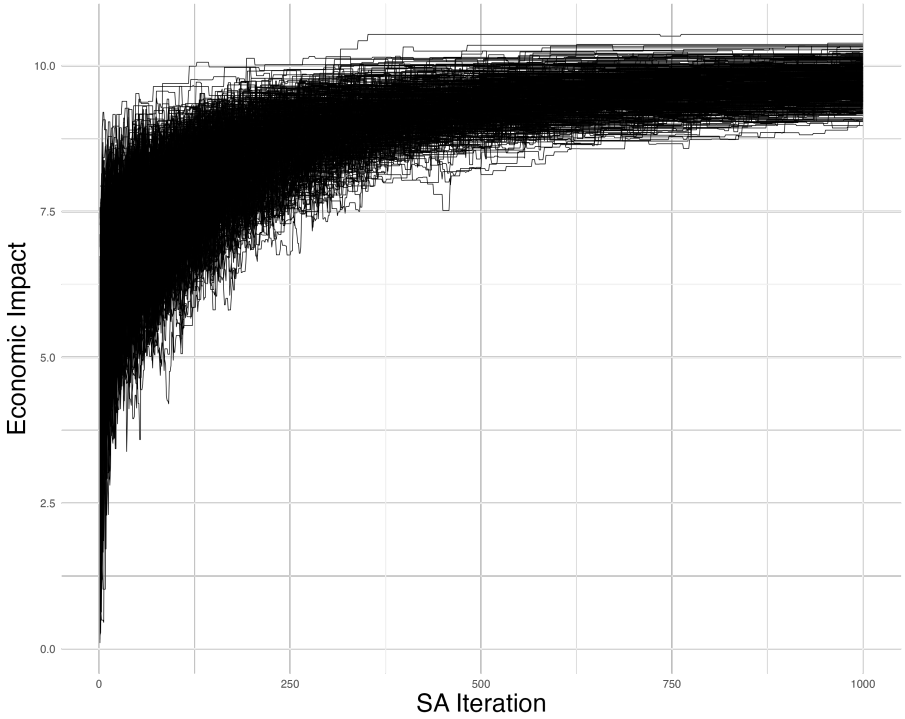

Notes: This figure shows the convergence of the simulated annealing algorithm over 1,000 iterations, with each line representing a different run.

Size of metro network and economic impact factor The simulations provide 500 selected metro networks sampled from π varying in the number of metro stations S, residence and workplace employments across locations, total population, commuting patterns, as well as economic impact factor W.

Panel (a) of Figure 2.13 shows the distribution of the economic impact factor from sampled metro networks. They are centered around 9.71, with a minimum of 8.97 and a maximum of 10.53. This range is comparable in magnitude to the findings of Heblich et al. (2020) for the London metro. Panel (b) of Figure 2.13 shows the distribution of the total number of metro stations from sampled metro networks. While there is a peak at 55 metro stations, some metro networks are extremely different, with a minimum of 33 stations and a maximum of 94 stations. Panel (c) of Figure 2.13 displays the correlation between the

Figure 2.12
Optimal urban transport example

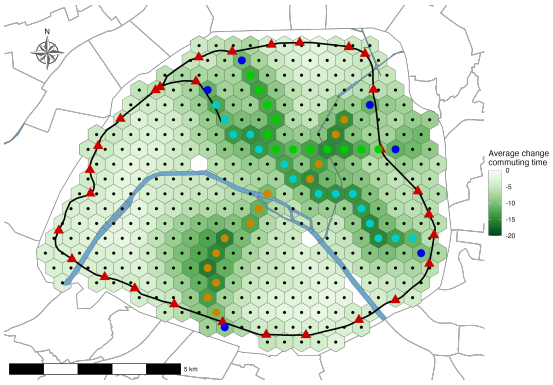

(a) Example 1: $S = 49$, Impact factor $= 10$

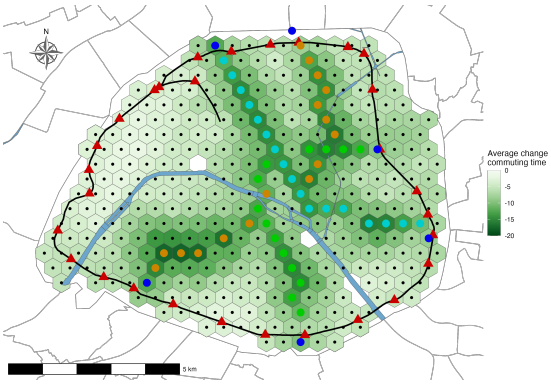

(b) Example 2: $S = 57$, Impact factor $= 10$

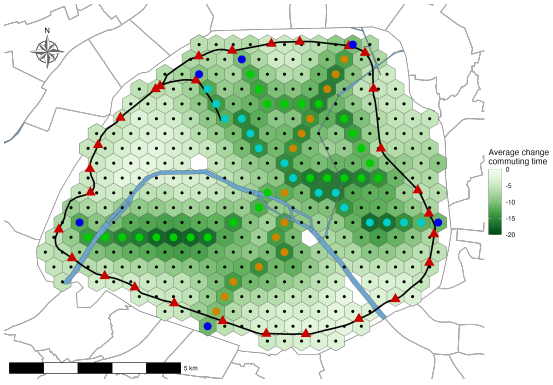

(c) Example 3: $S = 65$, Impact factor $= 9$

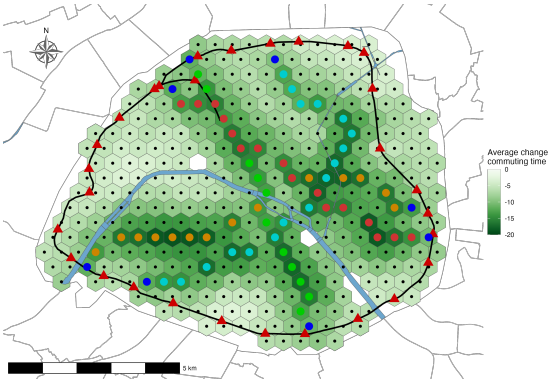

(d) Example 4: $S = 75$, Impact factor $= 9$

Notes: Each subfigure represents an example of an optimal urban transport, showing the number of train stations (S) and the associated impact factor. The economic impact factor is defined as the ratio between the net present value of change in rateable values (considering an infinite lifetime and a 5% discount rate) and the metro construction cots. Darker shades indicate areas with a higher decrease in average commuting time with respect to the initial. Colored dots indicate metro stations, with a single color for each line. Red triangles represent *Petite Ceinture* stations, and the black line represents the *Petite Ceinture* railroad.

number of metro stations S and economic impact W for the sampled metro networks.[10] Since W is a function of the metro construction cost, there is a negative relationship between the number of metro stations and the economic impact factor. However, there is still heterogeneity between metro networks with the same number of stations, as shown by the R-squared of 0.119. It suggests that urban transport infrastructure design matters since metro networks display heterogeneity in economic impact factor for a given number of stations.

Figure 2.13

Size and economic impact of sampled metro networks

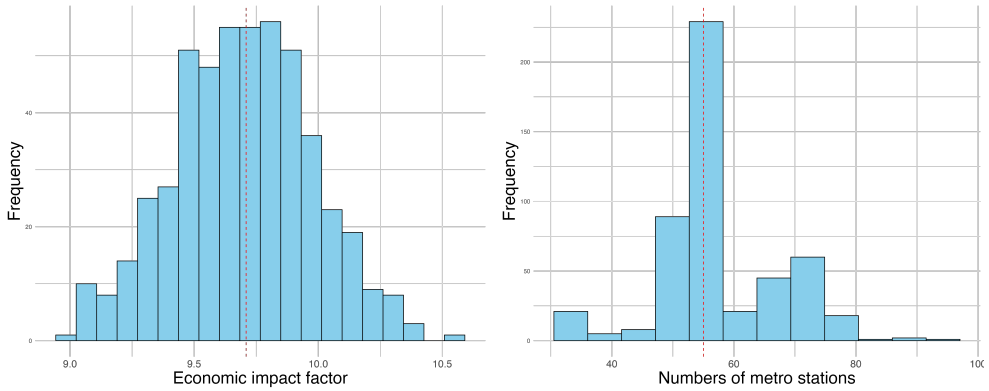

(a) Distribution of economic impact

(b) Metro size

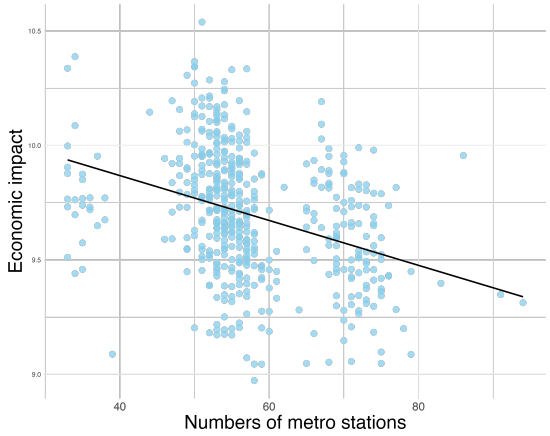

(c) Metro size and economic impact

Notes: Panel (a) depicts the distribution of the economic impact factor from the SA runs. Panel (b) shows the distribution of the total number of metro stations in the SA runs. Panel (c) illustrates the relationship between the number of metro stations and the economic impact, with each blue dot representing a SA run. This figure shows results from 500 independent runs of the SA algorithm with 1,000 iterations. The economic impact factor is defined as the ratio between the net present value of change in rateable values (considering an infinite lifetime and a 5% discount rate) and the metro construction cots.

City, location, and commuting characteristics Over the 500 sampled metro networks, the total production and population increase by, on average, 32.0% and 23.7%, respectively. Figure 2.14 shows the relative increase in population by skill. Both have

[10] Figure B.3 shows the relationship for all the iterations and not only the final sampled metro networks.

similar inflows within the city with medians around 1.22 and 1.24 for high-skilled and low-skilled workers, respectively.

Figure 2.14
Population distribution by skill level

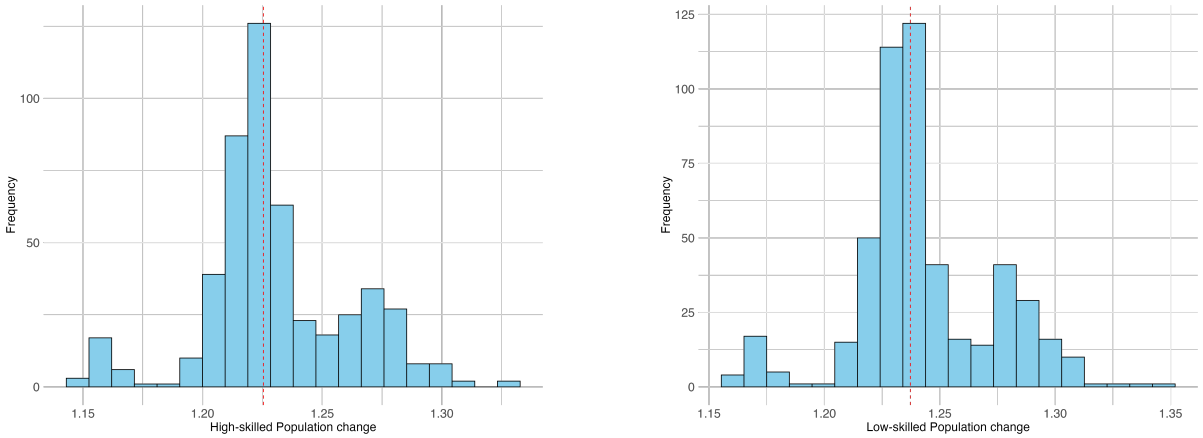

(a) High-skilled **(b)** Low-skilled

Notes: This figure shows the relative changes in population distribution by skill level with respect to the initial. Panel (a) depicts the distribution of population change for high-skilled workers. Panel (b) shows the distribution of population change for low-skilled workers.

Regarding savings in commuting time, Panel (a) of Figure 2.15 shows the distribution of change in total commuting time over the 500 sampled metro networks. The average total decrease in commuting time within the city is 20.4%. However, this aggregate value hides large heterogeneity. Panel (b) of Figure 2.15 shows the change in average commuting time by location with respect to distance from the city center. While all locations experience a decrease in average commuting time, those that are closer to the city center experience a relatively higher decrease in commuting time.

Figure 2.15
Commuting time change

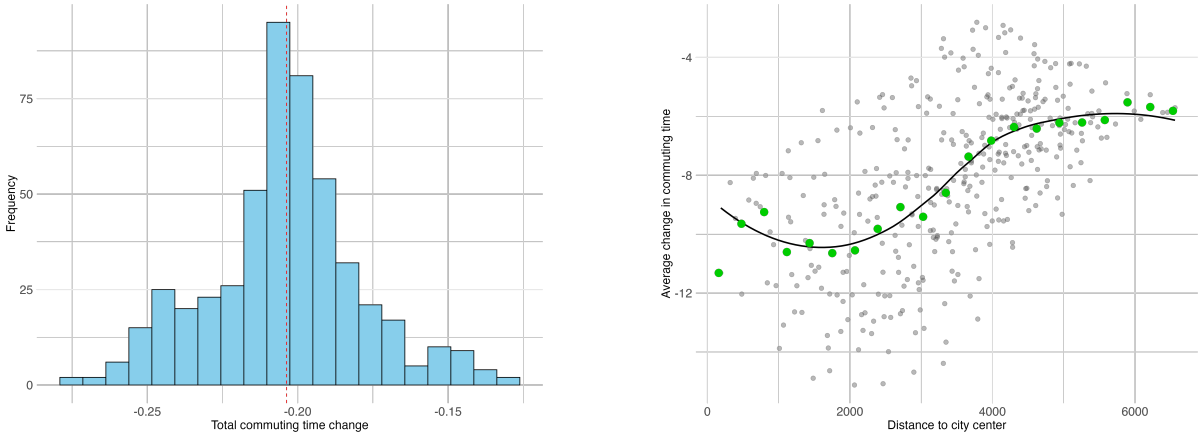

(a) Total commuting time change **(b)** Location commuting time change

Notes: This figure illustrates changes in commuting time with respect to the initial. Panel (a) shows the relative changes in total commuting time. Panel (b) depicts the average change in percentage points of each location with respect to distance to the city center.

Figure 2.16 shows the average change of economic activities for each location with respect to distance from the city center over the 500 sampled metro networks (see Figure B.4 for maps in appendix). While Panel (a) displays that locations close to the periphery experience higher growth in residence employment, Panels (b) and (c) show that locations close to the city center experience higher growth in workplace employment and production, respectively. This aligns with Heblich et al. (2020), who show that implementing a railroad connecting the city center to the suburbs creates a separation between workplace and residence.

Figure 2.16

Change in economic activities with respect to city center

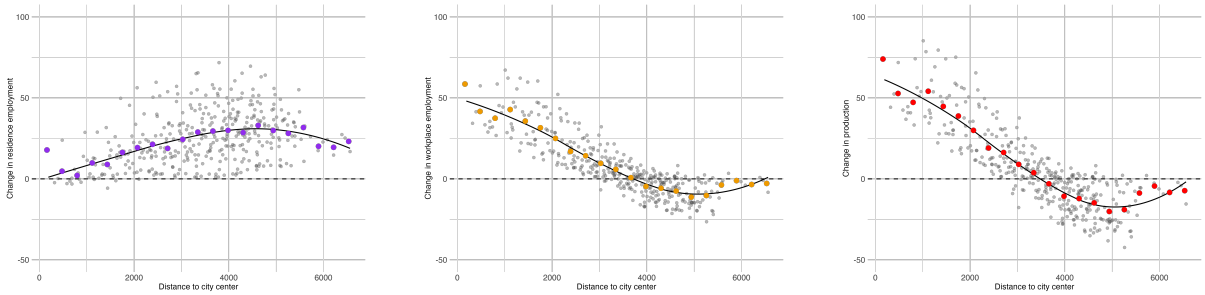

(a) Residence employment **(b)** Workplace employment **(c)** Production

Notes: This figure shows changes in percentage points of location economic activities with respect to distance from the city center. Panel (a) depicts the change in residence employment. Panel (b) shows the change in workplace employment. Panel (c) illustrates the change in production.

Figure 2.17 examines the change in commuting patterns by plotting the cumulative distribution of commuting by skill level over distance (as in Figure 2.9) following the implementation of the 500 sampled metro networks. Overall, these infrastructure changes create similar disconnections between workplace and residence, with a decline in the share of commuters working in their place of residence and a rise in long-distance commuting for both skill groups.

Figure 2.17

Commuting decisions by level of workers

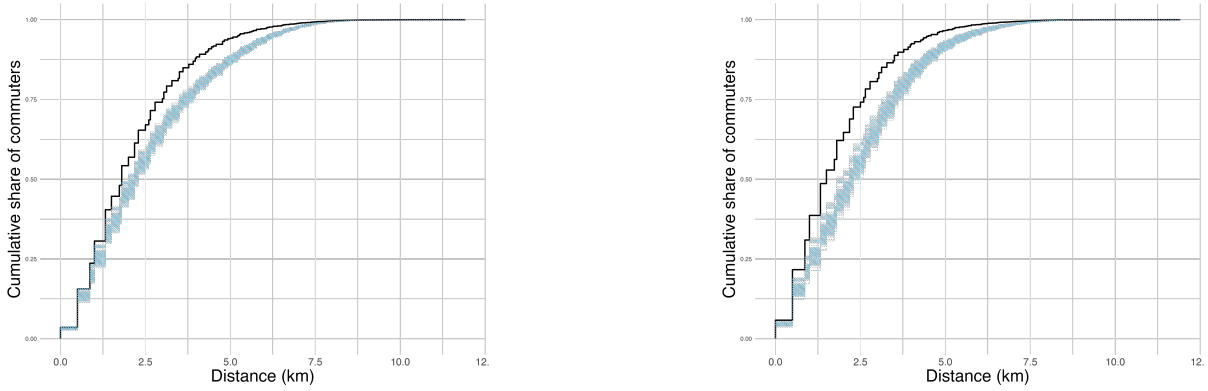

(a) High-skilled workers **(b)** Low-skilled workers

Notes: This figure shows the cumulative distribution of commuters by skill level. Each blue line represents one cumulative distribution of commuters resulting from a SA run, while the black line represents the initial cumulative distribution of commuters. Panel (a) depicts the distribution for high-skilled workers, and Panel (b) shows the distribution for low-skilled workers.

Strategic locations Previous Figure 2.12 shows that different metro designs can achieve similar economic criteria. However, some stations may be more strategic and appear more frequently than others across the 500 sampled metro networks. To explore this pattern, Figure 2.18 shows the frequency of appearance of each metro station across the 500 sampled metro networks. Metro stations within the city center of Paris appear to be strategic locations as they depict a high level of frequency. Consequently, simulations of the simulated annealing algorithm converge toward this design where the lines tend to pass through the city center, regardless of its initial design and the starting/ending metro stations. However, this result could be mechanical, due to the centrality of these stations in the network.

Figure 2.18
Metro stations frequency in sampled metro networks

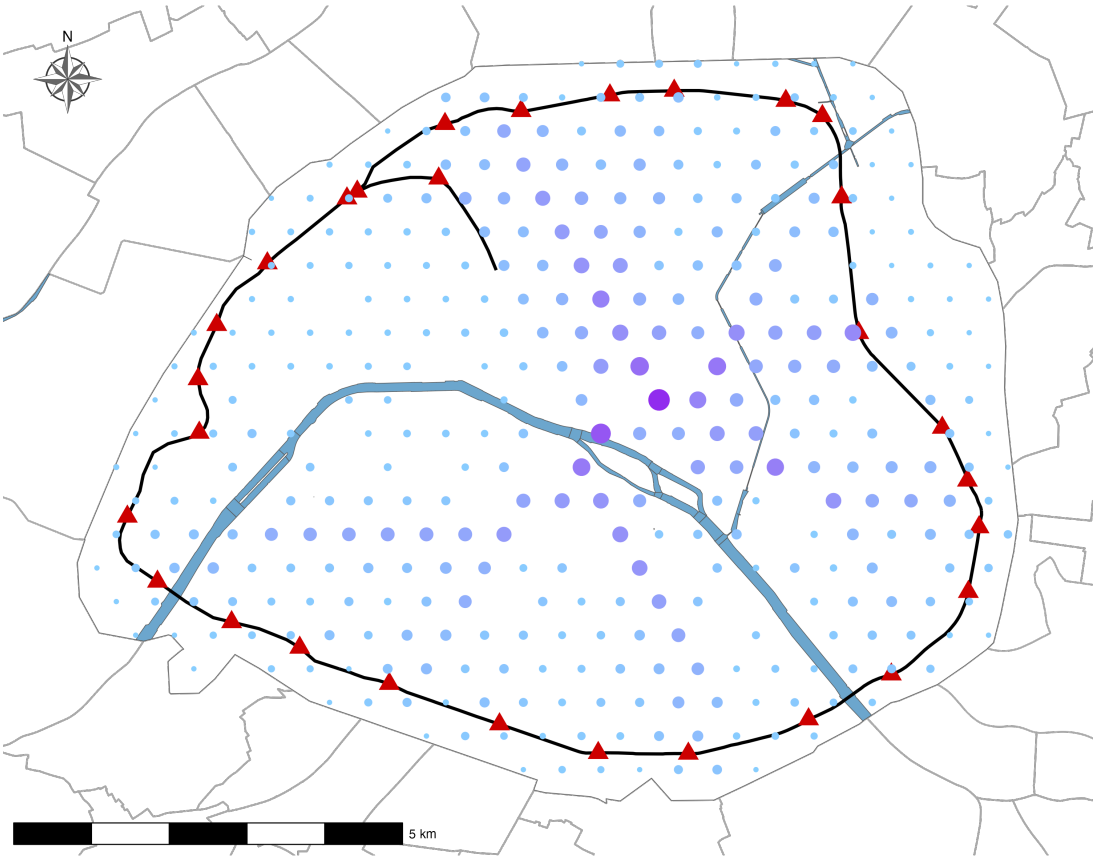

Notes: This figure illustrates the frequency of metro stations occurring in 500 simulated annealing runs. The size of each station is proportional to its frequency, with larger dots indicating higher frequency, while the varying shades of purple dots indicate different levels of station frequency. Red triangles represent *Petite Ceinture* stations.

To further investigate which factors explain strategic metro stations, I implement the following OLS regression,

$$\mathrm{F}_m = \beta_0 + X_m\beta + \varepsilon_m, \tag{2.31}$$

where F_m is the frequency of a metro station m, X_m is a vector of location characteristics associated with metro station m including: A_m the (log) productivity (see Panel (c) of Figure 2.8), $B_{m,g}$ the (log) type-specific amenities (see Panel (a) and Panel (b) of Figure 2.8), Costs_m the (log) construction costs, and the (log) distance to the city center (defined as Notre-Dame, which is at the center of Paris) of metro station m.

Table 2.2 shows the results. Each column reports a separate regression. The first four columns investigate the effect of productivity, low-amenities, high-amenities, and distance to the city center on the metro station frequency separately, holding construction costs constant. These estimates suggest a positive and significant effect of productivity and type-specific amenities on the frequency of sampled metro stations. By contrast, the coefficient associated with the distance to the city center is negative and significant, suggesting that potential stations that are closer to the city center are more represented in the sampled metro stations. This result could be partly mechanical since radial lines necessarily cross the city center. However, productivity and amenities are highly geographically correlated, and both are higher in the city center (see Figure 2.8). Controlling for the four independent variables in column (4) decreases the magnitude of the effects associated with productivity and low-skilled amenities variables. However, the coefficient associated with high-skilled amenities becomes negative. Since the economic objective is based on gains in rateable values, connecting locations with higher low-skilled amenities is more strategic than connecting those with higher high-skilled amenities. This is primarily because these locations attract low-skilled workers, representing the city's main workforce with 54% of the Parisian population being low-skilled. Additionally, low-skilled workers tend to spend a higher proportion of their income on housing. Therefore, implementing a metro network within these areas increases low-skilled workers' market access and total income, which in turn increases payments to landlords. Moreover, estimates suggest that, on average, after accounting for the location centrality, construction costs, and the level of amenities, a 1% increase in productivity leads to a 1.7 increase in frequency within the sampled metro networks compared to other stations.

Overall, results from this historical application confirm the findings of the numerical example and highlight the importance of targeting metro stations that connect locations with high productivity and amenities.

Table 2.2
Determinants of metro stations frequency

	Metro Station Frequency				
	(1) OLS	(2) OLS	(3) OLS	(4) OLS	(5) OLS
Log. Productivity	274.5***				170.9***
	(36.2)				(36.7)
Log. Costs	-54.3***	6.8	9.2	-26.0***	-66.4***
	(12.0)	(9.1)	(9.1)	(7.1)	(10.5)
Log. Low-skilled Amenities		174.9***			159.8***
		(34.7)			(38.6)
Log. High-skilled Amenities			91.0***		-114.9***
			(15.5)		(30.4)
Log. Distance to CC				-162.2***	-139.1***
				(20.5)	(22.0)
Observations	334	334	334	334	334
R^2	0.21	0.14	0.11	0.35	0.42

Notes: Each column reports estimates from a separate regression. Regressions use potential metro stations derived from 500mx500m grid cells. The dependent variable is the frequency of metro stations within 500 SA runs. Heteroskedasticity-robust standard errors are in parentheses and ***, **, * indicate significance at the 1%, 5% and 10% level, respectively.

IV.5.4 Comparative static

Next, I run comparative statics exercises on parameters and show how the characteristics of sampled metro networks change. These experiments allow to refine the results obtained previously and investigate what other factors determine convergence towards specific metro networks.

An alternative CBD First, I conduct a comparative static experiment in order to check whether productivity is the main factor explaining metro station frequency with the sampled metro networks. To achieve this, I simulate a productivity shock in locations near the city center, with positive shock for those located on the southern bank of the Seine in Paris and negative shock for those located on the northern bank as illustrated in Panel (a) of Figure 2.19. Then, I sample again 500 metro networks using the simulated annealing algorithm and considering the same parameters. Panel (b) of Figure 2.19 shows the counterfactual frequency of metro stations within the sampled metro networks, and another pattern emerges from it. Compared to previous simulations in Figure 2.18, metro stations in the South seem to appear more often in the SA runs. Panel (c) of Figure 2.19 shows the change between baseline and counterfactual metro station frequency, and it clearly depicts an increase around areas that experienced a productivity shock. Hence,

this experiment suggests that productivity is one of the main driver of strategic location, confirming previous results in Table 2.2.

Figure 2.19
Comparative static: new city center

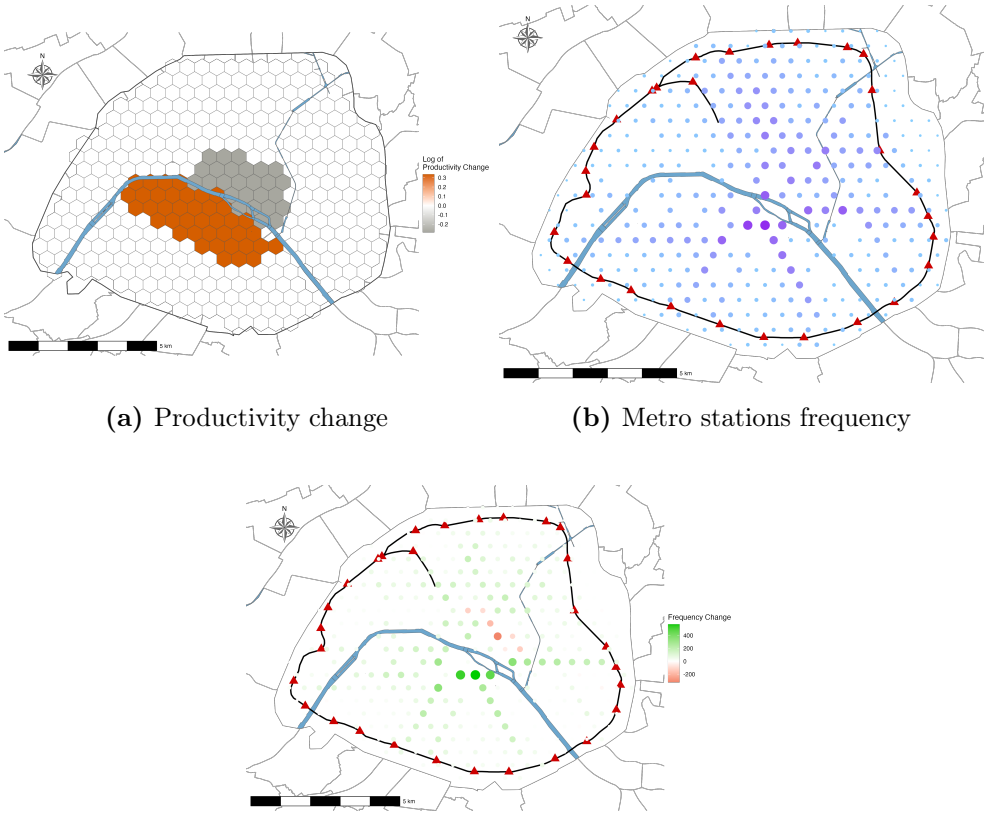

(a) Productivity change

(b) Metro stations frequency

(c) Strategic stations change

Notes: Panel (a) shows the productivity shock with an alternative central business district (CBD) in orange, and the old CBD in grey. Panel (b) illustrates the frequency of metro stations occurring in 500 simulated annealing runs following this new CBD. Panel (c) shows the change in frequency of metro stations between the baseline and the new CBD scenario. Green indicates a positive change in frequency, while red indicates a negative change. The size of the dots is proportional to the absolute value of the frequency change.

Metro construction fixed cost Second, I conduct a comparative static experiment investigating the role of the metro construction fixed-cost ϑ_0. The metro cost functional form equation (2.30), by assuming fixed and linear costs, should provide an incentive for planners to build larger metro networks in order to smooth large fixed-investments. To explore this, I implement simulations and investigate the size of the metro network while gradually increasing the fixed-cost by a factor. For a given ϑ_0, I consider 100 runs of the simulated annealing algorithm with 1,000 iterations each in order to sample metro networks from the distribution π. Then, I compute the average number of stations and lines of the sampled metros. Figure 2.20 shows the results, where the x-axis represents the multiplication factor of ϑ_0, the y-axis represents the average number of metro stations in

Panel (a), and the average number of metro lines in Panel (b). Overall, this experiment shows that increasing the fixed-cost ϑ_0 leads to sampled metro networks being larger in terms of lines and stations.

Figure 2.20
Comparative static: metro construction fixed-cost

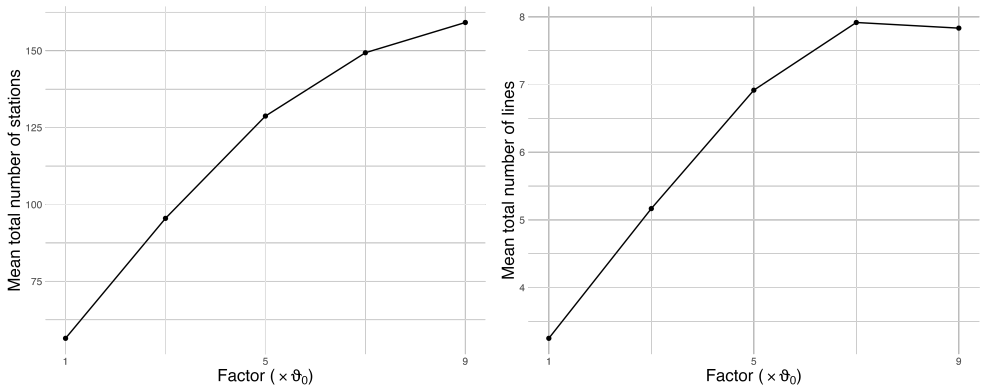

(a) Mean number of total stations **(b)** Mean number of total stations

Notes: Panel (a) shows the average total number of stations over the SA runs as a function of the cost factor. Panel (b) illustrates the average total number of metro lines over the SA runs as a function of the cost factor.

Agglomeration forces In this last comparative static experiment, I investigate the role of agglomeration forces. To do so, I allow agglomeration forces by letting type-specific amenities and productivity be functions of two components: (i) exogenous type-specific residential ($b_{n,g}$) and production (a_n) fundamentals, and (ii) own location residence or workplace density, as in Heblich et al. (2020). Hence, both productivity and amenities can be written as,

$$B_{n,g} = b_{n,g} \left(\frac{R_n}{K_n} \right)^{\eta^R},$$
$$A_n = a_n \left(\frac{L_n}{K_n} \right)^{\eta^L},$$

where endogenous residential externalities depend on the location's own residence employment density weighted by a constant elasticity (η^R) parameter, and endogenous production externalities depend on the location's own workplace employment density weighted by a constant elasticity (η^L) parameter. I calibrate η^L to 0.07, and η^R to 0.16, which are standard values estimated in the urban literature (Ahlfeldt et al., 2015; Heblich et al., 2020; Cosentino, 2025). Then, I repeat the baseline simulation procedure considering agglomeration forces, resulting in 500 sampled metro networks.

Across the 500 sampled metro networks, total productivity, total low-skilled amenities,

and total high-skilled amenities increase on average by 0.6%, 3.2%, and 3.0%, respectively, due to agglomeration gains. Panel (a) of Figure 2.21 displays the spatial distribution of metro station frequency within the sampled metro networks. A similar pattern emerges from it, compared to Figure 2.18, with higher strategic stations in the city center. Panel (b) of Figure 2.21 displays the change in metro station frequency between the baseline and this comparative static experiment. While metro stations located in the city center experience small changes, those on the periphery show very different patterns with an increase, especially in the south and north of Paris. Therefore, strategic metro stations seem to be more evenly distributed. Panel (c) of Figure 2.21 also explores this pattern by displaying the distribution of metro station frequency, indicating the concentration of strategic stations. As a result, introducing agglomeration forces seems to decrease the concentration of strategic metro stations in certain locations and the number of metro stations with zero appearances in the simulations. Overall, this comparative static experiment shows that introducing agglomeration forces leads the simulated annealing algorithm to converge towards an optimal metro pattern that goes through the city center, with fewer discernible strategic stations on the periphery.

Green indicates a positive change in frequency, while red indicates a negative change. The size of the dots is proportional to the absolute value of the frequency change.

IV.6 Egalitarian versus Utilitarian

In this subsection, I explore whether the maximization of utility by a planner, distinguishing between an egalitarian and an utilitarian approach, leads to different metro designs. Previous results used an economic impact factor based on rateable value gains and metro construction costs as the economic objective W. However, a planner can also build a metro network within a given budget $\mathcal{B}$, aiming to maximize an economic objective W. An utilitarian planner seeks to maximize the sum of the utilities of the two agents, treating all individuals as having equal weight within the city. Conversely, an egalitarian planner aims to maximize the minimum utility between the two agents, following a Rawlsian welfare approach that focuses on enhancing the well-being of the worst-off workers within the city. To investigate whether different planner objectives result in different metro designs, I define the following utilitarian planner maximization problem,

$$\begin{aligned} \max \quad & \widehat{\overline{U}}_H(M;\theta) + \widehat{\overline{U}}_L(M;\theta) \\ \text{subject to} \quad & \mathcal{B} \geq \text{Cost}(M), \end{aligned} \tag{2.32}$$

Figure 2.21
Comparative static: agglomeration forces

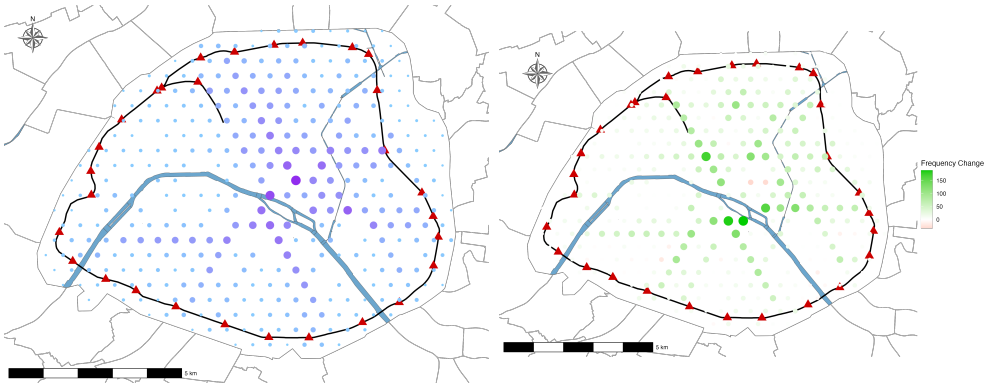

(a) Metro stations frequency **(b)** Strategic stations change

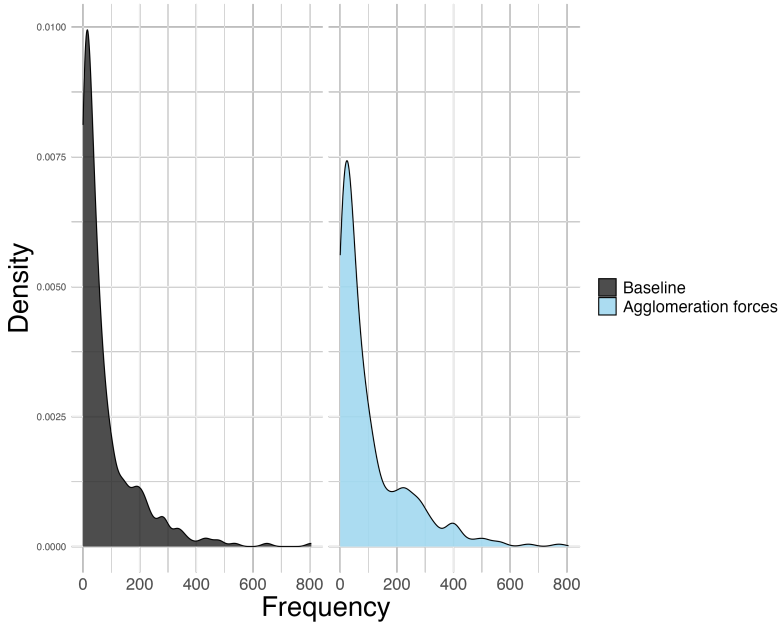

(c) Distribution of metro stations frequency

Notes: Panel (a) shows the frequency of metro stations occurring in the simulated annealing runs considering agglomeration forces. The size of each station is proportional to its frequency, with larger dots indicating higher frequency, while the varying shades of purple dots indicate different levels of station frequency. Panel (b) illustrates the change in frequency of metro stations between the baseline and the agglomeration forces scenario. Green indicates a positive change in frequency, while red indicates a negative change. The size of the dots is proportional to the absolute value of the frequency change. Panel (c) depicts the distribution of frequency in both the baseline and agglomeration forces scenarios.

and the following egalitarian planner maximization problem,

$$\begin{aligned} \max \quad & \min\left(\widehat{\overline{U}}_H(M;\theta), \widehat{\overline{U}}_L(M;\theta)\right) \\ \text{subject to} \quad & \mathcal{B} \geq \text{Cost}(M). \end{aligned} \tag{2.33}$$

In both equations, $\widehat{\overline{U}}_H$ and $\widehat{\overline{U}}_L$ represent the indirect utility change in percentage points for high-skilled and low-skilled workers, respectively. $\mathcal{B}$ denotes the total budget for metro construction, and $\text{Cost}(M)$ represents the construction costs of metro M.

Again, I sampled 500 metro networks using the simulated annealing algorithm for both an utilitarian and an egalitarian planner problem. Figure 2.22 shows the difference in metro station frequency between the utilitarian scenario and the egalitarian scenario. Blue dots indicate metro stations that appear more often in the utilitarian scenario than in the egalitarian scenario, while red dots indicate the opposite. This visualization clearly shows a two-sided pattern: metro stations in the west appear more frequently in the utilitarian scenario, whereas those in the east appear more frequently in the egalitarian scenario. As a consequence, the utilitarian scenario tends to implement more often a metro within locations that have high-level amenities for high-skilled workers, while the egalitarian scenario tends to implement more often a metro within locations that have high-level amenities for low-skilled workers. This overall pattern can be explained by the fact that, in an open city setting, an inflow of workers from the outside economy creates pressure on the housing market, increasing housing prices. Since low-skilled workers spend a relatively higher share of their income on housing, they suffer relatively more from an increase in housing prices. Hence, within the scenario of an utilitarian planner maximizing the sum of utilities, the change in expected utility for high-skilled workers will be relatively larger than that for low-skilled workers. As a consequence, this will drive the metro network design towards locations with a high level of amenities for high-skilled workers. Given that the egalitarian scenario maximizes the minimum utility between the two types of workers, the metro design converges on locations where the amenities of low-skilled workers are large, as their expected utility increases relatively less than that of high-skilled workers. Note that I find similar results when considering a maximization problem where a planner targets a specific type of workers with a weight z ($\max: \ (1-z)\times\widehat{\overline{U}}_H(M;\theta)+z\times\widehat{\overline{U}}_L(M;\theta)$). Specifically, when comparing a weight $z = 1$ (targeting low-skilled workers) with a weight $z = 0$ (targeting high-skilled workers), the difference in frequency displays the same pattern as in Figure 2.22 (see Figure B.5 in the appendix).

Figure 2.22
Difference between Utilitarian and Egalitarian sampled metro networks

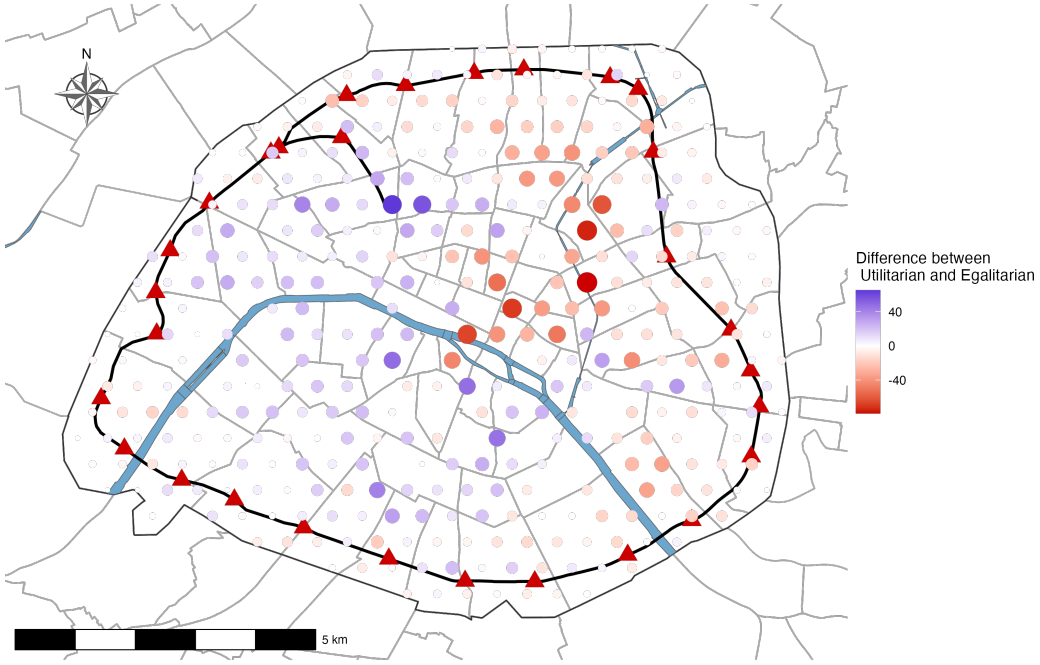

Notes: This figure shows the change in frequency of metro stations occurring in the simulated annealing runs between the Utilitarian and the Egalitarian scenarios. Blue indicates a positive change in frequency, while red indicates a negative change. The size of the dots is proportional to the absolute value of the frequency change.

V Comparison with metro network projects

Once the planner has sampled metros from $\mathcal{M}$, she can use this information to compute proximity indexes for her metro projects,

$$\text{Index}_m = \sum_s \left(\frac{wgt_s}{\text{Dist}_{sm}} \right), \tag{2.34}$$

with Dist_{sm} the distance between lines of the metro project m, and the potential metro stations s. Moreover, wgt_s is the station weight based on the frequency, which is specific to the simulated annealing algorithm parameters (represented in Figure 2.18 for the baseline results). Hence, this index aims to capture whether a metro project is more or less far from strategic metro locations resulting from runs of the SA algorithm. Since distance appears in the denominator, a higher index will translate to a greater proximity of the metro project to strategic metro stations.

Table 2.3 shows the indexes for the metro projects presented in section IV.1, and based on the different scenarios with general equilibrium and without agglomeration forces: maximization of economic impact factor (baseline results) in column (1), maximization of utility with an utilitarian planner in column (2), maximization of utility with an egalitarian planner in column (3). Column (4) shows the total length for each metro project, and the last 3 columns show the indexes normalized by the length.

Regarding the Fulgence Bienvenüe metro project, which was selected and implemented by public authorities, it exhibits a relatively high index in the baseline scenario that maximizes the economic impact factor, but a relatively low index in the utilitarian and egalitarian scenarios. This suggests that the adopted metro design by Fulgence Bienvenüe was not intended for a specific group of workers. Interestingly, the Alphand-Huet metro project (illustrated in Figure 2.7(b)) displays the highest index once standardized by metro length, regardless of the scenario considered. Hence, these simulations indicate that the Alphand-Huet metro project would outperform the Fulgence Bienvenüe metro project when considering project length. Moreover, the Léon Say metro project, the Alphand-Huet metro project, and the Council project exhibit a higher index for the utilitarian scenario compared to the egalitarian scenario. Hence, these projects appear to be more oriented toward high-skilled workers than low-skilled workers.

Table 2.3
Metro projects

Metro project	General	Uti	Ega	Length (km)	Normalized Index		
	(1)	(2)	(3)	(4)	(1)/(4)	(2)/(4)	(3)/(4)
Léon Say	3.51	3.87	3.80	21.22	0.17	0.18	0.18
Alphand-Huet	6.92	7.64	7.52	27.94	0.25	0.27	0.27
Council 1883	6.62	7.17	7.15	63.01	0.11	0.11	0.11
Fulgence Bienvenüe	12.68	11.27	11.75	57.90	0.22	0.19	0.20

VI Conclusion

This paper connects the quantitative urban model literature with a simulated annealing algorithm to identify optimal urban transport infrastructure design. The developed framework incorporates general equilibrium effects induced by improvements in commuting costs, enabling the identification of strategic within-city locations for urban transport design that maximize workers' welfare. By applying this framework to historical Paris and a numerical example, results show that strategic metro stations are predominantly located within areas of high centrality, high productivity, and high amenities.

A potential application of this framework is the use of strategic station locations as instrumental variables, given that they are driven by welfare considerations. This approach allows to differentiate parts of the network designed to maximize well-being from those influenced by other non-random factors, thereby offering valuable insights for urban planning and policy-making.

Chapter 3

Racial Preferences and Local Public Goods

Acknowledgements

I am particulary grateful to Clément Bosquet for his guidance and support. I benefited from conversations with Pierre-Philippe Combes, Stephan Heblich, Camille Hémet, Gabriel Loumeau, Fabien Moizeau, and Clara Santamaria. I thank participants of DESIR seminar, Doctorissimes, PSE Interdisciplinary Worshop: Neighborhoods and Local Interactions, JMA, and AFSE annual congress for their valuable comments and suggestions. Responsibility for results, opinions and errors lies with the author alone.

I Introduction

Racial segregation across United States (U.S.) cities persists over time and exhibits significant disparities (Cutler et al., 1999). Figure 3.1 illustrates this pattern by comparing the dissimilarity index measuring segregation between blacks and whites in 1990 and 2010 across 265 core-based statistical areas (CBSAs). While there is an overall decline in racial segregation over these 20 years, 50% of CBSAs experienced an absolute change of 0.06 or less in the dissimilarity index. Hence, only a few cities experienced substantial shifts in racial segregation.

Figure 3.1
Racial segregation in U.S cities 1990-2010

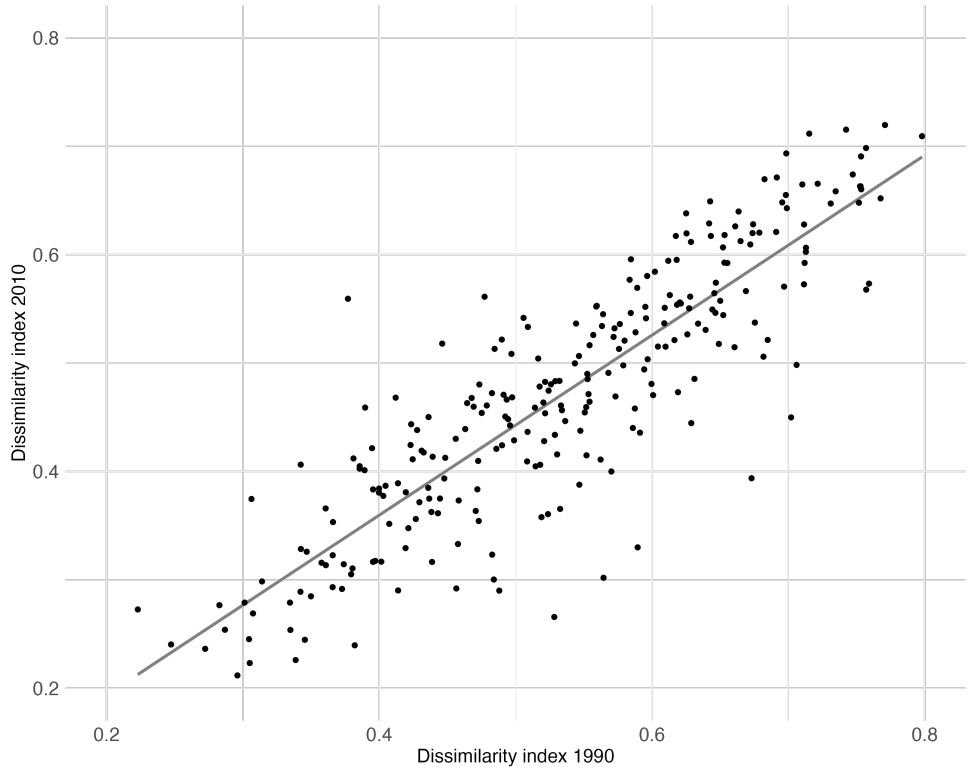

Notes: This figure illustrates the correlation between racial segregation in 1990 and 2010 for U.S. Core-Based Statistical Areas (CBSAs). Each black dot represents a CBSA. The measure of racial segregation is derived from a dissimilarity index between whites and blacks, using census tract data based on 2010 geography.

Natural amenities emerge as a candidate to explain the persistence of racial segregation over time and its variation across cities, since they represent a persistent factor influencing within-city sorting (Lee and Lin, 2018). In 2010, racial segregation was, on average, 5.4 percentage points higher in coastal cities than in interior cities, highlighting the potential role of natural amenities in shaping differences in racial segregation patterns, given that coastal cities are more abundant in natural amenities. Beyond city-level differences, natural amenities also shape racial sorting within cities. Neighborhoods near persistent natural features like coastlines, lakes, rivers, and hills tend to have a higher proportion of white residents compared to other neighborhoods. The average difference was 5.5 percentage points in 1990 and increased to 6.4 percentage points in 2010. Overall, these patterns suggest that natural amenities contribute to racial sorting by making certain neighborhoods more predominantly white, ultimately increasing racial segregation between blacks and whites.

Two potential channels could explain this result. First, natural amenities can increase rent and endogenous amenities through a market effect resulting from higher demand from households for these locations. Second, natural amenities can represent a local

public good creating ethnic division through an exclusion effect. For example, natural amenities could increase racial hostility from whites towards blacks since they want to keep privileged access and do not want to share the local public good. This mechanism aligns with the public goods complementarity described by Albouy et al. (2020).

This paper explores whether natural amenities play a role in shaping racial sorting and racial segregation within the U.S., considering these two channels, namely the market effect and the exclusion effect, and assuming that the place of residence determines (almost entirely) the access to these natural amenities.

In a first step, I exploit spatial variation in natural amenities abundance and anti-black attitudes to shed light on market and exclusion effects created by natural amenities. Changes in anti-black attitudes are proxied by the city-wide expansion of Confederate monuments over time. Since Confederate monuments represent symbols of oppression and are dedicated by local authorities (as documented by Henderson et al. (2021b) and Ferlenga (2023)), a higher level should reflect a higher hostility from whites toward blacks and a greater possibility for whites to exclude blacks from their neighborhoods to maintain this privileged access. To do so, I use a database with consistent-boundary neighborhoods in several U.S. metropolitan areas, spanning the census years from 1880 to 2010. These data contain racial information, spatial information on many persistent natural features, and the city-wide number of Confederate monuments.

In a second step, I use a quantitative spatial model of heterogeneous agents on 16 of the 17 largest cities covering 29% of the urban population commuting flows.[1] This general equilibrium model of within-city commuting choices allows me to recover amenities and to quantify racial preferences as well as their interactions with natural amenities, by exploiting variation across neighborhoods. Finally, I conduct two counterfactual exercises to investigate the role of racial preferences on racial segregation within these U.S. cities.

This paper provides evidence that natural amenities have a major influence on racial sorting. Reduced-form results suggest that both channels of natural amenities are at play. First, regarding the market effect, neighborhoods that have access to natural amenities are, on average, more white by 2.2 percentage points compared to other neighborhoods within a city over the 1880-2010 period. Second, regarding the exclusion effect, neighborhoods close to natural amenities experience a 5.4 percentage point increase in their white shares following a one standard deviation increase in citywide Confederate monuments.

[1] I exclude New York from the analysis because I don't observe the commuting time matrix between census tracts.

Structural analysis then highlights that racial preferences matter when explaining residential choices of blacks and whites. Exploiting the variation across neighborhoods of amenities recovered from the quantitative spatial model, I find strong and significant homophily parameters for both groups of residents, with a higher parameter for whites. I find that the average semi-elasticity of amenities with respect to the white share is 0.5 for whites and -0.26 for blacks. On average, a 10 percentage point increase in the neighborhood white share is associated with a 5% increase in amenities for whites, while it is associated with a 2.6% decrease in amenities for blacks. This is consistent with the idea that whites place more importance on the racial composition of the neighborhood (Krysan and Farley, 2002; Ihlanfeldt and Scafidi, 2002). In addition, I find a positive effect of natural features proximity (such as coastlines, lakes, rivers, and hills) on structural amenities, and a complementarity effect with respect to racial composition. For both black and white residents, the presence of their own racial group in the neighborhood makes access to a local public good even more valuable. For blacks, I estimate a positive marginal effect of natural amenities, with a white share turning point of 0.95; beyond this threshold, they no longer value proximity to natural amenities. Similarly, I estimate a positive marginal effect for whites, with a turning point of 0.71. These results highlight the role of racial composition in unlocking local public goods (Albouy et al., 2020). In a first counterfactual exercise, I show that removing this complementarity effect between racial composition and natural amenities leads to a decrease in the white share within neighborhoods near natural amenities. As a consequence, it improves the access of black residents to natural amenities. However, through general equilibrium effects, it leads to a small (yet non-statistically significant) increase in racial segregation of 2.4 percentage points, since homophily parameters are still at play. The second counterfactual exercise shows that, on average, removing racial preferences and the complementarity effect reduces racial segregation by 11.6 percentage points. Overall, these results suggest that racial preferences and natural amenities play an important role in determining the spatial structure through residential choices.

My paper connects to several strands of existing research. First, this study is related to the literature on neighborhood sorting. For income sorting, previous work has highlighted the role of historical amenities (Brueckner et al., 1999; Gaigné et al., 2022), transportation (Baum-Snow, 2007), aging houses (Brueckner and Rosenthal, 2009), and endogenous amenities, especially non-tradable services (Couture and Handbury, 2020; Baum-Snow and Hartley, 2020). For racial sorting, studies have shown the importance of collective action by whites in the development of urban neighborhoods (Sood et al., 2019; Aaronson

et al., 2021), and whites' racial preferences (Card et al., 2008; Boustan, 2010). My work relates to the seminal paper by Lee and Lin (2018), which provides evidence on the role of natural amenities in income segregation and income sorting. However, my paper bridges these two literature and distinguishes itself from Lee and Lin (2018) by investigating the role of natural amenities in spatial sorting by race on top of income, as I control for the latter. Moreover, despite a strong correlation between the two, Aliprantis et al. (2022) explains that financial constraints, such as high housing prices, are not the reason why high-income black households live in neighborhoods of similar quality to low-income white households. Instead, the role of racial preferences matters for understanding racial sorting. In other words, blacks trade-off neighborhood quality with racial composition, in order to not suffer racial prejudice. In this vein, my analysis of natural amenities and their interaction with racial preferences through an exclusion effect allows us to delve deeper than Lee and Lin (2018). Second, this work connects to the long-lasting literature on ethnic diversity and public goods. Literature has investigated the impact of ethnic diversity on economic growth through cross-country comparisons (Easterly and Levine, 1997; Alesina et al., 2003), productivity (Ottaviano and Peri, 2006; Peri, 2012), local public goods provision and neighborhood quality (Alesina et al., 1999; Miguel and Gugerty, 2005; Algan et al., 2016; Alesina et al., 2019; Hennig, 2021), and preferences and social behavior (Alesina et al., 2021; Egorov et al., 2021). However, this paper takes the relationship in the opposite direction by looking at whether proximity to fixed local public goods, such as natural amenities, can influence ethnic diversity by examining neighborhood racial composition. Finally, my study relates to the ongoing literature on within-city quantitative spatial models. Recent works have developed heterogeneous agents models to study transit improvements (Tsivanidis, 2024; Loumeau, 2024; Balboni et al., 2020), public housing policies (Almagro et al., 2023), path dependency (Heblich et al., 2021), and neighborhood effects (Bayer et al., 2022; Redding and Sturm, 2024). My setup relates to Bagagli (2023) and Weiwu (2024), which also estimate racial preference parameters. Both papers focus on highway improvements as a source of variation for estimating homophily parameters. The former focuses on Chicago without observing workplace employment data (i.e. where workers work) and makes the assumption of a monocentric city, while the latter focuses on 25 U.S. cities with several workplaces but in a historical setting. By contrast, my paper focuses on a contemporaneous context with 2010 LODES data, allowing observation of workplace and residence employment at the census tract level for the 16 largest CBSAs (except for New York).[2] My strategy relies on within-city variation

[2] The LEHD Origin-Destination Employment Statistics (LODES) data provide information over com-

across neighborhoods to estimate racial preferences. Additionally, I investigate whether first-nature factors, such as natural amenities, increase endogenous forces.

The remainder of the paper is organized as follows. Section II provides a description of my database and a brief review of the historical context of racial discrimination through the lens of natural amenities. Section III shows how natural amenities influence racial segregation and racial sorting. Section IV presents a heterogeneous agents quantitative spatial model to estimate racial preferences and undertake counterfactual exercises. Finally, Section V summarizes the main results and discusses the role of natural amenities.

II Data and historical context

In this section, I introduce the data used to conduct the analysis. Then, I briefly present historical events suggesting that natural amenities have been subject to racial conflict within the U.S.

II.1 Data and stylized facts

Geography I test whether natural amenities have an impact on racial composition through market and exclusion effects with a database of decennial census tracts from 1880 to 2010 with consistent boundaries. Census tracts are small geographic units similar to neighborhoods with a population size between 1,200 and 8,000 people, providing consistency over time. The normalization to 2010 neighborhood boundaries is ensured through different crosswalks provided by Lee and Lin (2018) and the Longitudinal Tract Data Base project.[3] This gives me an unbalanced panel dataset due to growing cities and census coverage with more complete data from 1960 onwards, as Table 3.1 details. There is no data for 1890 and 1900. Each neighborhood is assigned to a single city (metropolitan area) according to the Office of Management and Budget's definitions of core-based statistical areas (CBSAs) from December 2009.[4]

Race I recover race data from IPUMS (American Community Survey and National Historical Geographic Information System) for the entire period, and I use this information

muting flows of workers by race.

[3] For example, they calculate average household income in 1940 for each 2010 tract by weighting the average household income reported for overlapping 1940 census tracts, where the weights are determined by overlapping land area.

[4] Some CBSAs are aggregated; for example, the Los Angeles-Long Beach-Santa Ana CBSA is combined with the Oxnard-Thousand Oaks-Ventura and Riverside-San Bernardino-Ontario CBSAs.

to compute the white share and two measures of racial segregation between blacks and whites at the city level. First, I consider a dissimilarity index (Duncan and Duncan, 1955) between whites and blacks,

$$\text{Dissimilarity}_m^{BW} = \frac{1}{2}\sum_{n=1}^{N}\left|\frac{b_n}{B_m} - \frac{w_n}{W_m}\right|, \tag{3.1}$$

where N is the number of tracts within the city m, w_n (resp. b_n) is the number of whites (resp. blacks) in the tract n, W_m (resp. B_m) is the total number of whites (resp. blacks) within the city m. The index measures the share of black residents that would need to change neighborhoods in order for all neighborhoods to reflect the demographics of the city as a whole. However, the dissimilarity index presents several issues; in particular, it is insensitive to racial permutations between neighborhoods.

Second, I consider a distance segregation index (White, 1983; Harari, 2024) as another measure of racial segregation,

$$\text{Distance}_m^{BW} = \frac{\sum_i D_i^W \mathbb{1}_{i\in S_B}}{\sum_i \mathbb{1}_{i\in S_B}}, \tag{3.2}$$

with $D_i^W \equiv \frac{\sum_j d_{ij}\mathbb{1}_{j\in S_W}}{\sum_j \mathbb{1}_{j\in S_W}}$. The subscript B corresponds to a black neighborhood (where the proportion of whites is less than 50%), and the subscript W corresponds to a white neighborhood (where the proportion of whites is greater than or equal to 50%), S_g is the set of neighborhoods of type g, and $d_{i,j}$ is the Euclidean distance between neighborhood i and neighborhood j. Overall, Distance_m^{BW} represents the distance segregation index between groups B and W for city m, which is the average distance between B and W neighborhoods.

Both racial segregation indexes aim to capture different patterns of segregation. The dissimilarity index focuses on the racial composition of a neighborhood with respect to the city level, while the distance index provides information on the spatial proximity between the two groups. However, Figure 3.2 displays their correlation conditional on the year and shows a positive and strong correlation between both indexes. Cities displaying a higher level of racial segregation, as measured by the dissimilarity index, are also cities where blacks are more distance-segregated from whites.

Natural amenities and other neighborhoods characteristics I obtain all necessary controls, such as population density, distances to the nearest seaport and the central

Figure 3.2
Distance and dissimilarity indexes

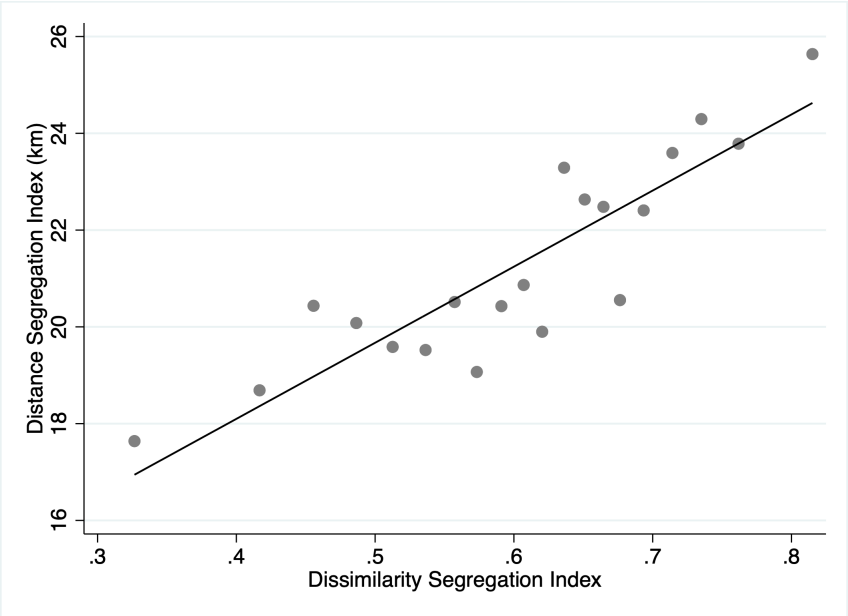

Notes: This figure presents a binned scatter plot illustrating the city-level correlation between the dissimilarity index for whites and blacks and the distance segregation index between majority white and majority non-white neighborhoods over the period from 1880 to 2010. The regression includes year fixed effects.

business district (CBD), and the median income, from Lee and Lin (2018)'s database. It also provides information on a large number of highly visible and persistent natural amenities: the distance from the neighborhood centroid to the nearest (1) coastline (i.e., the Atlantic or Pacific Ocean, the Gulf of Mexico, or a Great Lake), (2) (non-Great) lake, and (3) major river. They also calculate (4) the average slope, (5) the flood-hazard risk, (6) the average 1971–2000 annual precipitation, (7) July maximum temperature, and (8) January minimum temperature. Finally, Lee and Lin (2018) also provides a rank of tracts based on average household income within each metropolitan area, which allows me to control for endogenous amenities. In historical census years 1880–1940, income data are not available. For 1930 and 1940, Lee and Lin (2018) uses average housing rents to rank tracts. In 1880–1920, lacking data on both income and prices, Lee and Lin (2018) uses an imputed occupational income score or the literacy rate. The assumption behind these substitutions is that the ordering of average income among neighborhoods is the same as that of housing rent, occupational income score, or the literacy rate.

Overall, this rich database of 61,082 neighborhoods across 308 CBSAs from 1880 to 2010 enables me to study racial dynamics at the neighborhood and city levels within the U.S. with a long-term perspective. The variety of information on proximity to natural features allows for the distinction between neighborhoods that are rich in natural amenities and those that are not. While the number of observations used in my empirical analysis varies

across periods due to data availability, the share of neighborhoods having access to a natural feature is relatively stable over time, as Table 3.1 indicates. The level of racial segregation, as measured by the dissimilarity index, differs from what Cutler et al. (1999) found due to differences in data availability and geographic precision, but the trends are roughly similar with distinct periods.[5] Since the distance segregation index is a function of city size, it varies widely due to the variation in the CBSAs sample. The last column of Table 3.1 accounts for the city size effect by normalizing the distance segregation index of a city with the average distance between two neighborhoods within the city. While the dissimilarity segregation index decreased over time, the distance segregation index slightly increased from 1950 to 2010.

Table 3.1
Population, Neighborhoods and Dissimilarity Index in U.S.

	Metropolitans Areas			Neighborhoods			Racial Segregation		
Year	Total	Population	U.S	Total	Coastal	N.A	Dissimilarity	Distance	Norm.
1880	26	6,284,298	12.52%	2,795	15.71%	23.26%	0.32	7.0	1.10
1910	1	4,695,832	5.09%	1,748	18.19%	20.65%	0.62	12.7	0.89
1920	2	8,253,532	7.78%	2,505	16.73%	19.56%	0.78	12.5	0.92
1930	10	8,249,909	6.72%	1,808	10.95%	20.08%	0.71	6.1	0.84
1940	43	36,076,605	27.30%	11,527	8.12%	19.53%	0.66	9.4	0.89
1950	51	52,247,779	34.67%	17,681	7.41%	18.38%	0.71	12.5	0.86
1960	136	102,771,452	57.31%	38,669	5.27%	17.94%	0.72	16.0	0.88
1970	229	143,187,161	70.40%	49,888	5.01%	18.44%	0.68	18.4	0.87
1980	277	166,237,695	73.38%	56,176	5.00%	19.19%	0.60	20.8	0.86
1990	308	192,328,911	77.33%	60,299	4.77%	19.63%	0.54	24.2	0.87
2000	308	239,146,648	84.98%	60,766	4.74%	19.65%	0.51	24.8	0.91
2010	308	264,609,448	85.70%	60,757	4.72%	19.63%	0.46	25.4	0.91

Notes: This table presents information at the neighborhood level, sourced from IPUMS data. The geospatial information on natural amenities is derived from Lee and Lin (2018) database. The neighborhoods are normalized to 2010 neighborhood boundaries. The "Coastal" column indicates whether a neighborhood is coastal if its centroid is within 500 meters of an ocean, the Gulf of Mexico, or a Great Lake. The "N.A" column indicates whether a neighborhood's centroid is within 500 meters of a coast, a river, a lake, or a hill. The "Dissimilarity" column represents the average dissimilarity index calculated between whites and blacks. The "Distance" column shows the average distance segregation between white and non-white neighborhoods. The last column represents the distance segregation index normalized by the average distance within the city.

Confederate monuments Lastly, I use data from the Southern Policy Law Center to document Confederate monuments in the United States. This allows me to approximate anti-black attitudes over time across U.S. cities (Henderson et al., 2021b; Ferlenga, 2023). Figure 3.3 shows their spatial expansion. Initially, they were concentrated in the South region, and then they progressively expanded towards the rest of the territory. I document the location of Confederate monuments (see Table C.1 in the appendix for the empirical specification and complete results) and find that, on average, neighborhoods close to the city center and close to the coast are more likely to receive a Confederate monument. These two features suggest that there might be a strategy behind the dedica-

[5] They use census blocks, which provides more precision compared to census tracts.

tion of Confederate monuments to signal anti-black attitudes, as locations close to the city center maximize exposure and locations close to the coast have higher levels of natural amenities.

II.2 Historical context: racial preferences and natural amenities

Natural amenities might reinforce racial sorting and, ultimately, racial segregation through two channels. Their perceived value to households can increase the rent of neighborhoods near natural amenities through a market effect. Moreover, it can reasonably be argued that natural amenities may be subject to racial conflict since they represent a local public good.

During the Jim Crow era (1877-1964), local governments across the United States enacted a host of policies and practices designed to segregate places of outdoor leisure (such as natural amenities) by race.[6] Beaches illustrate how natural amenities may create an exclusion effect. As Kahrl (2018) documented, the American coastline has long been a flashpoint of racial conflict and contestation since many cities prohibited blacks from stepping on beaches. For example, the Chicago race riot of 1919, which lasted seven days and killed 38 people, began on the shores of Lake Michigan when members of a gang of white youths stoned a black teenager to death after he accidentally crossed a color line in the water. Another example is the non-violent wade-ins movements in the 1950s, which aimed to demand leisure access for blacks.[7] As a result, the Kerner Commission listed "poor recreation facilities and programs," which include the lack of access to natural amenities, as the fifth most intense grievance of black populations (behind policing practices, unemployment and underemployment, housing, and education).

Before the end of the Jim Crow era, these exclusion mechanisms were explicit and legal. But even after the Civil Rights Act of 1964, cities used different strategies to keep natural amenities segregated, such as pricing (parking fees), quotas (number of passes sold to non-residents), or even illegal actions such as violence.[8]

[6] Jim Crow laws were national and local laws enacted by Southern state legislatures from 1877 to 1964. These laws were put in place to restrict the constitutional rights of African Americans acquired after the Civil War. See Althoff and Reichardt (2022) for an analysis of their long-term consequences.

[7] Even if separated beaches were established for blacks, they were small, far away, and sometimes dangerous. For example, in New Orleans, the city-designated black beach was an area grossly polluted with sewage from nearby fishing camps.

[8] An example is the Lunada Bay Boys, a gang of wealthy white Californians who, for several decades, have engaged in a terror campaign by assaulting and harassing non-residents, particularly African Americans, seeking access to the city's public beach, all with the tacit approval of local law enforcement.

Figure 3.3
Spatial expansion of Confederate monuments within the U.S.

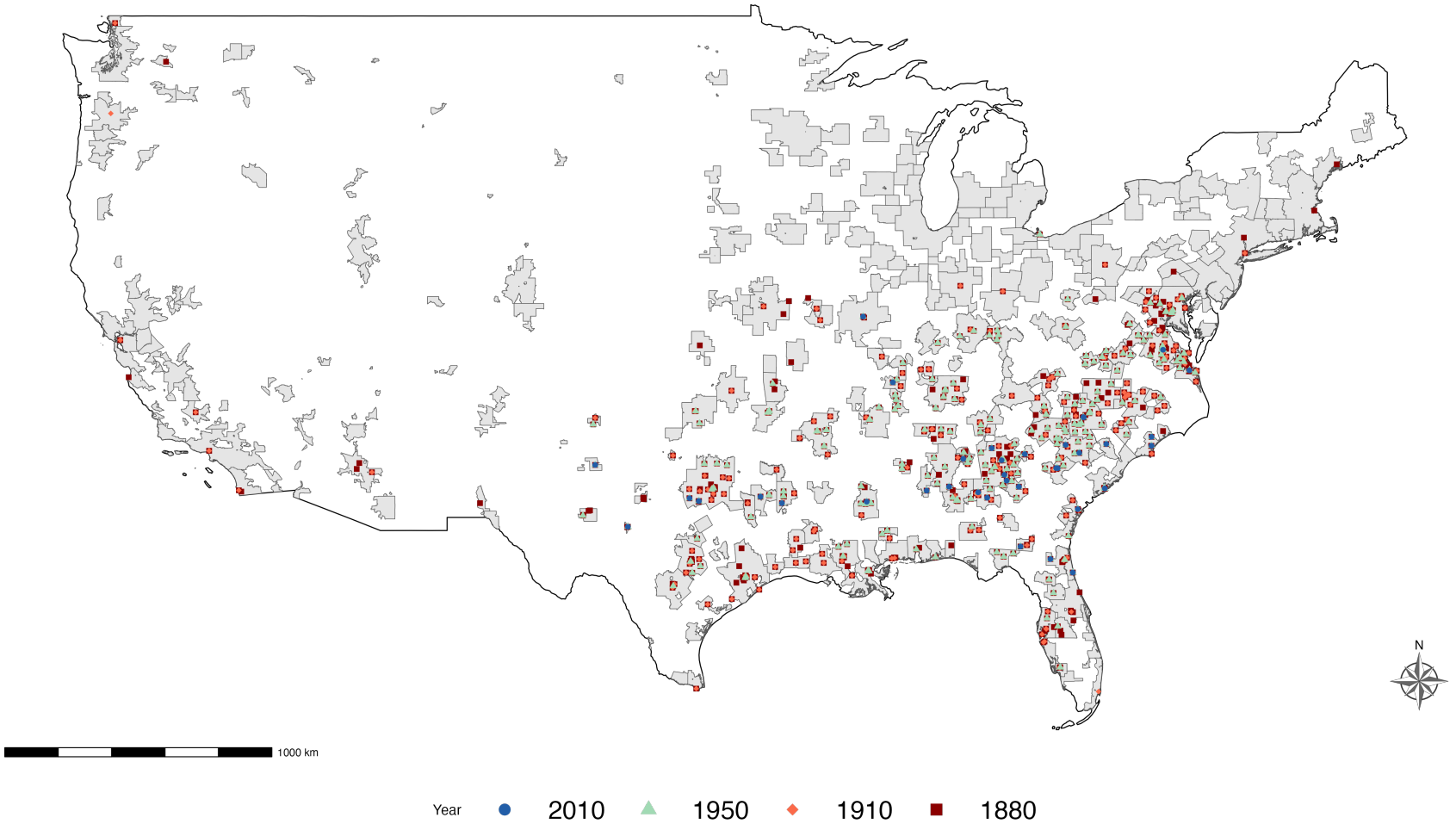

Notes: This figure illustrates the spatial expansion of Confederate monuments over time within the United States. Each shape represents a Confederate monument, with different colors indicating the time period of their establishment: red square for 1880, orange diamond for 1910, light green triangle for 1950, and blue dot for 2010. Grey areas represent Core-Based Statistical Areas (CBSAs) as observed in 2010.

Thereby, this persistence effect on racial sorting and racial segregation seems to be a combination of a market effect and an exclusion effect induced by public policies, collective actions, and individual actions that aimed to segregate natural amenities by race. Many of these policies and practices persist over time, and removing these restrictions is fundamental to ensuring that these natural amenities are truly public.

III Reduced-form evidence

In this section, I test whether natural amenities imply higher racial segregation at the city level. Then, I investigate whether they impact racial sorting at the neighborhood level.

III.1 City-wide racial segregation

III.1.1 Natural amenities

In order to investigate whether natural amenities abundance increases city-wide racial segregation over the 1880-2010 period, I run the following specification:

$$D_{m,t} = \theta_t + \beta \, \text{NA}_m + X_{m,t}\gamma + \epsilon_{m,t}, \tag{3.3}$$

where $D_{m,t}$ is the racial segregation index between blacks and whites within city m at time t (either the dissimilarity index equation (3.1) or the distance index equation (3.2)), NA_m is a variable indicating if city m is abundant in terms of natural amenities, $X_{m,t}$ is a vector of time-varying controls at the city level, and θ_t represents time fixed effects. The standard errors $\epsilon_{m,t}$ are clustered at the city level. The coefficient of interest β is estimated through variation in natural amenities between cities.

Table 3.2 shows the results for both the dissimilarity segregation index and the distance segregation index. First, I consider a simple dummy variable indicating the coastal status of city m, since coastal cities are naturally more abundant in natural amenities than interior cities. In column (1), blacks are more distance-segregated from whites by, on average, 6 km compared to interior cities. In column (5), coastal cities are, on average, 6.1 percentage points more racially segregated compared to interior cities. According to both measures, racial segregation is higher in coastal cities compared to interior cities. However, interior and coastal cities may have different characteristics in terms of total population, area, and total number of blacks due to natural advantages (Bleakley and Lin, 2012) or housing constraints (Saiz, 2010), for example. Therefore, this would bias the estimation of the effect of natural amenities' abundance on racial segregation. Moreover,

population and area significantly influence city-wide dissimilarity in racial segregation, with larger and denser cities having higher levels of racial segregation, as shown by Cutler et al. (1999). Additionally, the distance segregation index is mechanically correlated with city size. Hence, I control for the log of the total number of neighborhoods, the log of the total area, the log of the total population, and the log of the total number of blacks to correct the effect of natural amenities on both racial segregation indexes. I also complement these controls with the number of highway rays (Baum-Snow, 2007) to capture suburbanization during this period, enabling the separation between whites and blacks within cities (Boustan, 2010; Mahajan, 2024). After controlling for these factors in columns (2) and (6), the effect associated with the coastal status remains positive and significant for both racial segregation measures. According to the distance index, blacks are more distance-segregated from whites by, on average, 2.6 km compared to interior cities, everything else being equal. According to the dissimilarity index, coastal cities are, on average, 2.8 percentage points more racially segregated than interior cities, everything else being equal. Finally, I use a continuous measure of natural amenities, which is the share of neighborhoods having access to a coastline, a lake, a river, or being over a hill. In addition, I add its squared term to capture the diminishing marginal effect due to the market effect. A higher share of neighborhoods near natural amenities makes the advantage of these neighborhoods less salient in the market. Estimated coefficients in columns (3) for the distance index and (7) for the dissimilarity index suggest that cities that have a higher share of neighborhoods with access to natural amenities are more racially segregated. As expected, the marginal effect is decreasing due to the negative coefficient associated with the squared term (with a turning point of approximately 0.35 for both indexes). Adding controls in columns (4) and (8) decreases the magnitude of the estimated effect on both indexes. I don't find any heterogeneity over time when investigating the differences in racial segregation between coastal and interior cities (see Figure C.4 in the appendix).

Table 3.2
Natural amenities and racial segregation

	Distance				Dissimilarity			
	(1)	(2)	(3)	(4)	(5)	(6)	(7)	(8)
$\mathbb{1}_m^{Coast}$	6.017***	2.616***			0.061***	0.028**		
	(1.546)	(0.962)			(0.016)	(0.014)		
% NA neigh.			27.320***	10.538*			0.163*	0.094
			(10.092)	(6.300)			(0.097)	(0.088)
(% NA neigh.)^2			-38.851***	-13.178*			-0.224**	-0.066
			(12.287)	(7.575)			(0.104)	(0.092)
Year FE	Yes	Yes	Yes	Yes	Yes	Yes	Yes	Yes
Set of Controls	○	✓	○	✓	○	✓	○	✓
Mean Seg.	21.32	21.32	21.32	21.32	0.57	0.57	0.57	0.57
R^2	0.229	0.572	0.186	0.565	0.374	0.533	0.350	0.530
Observations	1,096	1,018	1,096	1,018	1,521	1,405	1,521	1,405

Notes: Each column reports estimates from separate regressions. The dependent variable from columns (1) to (4) is the distance segregation index between blacks and whites. All estimations include year fixed effects. The dependent variable from columns (5) to (8) is the dissimilarity index between blacks and whites. Controls include the log total number of neighborhoods, the log total area, the log of the total population, the log of the total number of blacks, and the total number of highway rays. The independent variable in columns (1)-(2) and (5)-(6) is a dummy variable indicating coastal city status. The independent variable in columns (3)-(4) and (7)-(8) is the share of neighborhoods having access to natural amenities (coastline, lake, hill, river). Standard errors are clustered by city, and ***, **, * indicate significance at the 1%, 5%, and 10% levels, respectively.

III.1.2 Confederate monuments

Then, I investigate whether the implementation of Confederate monuments increases city-wide racial segregation over the 1880-2010 period. To do so, I run the following difference-in-difference empirical specification:

$$D_{m,t} = \alpha_m + \theta_t + \beta \, \text{CM}_{m,t} + X_{m,t}\gamma + \epsilon_{m,t}, \tag{3.4}$$

where the variable of interest $\text{CM}_{m,t}$ is the total number of Confederate monuments within a city m at time t, and I now include city fixed effects compare to the previous equation (3.3).

Therefore, the coefficient of interest β is estimated through within-city variation in Confederate monuments. As shown by Ferlenga (2023), Confederate monuments are symbols of white oppression toward blacks, and their dedication reflects the racial prejudice in the air. This is primarily due to the symbols of support for slavery that these monuments represent.

Table 3.3 shows the results for both the dissimilarity segregation index and the distance segregation index. Overall, there is a positive and significant effect of the implementation of Confederate monuments on racial segregation. In column (1), a one-unit increase in the number of Confederate monuments increases, on average, by 266 meters the average distance of blacks from whites within the city. In column (4), a one-unit increase in the

number of Confederate monuments increases, on average, by 0.2 percentage points the dissimilarity index within the city. Adding the same controls as in the previous empirical specification (3.3) in columns (2) and (5) decreases the magnitude of the estimated coefficients. However, I explore the heterogeneity between cities based on their coastal status, as cities with more abundant natural amenities may have a greater incentive to exclude minority groups to maintain privileged access to them. After controlling for city characteristics, I find that coastal cities experience an increase in distance segregation following an increase in Confederate monuments, whereas the effect for interior cities remains statistically indistinguishable from zero. However, there is no heterogeneity effect by coastal status for the dissimilarity index.

Table 3.3

Confederate monuments and racial segregation

	Distance			Dissimilarity		
	(1)	(2)	(3)	(4)	(5)	(6)
CM	0.266*	0.005	0.051	0.002***	0.001	0.001
	(0.142)	(0.097)	(0.087)	(0.001)	(0.001)	(0.001)
$\mathbb{1}_m^{Coast} \times$ CM			0.537***			-0.001
			(0.199)			(0.003)
Year FE	Yes	Yes	Yes	Yes	Yes	Yes
MSA FE	Yes	Yes	Yes	Yes	Yes	Yes
Set of Controls	○	✓	✓	○	✓	✓
Mean Seg.	21.32	21.32	21.32	0.57	0.57	0.57
R^2	0.904	0.940	0.941	0.882	0.909	0.909
Observations	1,078	1,000	1,000	1,509	1,393	1,393

Notes: Each column reports estimates from separate regressions. The dependent variable from columns (1) to (3) is the distance segregation index between blacks and whites. All estimations include year and city fixed effects. The dependent variable from columns (4) to (6) is the dissimilarity index between blacks and whites. Controls include the log total number of neighborhoods, the log total area, the log of the total population, the log of the total number of blacks, and the total number of highway rays. The independent variable is the total number of Confederate monuments within the city. $\mathbb{1}_m^{Coast}$ is a dummy variable indicating the coastal status of the city. Standard errors are clustered by city, and ***, **, * indicate significance at the 1%, 5%, and 10% levels, respectively.

III.2 Racial sorting

III.2.1 Empirical strategy

To test if natural amenities influence neighborhood racial sorting over time through a market effect and an exclusion effect, I implement the following empirical specification,

$$s_{n(m),t} = \beta_1 \, \mathbb{1}_{n(m)}^{NA} + \beta_2 \, \mathbb{1}_{n(m)}^{NA} \times \text{CM}_{m,t} + X_{n(m),t}\gamma + \delta_{m,t} + \epsilon_{n(m),t}, \tag{3.5}$$

where the dependent variable $s_{n(m),t}$ is the white share of neighborhood n in city m in period t, the dummy $\mathbb{1}_{n(m)}^{NA}$ indicates whether neighborhood n within city m has access

to a coastline, a lake, a river, or is over a hill.[9] $CM_{m,t}$ is the number of Confederate monuments within city m at time t, which is used as a proxy for city-level anti-black attitudes. The city-year fixed effect $\delta_{m,t}$ ensures that the identification comes from within the city, and I control for a vector of neighborhood characteristics $X_{n(m),t}$. The standard errors $\epsilon_{n(m),t}$ are clustered at the fixed effect level to allow for correlations between error terms within the city each year.

There are two coefficients of interest in this specification. First, β_1, which is estimated by comparing neighborhoods abundant in natural amenities to other neighborhoods, aims to capture the market effect induced by natural amenities. Access to natural amenities makes it less affordable to live in these neighborhoods, especially for blacks, who have, on average, lower incomes than whites. Second, β_2 from the interaction between the natural amenities dummy and the city-wide Confederate monuments aims to capture the exclusion effect of natural amenities. The coefficient is estimated through variation in Confederate monuments across cities and over time. Ferlenga (2023) finds causal evidence that Confederate monument dedication creates an outmigration of blacks at the county level. I confirm these results by investigating the effect of Confederate monument dedication on the neighborhood white share (see event-study plots of Figure C.3 in the appendix). Therefore, because Confederate monuments are related to anti-black attitudes, I assume that an increase in Confederate monuments is associated with a greater likelihood of white individuals exhibiting actions or hostility aimed at excluding blacks from their neighborhoods. In addition, the willingness of whites to exclude blacks is assumed to be even greater in the presence of local public goods such as natural amenities.

III.2.2 Baseline results

Table 3.4 reports the baseline results. In the simplest specification (without the interaction term) in column (1), there is a positive and significant coefficient associated with the natural amenities dummy, suggesting that, on average, neighborhoods near natural amenities are 3.5 percentage points more white than other neighborhoods. Overall, natural amenities influence racial sorting by making neighborhoods more white, but this aggregate effect includes both market and exclusion channels. In order to disentangle these effects, I control for the interaction between natural amenities and Confederate monuments in column (2). The estimated coefficient of the interaction term between Confederate monuments and the natural amenities dummy is positive and significant, and the coefficient associated

[9] The neighborhood is within 500 meters of a natural feature such as an ocean, the Gulf of Mexico, a lake, a major river, or has an average slope greater than 15°.

with natural amenities, capturing the market effect, remains similar in magnitude. This suggests that the increase in anti-black attitudes within the city amplifies the sorting of whites towards neighborhoods abundant in natural amenities. On average, a one standard deviation increase in Confederate monuments makes neighborhoods near natural amenities 0.6 percentage points more white compared to other neighborhoods. In column (3), I control for neighborhood characteristics, such as distance to the nearest seaport (interacted with metropolitan coastal status), distance to the Central Business District, population density, and income percentile rank (capturing better endogenous amenities and infrastructure) in order to reduce omitted variable bias. This allows for the disentangling of income effects from racial composition effects due to the strong correlation between both. Both coefficients associated with the market and exclusion effects decrease in magnitude but still remain positive and significant. I apply the Oster (2019) test for unobservables by comparing the variation of estimated coefficients and R^2 in models with and without controls. This ultimately quantifies the strength of selection on unobservables required for the coefficient to be non-different from 0. I set the model without controls to column (2) and the model with full controls to column (3), and find estimated $\hat{\delta}$ values of 2.55 for the natural amenities variable and 2.22 for the interaction term between Confederate monuments and the natural amenities dummy. Both values are larger than 1, suggesting that bias from unobservables is unlikely to drive the coefficients toward 0. On average, neighborhoods near natural amenities tend to be 2.2 percentage points more white than other neighborhoods, everything else being equal. Lastly, in column (4), I control for neighborhood fixed effects, capturing time-invariant characteristics. Because natural amenities are fixed over time, the market effect on racial sorting is no longer identified, and only the exclusion effect remains estimated through variation in city-wide Confederate monuments. On average, neighborhoods that have access to natural amenities experience a 5.4 percentage point increase in their white shares when the number of Confederate monuments increases by one standard deviation. Additional results show that both market and exclusion effects hold when using a long-difference strategy (see appendix section C.2.4). While I do find a higher market effect in the Midwest region (see Figure C.5 in the appendix), I do not find any significant heterogeneity by region for the exclusion effect (see Figure C.6 in the appendix).

III.2.3 Heterogeneity in natural amenities

Figure 3.4 shows that both market and exclusion effects are robust when decomposing the baseline natural amenities measure or using alternative measures. Panel (a) displays

Table 3.4
Baseline: natural amenities and white share

	$s_{n,t}$			
	(1)	(2)	(3)	(4)
Natural Amenities	0.0354***	0.0328***	0.0224***	
	(0.0030)	(0.0035)	(0.0024)	
NA × Conf. Monu.		0.0005***	0.0003**	0.0045***
		(0.0001)	(0.0001)	(0.0006)
S.D Conf. Monu.	12	12	12	12
Neigh. FE	○	○	○	✓
Share of NA Neigh.	0.190	0.190	0.190	0.190
Set of Controls	○	○	✓	✓
R^2	0.257	0.257	0.463	0.808
Observations	364,605	364,605	362,874	364,405
MSA-years FE	1,697	1,697	1,638	1,697

Notes: Each column reports estimates from separate regressions. The dependent variable is the neighborhood white share. All estimations include city-year fixed effects. Column (4) includes neighborhood fixed effects. Controls include the percentile income rank, the log distance to seaport, the log distance to CBD, and the log population density. The independent variable Natural Amenities is a dummy variable equal to one if the neighborhood is within 500 meters of a natural feature such as an ocean, the Gulf of Mexico, a lake, a major river, or has an average slope greater than 15°. The independent variable Conf. Monu. represents the total number of Confederate monuments within the city. Standard errors are clustered by city-year, and ***, **, * indicate significance at the 1%, 5%, and 10% levels, respectively.

the market effect of natural amenities referring to column (1) in Table 3.4, and the added controls are percentile income rank, distance to seaport, distance to CBD, and population density. Panel (b) displays the exclusion effect of natural amenities referring to column (4) in Table 3.4, and the added controls are percentile income rank and population density.

Following Lee and Lin (2018), I use different indicators for natural features, which are, from left to right, coast, lakes, rivers, hills, temperate climates, low flood risk, and a hedonic index.[10] Overall, estimates are positive and robust to including controls, confirming previous findings. Note that estimates for the exclusion effect do not vary significantly between specifications, unlike the market effect estimates. This is primarily due to the neighborhood fixed effects, which control for unobserved characteristics and reduce omitted variable bias.

[10] Lee and Lin (2018) regress the logarithm of neighborhood median housing rent, reported in censuses from 1930 to 2010, against a complete vector of dummy variables indicating proximity to all natural features (at many thresholds), log population density, log distance to the CBD, log number of housing units, average housing age, log distance to the nearest seaport, and metropolitan area–year fixed-effects. Then, they predict values for housing rents based on just the estimated natural feature coefficients.

Figure 3.4
Heterogeneity in Natural Amenities

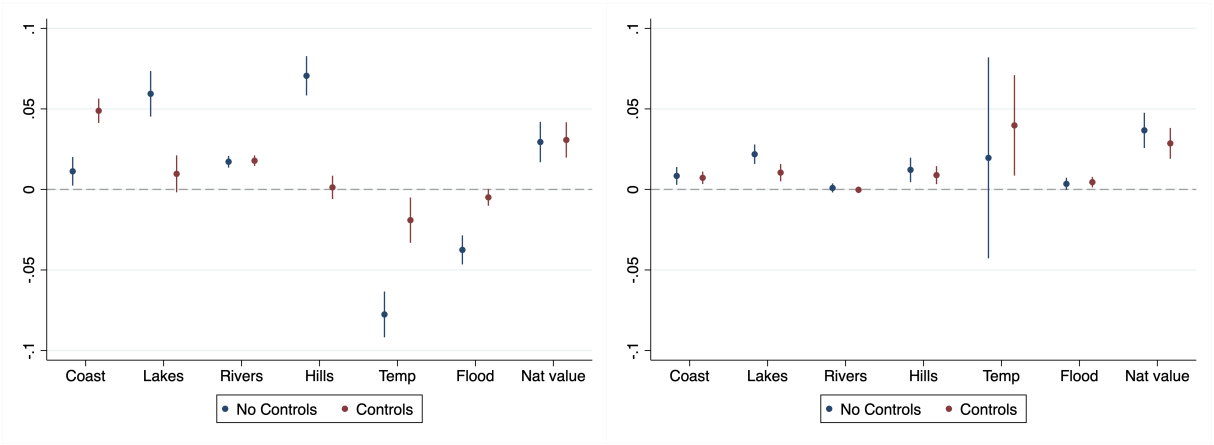

(a) Market effect **(b)** Exclusion effect

Notes: Each dot represents a coefficient from baseline regression with different natural amenity measures. Panel (a) displays the market effect of natural amenities referring to column (1) in Table 3.4, and the added controls are the percentile income rank, the log distance to seaport, the log distance to CBD, and the log population density. Panel (b) displays the exclusion effect of natural amenities referring to column (4) in Table 3.4, and the added controls are the percentile income rank and the log population density.

III.2.4 Placebos

I conduct placebo tests in order to assess whether Confederate monuments capture the exclusion effect by using the share of blacks and the share of others (referring to Asian and Hispanic/Latino individuals) within the neighborhood as the dependent variable instead of using the white share. If Confederate monuments truly capture changes in anti-black attitudes, the exclusion effect should be null for the share of others and negative and significant for the share of blacks.

Table 3.5 shows the results. Regarding the market effect of natural amenities, it is negative and significant for both racial groups, with a larger effect for blacks. This might be due to the fact that, on average, Asian and Hispanic/Latino individuals have greater income than blacks. Regarding the exclusion effect captured by the interaction term between Confederate monuments and the natural amenities dummy, it is negative and significant for blacks, and the effect is null for others. Whatever the specification used, the exclusion effect for blacks is about the same size as that for whites in Table 3.4. This suggests a substitution between blacks and whites within neighborhoods near natural amenities following an increase in city-wide anti-black attitudes.

III.3 Discussion

Previous results show that cities with more natural amenities tend to be more racially segregated. Within a city, neighborhoods with access to natural amenities are associated

Table 3.5
Placebo: share of Others and Black

	Others		Black	
	(1)	(2)	(3)	(4)
Natural Amenities	-0.0050***		-0.0174***	
	(0.0018)		(0.0024)	
NA × Conf. Monu.	-0.0000	-0.0004	-0.0003**	-0.0041***
	(0.0001)	(0.0003)	(0.0001)	(0.0006)
S.D Conf. Monu.	12	12	12	12
Neigh. FE	○	✓	○	✓
Share of NA Neigh.	0.190	0.190	0.190	0.190
Set of Controls	✓	✓	✓	✓
R^2	0.680	0.768	0.347	0.795
Observations	362,874	364,405	362,860	364,391
MSA-years FE	1,638	1,697	1,638	1,697

Notes: Each column reports estimates from separate regressions. The dependent variable in columns (1) and (2) is the share of Asian and Hispanic/Latino individuals within the neighborhood. The dependent variable in columns (3) and (4) is the share of blacks within the neighborhood. All estimations include city-year fixed effects. Columns (2) and (4) include neighborhood fixed effects. Controls include the percentile income rank, the log distance to seaport, the log distance to CBD, and the log population density. The independent variable Natural Amenities is a dummy variable equal to one if the neighborhood is within 500 meters of a natural feature such as an ocean, the Gulf of Mexico, a lake, a major river, or has an average slope greater than 15°. The independent variable Conf. Monu. represents the total number of Confederate monuments within the city. Standard errors are clustered by city-year, and ***, **, * indicate significance at the 1%, 5%, and 10% levels, respectively.

with a higher share of whites. Additionally, an increase in city-wide Confederate monuments is associated with greater city-level distance segregation, and the effect is stronger in cities with abundant natural amenities. Within a city, more Confederate monuments are associated with a higher share of whites in neighborhoods that have access to natural amenities. Overall, natural amenities and their interaction with anti-black attitudes (captured through Confederate monuments) appear to play a substantial role in explaining racial sorting.

One concern could be related to income. Since blacks are, on average, poorer than whites, they could be excluded from locations close to natural amenities by a simple market effect. While I do not observe individual income data by race to control for that, Derenoncourt et al. (2024) documents a convergence of the racial wealth gap throughout the 20th century. Specifically, the white-to-black per capita wealth ratio decreased from nearly 60 to 1 at the start to 10 to 1 by 1920 and further to 7 to 1 by the 1950s, after which it stabilized.

Moreover, Aliprantis et al. (2022) explains that financial constraints, such as high housing prices, are not the reason why high-income Black households live in neighborhoods of similar quality to low-income white households. Indeed, Black and white households are distributed across metropolitan areas with similar housing price-quality gradients. In-

stead, they highlight the role of racial composition and racial preferences of neighborhoods in understanding neighborhood sorting by income and race.

Finally, Bayer et al. (2021) confirms these results by showing that in every metropolitan area, Blacks and whites who are identical in every other way often end up living in neighborhoods that differ significantly in terms of available resources. They document that it takes more than $65,000 in household income for a Black household to live in a neighborhood with the median level of neighborhood income. By contrast, white households with only $21,000 in income reside in such neighborhoods. More generally, Black households at every income level reside in neighborhoods that are, on average, much poorer than those of comparable white households.

This evidence suggests that prices alone are not a central determinant of racial segregation and that racial preferences or racial prejudice play a significant role in explaining racial sorting. Therefore, there are good reasons to believe that the previous results are not solely driven by income differences between Blacks and whites.

IV A simple heterogeneous quantitative spatial model

In this section, I introduce a simple heterogeneous quantitative spatial model of black and white workers that differ in preferences. First, black workers spend a higher share of their income on housing compared to white workers. Second, they are also more sensitive to neighborhood and workplace characteristics. These assumptions introduce non-homothetic preferences and accommodate the fact that blacks are, on average, poorer than whites (Weiwu, 2024). In addition to preferences, both groups are substitutes in the production function. For simplification, I assume that black workers represent low-skilled workers and consider white workers as high-skilled workers. As a consequence, they earn different wages and are differently used by firms.

This model is useful for bringing theory to data, allowing the estimation of the impact of first-nature factors (such as natural amenities) and second-nature factors (such as racial preferences) on group-specific residential choices, taking into account work opportunities. Finally, counterfactuals allow for the disentangling of mechanisms at play.

In this class of urban models, researchers need to observe the rents, the land area, the number of workers, and residents by neighborhoods within the city in order to recover unobserved characteristics (such as wages, amenities, productivity) by inverting the model step by step. I apply the quantitative spatial model to the 2010 data of the 16 largest

CBSAs (excluding New York), covering 29% of the U.S. urban population commuting flows. I observe the workplace and residence employment by race from LODES data, the commuting time between neighborhoods from the pysal project, and finally, neighborhood rents and land from Lee and Lin (2018)'s database.[11]

IV.1 Model set-up

IV.1.1 Workers

I consider a mass of workers composed of two groups (blacks and whites, $g \in \{b, w\}$) within a closed city of N discrete locations. Workers choose a place of residence and a place of work as a pair of locations. Worker ν of group g choosing pair locations ni derives the following indirect utility:

$$U_{ni,g} = \frac{B_{n,g} w_{i,g}}{d_{ni} P_n^{1-\beta_g} Q_n^{\beta_g}} \epsilon_{ni,g}(\nu),$$

where $B_{n,g}$ are group-specific amenities in neighborhood n, $w_{i,g}$ is the group-specific wage in workplace i, d_{ni} is the bilateral commuting cost between neighborhood n and workplace i, P_n is the price of the final consumption good in neighborhood n, Q_n is the rent of neighborhood n, and $\epsilon_{ni,g}(\nu)$ is a pair-locations idiosyncratic shock of worker ν drawn from a Fréchet distribution. Finally, β_g represents the group-specific share of income spent on housing, and by making the assumption that the final good is freely traded within the city, its price is taken as numeraire ($P_n = 1$ for all n).

Using standard properties of the Fréchet distribution (McFadden, 1974), the probability that a worker chooses to live in n and work in i,

$$\lambda_{ni,g} = \frac{L_{ni,g}}{L_{N_g}} = \frac{(B_{n,g} w_{i,g})^{\epsilon_g} (d_{ni} Q_n^{\beta_g})^{-\epsilon_g}}{\sum_{k \in N} \sum_{l \in N} (B_{k,g} w_{l,g})^{\epsilon_g} (d_{kl} Q_l^{\beta_g})^{-\epsilon_g}} = \frac{\Phi_{ni,g}}{\sum_{k \in N} \sum_{l \in N} \Phi_{kl,g}}, \tag{3.6}$$

where $L_{ni,g}$ is the group-specific number of commuters from n to i and L_{N_g} is the group-specific total number of workers that choose the city. As Redding (2022) detailed, the probability of commuting between both locations n and i depends on neighborhood characteristics, workplace characteristics, and the bilateral cost (numerator), but also on all other residence and workplace characteristics, and bilateral commuting costs (denominator).

[11] Data on the pysal project are available here.

By summing across workplaces, I obtain the probability that a worker of group g lives in n,

$$\lambda_{n,g}^{R} = \frac{R_{n,g}}{L_{N_g}} = \frac{\sum_{i \in N} \Phi_{ni,g}}{\sum_{k \in N} \sum_{l \in N} \Phi_{kl,g}}, \tag{3.7}$$

and by summing across residence places, I obtain the probability that a worker of group g works in i,

$$\lambda_{i,g}^{L} = \frac{L_{i,g}}{L_{N_g}} = \frac{\sum_{n \in N} \Phi_{ni,g}}{\sum_{k \in N} \sum_{l \in N} \Phi_{kl,g}}. \tag{3.8}$$

Finally, population mobility ensures that everyone derives the same expected utility within the city, which is written as,

$$\overline{U}_g = \delta_g \left[\sum_{k \in N} \sum_{l \in N} \Phi_{kl,g} \right]^{1/\epsilon_g}, \tag{3.9}$$

with $\delta_g \equiv \Gamma\left(\frac{(\epsilon_g - 1)}{\epsilon_g}\right)$, and $\Gamma(.)$ the gamma function.

IV.1.2 Firms

The final good is produced by a representative firm with a Cobb-Douglas technology under constant returns to scale,

$$Y_i = A_i \left(\frac{L_i}{\alpha}\right)^{\alpha} \left(\frac{H_i^L}{1-\alpha}\right)^{1-\alpha}, \tag{3.10}$$

where A_i represents the productivity in workplace i, $L_i = \left(\sum_g a_{i,g} L_{i,g}^{\rho}\right)^{1/\rho}$ is the aggregate labor supply following a constant elasticity of substitution (CES) between both groups of workers. The parameter ρ governs the substitution between black workers and white workers, and $a_{i,g}$ represents the location racial intensity of group g ($\sum_g a_{i,g} = 1$). Finally, H_i^L is the commercial housing used for production in location i, and α is the share of labor in the production function.

The first-order conditions of the firm's profit with respect to group-specific labor and housing are,

$$w_{i,g} = \alpha^{(1-\alpha)} a_{i,g} L_{i,g}^{\rho-1} A_i L_i^{\alpha-\rho} \left(\frac{H_i^L}{1-\alpha}\right)^{1-\alpha}, \tag{3.11}$$

$$Q_i = (1-\alpha)^{\alpha} A_i \left(\frac{L_i}{\alpha}\right)^{\alpha} (H_i^L)^{-\alpha}. \tag{3.12}$$

IV.1.3 Housing

I assume that firms and residents compete for housing and that there is no distortion in the allocation of it. Housing is supplied by a large number of developers who combine land (K_n) and capital with a Cobb-Douglas technology to produce housing,

$$H_n^S = K_n^{\mu} M_n^{1-\mu}. \tag{3.13}$$

This housing is then rented at price Q_n. Maximizing profit, we obtain,

$$H_n = k_n \, Q_n^{\frac{1-\mu}{\mu}}, \tag{3.14}$$

where $\frac{1-\mu}{\mu}$ is the housing supply elasticity, and $k_n = (1-\mu)^{\frac{1-\mu}{\mu}} K_n$.[12]

IV.2 From theory to data

IV.2.1 Wages

Using the commuting probability (3.6) and the residential probability (3.7), it is possible to write the probability that a type-g worker commutes from n to i, conditionally on living in neighborhood n, as,

$$\lambda^R_{ni|n,g} = \frac{\lambda_{ni,g}}{\lambda^R_{n,g}} = \frac{(w_{i,g}/d_{ni})^{\epsilon_g}}{\sum_{l \in N}(w_{l,g}/d_{nl})^{\epsilon_g}}. \tag{3.15}$$

Finally, combining the conditional commuting probability (3.15) with the labor market clearing condition,

$$L_{i,g} = \sum_{n \in N} \frac{(w_{i,g}/d_{ni})^{\epsilon_g}}{\sum_{l \in N}(w_{l,g}/d_{nl})^{\epsilon_g}} R_{n,g}, \tag{3.16}$$

there exists a unique vector of wages that solves the labor market, given the observed vectors of residence employment, workplace employment, and commuting cost parametrization.

IV.2.2 Location racial intensity in the production function

From the labor first-order condition of the firm (3.11) and with two groups of workers, it is possible to recover the intensity of black workers within each workplace since group-

[12] Combes et al. (2021) find evidence that a Cobb-Douglas technology is a good approximation for the production function of housing.

specific wages have been recovered,

$$\frac{1-a_i}{a_i} = \frac{w_{i,w}}{w_{i,b}} \left(\frac{L_{i,b}}{L_{i,w}} \right)^{\rho-1}, \tag{3.17}$$

where a_i is the intensity of black workers in i, $w_{i,w}$ is the wage of white workers in i, and $w_{i,b}$ is the wage of black workers in i, $L_{i,b}$ is the total number of black workers in i, and $L_{i,w}$ is the total number of white workers in i.

IV.2.3 Productivity

From the zero-profit condition due to free entry and the first-order conditions (3.11 and 3.12), it is possible to express the location productivity as,

$$A_i = W_i^{\alpha} Q_i^{1-\alpha}, \tag{3.18}$$

which is a function of aggregate wages W_i and rents Q_i in workplace i.[13] Intuitively, a higher cost (wages, rents) implies a higher productivity in order for the zero-profit condition to hold, as it can be seen by rewriting the last equation (3.18) as $1 = \frac{W_i^{\alpha} Q_i^{1-\alpha}}{A_i}$.

IV.2.4 Amenities

Combining the residential probability (3.7) and the expected utility (3.9), it is possible to derive group-specific amenities as,

$$B_{n,g} = \frac{(\lambda_{n,g}^R)^{1/\epsilon_g} Q_n^{\beta_g}}{\left(\sum_{i \in N} (w_{i,g}/d_{ni})^{\epsilon_g}\right)^{1/\epsilon_g}} \frac{\overline{U}_g}{\delta_g}, \tag{3.19}$$

where amenities are considered as residuals explaining residential choices in this commuting model. Recalling that $\frac{\overline{U}_g}{\delta_g}$ is a scalar, for a given residential market access (denominator), and a given rent, a higher share of group g living in location n implies higher group-specific amenities.

[13] Aggregate wage cost for firm $W_i = \left(\sum_g a_{i,g}^{\frac{1}{1-\rho}} w_{i,g}^{\frac{\rho}{\rho-1}} \right)^{\frac{\rho-1}{\rho}}$ is obtained through $W_i L_i = \sum_g w_{i,g} L_{i,g}$ and group-specific wage (3.11).

IV.2.5 Density of development

Finally, using the total housing demand by residents and firms and the housing market clearing condition, it is possible to recover the total housing supply,

$$H_n^S = H_n^R + H_n^L, \tag{3.20}$$

where H_n^R is the residential housing demand in n, and H_n^L is the commercial housing demand in n.

The housing demand from residents takes the form of,

$$H^R = \sum_g \beta_g \sum_{i \in N} \lambda^R_{ni|n,g} \frac{w_{i,g}}{Q_n} R_{n,g}, \tag{3.21}$$

where $\sum_{i \in N} \lambda^R_{ni|n,g} w_{i,g}$ is the expected income from residents of group g living in neighborhood n. The housing demand of firms in workplace i is derived from the first-order condition (3.12),

$$H_i^L = \frac{1-\alpha}{\alpha} \left(\frac{A_i}{Q_i} \right)^{1/\alpha} L_i. \tag{3.22}$$

IV.3 Racial preferences

I allow group-specific amenities $B_{n,g}$ to be endogenous,

$$B_{n,g} = b_{n,g} \left(\frac{R_n}{K_n} \right)^{\eta_g^r} (s_n)^{\eta_g^w} \left(e^{\eta_g^c \, s_n \times \mathbb{1}_n^{NA}} \right), \tag{3.23}$$

depending on a fundamental amenities component ($b_{n,g}$), residential density within the neighborhood n ($R_n/K_n \equiv \text{Dens}_n$), the share of whites within the neighborhood n (s_n), and its interaction with a dummy variable ($\mathbb{1}_n^{NA}$) indicating whether the neighborhood has access to natural amenities as in the reduced-form section.

First, the parameter η_g^w is the racial composition elasticity, which aims to capture preferences towards the white presence of group g. This relates to the neighborhood effect literature, such as Tsivanidis (2024), which develops a framework to quantify the impact of the college share of residents on amenities rather than the total density of residents (as in Ahlfeldt et al. (2015)). By contrast, my setting estimates homophily parameters referring to racial preferences as in Bagagli (2023) and Weiwu (2024). If white workers value living within more white neighborhoods, the racial composition elasticity for whites will

be positive ($\eta_w^w > 0$). By contrast, if black workers value living within more black neighborhoods, the racial composition elasticity for blacks will be negative ($\eta_b^w < 0$). Second, the parameter η_g^c aims to capture the complementarity between natural amenities and white presence. Finally, η_g^r relates to standard residential agglomeration forces elasticity in quantitative urban models (Ahlfeldt et al., 2015; Heblich et al., 2020).

IV.4 Model Quantification

IV.4.1 Calibration

Housing consumption From the Consumer Expenditure Survey (U.S. Bureau of Labor Statistics), I calibrate the share of income dedicated to housing to $\beta_b = 0.38$ for blacks and $\beta_w = 0.33$ for whites.[14] Hence, these values aim to capture the fact that black workers are more sensitive to housing prices than white workers (see, for example, Weiwu (2024), Redding and Sturm (2024), Tsivanidis (2024)).

Production function Regarding the share of labor in the production function, I take $\alpha = 0.7$, which is a standard value in the literature for modern contexts. Finally, I calibrate the substitution parameter between low-skilled and high-skilled worker groups to $\rho = 0.3$, corresponding to the estimate from Card (2009) and to the value widely used in the quantitative urban model literature (see, for example, Weiwu (2024), Redding and Sturm (2024), Herzog (2024), Tsivanidis (2024)).

Housing supply elasticity I calibrate the housing supply elasticity based on estimates of Saiz (2010) for U.S. cities. Table 3.6 shows the values by CBSA.

Commuting elasticity I use the standard value in the urban economics literature, $\kappa = 0.01$ (Ahlfeldt et al., 2015), and I do not differentiate it by worker type since Tsivanidis (2024) finds no significant difference in commuting elasticity between low-skilled and high-skilled workers.

IV.4.2 Estimation

Fréchet parameter Given the commuting cost functional form $d_{ni} = e^{\kappa t_{ni}}$ with the calibrated commuting cost elasticity κ and t_{ni} the commuting time, both group-specific

[14] This survey is available via this link.

Table 3.6
Housing Supply Elasticity by CBSA

CBSA	Housing supply elasticity
Houston, TX	2.30
Los Angeles, CA	0.63
Chicago, IL	0.81
Phoenix, AZ	1.61
Philadelphia, PA	1.65
San Diego, CA	0.67
San Jose, CA	0.76
Seattle, WA	0.88
San Antonio, TX	2.98
Dallas, TX	2.18
Austin, TX	3.00
Jacksonville, FL	1.06
Columbus, GA	2.71
Charlotte, NC	3.09
Indianapolis, IN	4.00
Denver, CO	1.53

Notes: This table displays the calibrated values of housing supply elasticity for each city, based on Saiz (2010).

Fréchet parameters can be estimated by taking the log of the commuting probability equation (3.6),

$$\ln \lambda_{ni,g} = \underbrace{\ln(w_{i,g})^{\epsilon_g}}_{\zeta_{i,g}} + \underbrace{\ln(B_{n,g}Q_n^{-\beta_g})^{\epsilon_g}}_{\vartheta_{n,g}} - \epsilon_g \kappa t_{ni} - \underbrace{\ln\left(\sum_{k\in N}\sum_{l\in N}\Phi_{kl,g}\right)}_{\xi_{ni,g}}, \tag{3.24}$$

where $\lambda_{ni,g}$ is the group-specific commuting flows between n and i, $\vartheta_{n,g}$ is an origin fixed effect capturing residence characteristics, $\zeta_{i,g}$ is a destination fixed effect capturing workplace characteristics, and $\xi_{ni,g}$ is a residual term.

Since I do not observe commuting flows by race in the LODES data, I use the American Community Survey, which provides, at the individual level, the race, the residence and workplace at the county level, and the reported commuting time. I estimate the previous equation (3.24) by using the PPML estimator that allows for zero commuting flows.

Table 3.7 shows the results. For $\kappa = 0.01$, it implies values of $\epsilon_w = 2.7$ and $\epsilon_b = 4.5$, which are in line with Tsivanidis (2024), which finds for high-skilled workers 2.65 and for low-skilled workers 3.98. According to these estimates, black workers are more sensitive to residence and workplace characteristics, and commuting times compared to white workers.

Table 3.7
Commuting flows by race

	Whites	Blacks
	(1)	(2)
$-\epsilon_g \kappa$	-0.027^{***}	-0.045^{***}
	(0.002)	(0.004)
Origin-Destination FE	Yes	Yes
Pseudo R-squared	0.18	0.42
Observations	10,603	2,994

Note: This table displays group-specific commuting cost estimations. Dependent variables are group-specific commuting flows and independent variable is the average commuting time. Both regressions contain origin and destination fixed-effects and are estimated through PPML, and ***, **, * indicate significance at the 1%, 5% and 10% level, respectively.

Racial preferences By taking the log of the group-specific amenities equation (3.23), I obtain,

$$\ln B_{n,g} = \eta_g^r \ln \text{Dens}_n + \eta_g^w \ln s_n + \eta_g^c s_n \times \mathbb{1}_n^{NA} + \ln b_{n,g}, \tag{3.25}$$

which can be estimated using an OLS model. Structural parameters η_g^r, η_g^w, and η_g^c are going to be estimated through variation across neighborhoods within the city, and $\ln b_{n,g}$ is considered as a residual term. Moreover, I also control for neighborhood time-unvarying characteristics (such as natural feature proximity, distance to city center, distance to seaport, and housing age) that are directly correlated with amenities in order to avoid attributing their influence to the effect of racial preferences, and a city fixed effect.

Table 3.8 shows the results. Column (1) shows racial preferences estimates only. These homophily parameters suggest that white workers have strong preferences towards the presence of whites within their neighborhood. By contrast, blacks have preferences against the presence of whites within their neighborhood. Moreover, the magnitude of the homophily parameter for whites is 3 times higher than that for blacks. This result implies that white workers have a stronger homophily parameter than blacks, which is consistent with Bagagli (2023) and Weiwu (2024). Column (2) controls for time-unvarying factors, which reduce the absolute size difference between blacks' and whites' racial preferences. Finally, column (3) adds residential agglomeration forces and complementarity between natural amenities and racial preferences parameters. There is no sizeable change in racial preferences estimates between columns (2) and (3). Regarding residential agglomeration

forces parameters, they are positive and significant and of similar magnitude for both racial groups. A higher density of residents is associated with a higher level of amenities. However, the magnitude is lower than those estimated in Ahlfeldt et al. (2015). Finally, complementarity between racial preferences and natural amenities parameters suggest that the marginal effect of natural amenities proximity differs according to the white share. For both groups, the presence of its own racial group in the neighborhood makes access to natural amenities even more valuable. This indicates the matter of homophily for enjoying local public goods such as natural amenities. For black workers, the marginal effect of natural amenities (see Table C.3 for full results) is positive with a turning point around 0.95, meaning that when the share of whites within the neighborhood reaches this threshold, natural amenities access is no longer valued by black workers. For white workers, the marginal effect of natural amenities is negative with a turning point around 0.71, meaning natural amenities become enjoyable only when the neighborhood white share reaches this level.

Table 3.8
Structural Estimation

	Baseline	Controls	
	(1)	(2)	(3)
η^w : racial preferences			
Blacks	-0.20***	-0.27***	-0.26***
	(0.03)	(0.04)	(0.04)
Whites	0.62***	0.52***	0.50***
	(0.03)	(0.02)	(0.02)
η^r : residential agglo. forces			
Blacks			0.03***
			(0.01)
Whites			0.04**
			(0.02)
η^c : complementarity			
Blacks			-0.20***
			(0.04)
Whites			0.28***
			(0.07)

Note: This table displays structural parameter estimations from group-specific separated regressions of the amenities equation (3.25). Dependent variables are group-specific amenities. Each regression controls for a city fixed effect, and ***, **, * indicate significance at the 1%, 5%, and 10% levels, respectively. Column (1) shows the racial composition elasticity for blacks and whites, and column (2) controls for a natural amenities dummy, distance to CBD, distance to seaport, and housing age. Column (3) adds the residential elasticity and the complementarity parameter. See Table C.3 for detailed results.

IV.4.3 Model fit

In order to test whether the model fits the observed data, I compare the residential floorspace demand density with the observed housing density. Figure 3.5 shows the correlation between both the estimated and observed variables for the 6 largest CBSAs in my sample. A slope of 1 represents a perfect correlation on average. For all the cities, there is a very good fit of the model with all R-squared values and slopes above 0.83, despite some overestimations (see Table C.5 for the model fit of all cities).

IV.5 Counterfactuals

IV.5.1 Complementarity between racial preferences and natural amenities ($\eta^c = 0$)

For the first experiment, I remove the complementarity between racial preferences and natural amenities by setting the parameter $\eta^c = 0$. For both groups, the presence of its own racial group in the neighborhood does not make access to natural amenities more valuable.

Racial segregation Figure 3.6 shows the variation of racial segregation for each of the 16 cities between initial and counterfactual equilibria. Surprisingly, removing complementarity between racial preferences and natural amenities makes only one city decrease in racial segregation. On average, cities see their racial segregation level increase by 2.4 percentage points. This result can be explained by two forces. First, the distaste of blacks to live in a neighborhood that has access to natural amenities and a high white presence is higher than the taste of whites to live in these neighborhoods ($|\epsilon_b \eta_b^c| > |\epsilon_w \eta_w^c|$). Second, the taste for homophily is higher for whites than for blacks ($|\epsilon_w \eta_w^w| > |\epsilon_b \eta_b^w|$). As a consequence, black workers live relatively more than before in neighborhoods that have access to natural amenities in this counterfactual, and this results in white flight from these neighborhoods. This is reflected by an average decrease of 14.4 percentage points of the share of white residents living in neighborhoods close to natural amenities (see Table C.4 in the appendix). Finally, through general equilibrium effects in the presence of racial preferences parameters (η_w^w, η_b^w), it makes racial segregation levels increase slightly since whites reallocate. Figure 3.7 illustrates this reallocation for two cities: Chicago and San Jose. The first two panels, 3.7(a) and 3.7(b), show the initial spatial sorting by plotting the white share across neighborhoods. The last two panels, 3.7(c) and 3.7(d), show the change in white share between the initial and counterfactual. Hence, neighborhoods

Figure 3.5
Validity of estimated density of development

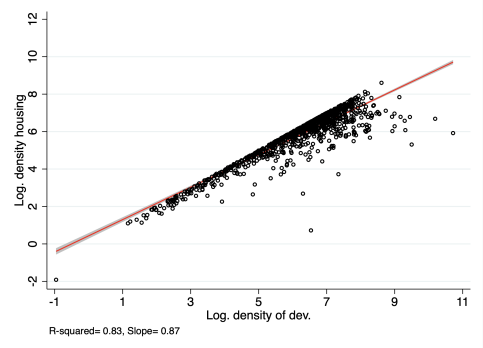

(a) Houston, TX

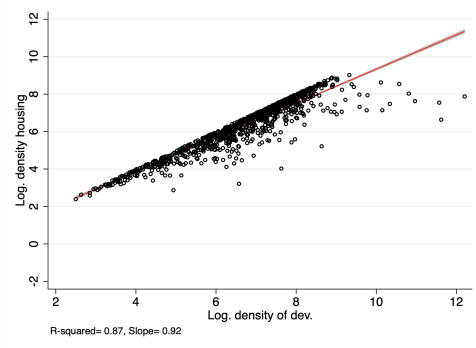

(b) Philadelphia, PA

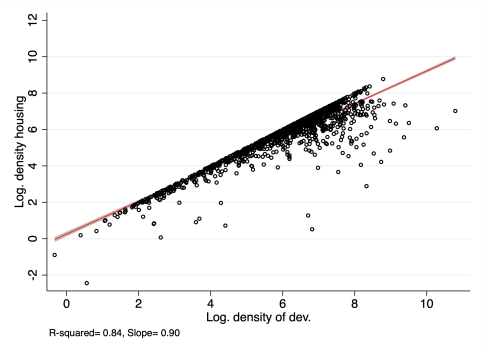

(c) Dallas, TX

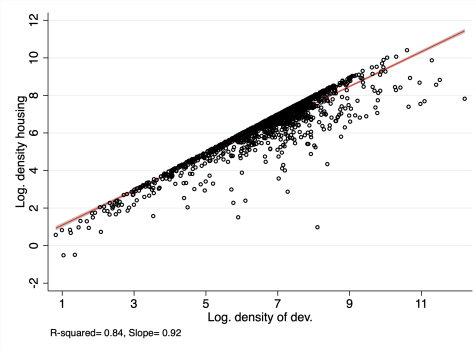

(d) San Jose, CA

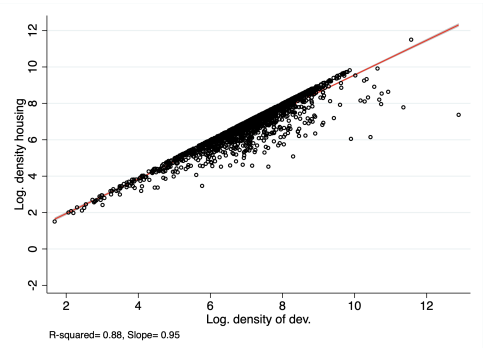

(e) Chicago, IL

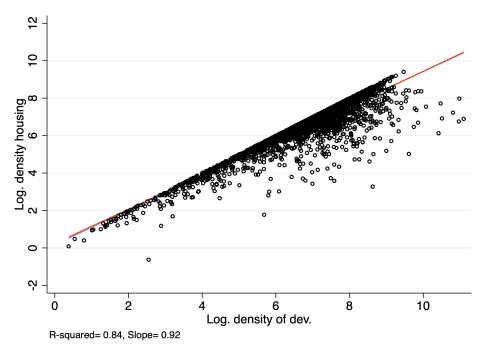

(f) Los Angeles, CA

Notes: This figure shows the model fit of the land market by comparing the log of estimated residential housing demand with the log of actual housing density for six of the largest observed Core-Based Statistical Areas (CBSAs) in the sample. Each black dot represents a neighborhood within a city. The red line represents the linear fit.

with access to natural amenities (indicated by a green triangle) exhibit a reduction in the proportion of white residents.

Figure 3.6

Counterfactual ($\eta^c = 0$): racial segregation changes

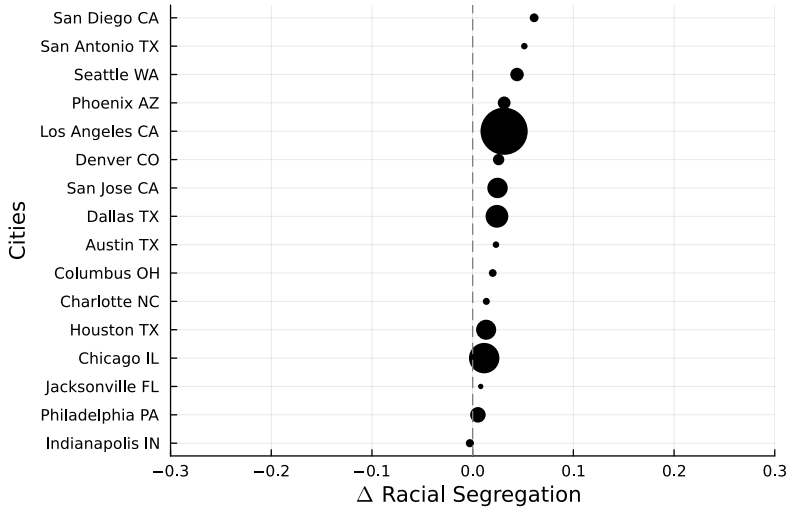

Notes: This figure shows the change in percentage points of racial segregation for each city following the counterfactual: removing the complementarity between natural amenities access and racial preferences. Each circle represents a Core-Based Statistical Area (CBSA), and its size depends on the initial total population. The x-axis shows the change in racial segregation.

Figure 3.7
Baseline white share and counterfactual change

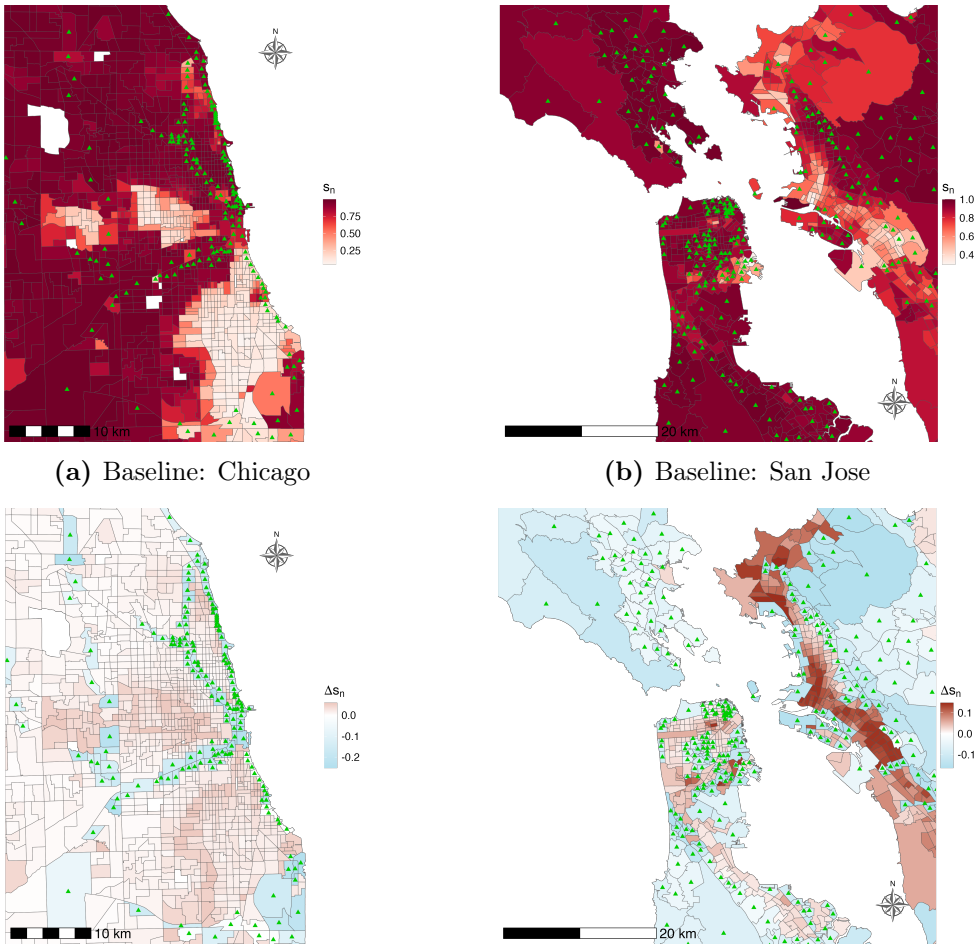

(a) Baseline: Chicago

(b) Baseline: San Jose

(c) Counterfactual $\eta^c = 0$: Chicago

(d) Counterfactual $\eta^c = 0$: San Jose

Notes: Panel (a) and Panel (b) show the neighborhood white share for Chicago and San Jose in the initial equilibrium. Darker shades represent higher levels of white share. Panel (c) and Panel (d) represent the change in white share in Chicago and San Jose following the counterfactual: removing the complementarity between natural amenities access and racial preferences. Green triangles indicate whether the neighborhood is close to natural amenities.

IV.5.2 Racial preferences ($\eta^c = 0$ & $\eta^w = 0$)

For the second experiment, I remove all racial preferences impacts by setting $\eta^c = 0$ and $\eta^w = 0$. In this scenario, blacks and whites no longer value racial composition and only residential agglomeration forces remain.

Racial Segregation As expected, removing racial preferences for both groups decreases the overall racial segregation in cities, as shown by Figure 3.8. On average, racial segregation decreases by 11.6 percentage points.

Figure 3.8
Counterfactual ($\eta^c = 0$ & $\eta^w = 0$): racial segregation changes

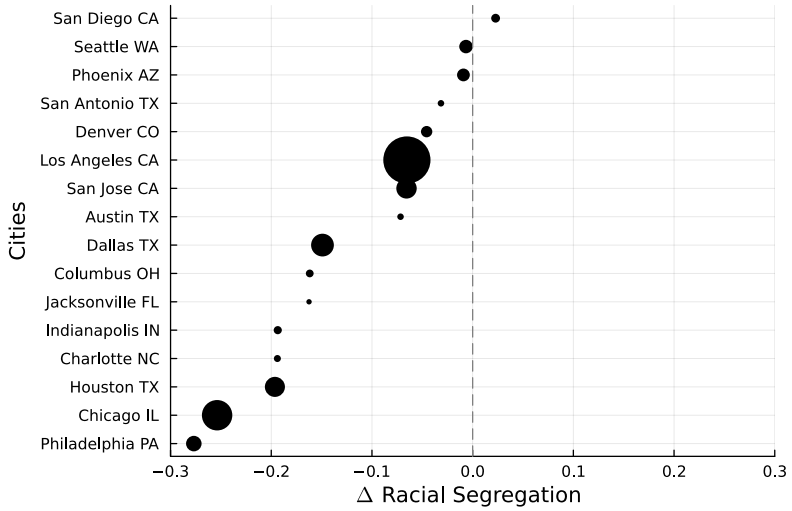

Notes: This figure shows the change in percentage points of racial segregation for each city following the counterfactual: removing the racial preferences. Each circle represents a Core-Based Statistical Area (CBSA), and its size depends on the initial total population. The x-axis shows the change in racial segregation.

V Conclusion

In this paper, I highlight the role of natural amenities in racial sorting and racial segregation within the U.S. using a neighborhood database from 1880 to 2010.

The reduced-form analysis shows that natural amenities influence racial sorting through two effects. First, a market effect: neighborhoods near natural amenities are, on average, more white since they are less affordable for households. Second, an exclusion effect: changes in anti-black attitudes, approximated by city-wide Confederate monuments, create an additional effect making neighborhoods near natural amenities more white. As a result, natural amenities affect citywide racial segregation.

Finally, the structural analysis based on a heterogeneous agents quantitative spatial model confirms the existence of strong racial preferences for both blacks and whites. Moreover, these homophily parameters are even greater in the presence of natural amenities. This highlights the close interaction between racial composition and local public goods, creating incentives for whites to exclude blacks from rich neighborhoods. The first experiment shows that removing the complementarity between natural amenities and racial preferences increases racial segregation slightly. By contrast, the second experiment finds that removing all racial preferences reduces racial segregation by 11.6 percentage points.

Appendix

A Appendix to Circular railroad: Evidence from the Parisian *Petite Ceinture*

A.1 Supplement

A.1.1 Industrial activity in 1860

Data The survey of industry in Paris in 1860 provides a range of information by *arrondissement*. The Parisian industry has been divided in 10 groups,

1. Alimentation (marchands de vin; boucher; épiciers; restaurateurs; raffineurs; boulangers; limonadiers; etc.)

2. Construction (macons; menuisiers; serruriers; charpentiers; peintres; couverture et plomberie; etc.)

3. Home Furnishing (ébenistes et menuisiers en meubles; tapissiers; fabricants de bronzes; papiers peints; etc.)

4. Clothing (tailleurs; cordonniers; lingerie; chapeliers; etc.)

5. Thread and Fabrics (passementrie; tissue pour robes; chales; filateurs et retordeurs de coton; etc.)

6. Steel, Iron, Copper, Zine, Lead (mécanicier constructeurs de machines; fondeurs de métaux; chaudronnier; etc.)

7. Gold, Silver, Platinum (bijouterie fine; métaux précieux; bijouterie fausse; orfévrerie; etc.)

8. Chemical and Ceramic Industry (pharmacien; parfumeurs; herboristes; droguistes; poterie; etc.)

9. Printing, engraving and Paper (imprimeurs; bureau; relieurs; éditeurs; graveurs; etc.)

10. Precision instruments, Watchmaking, Music, Leather, etc.

Figure A.1
Spatial distribution of industries in 1860

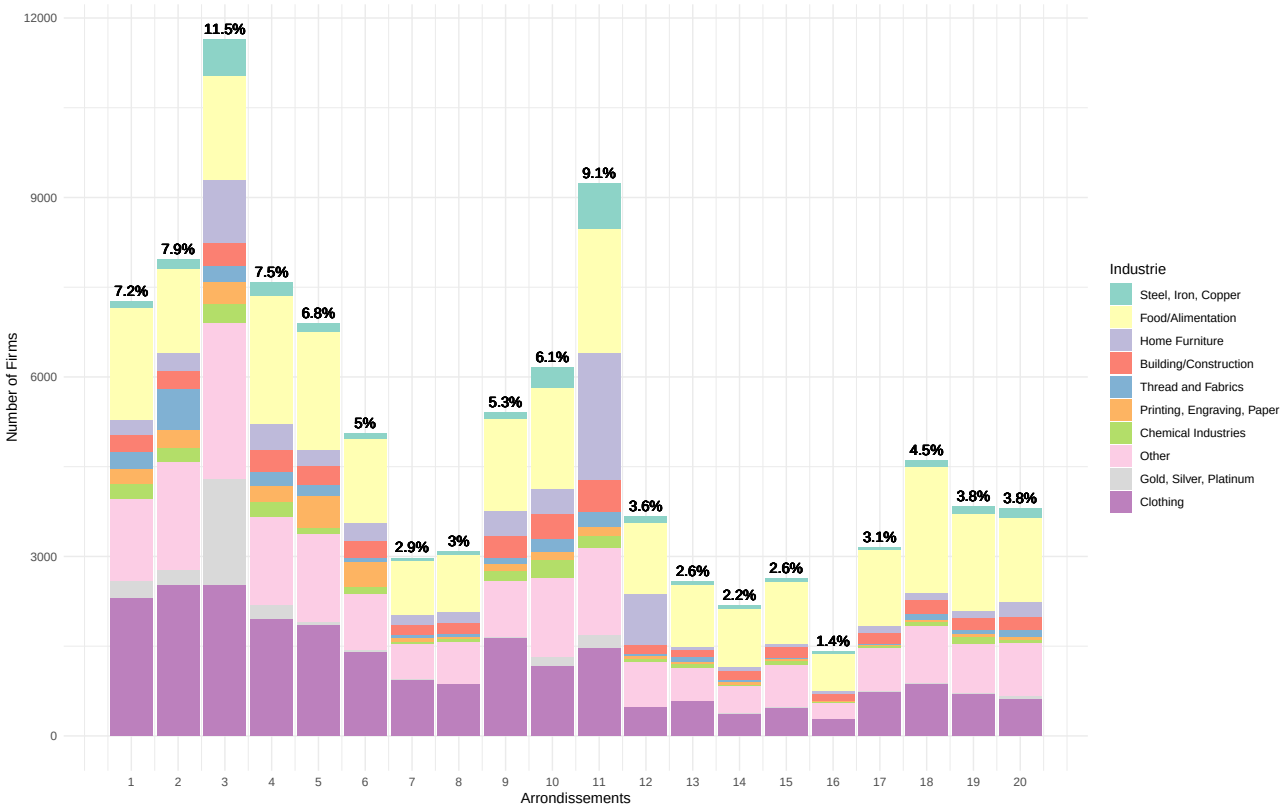

Notes: This graphic illustrates the Parisian spatial distribution of firms by industry in 1860. Percentages above bars represent the share of total surveyed firms within each *arrondissement*.

Firms The total number of firms is 101, 171 with a distribution in descending order of 11.5% in the 3rd *arrondissement*, 9.12% in the 11th *arrondissement*, and 7.82% in the 2nd *arrondissement*.

Over the total number of firms (101, 171), 7, 492 have more than 10 workers, 31, 480 have between 2 and 10 workers and 62, 199 have 1 worker or work alone. This demonstrates the fragmentation of the Parisian industry.

The Alimentation group displays the most number of firms, 29, 069, followed by the clothing group with 23, 800. Note that there is very few number of firms within Alimentation group that used more than 2 worker.

Regarding the women, they are less likely to be at the head of the firm. The maximum share observed of women leading the firm is within the clothing group, 33%.

Employment The total number of employed workers is 416, 811 with 285, 861 men, 105, 410 women, 19, 059 boys (less than 16y.), 6, 481 girls (less than 16y.). The daily

wages go from 50 cents to 20 francs. The industrial group having the higher wages are the Construction; the Home furnishing, and the construction de machines groups. Across the 101, 171 firms, 6, 929 employ workers less than 12 hours, 37, 061 employ workers 12 hours, 37, 216 employ workers more than 12 hours, and 19, 965 employ worker without hours limitations.

Figure A.2
Distribution of daily wages in 1860

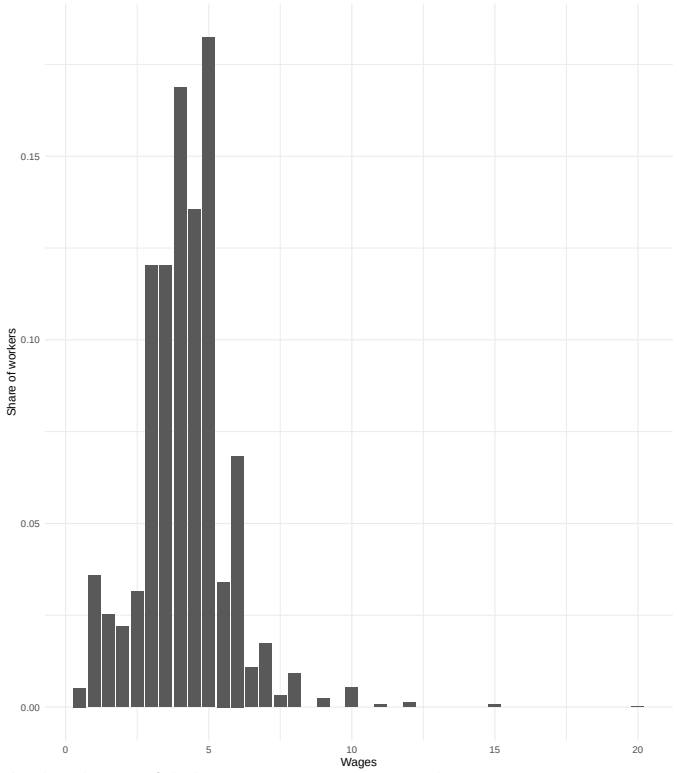

Notes: This graphic illustrates the distribution of daily wages across Parisian workers in 1860.

Rents The total sum of the rents paid of firms within Paris is 107, 390, 710 francs, and represents on average 3.18% of the total revenues. However, there is spatial heterogeneity in the share dedicated to the housing. The 19th *arrondissement* displays a share of 1.6% of revenues spent in housing, whereas the share is 4.33% in the 9th *arrondissement*. There is also heterogeneity between industrial groups with Alimentation; Home furnishing and clothing having the greater share of revenues spent in housing.

Revenues The total sum of the revenues of firms is 3, 369, 092, 949 francs, with the Alimentation group representing 32.3% of this amount (1, 087, 904, 367 francs), followed by the clothing group with 13.49% (434, 538, 168 francs). Diving the total sum of revenues of each group by its number of firms, we get the average revenues by group. Leather; Chemical and Ceramic Industry; Construction; Gold, Silver, Platinum groups have the

highest average revenues by firms.

Figure A.3

Firms, workers, total rents, and revenues *Arrondissement* in 1860.

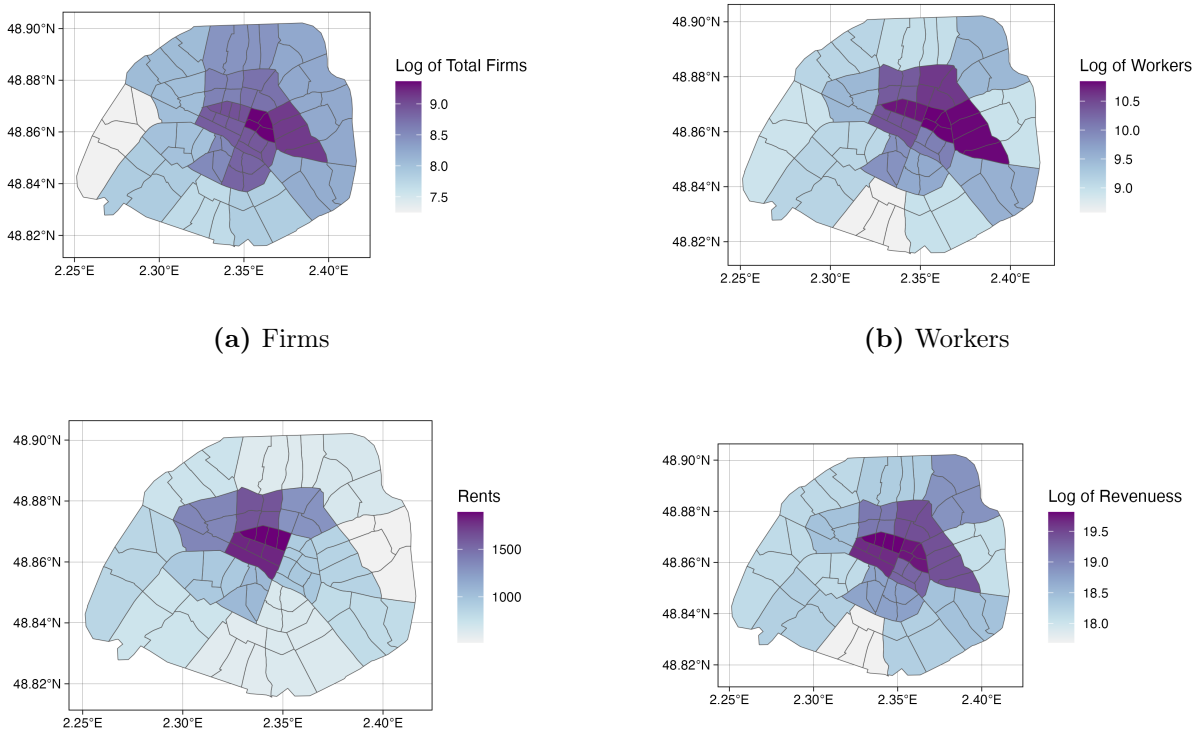

(a) Firms

(b) Workers

(c) Total Rents

(d) Revenues

Notes: This figure displays the spatial distribution of firms, workers, total rents, and revenues across *arrondissements* in 1860.

A.1.2 Paris income segregation

As expected, panel (a) of Figure A.4 shows that the spatial sorting of individuals by skilled within Paris is characterized by high income households living in the west of Paris. This sorting could be due to desamenities mechanisms such as air pollution as suggested by Heblich et al. (2021). Moreover, panel (b) displays the low-skilled population growth during a decade. Low-skilled individuals tend to leave the city center.

Figure A.4

Paris Income Segregation

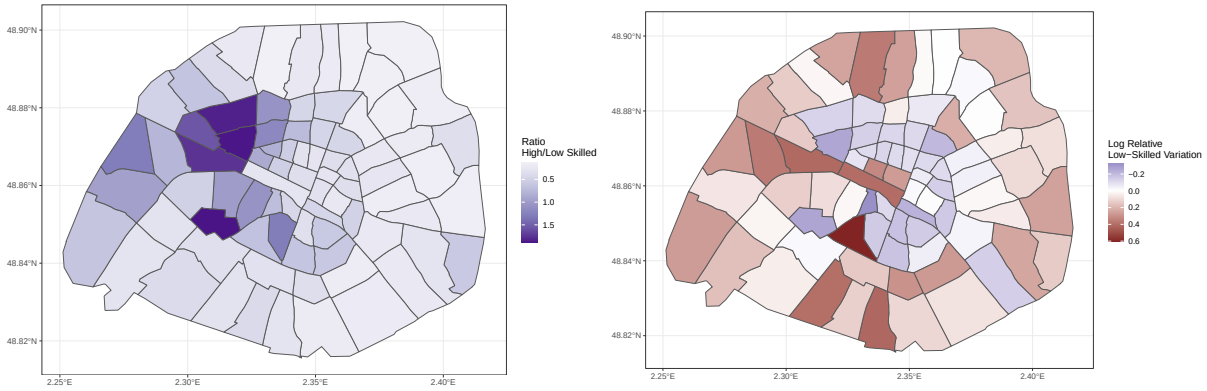

(a) Ratio High/Low-Skilled in 1891

(b) Low-Skilled Difference 1881-1891

Notes: This map displays the ratio high over low skilled in 1891, and the decentralization of the low-skilled population between 1881 and 1891.

A.2 Stylized Facts

A.2.1 Lexicometrics

Figure A.5

Lexicometrics - Parisian issues during 1830-1850 period

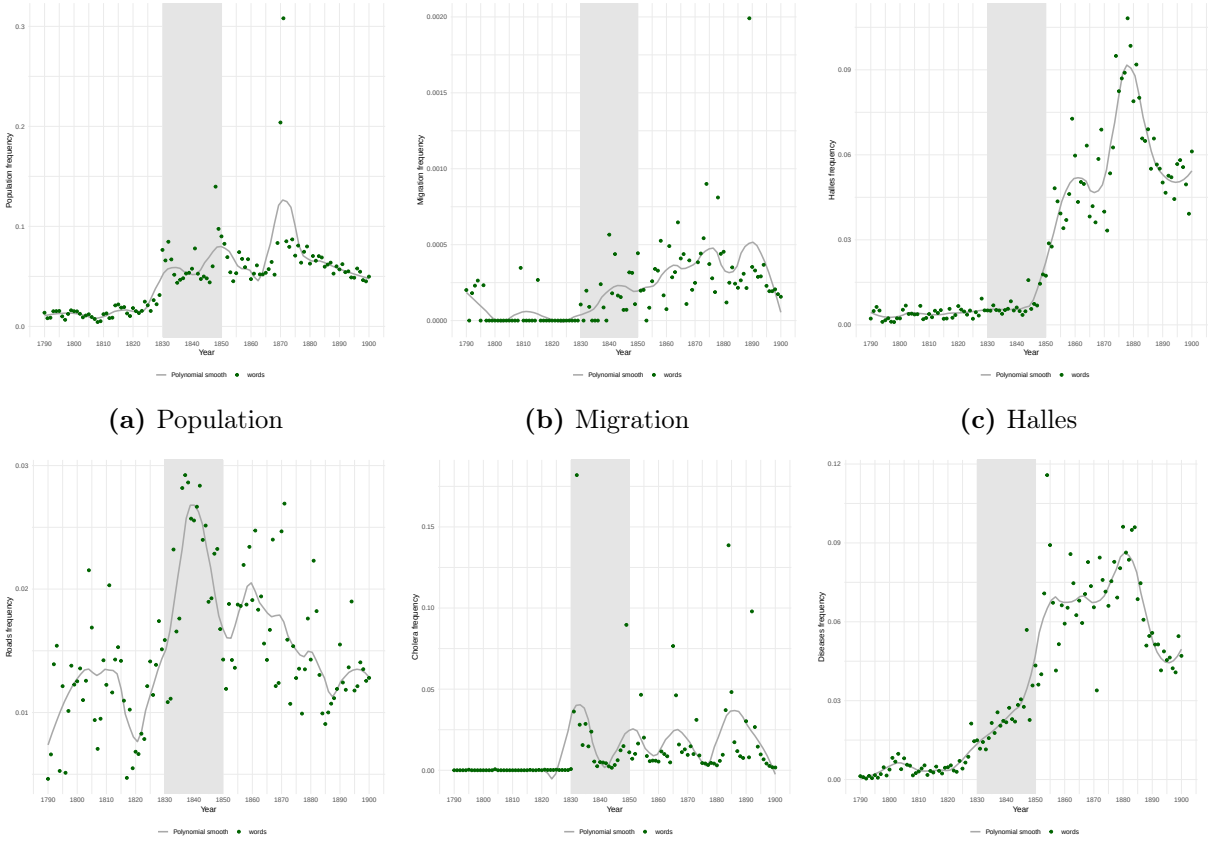

(a) Population **(b)** Migration **(c)** Halles

(d) Roads **(e)** Cholera **(f)** Disease

Notes: Each figure reports the frequency of specific words in French newspapers for Paris over the period 1790-1900. Panels (a) to (f) show the frequency of *population*, *migration*, *Halles*, *roads*, *cholera*, and *disease*, respectively.

Figure A.6
Lexicometrics - City planification

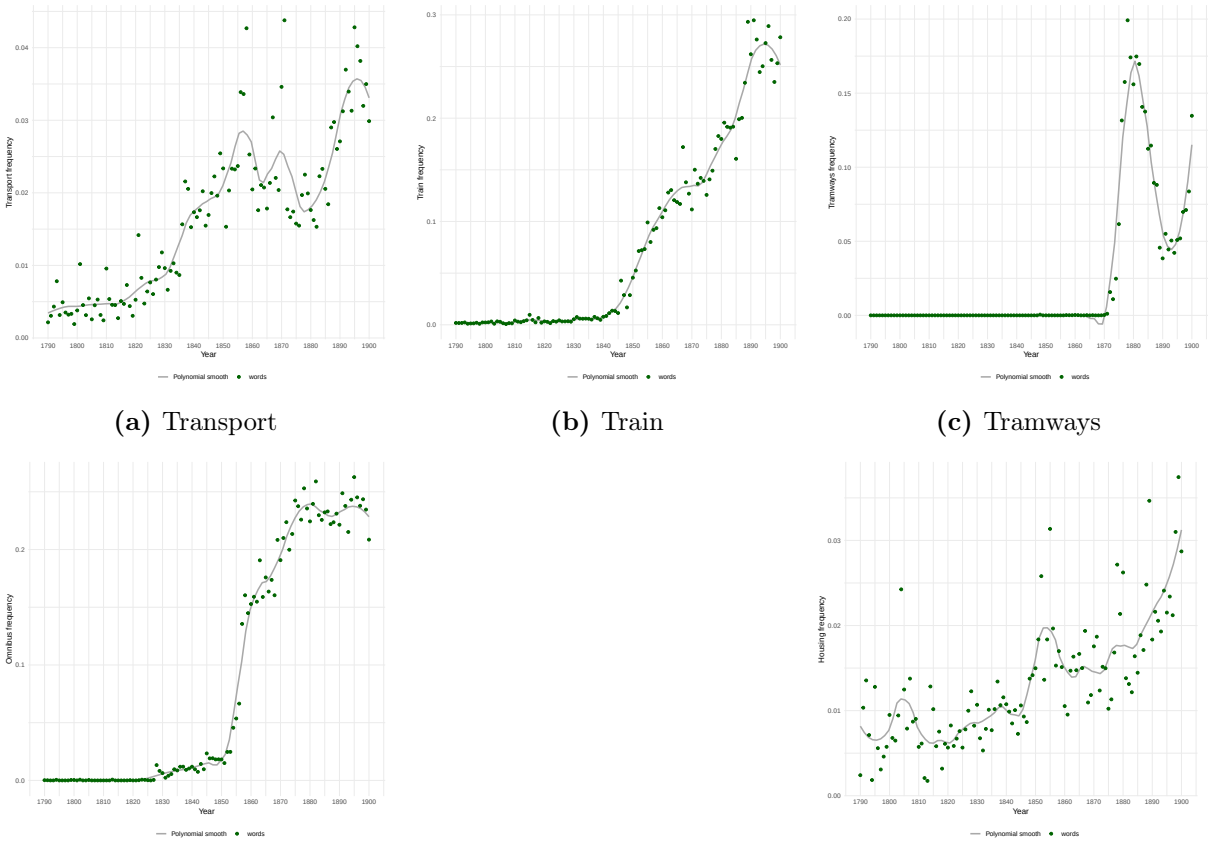

(a) Transport

(b) Train

(c) Tramways

(d) Omnibus

(e) Housing

Notes: Each figure reports the frequency of specific words in French newspapers for Paris over the period 1790-1900. Panels (a) to (e) show the frequency of *transport*, *train*, *tramways*, *omnibus*, and *housing*, respectively.

Figure A.7
Lexicometrics — Unemployment

Notes: This figure reports the frequency of the word *unemployment* in French newspapers for Paris over the period 1790-1900.

A.2.2 Average buildings heights in Paris (1891)

Figure A.8
Density of development

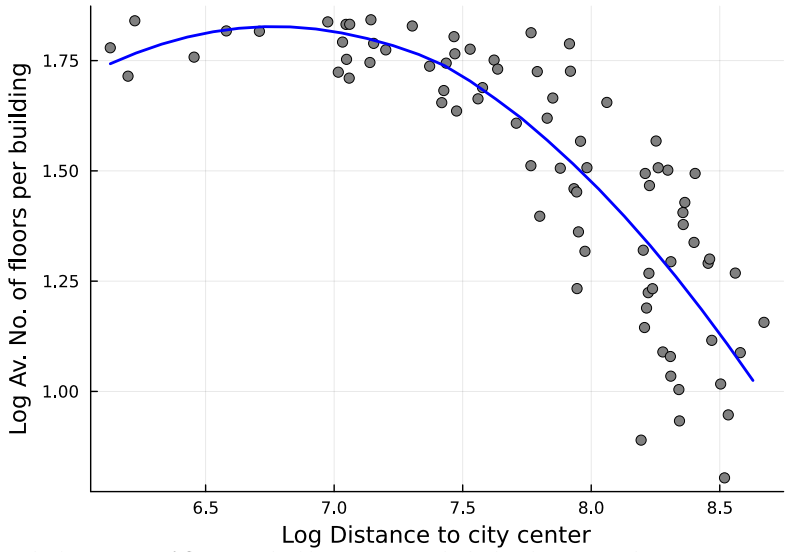

Notes: This figure compares the log average of floors per building in 1891 with the log distance to the city center. Each dots represents a neighborhood.

A.2.3 Greater Paris Population Dynamics

To explore Greater Paris population dynamics, I employ a OLS model to determine whether there has been a population agglomeration effect along the Paris border, using the population growth rate of neighborhoods between 1801 and 1906 as the dependent

variable and the logarithm of the distance from the Paris border (represented by the thick black line on Figure 1.6) as the independent variable. Figure A.9 displays a distinct negative correlation between population growth from 1801 to 1906 and the distance from the Paris border. This implies that the population of Greater Paris concentrated towards the Paris border during this period. It's important to emphasize that this correlation is particularly pronounced for the Paris neighborhoods. In addition, Parisian neighborhoods that experienced low or even negative growth during the period were initially the most populated. More precisely, the coefficient associated with the Paris sample, which stands at $-2.214(0.178)$, suggests a strong negative relationship between the population growth from 1801 to 1906 and the distance from the Paris border. This suggests that for neighborhoods within Paris, doubling the distance from the Paris border decreases the population growth by approximately 221.4%. Additionally, the R-squared indicates that the log distance to the Paris border explains approximately 66.3% of the variation in population growth within the Paris sample, highlighting the substantial explanatory power of this factor. In contrast, for the suburb sample, the coefficient of $-0.827(0.106)$ still demonstrates a negative relationship, though it is less pronounced.[1]

[1] The test whether both coefficients are significantly different gives a p-value of approximately 0.000000005. There is overwhelmingly strong evidence against the hypothesis that the coefficients of the variables in the two regression models are equal.

Figure A.9
Greater Paris population growth and distance to Paris border

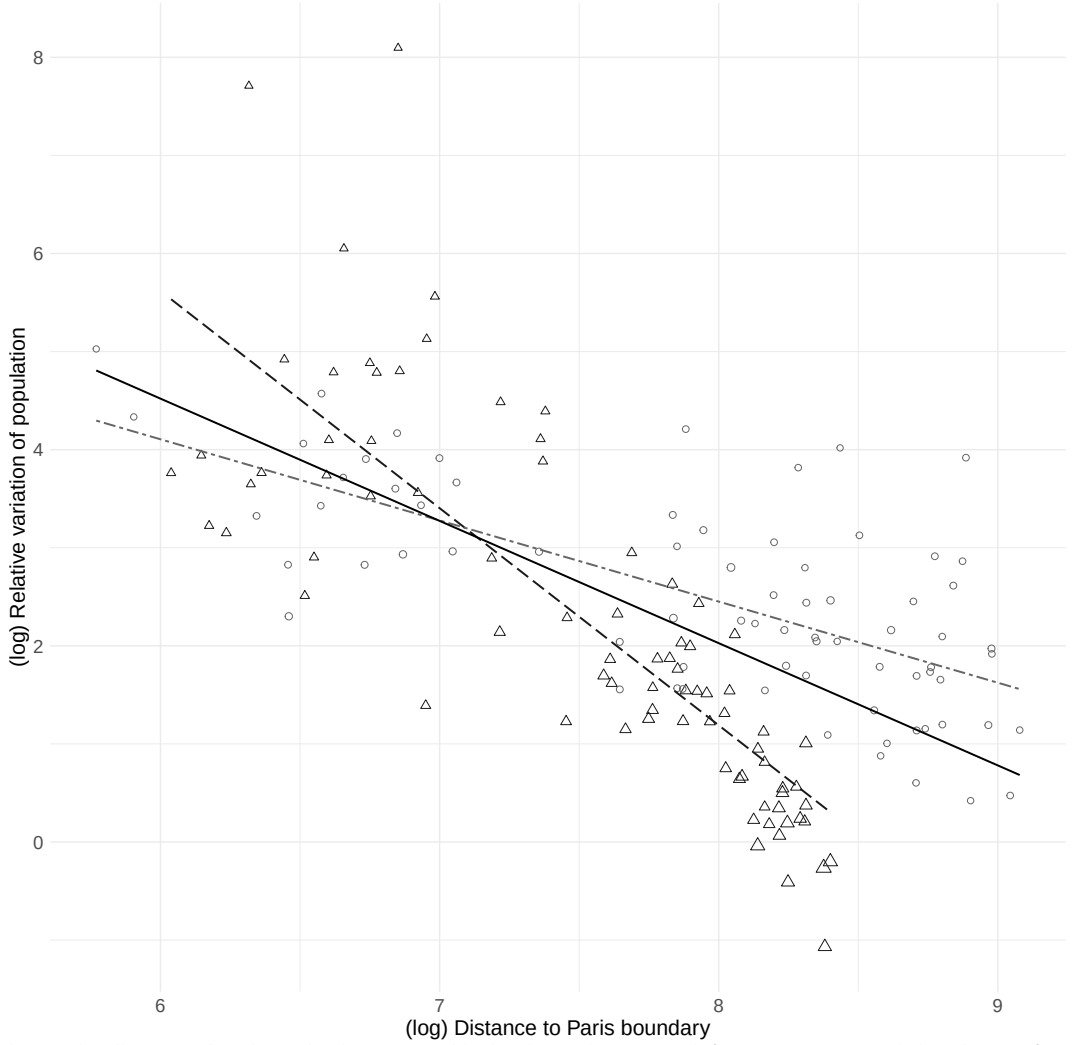

Notes: This graphic illustrates the relationship between neighborhoods population growth from 1801 to 1906 and their distance from the Paris boundary. Triangles represent spatial units within Paris, while circles represent spatial units in the suburb. The size of triangles and circles is function of 1801 population. The solid line represents the regression analysis for the entire sample, the double-dash line represents the suburb sample, and the long-dash line represents the Paris sample.

I run two econometrics specifications in order to describe the long-term population dynamics over the great Paris. Specifically, I look at whether individuals agglomerate to the edge of Paris boundary as suggested the graphic. First, I use the panel dimension and run the following specification,

$$ln\left(\frac{\text{Population}_{n(a),t+1}}{\text{Population}_{n(a),t}}\right) = \beta \text{ Distance to Paris boundary}_{n(a)} + \vartheta_t + \mu_a + \epsilon_{n(a),t}$$

where the dependent variable aims to capture the forward population growth, the independent is the distance between Paris boundary and the location n, ϑ_t is a time FE, and μ_a is a *arrondissement* FE.

Secondly, I use long-differences between 1801 and 1906 and run the following specification,

$$ln\left(\frac{\text{Population}_{n(a),1906}}{\text{Population}_{n(a),1801}}\right) = \beta \text{ Distance to Paris boundary}_{n(a)} + \mu_a + \epsilon_{n(a),t}$$

which is very similar to previous specification.

Table A.1

Great Paris Population Dynamics (1801-1906)

	Specification							
	Panel				Long-Differences			
	(1)	(2)	(3)	(4)	(5)	(6)	(7)	(8)
Distance to	−0.069	−0.045	−0.123	−0.045	−1.247	−0.836	−2.214	−0.827
Paris boundary	(0.005)	(0.006)	(0.009)	(0.005)	(0.117)	(0.101)	(0.179)	(0.106)
Year FE	Yes	Yes	Yes	Yes	No	No	No	No
Arrond. FE	No	Yes	No	No	No	Yes	No	No
Area	GP	GP	Paris	Suburb	GP	GP	Paris	Suburb
Observations	2,746	2,746	1,440	1,306	153	153	80	73
R^2	0.206	0.253	0.292	0.240	0.430	0.783	0.663	0.460

Notes: Each column reports an estimate from a separate regression. Regressions use 80 Parisian neighborhoods and 72 suburban municipalities. The independent variable is the log distance to Paris boundary. Columns (1) to (4) use the population growth each 10 years as dependent variable, panel data specification with year fixed-effects, and columns (3) and (4) use respectively the Parisian and suburban sample. Column (2) controls for *arrondissement* fixed-effects. Columns (5) to (8) use the population growth between 1801 and 1906 as dependent variable, and columns (7) and (8) use respectively the Parisian and suburban sample. Column (6) controls for *arrondissement* fixed-effects. Heteroskedasticity-robust standard errors are in parentheses.

A.3 Urban transport

A.3.1 *Petite Ceinture* railroad

Figure A.10
Representation of the PC railroad by a cartoon from Cham

Figure A.11
Construction of the *Petite Ceinture* railroad overtime

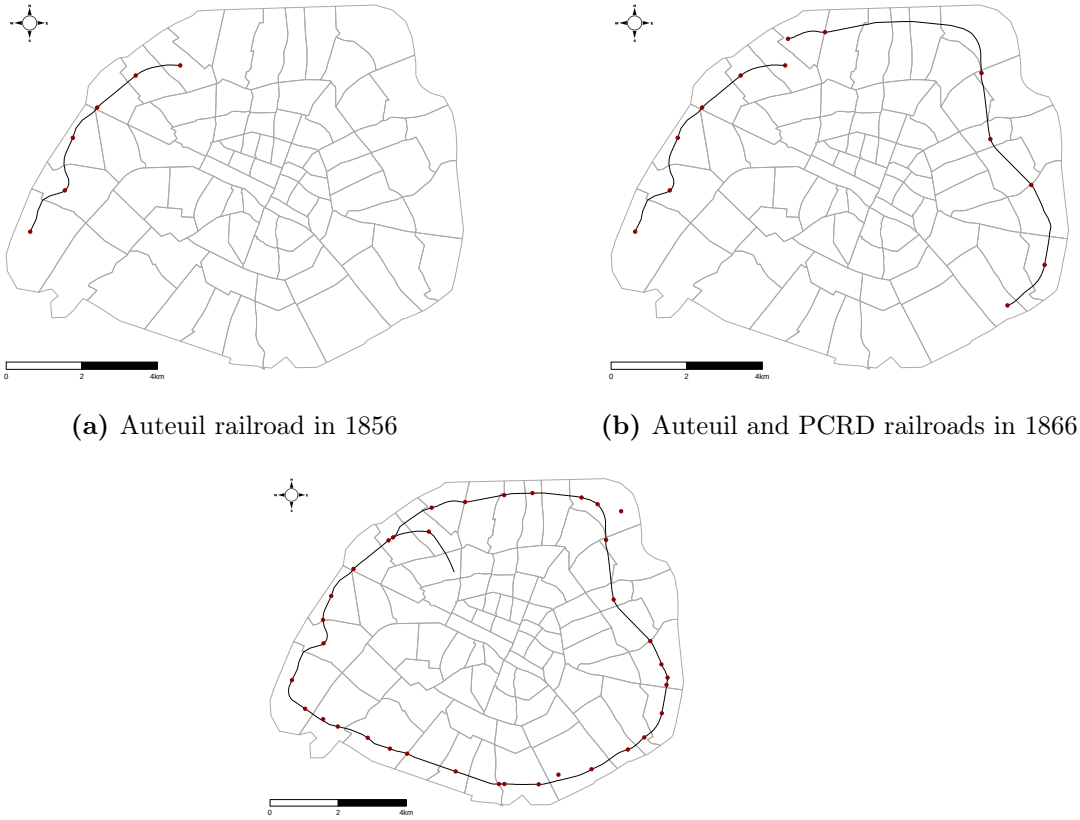

(a) Auteuil railroad in 1856

(b) Auteuil and PCRD railroads in 1866

(c) *Petite Ceinture* railroad in 1872

Notes: This figure displays the evolution of *Petite Ceinture* network overtime. Red dots represent train stations, dark line the railroad. The railroad has been built in 4 main phases:) Auteuil line (1854); ii) PCRD line (1862); iii) PCRG line (1867); iv) the completion of the circle with the connection between the Auteuil line and PCRD line in 1869. The Paris-Bestiaux station, a merchandise train station in the northeastern part of Paris, is not directly linked to the main *Petite Ceinture* railway network. Instead, it connects through a smaller section not displayed on this map.

Figure A.12
Treated spatial units overtime considering 500m threshold

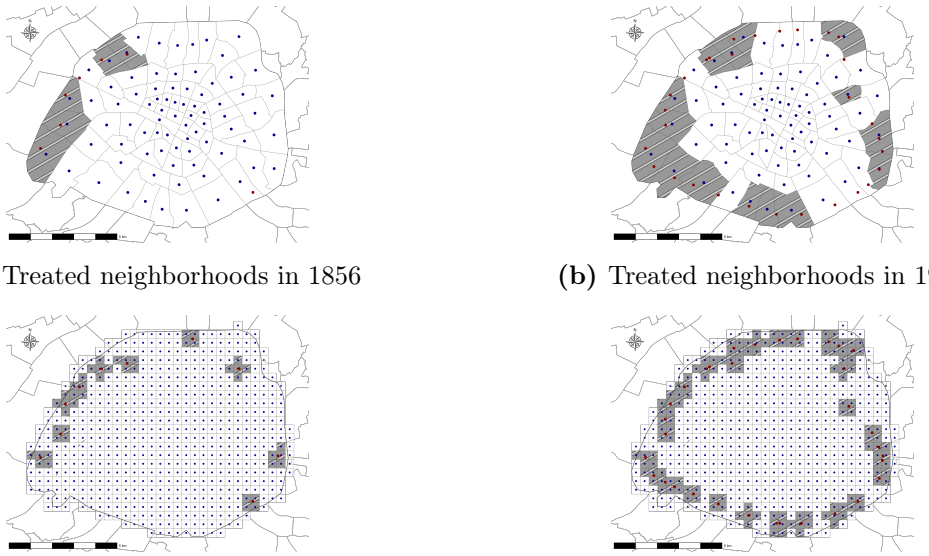

(a) Treated neighborhoods in 1856

(b) Treated neighborhoods in 1900

(c) Treated grids in 1856

(d) Treated grids in 1900

Figure A.13
Traffic of the *Petite Ceinture* in 1901

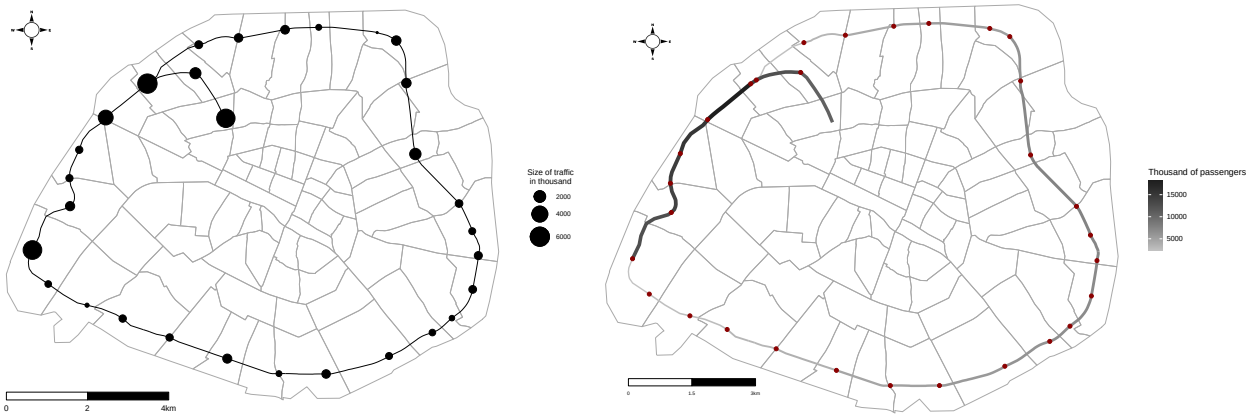

(a) By Train Station

(b) By Segment

Notes: The Panel (a) represents the traffic of the PC by train station, and Panel (b) represents the traffic of the PC by railroad segment. The actual number of stations was 30 in 1900. Here, some stations are missing from the data or have been merged (e.g. Bel-Air Vincennes and Bel-Air Ceinture). The traffic data is derived from bilateral flow matrices between stations. Traffic for each segment is calculated by finding the shortest path between the origin and destination stations. Then, the sum of traffic for each section is computed.

A.3.2 Streets network in 1896

Figure A.14
Streets in 1896

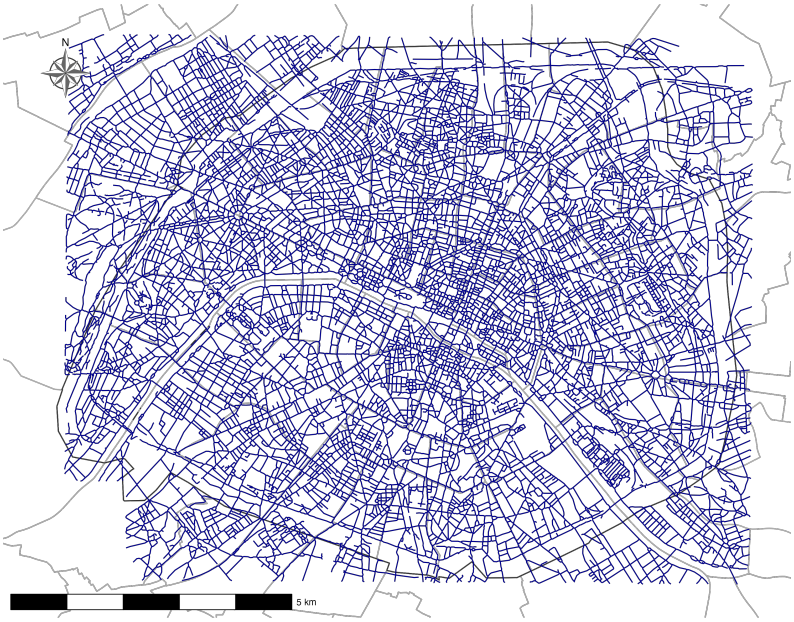

A.3.3 Speed of urban transport

Table A.2
Speed commuting modes

Transport Mode	Source	Value
	Structural Analysis	
Walk		5km/h
Omnibus & Tramways	Passalacqua (2012)	9km/h
Petite Ceinture	*Association Sauvegarde Petite Ceinture*	20km/h
	Reduced-Form Analysis	
Metro	*RATP/Wikipedia*	20km/h

A.3.4 Omnibuses and Tramways network

Figure A.15
Omnibus and tramways in 1896

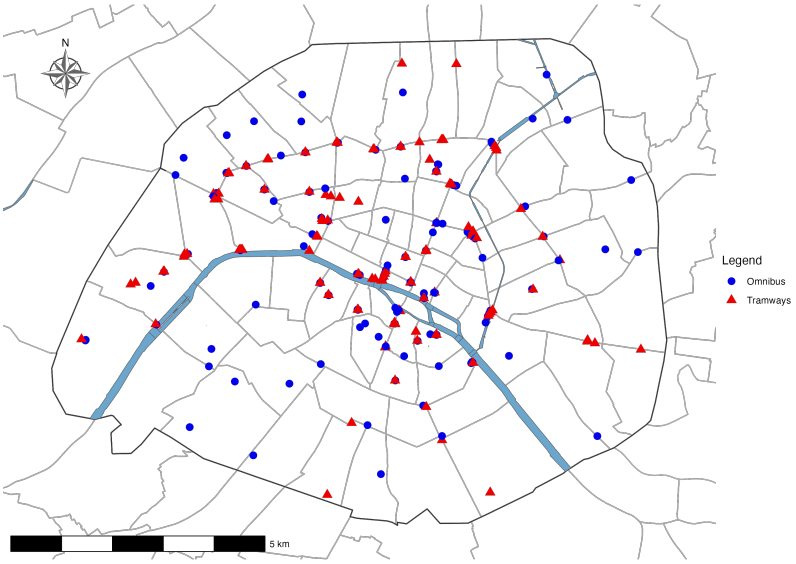

Figure A.16
Bilateral commuting time in 1896 with fixed omnibus and tramway

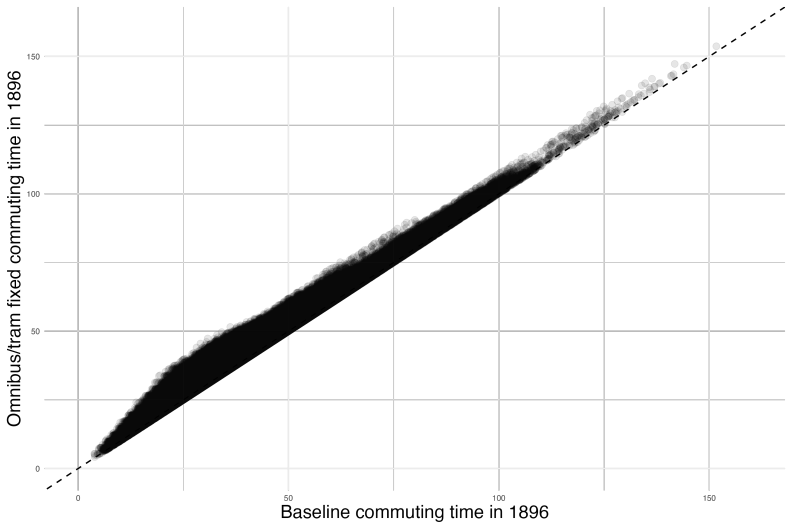

A.4 Robustness checks and others results

A.4.1 Short-term effects: freight market access using NLS

I use non-linear least squares (NLS) to disentangle market access. Following Redding and Venables (2004), access to suppliers and consumers should matter for firms selling final goods (such as retail establishments). To do so, I consider a freight travel time matrix $(t^T_{ni,t})$ for supplier access, and a commuting time matrix $(t^C_{ni,t})$ for consumer access. For factories, only access to the labor supply should matter, and for the population, access to all firms should matter. I consider the same long-difference specification as equation (1.2), and estimate the commuting time elasticity ν instead of calibrating it. As previously, I control for the initial building share as well as the proximity to Haussmann renovations. Moreover, I allow ν to vary across access to suppliers and consumers for retail. Finally, I consider two time functional forms: (i) an exponential functional form (as in the baseline), and (ii) a power functional form.

Retails As mentioned above, I consider two market access measures for retail growth. I use the NLS estimator and run both specifications,

$$\Delta \text{ Retail}_i = \eta_0 + \beta_1 \ln\left(\frac{\sum_n e^{-\nu_1 t^C_{ni,1896}} \text{Pop}_{n,1896}}{\sum_n e^{-\nu_1 t^C_{ni,1861}} \text{Pop}_{n,1861}}\right) + \beta_2 \ln\left(\frac{\sum_n e^{-\nu_2 t^T_{ni,1896}} \text{Fact}_{n,1896}}{\sum_n e^{-\nu_2 t^T_{ni,1861}} \text{Fact}_{n,1861}}\right) + X_i\gamma + \epsilon_i,$$

$$\Delta \text{ Retail}_i = \eta_0 + \beta_1 \ln\left(\frac{\sum_n \left(t^C_{ni,1896}\right)^{-\nu_1} \text{Pop}_{n,1896}}{\sum_n \left(t^C_{ni,1861}\right)^{-\nu_1} \text{Pop}_{n,1861}}\right) + \beta_2 \ln\left(\frac{\sum_n \left(t^T_{ni,1896}\right)^{-\nu_2} \text{Fact}_{n,1896}}{\sum_n \left(t^T_{ni,1861}\right)^{-\nu_2} \text{Fact}_{n,1861}}\right) + X_i\gamma + \epsilon_i,$$

where the dependent variable Δ Retail$_i$ is the growth of retail establishments within grid cell i between 1861 and 1896, $t^C_{ni,t}$ is the commuting time between locations n and i at time t, $\text{Pop}_{n,t}$ is the population in neighborhood n at time t, $t^T_{ni,t}$ is the freight travel time between locations n and i at time t, and $\text{Fact}_{n,t}$ is the total number of factories in grid cell n at time t. The vector X_i controls for grid cell initial share of buildings and distance to nearest Haussmann renovations. Figure A.17 shows the model fit, and Table A.3 shows the results, where column (1) considers the exponential functional form and column (2) considers the power functional form. While the estimated coefficients associated with the population (β_1) and factories (β_2) proximity are positive and significant, both their spatial decay parameters (ν_1, and ν_2) are really high whatever the commuting cost functional form. For example, factories no longer matter after 10 minutes of freight travel time $t^T_{ni,t}$

in both functional forms.

Figure A.17
Retail establishments - NLS fit

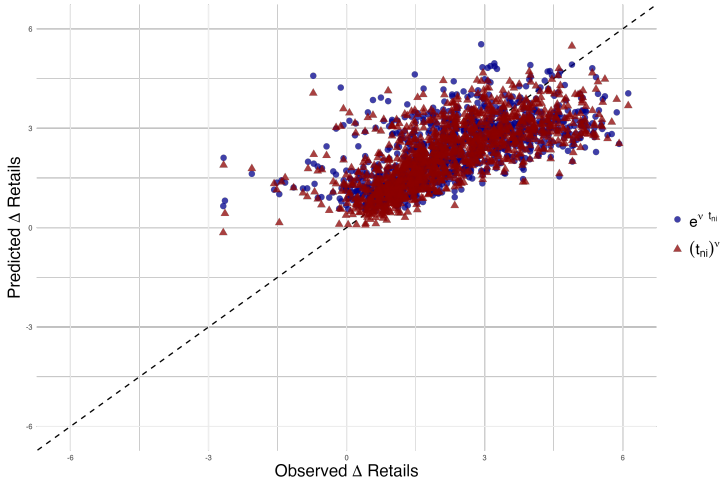

Table A.3
NLS: Retail establishments

	Retails	
	(1)	(2)
Population		
β_1	0.67	0.607
	(0.137)	(0.126)
ν_1	0.525	4.654
	(0.203)	(1.609)
Factories		
β_2	0.603	1.009
	(0.069)	(0.151)
ν_2	0.653	2.497
	(0.063)	(0.108)
Initial building share		
β_3	−0.905	−0.884
	(0.165)	(0.158)
Haussmann renovations		
β_4	−0.035	−0.028
	(0.029)	(0.028)
Commuting cost functional form	$e^{\nu\, t_{ni}}$	$(t_{ni})^{\nu}$
Observations	1,226	1,226

Factories As previously, I use the NLS estimator and run both specifications considering access to labor supply,

$$\Delta \text{ Factories}_i = \eta_0 + \beta_1 \ln\left(\frac{\sum_n e^{-\nu_1 \, t^C_{ni,1896}} \text{Pop}_{n,1896}}{\sum_n e^{-\nu_1 \, t^C_{ni,1861}} \text{Pop}_{n,1861}}\right) + X_i\gamma + \epsilon_i,$$

$$\Delta \text{ Factories}_i = \eta_0 + \beta_1 \ln\left(\frac{\sum_n \left(t^C_{ni,1896}\right)^{-\nu_1} \text{Pop}_{n,1896}}{\sum_n \left(t^C_{ni,1861}\right)^{-\nu_1} \text{Pop}_{n,1861}}\right) + X_i\gamma + \epsilon_i,$$

where the dependent variable Δ Factories$_i$ is the growth of factories within grid cell i between 1861 and 1896, $t^C_{ni,t}$ is the commuting time between locations n and i at time t, and $\text{Pop}_{n,t}$ is the population in neighborhood n at time t. The vector X_i controls for grid cell initial share of buildings and distance to nearest Haussmann renovations. Figure A.18 shows the model fit, and Table A.4 shows the results, where column (1) considers the exponential functional form and column (2) considers the power functional form. In the first specification considering the exponential functional form, the estimated coefficient associated with the population proximity (β_1) is positive and significant as in Table A.3. However, the magnitude of the spatial decay parameter (ν_1) is lower. Here, labor supply no longer matters after 20 minutes. The estimated parameters are not statistically significant for the second specification considering the power functional form.

Figure A.18
Factories - NLS fit

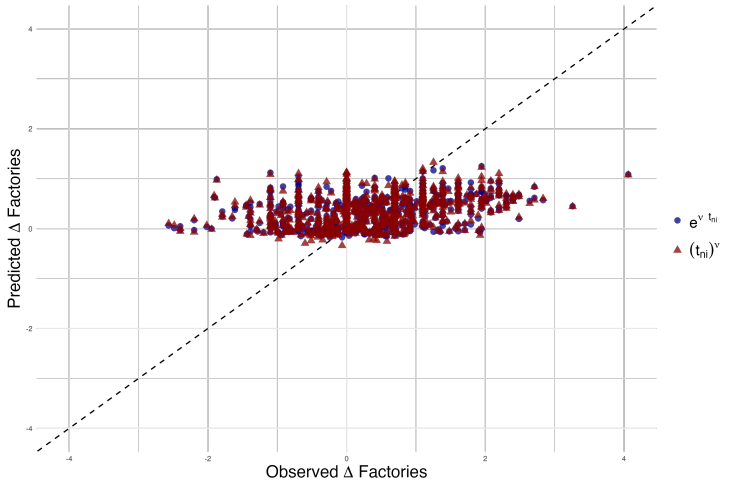

Table A.4
NLS - Factories

	Factories	
	(1)	(2)
Population		
β_1	0.592	1.623
	(0.134)	(1.19)
ν_1	0.289	1.041
	(0.132)	(0.637)
Initial building share		
β_3	−0.376	−0.333
	(0.18)	(0.181)
Haussmann renovations		
β_4	0.009	0.022
	(0.033)	(0.033)
Commuting cost functional form	$e^{\nu\, t_{ni}}$	$(t_{ni})^{\nu}$
Observations	743	743

Population As previously, I use the NLS estimator and run both specifications considering access to total number of firms,

$$\Delta \text{ Population}_n = \eta_0 + \beta_1 \ln\left(\frac{\sum_i e^{-\nu_1\, t^C_{ni,1896}} \text{Firms}_{i,1896}}{\sum_i e^{-\nu_1\, t^C_{ni,1861}} \text{Firms}_{i,1861}}\right) + X_n\gamma + \epsilon_n,$$

$$\Delta \text{ Population}_n = \eta_0 + \beta_1 \ln\left(\frac{\sum_i \left(t^C_{ni,1896}\right)^{-\nu_1} \text{Firms}_{i,1896}}{\sum_i \left(t^C_{ni,1861}\right)^{-\nu_1} \text{Firms}_{i,1861}}\right) + X_n\gamma + \epsilon_n.$$

where the dependent variable Δ Population$_n$ is the growth of population within neighborhood n between 1861 and 1896, $t^C_{ni,t}$ is the commuting time between locations n and i at time t, and Firms$_{i,t}$ is the total number of firms in grid cell i at time t. The vector X_n controls for neighborhood initial share of buildings and the total length of Haussmann renovations.

Figure A.19 shows the model fit, and Table A.5 shows the results, where column (1) considers the exponential functional form and column (2) considers the power functional form. The estimated coefficient associated with the firms proximity (β_1) is positive and significant, and the magnitude of the spatial decay parameter (ν_1) is similar to the result in Table A.4.

Figure A.19
Population - NLS fit

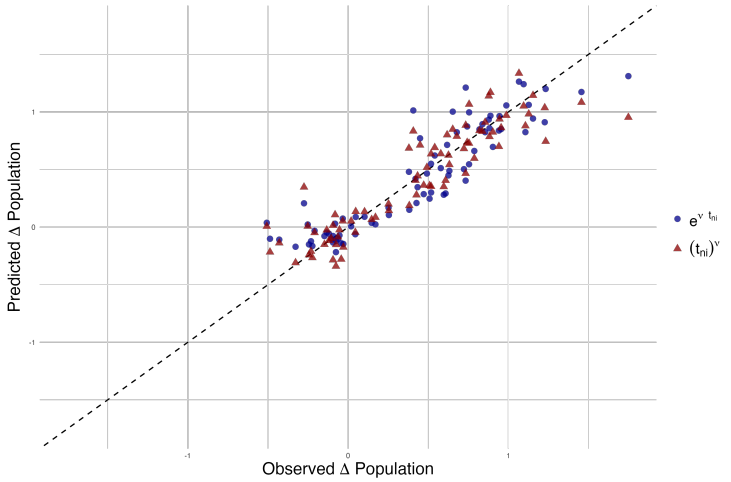

Table A.5
NLS - Population

	Population	
	(1)	(2)
Firms		
β_1	0.336	0.815
	(0.05)	(0.208)
ν_1	0.379	1.663
	(0.066)	(0.181)
Initial building share		
β_3	−0.426	−0.428
	(0.183)	(0.194)
Haussmann renovations		
β_4	0.009	0.016
	(0.027)	(0.028)
Commuting cost functional form	$e^{\nu\ t_{ni}}$	$(t_{ni})^{\nu}$
Observations	80	80

A.4.2 Short-term effects: additional results for market access strategy

Figure A.20
Instrumental variable for market access change between 1861 and 1896

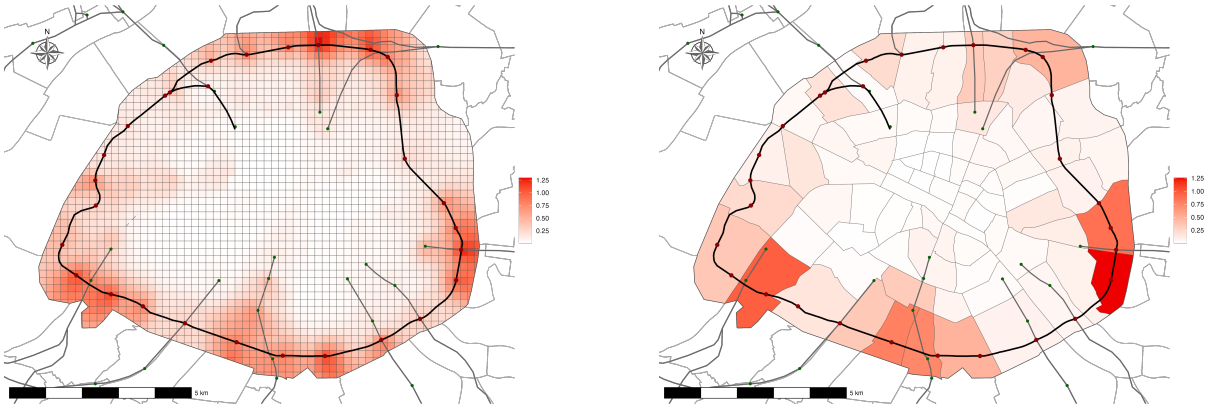

(a) IV for FMA change (1861- 1896)

(b) IV for RMA change (1861- 1896)

Notes: Both figures show growth in Market Access between 1861 and 1896 with the numerator fixed to the initial period. Panel (a) displays the firm market access growth in each 200m×200m grid cell. Panel (b) displays the residential market access growth in each Parisian neighborhood.

Table A.6
(Poisson regression) Firms and Market Access

	All			Factories			Retails		
	(1)	(2)	(3)	(4)	(5)	(6)	(7)	(8)	(9)
Log. FMA	2.85***	2.36***	1.92***	2.05***	1.68***	1.39***	3.11***	2.55***	2.07***
	(0.152)	(0.247)	(0.249)	(0.160)	(0.266)	(0.293)	(0.183)	(0.277)	(0.273)
Baseline controls		✓	✓		✓	✓		✓	✓
Old Paris border			✓			✓			✓
Observations	3,608	3,608	3,608	2,776	2,776	2,776	3,580	3,580	3,580
Grid cell fixed effects	✓	✓	✓	✓	✓	✓	✓	✓	✓
Year fixed effects	✓	✓	✓	✓	✓	✓	✓	✓	✓

Notes: Each column reports estimates from a separate regression using PPML. Regressions use 200mx200m grid cells. Dependent variable is the Firm Market Access growth between 1861 and 1896. From (1) to (3) the independent variable is the total firms. From (4) to (6) the independent variable is the total factories. From (7) to (9) the independent variable is the total retails. Baseline controls are the share of buildings in initial period interacted with year fixed-effects, and the distance to nearest Haussmann renovations. Columns (3), (6) and (9) control for a dummy indicating whether the grid cell is within boundary of 1859 Paris. Heteroskedasticity-robust standard errors are in parentheses and ***, **, * indicate significance at the 1%, 5% and 10% level, respectively.

Table A.7
Robustness checks ν - Firms growth and Market Access

	Total				Factories				Retails			
	(1)	(2)	(3)	(4)	(5)	(6)	(7)	(8)	(9)	(10)	(11)	(12)
Δ FMA	2.09***	0.770***	2.67***	0.971***	0.842***	0.396*	1.12***	0.454*	2.13***	0.681***	2.71***	0.812***
	(0.086)	(0.169)	(0.124)	(0.196)	(0.102)	(0.224)	(0.147)	(0.252)	(0.100)	(0.203)	(0.144)	(0.234)
Controls		✓		✓		✓		✓		✓		✓
ν	0.143	0.143	0.070	0.070	0.143	0.143	0.070	0.070	0.143	0.143	0.070	0.070
Observations	1,326	1,326	1,326	1,326	743	743	743	743	1,226	1,226	1,226	1,226
R^2	0.330	0.346	0.293	0.336	0.094	0.100	0.085	0.096	0.304	0.329	0.268	0.318
F-stat, Δ FMA		1,323.6		3,334.9		610.4		1,567.0		1,126.3		2,885.0

Notes: Each column reports estimates from a separate regression. Regressions use 200mx200m grid cells. Dependent variable is the Firm Market Access growth between 1861 and 1896. From (1) to (4) the independent variable is the growth in the total number of firms. From (5) to (8) the independent variable is the growth in the total number of factories. From (9) to (12) the independent variable is the growth in retail establishments. Baseline controls are the share of buildings in initial period and the distance to nearest Haussmann renovations. Columns (1), (2), (5), (6), (9), (10) use a calibrated $\nu = 0.143$ corresponding to 7×0.0204, and other columns use a calibrated $\nu = 0.07$ corresponding to ARSW's Berlin Wall paper. Instrumental variable is the Firm Market Access growth between 1861 and 1896 with the numerator fixed to the initial period. Heteroskedasticity-robust standard errors are in parentheses and ***, **, * indicate significance at the 1%, 5% and 10% level, respectively.

Table A.8
Robustness checks ν - Residential growth and Market Access

	Population				Rent			
	(1)	(2)	(3)	(4)	(5)	(6)	(7)	(8)
Δ RMA	0.642***	0.184***	1.16***	0.320***	0.726***	0.423*	1.31***	0.635*
	(0.049)	(0.066)	(0.107)	(0.108)	(0.096)	(0.232)	(0.198)	(0.369)
Controls		✓		✓		✓		✓
ν	0.143	0.143	0.070	0.070	0.143	0.143	0.070	0.070
Observations	80	80	80	80	80	80	80	80
R^2	0.747	0.759	0.698	0.750	0.524	0.516	0.488	0.493
F-stat, Δ RMA		79.3		154.6		79.3		154.6

Notes: Each column reports estimates from a separate regression. Regressions use 200mx200m grid cells. Dependent variable is the Residential Market Access growth between 1861 and 1896. From (1) to (4) the independent variable is the population growth. From (5) to (8) the independent variable is the rent growth. Baseline controls are the share of buildings in initial period and the total length of Haussmann renovations. Columns (1), (2), (5), (6) use a calibrated $\nu = 0.143$ corresponding to 7×0.0204, and other columns use a calibrated $\nu = 0.07$ corresponding to ARSW's Berlin Wall paper. Instrumental variable is the Residential Market Access growth between 1861 and 1896 with the numerator fixed to the initial period. Heteroskedasticity-robust standard errors are in parentheses and ***, **, * indicate significance at the 1%, 5% and 10% level, respectively.

Table A.9
Liberal profession and Market Access

	Liberal profession			
	(1)	(2)	(3)	(4)
Δ FMA	1.44***	0.989***	0.739***	0.098
	(0.136)	(0.194)	(0.225)	(0.248)
Baseline controls		✓	✓	✓
Old Paris border			✓	
Observations	871	871	871	871
R^2	0.154	0.171	0.176	0.141
F-stat, Δ FMA				1,131.8

Notes: Each column reports estimates from a separate regression. Regressions use 200mx200m grid cells. Dependent variable is the Firm Market Access growth between 1861 and 1896. The independent variable is the growth in total number of liberal professions. Baseline controls are the share of buildings in initial period and the distance to nearest Haussmann renovations. Columns (3) controls for a dummy indicating whether the grid cell is within boundary of 1859 Paris. Instrumental variable is the Firm Market Access growth between 1861 and 1896 with the numerator fixed to the initial period. Heteroskedasticity-robust standard errors are in parentheses and ***, **, * indicate significance at the 1%, 5% and 10% level, respectively.

Table A.10
1831-1856 Population growth and Market Access

	Population growth (1831-1856)		
	(1)	(2)	(3)
Δ RMA	0.852***	0.490**	0.082
	(0.117)	(0.190)	(0.192)
Controls		✓	✓
Observations	80	80	80
R^2	0.534	0.581	0.542
F-stat, Δ RMA			111.3

Notes: Each column reports estimates from a separate regression. Regressions use 80 Parisian neighborhoods. Dependent variable is the Residential Market Access growth between 1861 and 1896. Independent variable is the growth in population between 1831 and 1856. Controls are initial building share and the total length of Haussmann renovations within each neighborhood. Instrumental variable is the Residential Market Access growth between 1861 and 1896 with the numerator fixed to the initial period. Heteroskedasticity-robust standard errors are in parentheses and ***, **, * indicate significance at the 1%, 5% and 10% level, respectively.

Table A.11
Street networks and Market Access

	Street networks			
	(1)	(2)	(3)	(4)
Δ FMA	0.062*	-0.088	-0.130**	-0.082
	(0.035)	(0.056)	(0.064)	(0.069)
Initial building share		-0.183**	-0.156*	-0.176**
		(0.078)	(0.082)	(0.084)
Log. distance to Haussmann		-0.098***	-0.095***	-0.098***
		(0.018)	(0.018)	(0.018)
Old boundary			0.062	
			(0.047)	
Observations	2,145	2,145	2,145	2,145
R^2	0.001	0.029	0.029	0.029
F-stat, Δ FMA				4,999.2

Notes: Each column reports estimates from a separate regression. Regressions use 200mx200m grid cells. Dependent variable is the Firm Market Access growth between 1861 and 1896. The independent variable is the growth in the total length of streets. Instrumental variable is the Firm Market Access growth between 1861 and 1896 with the numerator fixed to the initial period. Heteroskedasticity-robust standard errors are in parentheses and ***, **, * indicate significance at the 1%, 5% and 10% level, respectively.

A.4.3 Short-term effects: staggered DiD strategy

Empirical Strategy To investigate whether the *Petite Ceinture* impacted the population and firms growth in the Parisian area taking into account staggered timing of the treatment, I rely on the estimator proposed by De Chaisemartin and d'Haultfoeuille (2024) and run the following Differences-in-Differences event-study specification,

$$ln\ Y_{n,t} = \psi_n + \eta_t + \sum_{\tau \neq -1} \beta_\tau \mathbb{1}\{t - E_n = \tau\} + X_{n,t}\gamma + \epsilon_{n,t}, \tag{A.1}$$

where $Y_{n,t}$ is the outcome of neighborhood n at time t, ψ_n and η_t are respectively neighborhood and year fixed effects, E_n is the time when neighborhood n initially receives the treatment, $\mathbb{1}$ corresponds to the binary treatment indicating whether a neighborhood is within 500m of a PC train stations. Neighborhoods are categorized into different cohorts based on their initial treatment timing. The identification strategy relies on the parallel trends assumption, which posits that before any treatment, treated and non-treated neighborhoods exhibit similar trends in a given observable outcome. In this context, neighborhoods that received the PC were not supposed to experience population or firm growth that differed from other neighborhoods prior to the deployment of the PC. To test for it, De Chaisemartin and d'Haultfoeuille (2024) enables the construction of an

event-study framework with placebo estimators computed by comparing the evolution of outcomes for neighborhoods treated for the first time and those not yet treated, prior to any changes in treatment status for first-time switchers. I employ a large period window (1831-1906) with data observed every 5 years to analyze pre-trends and dynamic treatment effects estimated by the coefficients β_τ associated with indicators for being τ periods relative to the treatment. The neighborhood fixed effect aims to capture invariant characteristics, such as distance to Paris city center or border, topography, altitudes, exogenous amenities, which is going to influence its population growth overtime. Additionally, I control for a binary variable capturing the area extension in 1860, other railroads proximity (Gare Saint-Lazare, Gare Montparnasse, Gare de l'Est, etc) and non-parametric trends with 10 indicator variables based on distance to the city center[2] in the vector of neighborhoods characteristics $X_{n,t}$ to capture other factors influencing the spatial distribution of the economic activity. The standard errors are clustered at the neighborhood level to allow for serial correlations.

Residential growth The outcome of interest is the logarithm of the total population within neighborhood n at time t, and I only consider train stations used for passenger purposes to investigate changes in commuting time. Moreover, I control for Haussmann renovations that reshape the urban structure and that could influence residential growth. Figure A.21 shows the results. Placebo estimates before the treatment are insignificant, indicating there are no significant pre-trends and the parallel trend assumption holds plausibly. Since I control for non-parametric trends based on the distance to the city center, results are interpreted in term of deviation from city center outmigration. The PC seems to have a positive impact on the residential growth 25 years following the implementation of train stations. This late effect result can be explained through the fact that the complete circle has been finished in 1869 (it is only at this moment it is relevant to use the PC as a commuting mode). On average, being close to 500 meters of a PC train station leads to a nearly 40% increase in the population within a neighborhood, 55 years later treatment.

Firms growth To investigate the effect on firm growth, I construct grid of 400×400m to exploit the granularity dimension of the city directories. These data document the locations of firms by their respective activities. I focus only on specific firms that have

[2] This allows population growth to vary according to distance to the city center and it aims to capture the city center outmigration pattern depicted in Figure 1.6.

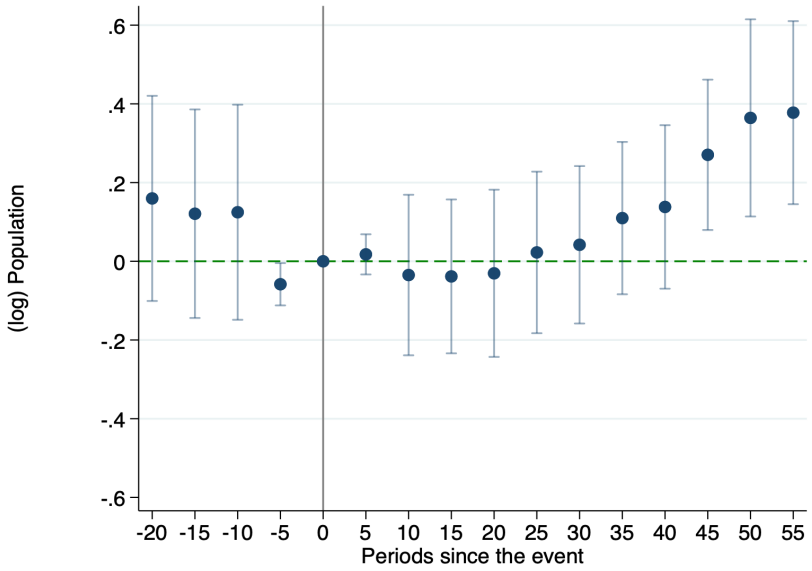

Figure A.21

Parisian Residential Growth and the *Petite Ceinture*

Notes: This figure shows the estimated effects of the PC on the logarithm of population and placebo estimates, using Parisian neighborhoods data from 1831-1906. The estimation is computed with did_multiplegt_dyn Stata command with 4 leads and 11 lags. Standard errors are clustered at the neighborhoods level. 95% confidence intervals relying on a normal approximation are shown in blue.

an interest to locate near to the PC. First, I take factories because they represent firms that extensively use the workforce to produce goods. A reduction in commuting costs for factories might broaden their access to a larger workforce supply, thus increasing their market potential. Moreover, it could be easier for them to export their final goods they produce. Second, I consider firms that are associated with small-scale activities, such as small shops (wine shops, retail store, creamery store, and grocery stores). The proximity to the PC would lower their merchandise costs. Therefore, I use the logarithm of the total number of specific firms within grid cell g at time t as the outcome variable and I consider both passengers and merchandise PC train stations. As previously, the treatment is binary indicating whether a grid cell is within 500m of a PC train stations, and I control for a binary variable capturing the area extension in 1860, other railroads proximity (Gare Saint-Lazare, Gare Montparnasse, Gare de l'Est, etc) and non-parametric trends with 10 indicator variables based on distance to the city center. Moreover, I control for a population market access measure at grid cell level. Figure A.22 displays the results when focusing specifically on these two categories. While the lead β_{-4} suggests large differences between treated and untreated units, others placebo estimates before the treatment are insignificant and close to zero for both types of activities. These differences 20 years before treatment could be explained by the low quality of city directories covering less areas at the beginning. Regarding retail activities, the effects appear to be quite substantial. On average, being close to 500 meters of a PC train station leads to a 66% increase in the

presence of retails within a grid cell, 45 years after treatment. A similar pattern emerges from the factories growth results. The size of the effect is in the same range as for retails, but the dynamics effects less reactive. This might be due to the fact that it's more costly to move a factory than a small retail shop. On average, being close to 500 meters of a PC train station leads to a 39% increase in the number of factories within a grid cell, 45 years after treatment.

Figure A.22

Specific firms and *Petite Ceinture*

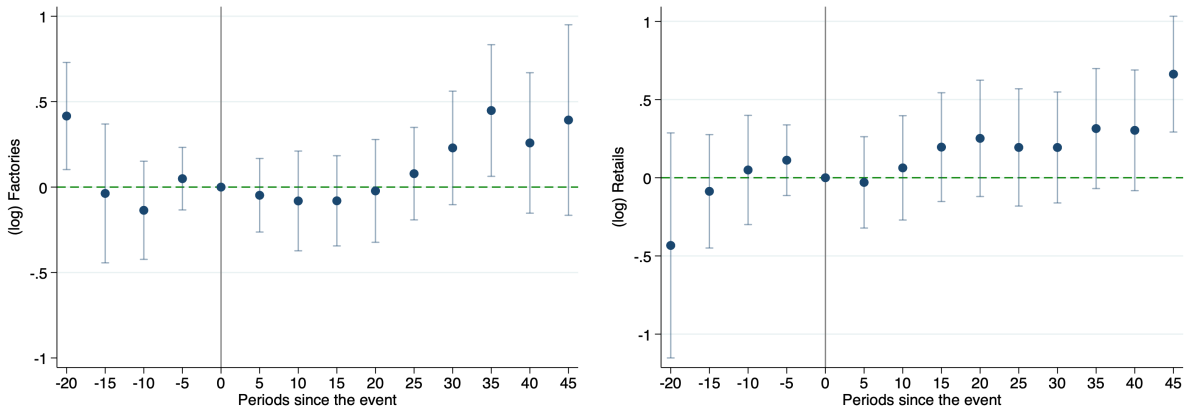

(a) Factories **(b)** Retail activities

Notes: This figure shows the estimated effects of the PC on the panels (a) and (c) logarithm of factories; panels (b) and (d) small shops, and placebo estimates, using Parisian neighborhoods data from 1831-1906. Panels (a) and (b) show results for a binary dummy based on 500m as treatment. Estimations are computed with did_ multiplegt_ dyn Stata command with 4 leads and 11 lags. Standard errors are clustered at the neighborhood level. 95% confidence intervals relying on a normal approximation are shown in blue.

Figure A.23
Streets development and the *Petite Ceinture*

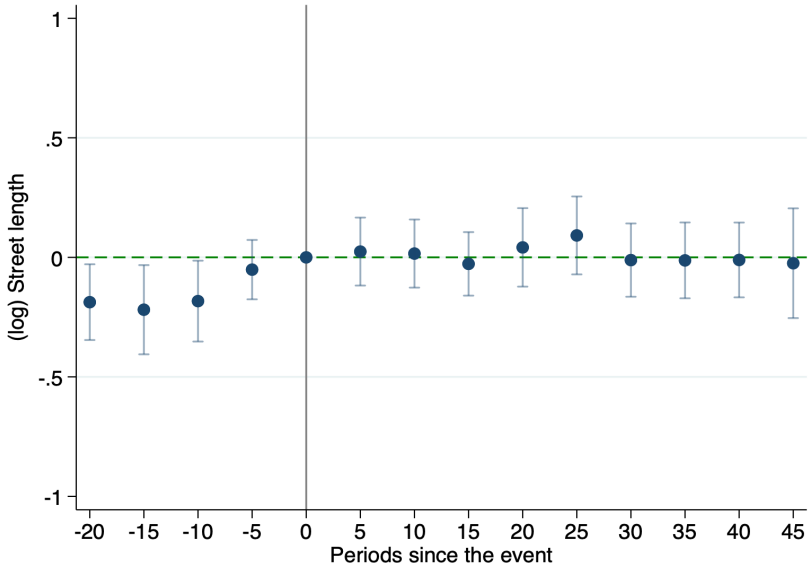

Notes: This figure shows the estimated effects of the PC on the logarithm of street length and placebo estimates, using grid cells as spatial units from 1831-1896. The estimation is computed with did_multiplegt_dyn Stata command with 4 leads and 9 lags. Standard errors are clustered at the grid cell level. 95% confidence intervals relying on a normal approximation are shown in blue.

Figure A.24
Liberal professions and the *Petite Ceinture*

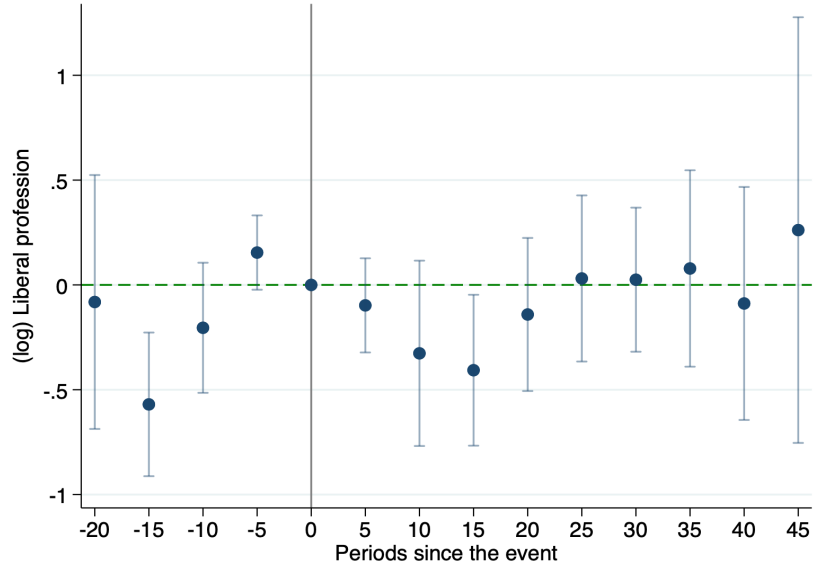

Figure A.25
Pre-trends sensitivity analysis

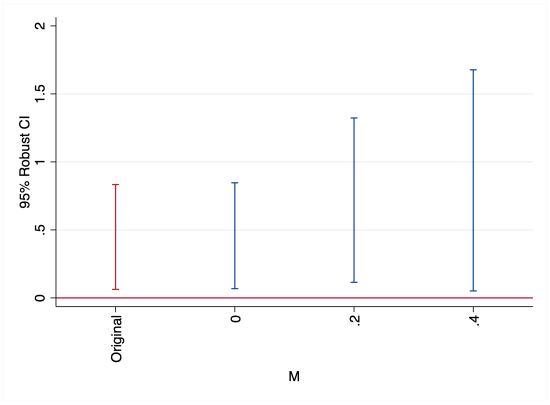

(a) Factories

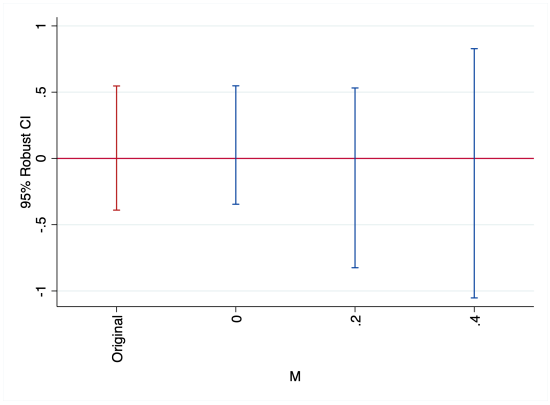

(b) Liberal professions

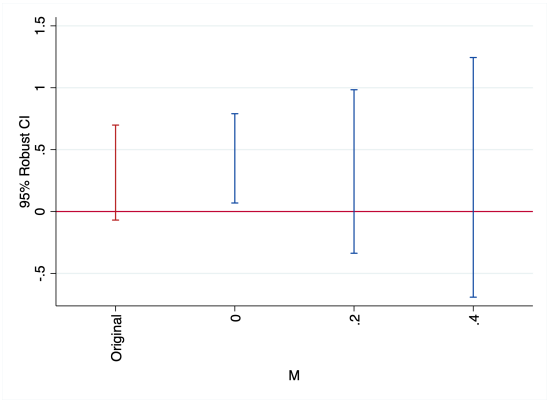

(c) Retails

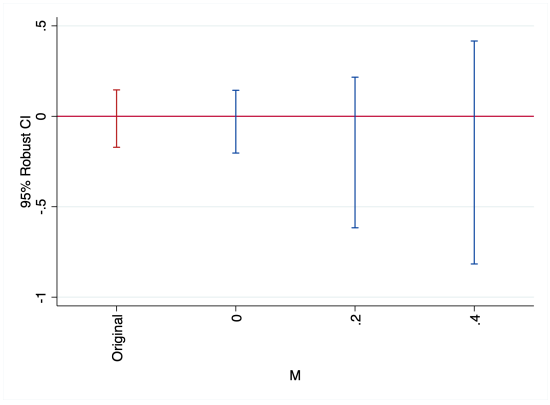

(d) Street Length

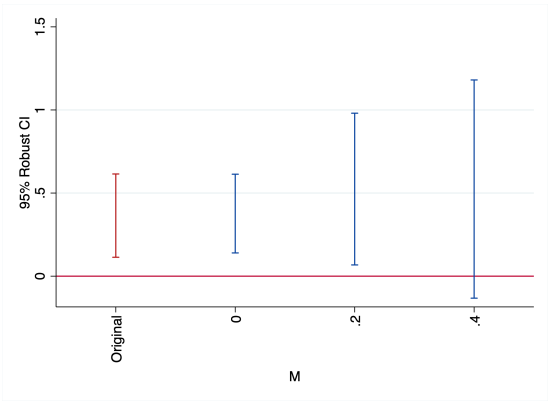

(e) Population

Figure A.26
Suburban Residential Sorting and the Chemin Fer

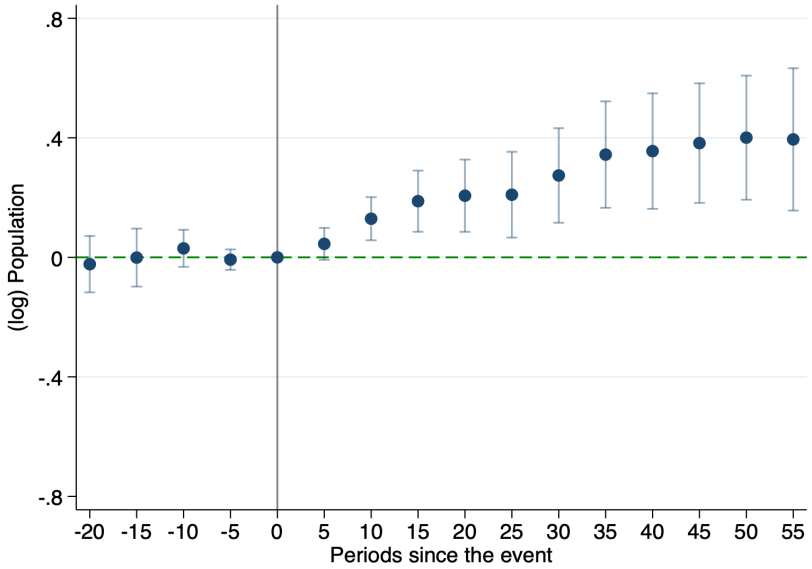

Notes: This figure shows the estimated effects of the railroad on the logarithm of population and placebo estimates, using suburban municipalities data from 1801-1896. The estimation is computed with did_ multiplegt_ dyn Stata command with 4 leads and 11 lags. Standard errors are clustered at the municipality level. 95% confidence intervals relying on a normal approximation are shown in blue.

Figure A.27
Replication of MMM: railways and population growth

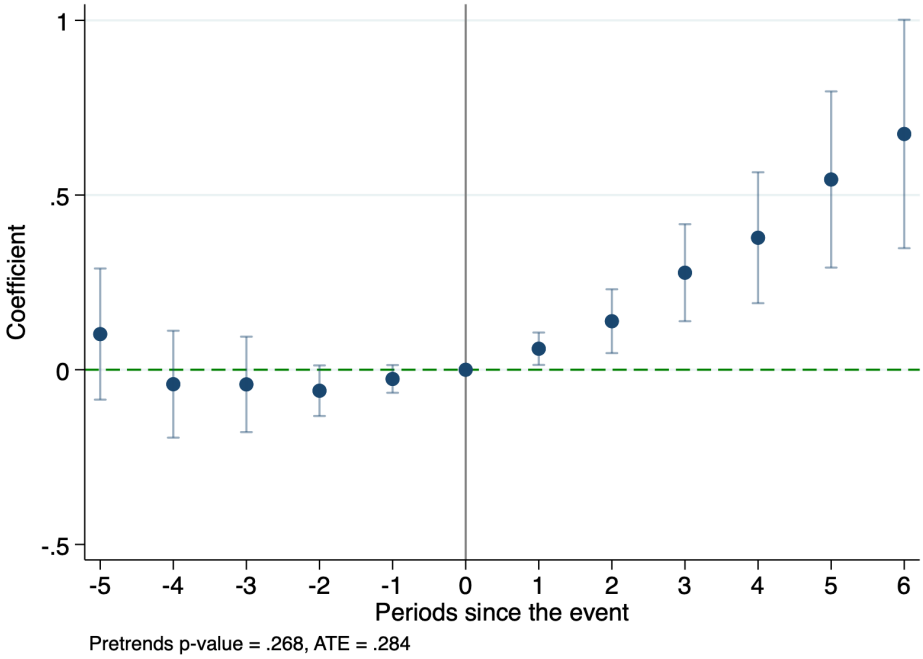

Notes: This figure shows the estimated effects of railways on the logarithm of population and placebo estimates, using parish data over 1801-1901 period from Heblich et al. (2020). The estimation is computed with did_ multiplegt_ dyn Stata command with 5 leads and 6 lags. Standard errors are clustered at the parish level level. 95% confidence intervals relying on a normal approximation are shown in blue.

A.4.4 Long-term effects

Table A.12
Long-Differences (1906-1954): Heterogeneity by traffic

	Δpop_n					
	(1)	(2)	(3)	(4)	(5)	(6)
$\text{Traffic}_{n(a),1901}$	0.12***	0.10*	0.00	0.12*	0.14*	0.15
	(0.03)	(0.05)	(0.05)	(0.07)	(0.08)	(0.12)
Log d2CC		0.22**	0.29**	0.23**	0.24**	0.26***
		(0.10)	(0.11)	(0.10)	(0.10)	(0.10)
Metro LCP Growth		-0.29	-0.38	-0.16	-0.10	-0.11
		(0.27)	(0.32)	(0.27)	(0.29)	(0.31)
Log area		0.14*	0.15*	0.14*	0.14*	0.15*
		(0.08)	(0.08)	(0.08)	(0.08)	(0.08)
Spatial Decay (δ)	1	1	0.5	1.5	2	3
Arrondissement FE	∘	✓	✓	✓	✓	✓
S.D indep. var	1.29	1.29	1.73	.96	.74	.49
R^2	0.242	0.766	0.751	0.772	0.771	0.766
Observations	80	80	80	80	80	80

Notes: Each column reports estimates from a separate regression. Regressions use 80 Parisian neighborhoods. Dependent variable is the log of relative population change within neighborhood between 1906 and 1954, and the independent is a measure of exposure to 1901 PC traffic computed through the sum of passengers from each station weighted by the distance between the neighborhood and the station. Spatial decay (δ) controls the importance of distance. Regressions from (2) to (6) include an *arrondissement* fixed effect. Heteroskedasticity-robust standard errors are in parentheses and ***, **, * indicate significance at the 1%, 5% and 10% level, respectively.

Table A.13
Long-Differences (1906-1954): housing supply

	$\Delta Buildings_n$		
	(1)	(2)	(3)
$\mathbb{1}_{n,1900}^{500\text{m}}$	0.27***	0.08	0.08
	(0.07)	(0.07)	(0.07)
Log d2CC		0.07	0.08
		(0.05)	(0.06)
Log area		0.15***	0.16***
		(0.03)	(0.03)
Metro LCP Growth		-0.11	-0.12
		(0.21)	(0.22)
Log initial Buildings			-0.07
			(0.05)
R^2	0.230	0.553	0.578
Observations	80	80	80

Figure A.28
Robustness check: varying LD ending-period

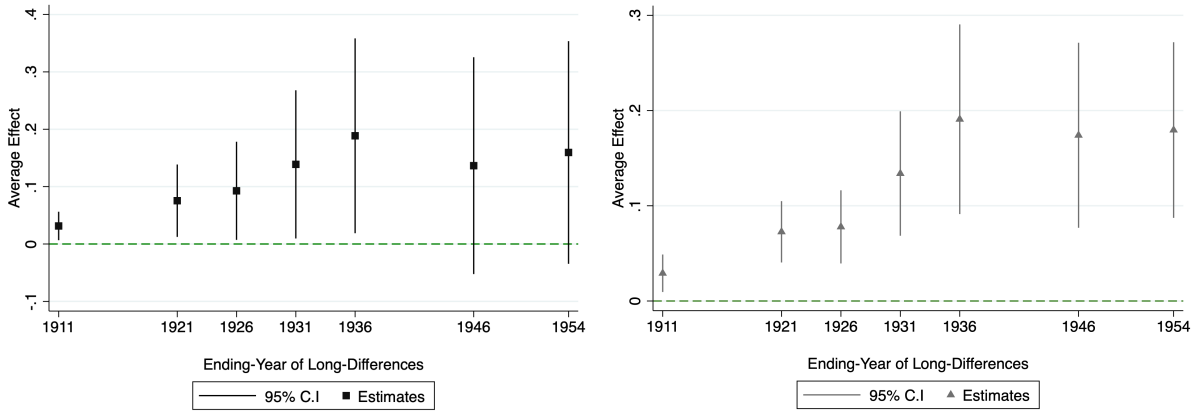

(a) Dummy 500m **(b)** Traffic Exposure ($\delta = 1$)

Notes: This figure displays estimates from several regression using different population growth ending periods. Panel (a) regressions use an indicator equal to one if neighborhood is within 500m of a train station as independent variable. Panel (b) use the traffic exposure measure as independent variable. Each regressions include an *arrondissement* fixed-effect and control for buildings growth.

A.4.5 Parisian urban growth

The construction of the PC not only changed the spatial distribution of economic activity within Paris but, due to its design and location in the periphery, also established a "physical" barrier separating the city from its suburbs. This goes in contrast with London which extended its underground railway system into the suburbs, creating an integrated urban growth (Heblich et al., 2020). This phenomenon was anticipated even at the time of the PC's approval, with the illustrator Cham remarking, "Paris won't need to be surrounded by walls once the circular railroad is completed" (see in appendix Figure A.10). To investigate whether the PC separated Paris and its suburbs by creating a barrier effect, Figure A.29 shows the population growth between 1861 and 1901 for Paris and its suburbs, and London and its suburbs, relative to the distance from each city's center. There is a stark differences between London and Paris after the threshold $5,800$ meters, corresponding to the maximum distance of Paris's peripheral neighborhoods. While London's population growth remained continuous with small change in slope beyond this distance, Paris exhibited a discontinuity. Beyond $5,800$ meters, the linear growth trend halted, with suburban cities growing at significantly lower rates than peripheral Parisian neighborhoods. Figure A.30 also confirms this result by running a RDD strategy. Hence, comparing both population growth with respect to distance to the city center highlights the barrier effect of the PC on Paris.

Figure A.29
Population growth of Paris and London relative to distance to the city center

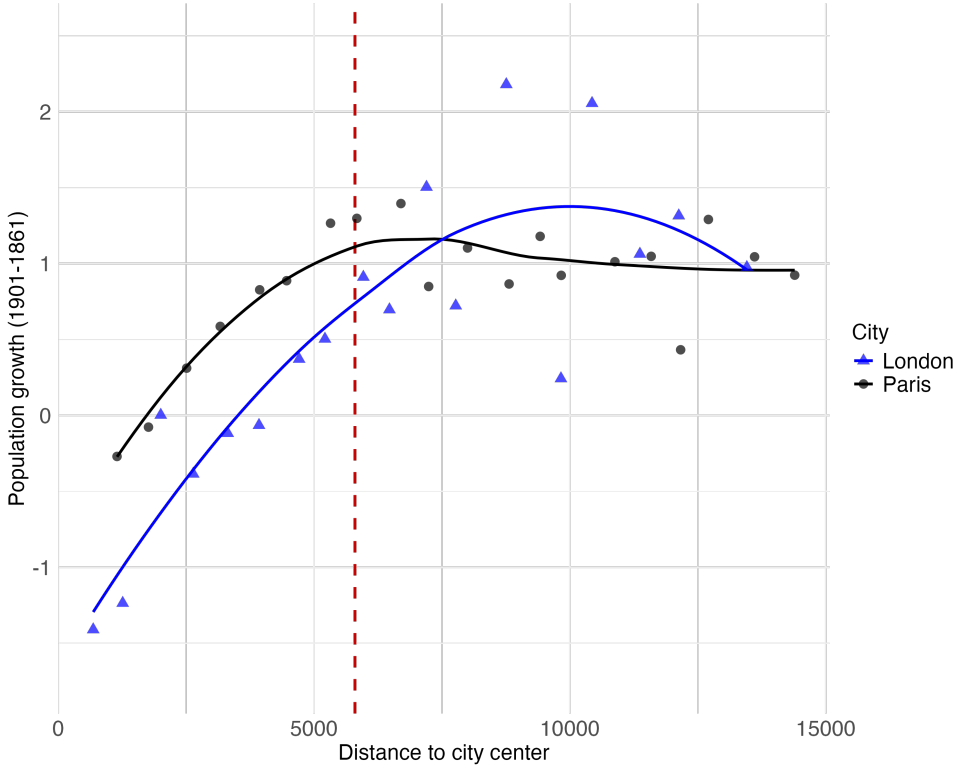

Figure A.30
Population growth (1861-1901) relative to distance to the city center

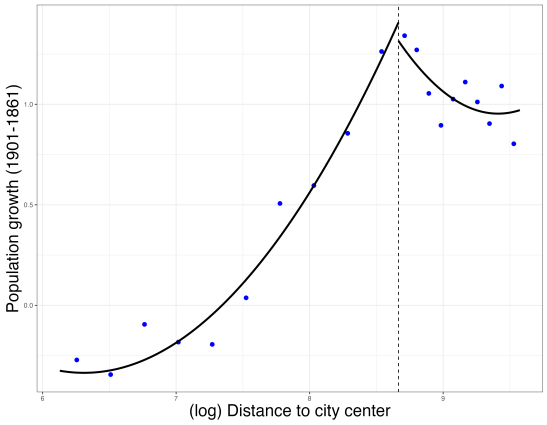

(a) Paris

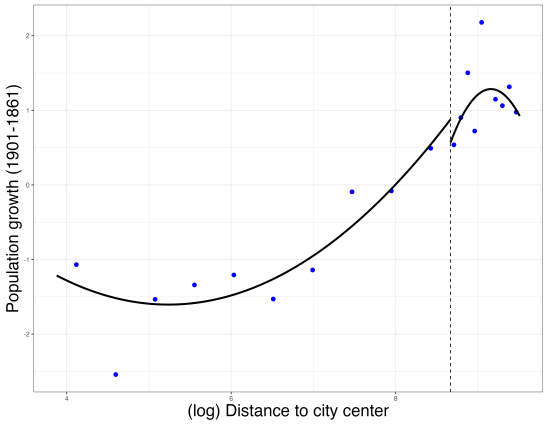

(b) London

A.4.6 Structural analysis additional results

Figure A.31

Residential floorspace demand and occupied housing units in 1891

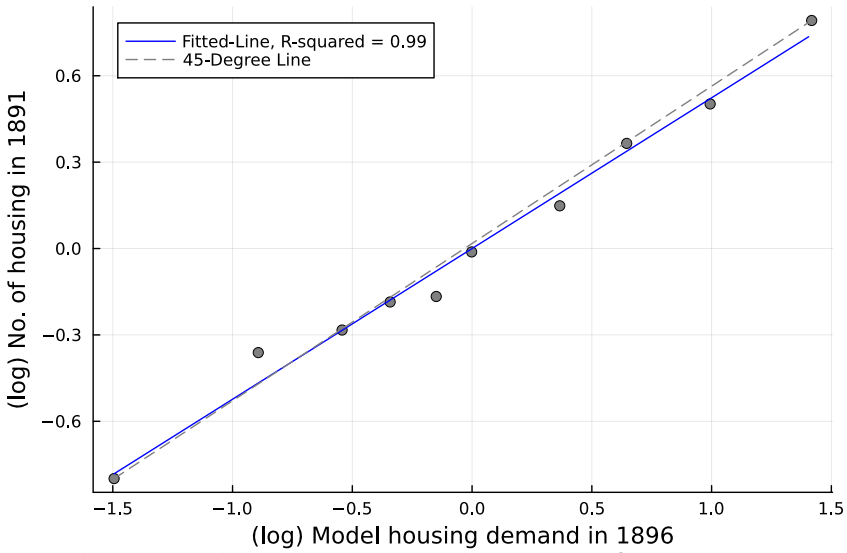

Notes: This figure compares the log occupied housing units in 1891 with the log residential floorspace demand in 1896. Each dot represents binned neighborhoods.

Figure A.32
Amenities

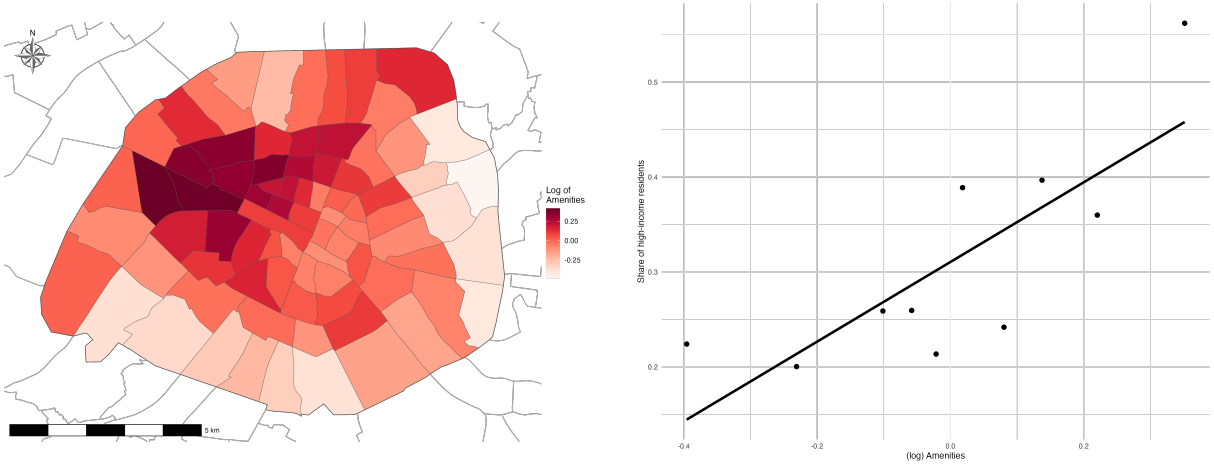

(a) Spatial distribution of amenities

(b) Amenities and high-income residents

Figure A.33
Changes in wages and distance to the city center

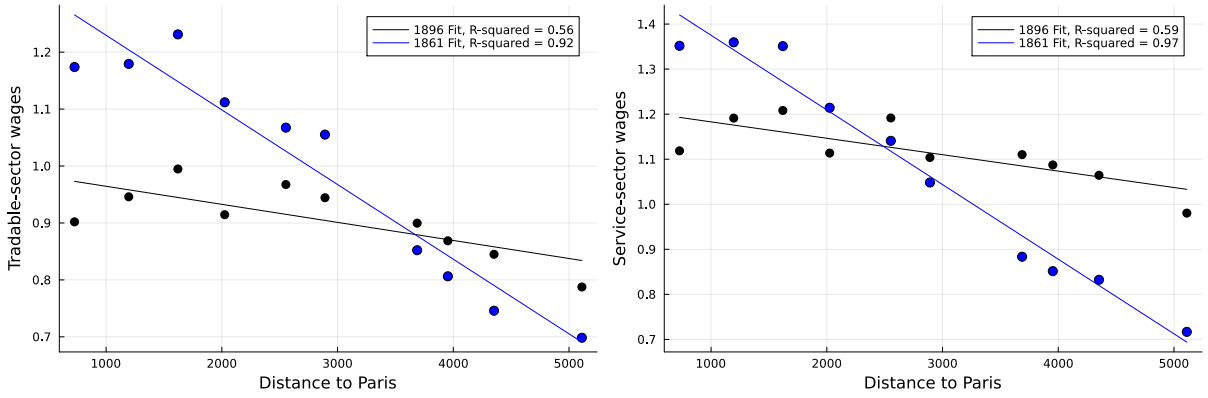

(a) Tradable sector

(b) Service sector

Notes: These figures represent the relationship between estimated wages and the distance to the city center in 1861 and 1896. In both Panel, binned blue dots represent industry specific wage estimates in 1861, and binned black dots represent industry specific wage estimates in 1896. Black and blue lines represents the fitted line from an OLS model.

Figure A.34
Haussmann Renovations

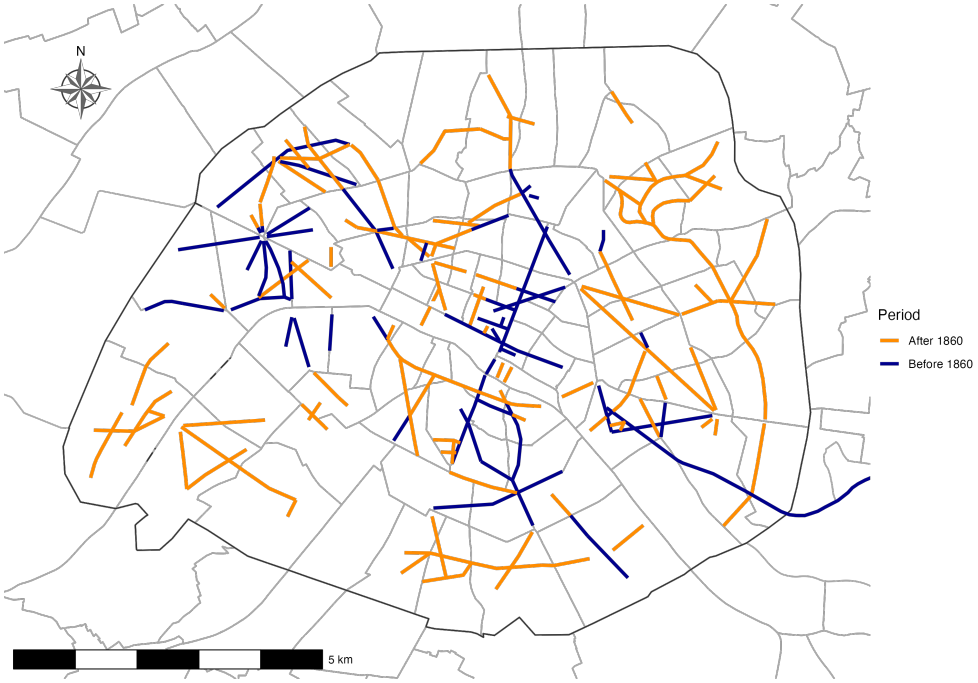

Notes: This map displays all the streets that have been created or renovated by Haussmann during the 19th century in Paris.

A.5 Data

A.5.1 Property values in 1876

Figure A.35
Property values in 1876

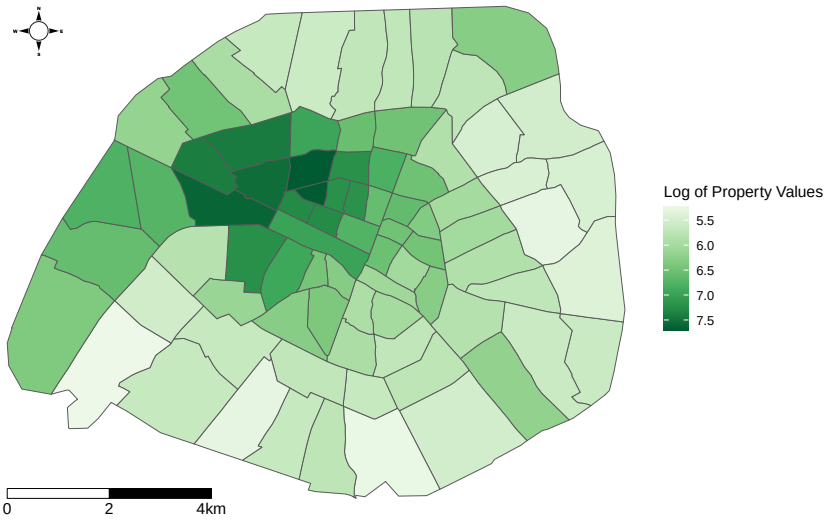

Notes: This map displays the logarithm of property values in 1876 across the 80 Parisian neighborhoods. Data are taken from the *révision cadastrale* of 1880.

A.5.2 City Directories

From firms to workplace employment City directories give informations on firms location but not on the workplace employment. In order to get an estimated total number of workers by sector per neighborhoods, I use the industrial survey of 1872 which provides information on the worker intensities by industries (see Table A.14). These average worker per firms can be seen as weights. For example, a factory is going to use more workforce than a small shop. Therefore, the total number of workers by sector per workplace in 1896 can be inferred following,

$$L_{ij} = \sum_{g \in j} \text{firms}_{ig} \times \text{weights}_{g,1872},$$

where L_{ij} is the total number of workers in i in sector j, firms_{ig} is the total of firms located in i belonging to industry g, and weights_{g} is the average number of workers used per firm within group industry g.

Table A.14
Average worker intensity by industries in 1872

Industry Name	Average Worker Intensity
Food/Alimentation	1.67
Building/Construction	8.4
Home Furniture	4.94
Clothing	4.37
Thread and Fabrics	11.72
Steel, Iron, Copper	8.25
Gold, Silver, Platinum	5.54
Chemical Industries	4.95
Printing, Engraving, Paper	8.51
Precision Instruments, Music and Watchmaking	5.04
Skins and Leathers	9.57
Military Equipment	14.16
Woodwork, Basketry and Brush Making	2.64
Parisian Articles	4.77
Miscellaneous Industries	2.01

A.5.3 Crosswalks and Old Greater Paris geography

I use the old geography of the Greater Paris (see Figure A.37) to compute weights in order to harmonize neighborhoods data over 1801-1856 period, to match 1860-1906 geography. More precisely, I compute weights based on overlapping areas. The method used is similar to Lee and Lin (2018). Moreover, I merge municipalities in order to be consistent with archives data (see Table A.15).

Figure A.36
Paris historical city center

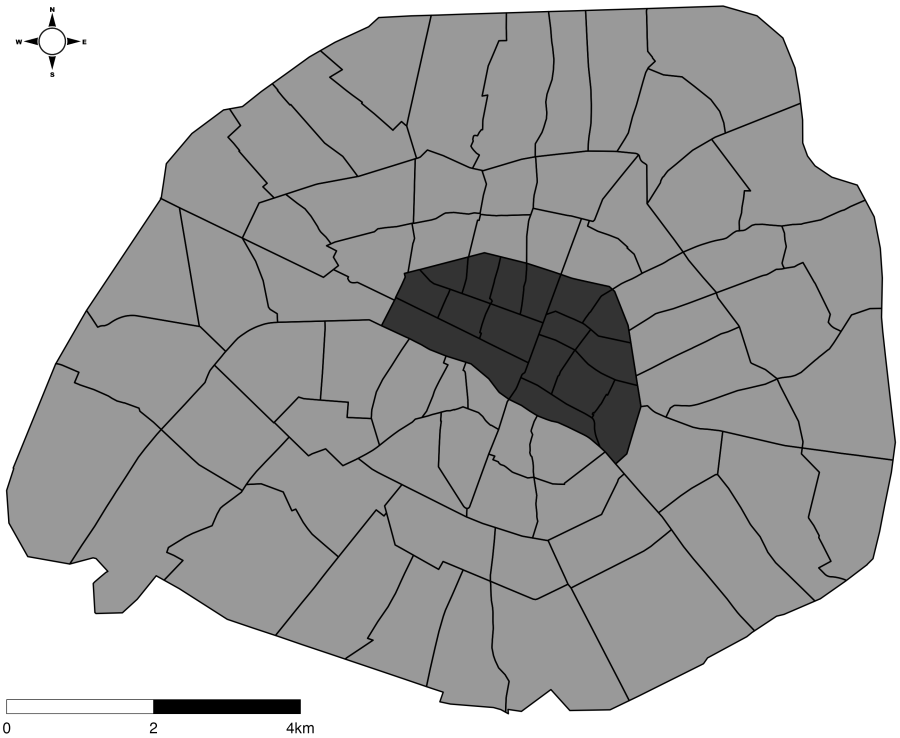

Notes: This map displays Paris boundaries after 1860. The dark grey area shows the historical city center, and in light grey the old periphery.

Figure A.37
Old geography of Great Paris

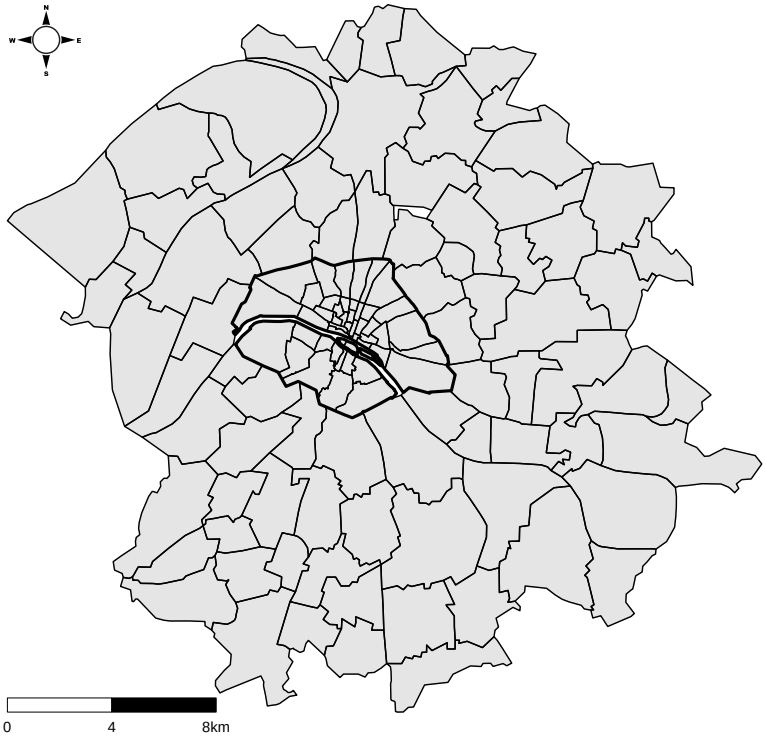

Notes: This map displays Greater Paris geography before 1860.

Table A.15
Merged Municipalities

Geography Name	Merged Municipalities
Arcueil	Arcueil, Cachan
Colombes	Colombes, La Garenne-Colombes, Bois-Colombes
Gennevilliers	Gennevilliers, Villeneuve-la-Garenne
Gentilly	Gentilly, Kremlin-Bicêtre

A.6 Theoretical Appendix

A.6.1 Residence and workplace-sector probabilities

$$\lambda_n^R = \frac{\sum_{j'} \sum_l \left(B_n w_{lj'}\right)^{\epsilon} \left(d_{nl}^C (P_n^T)^{\alpha^T} (P_n^S)^{\alpha^S} Q_n^{1-\alpha^T-\alpha^S}\right)^{-\epsilon}}{\sum_{j'} \sum_k \sum_l \left(B_k w_{lj'}\right)^{\epsilon} \left(d_{kl}^C (P_k^T)^{\alpha^T} (P_k^S)^{\alpha^S} Q_k^{1-\alpha^T-\alpha^S}\right)^{-\epsilon}}. \tag{A.2}$$

$$\lambda_{ij}^L = \frac{\sum_k \left(B_k w_{ij}\right)^{\epsilon} \left(d_{ki}^C (P_k^T)^{\alpha^T} (P_k^S)^{\alpha^S} Q_k^{1-\alpha^T-\alpha^S}\right)^{-\epsilon}}{\sum_{j'} \sum_k \sum_l \left(B_k w_{lj'}\right)^{\epsilon} \left(d_{kl}^C (P_k^T)^{\alpha^T} (P_k^S)^{\alpha^S} Q_k^{1-\alpha^T-\alpha^S}\right)^{-\epsilon}}. \tag{A.3}$$

A.6.2 Exact-hat algebra

The relative changes in amenities can be expressed as,

$$\widehat{B}_n = \widehat{R}_n^{\eta^R} \tag{A.4}$$

which includes only changes in residential employment ($\widehat{R}_n$) since land is fixed. The relative changes in bilateral trade of goods between locations can be expressed as,

$$\widehat{\pi}_{ni} = \frac{\left(\widehat{d}_{ni}^T \widehat{w}_{iT}^{\beta_L^T} \widehat{Q}_i^{\beta_H^T}\right)^{1-\sigma}}{\sum_{k \in \mathbb{J}} \pi_{nk} \left(\widehat{d}_{nk}^T \widehat{w}_{kT}^{\beta_L^T} \widehat{Q}_k^{\beta_H^T}\right)^{1-\sigma}} \tag{A.5}$$

which is function of changes in trade commuting costs ($\widehat{d}_{ni}^T$), and changes in prices of factors in the production function ($\widehat{w}_{iT}$,$\widehat{Q}_i$). The relative changes of tradable goods price index can be expressed as,

$$\widehat{P}_n^T = (\widehat{\pi}_{nn})^{-\frac{1}{(1-\sigma)}} \widehat{w}_{nT}^{\beta_L^T} \widehat{Q}_n^{\beta_H^T} \tag{A.6}$$

which is function of changes in domestic trade share ($\widehat{\pi}_{nn}$), and changes in prices of factors in the production function ($\widehat{w}_{nT}$, $\widehat{Q}_n$). The relative changes of non-tradable services price index can be expressed as,

$$\widehat{P}_n^S = \widehat{w}_{nS}^{\frac{1-\beta_L^S \sigma}{1-\sigma}} \widehat{Q}_n^{\frac{-\beta_H^S \sigma}{1-\sigma}} \widehat{L}_n^{1/(1-\sigma)} \tag{A.7}$$

which is function of changes in prices of factors in the production function ($\widehat{w}_{nS}$, $\widehat{Q}_n$), and changes in workplace employment ($\widehat{L}_n$). The relative changes of locations-sector choices

can be expressed as,

$$\widehat{\lambda}_{nij} = \frac{\left(\widehat{B}_n \widehat{w}_{ij}\right)^{\epsilon} \left(\widehat{d}^C_{ni} (\widehat{P}^T_n)^{\alpha_T} (\widehat{P}^S_n)^{\alpha_S} \widehat{Q}^{1-\alpha_S-\alpha_T}_n\right)^{-\epsilon}}{\sum_{j'} \sum_k \sum_l \lambda_{klj'} \left(\widehat{B}_k \widehat{w}_{lj'}\right)^{\epsilon} \left(\widehat{d}^C_{kl} (\widehat{P}^T_k)^{\alpha_T} (\widehat{P}^S_k)^{\alpha_S} \widehat{Q}^{1-\alpha_S-\alpha_T}_k\right)^{-\epsilon}} \tag{A.8}$$

which is function of changes in living cost ($\widehat{P}^T_n$, $\widehat{P}^S_n$, $\widehat{Q}_n$), changes in passengers commuting costs ($\widehat{d}^C_{ni}$), changes in amenities ($\widehat{B}_n$), and changes in sector-specific wages ($\widehat{w}_{ij}$). The relative changes in Parisian total population can be expressed as,

$$\left(\widehat{L}_{\mathbb{J}}\right)^{1/\epsilon} = \Big[\sum_{j'} \sum_k \sum_l \lambda_{klj'} \left(\widehat{B}_k \widehat{w}_{lj'}\right)^{\epsilon} \left(\widehat{d}^C_{kl} (\widehat{P}^T_k)^{\alpha_T} (\widehat{P}^S_k)^{\alpha_S} \widehat{Q}^{1-\alpha_S-\alpha_T}_k\right)^{-\epsilon} \Big]^{1/\epsilon} \tag{A.9}$$

which is function of changes in living cost ($\widehat{P}^T_n$, $\widehat{P}^S_n$, $\widehat{Q}_n$), changes in passengers commuting costs ($\widehat{d}^C_{ni}$), changes in amenities ($\widehat{B}_n$), and changes in sector-specific wages ($\widehat{w}_{ij}$). The changes in residential housing demand can be expressed as,

$$\widehat{H}^R_{nT} H^R_{nT} = \alpha_H \left[\sum_{i \in \mathbb{J}} \left(\frac{\lambda^R_{niT|n} \left(\frac{\widehat{w}_{iT}}{\widehat{d}^C_{ni}}\right)^{\epsilon}}{\sum_{l \in \mathbb{J}} \lambda^R_{nlT|n} \left(\frac{\widehat{w}_{lT}}{\widehat{d}^C_{nl}}\right)^{\epsilon}} \right) \right] \frac{\widehat{\lambda}^R_{nT} \lambda^R_{nT} \widehat{L}_{\mathbb{J}} L_{\mathbb{J}}}{\widehat{Q}_n Q_n} \tag{A.10}$$

$$\widehat{H}^R_{nS} H^R_{nS} = \alpha_H \left[\sum_{i \in \mathbb{J}} \left(\frac{\lambda^R_{niS|n} \left(\frac{\widehat{w}_{iS}}{\widehat{d}^C_{ni}}\right)^{\epsilon}}{\sum_{l \in \mathbb{J}} \lambda^R_{nlS|n} \left(\frac{\widehat{w}_{lS}}{\widehat{d}^C_{nl}}\right)^{\epsilon}} \right) \right] \frac{\widehat{\lambda}^R_{nS} \lambda^R_{nS} \widehat{L}_{\mathbb{J}} L_{\mathbb{J}}}{\widehat{Q}_n Q_n} \tag{A.11}$$

and the changes in commercial housing demand can be expressed as,

$$\widehat{H}^L_{nT} H^L_{nT} = \frac{\beta^T_H}{\beta^T_L} \widehat{\lambda}^L_{nT} \lambda^L_{nT} \widehat{L}_{\mathbb{J}} L_{\mathbb{J}} \frac{\widehat{w}_{nT} w_{nT}}{\widehat{Q}_n Q_n} \tag{A.12}$$

$$\widehat{H}^L_{nS} H^L_{nS} = \frac{\beta^S_H}{\beta^S_L} \widehat{\lambda}^L_{nS} \lambda^L_{nS} \widehat{L}_{\mathbb{J}} L_{\mathbb{J}} \frac{\widehat{w}_{nS} w_{nS}}{\widehat{Q}_n Q_n}. \tag{A.13}$$

Finally, the changes in rateable values can be expressed as,

$$\widehat{\mathbb{Q}}_n \mathbb{Q}_n = \widehat{Q}^{1+\mu}_n \mathbb{Q}_n. \tag{A.14}$$

A.7 Calibration

A.7.1 Overview of model quantification

Table A.16
Parameters Calibration and Estimation

Parameter	Description	Method	Value
	Calibrated		
ϵ	Fréchet parameter	Heblich et al. (2020)	5.25
α_S	Share of services consumption	Industrial survey 1872	0.5
α_T	Share of tradable consumption	Industrial survey 1872	0.25
α_H	Share of housing consumption	Heblich et al. (2020)	0.25
σ	Elasticity of substitution across services		4.5
β_H^S	Share of floorspace in services production function	Industrial survey 1872	0.266
β_L^S	Share of labor in services production function	Industrial survey 1872	0.534
β_M^S	Share of machinery in services production function	Industrial survey 1872	0.2
β_H^T	Share of floorspace in tradable production function	Heblich et al. (2020)	0.6
β_L^T	Share of labor in tradable production function	Heblich et al. (2020)	0.2
β_M^T	Share of machinery in tradable production function	Heblich et al. (2020)	0.2
	Estimated		
$d_{ni}^C = e^{\tau\, t_{ni}}$	Passenger commuting costs	PC bilateral flows	$\tau = 0.0204$
$d_{ni}^T = e^{\kappa\, t_{ni}}$	Freight commuting costs	Monte et al. (2018)	$\kappa = 0.0068$
η^R	Residential agglo. forces	OLS	0.168
μ	Housing supply elasticity	OLS	0.517

A.7.2 Commuting time disutility

Table A.17 shows the main and alternative specifications for estimating commuting cost elasticity τ in equation (1.35).

First two columns use a log specification, columns (3) and (4) use a PPML estimator to not drop flows with 0 passengers, and last column uses an IV specification. Since the *Petite Ceinture* network is designed in a circular shape, and it is possible to use it for leisure purposes; there are observations making the origin-to-origin journey. As it doesn't really make sense to study work commuting, I'm excluding most of these observations by excluding bottom and top 10% of commuters in columns (2) and (4). Lastly, I instrument commuting time between train stations with euclidean distances in column (5). Overall, coefficients associated to the commuting cost elasticity display similar magnitude and I use the first specification to calibrate $\tau = 0.204$ in the quantitative spatial model.

Table A.17
Estimation of τ

	$Log(Y)$		PPML		IV
	(1)	(2)	(3)	(4)	(5)
Commuting time	-0.0204***	-0.0169***	-0.0260***	-0.0190***	-0.0140***
	(0.0037)	(0.0023)	(0.0040)	(0.0044)	(0.0026)
Observations	575	457	593	475	457
R^2	0.548	0.840			—
F-test (1st stage), Commuting time					6,498.6
Sample	All	10% - 90%	All	10% - 90%	10% - 90%
Origin fixed effects	✓	✓	✓	✓	✓
Destination fixed effects	✓	✓	✓	✓	✓

Notes: Each column reports estimates from a separate regression. Regressions use bilateral flows between each train stations of the PC. The dependent variable is the traffic from an origin station to a destination station. Each regression includes origin and destination fixed-effects. The independent variable is the commuting time between two stations. Columns (1) and (2) use a OLS estimator, while (3) and (4) use a PPML estimator. Last column instruments the commuting time with the euclidean distance between two stations. Columns (2), (4), and (5) exclude stations that are within bottom and top 10% of commuters. Heteroskedasticity-robust standard errors are in parentheses and ***, **, * indicate significance at the 1%, 5% and 10% level, respectively.

A.8 Bootstrap: other results

A.8.1 Correlation

Figure A.38
Bootstrap results: ϵ

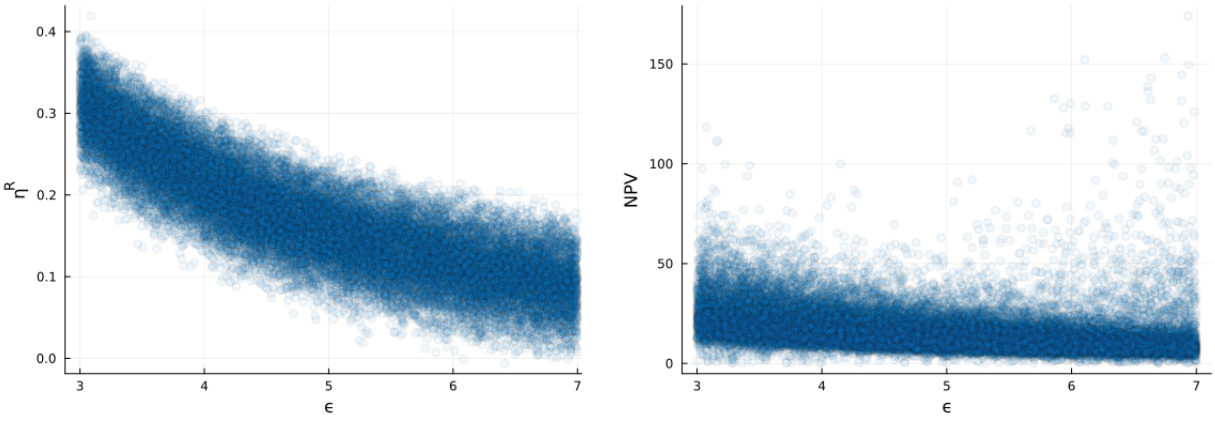

(a) Residential agglomeration forces (η^R) **(b)** Economic impact factor of the PC

Notes: These figures show the correlation of ϵ with: residential agglomeration forces in Panel (a), and economic impact factor of the PC removal in Panel (b), from a bootstrap procedure of 40,000 random draws of $\{\epsilon, \alpha_H, \alpha_T, \alpha_S, \kappa, \tau, \beta_H^S, \beta_L^S, \beta_M^S, \beta_H^T, \beta_L^T, \beta_M^T, \mu\}$.

Figure A.39
Bootstrap results: τ

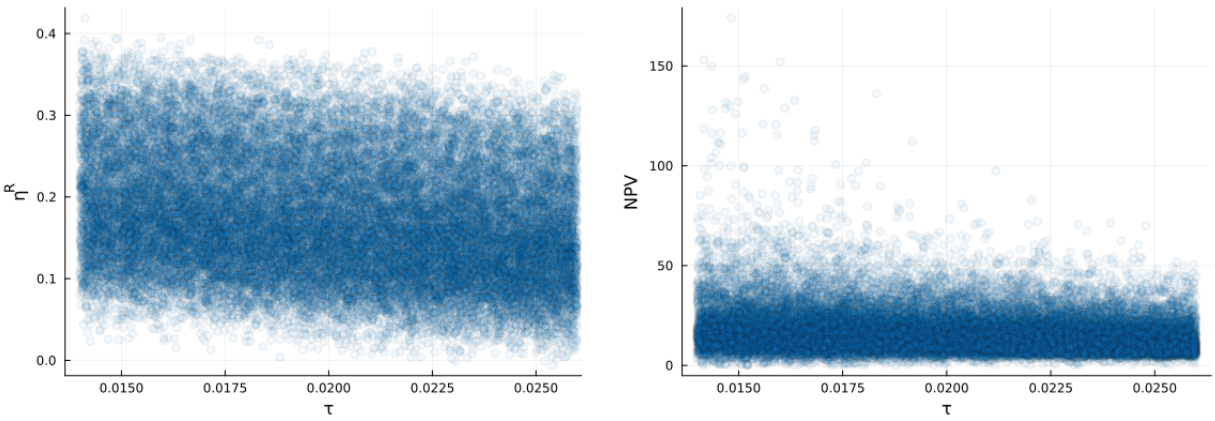

(a) Residential agglomeration forces (η^R) **(b)** Economic impact factor of the PC

Notes: These figures show the correlation of τ with: residential agglomeration forces in Panel (a), and economic impact factor of the PC removal in Panel (b), from a bootstrap procedure of 40,000 random draws of $\{\epsilon, \alpha_H, \alpha_T, \alpha_S, \kappa, \tau, \beta_H^S, \beta_L^S, \beta_M^S, \beta_H^T, \beta_L^T, \beta_M^T, \mu\}$.

Figure A.40
Bootstrap results: $\tau \times \epsilon$

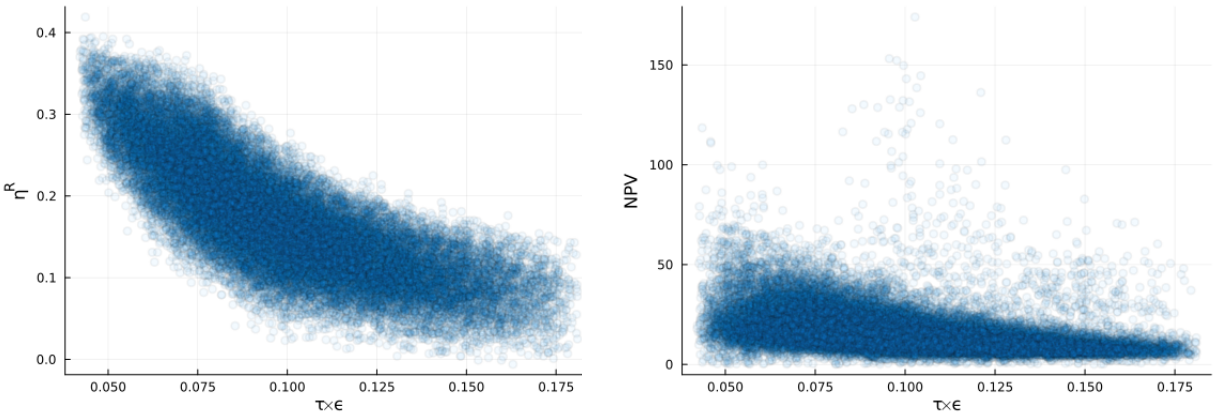

(a) Residential agglomeration forces (η^R) **(b)** Economic impact factor of the PC

Notes: These figures show the correlation of $\tau \times \epsilon$ with: residential agglomeration forces in Panel (a), and economic impact factor of the PC removal in Panel (b), from a bootstrap procedure of $40,000$ random draws of $\{\epsilon, \alpha_H, \alpha_T, \alpha_S, \kappa, \tau, \beta_H^S, \beta_L^S, \beta_M^S, \beta_H^T, \beta_L^T, \beta_M^T, \mu\}$.

Figure A.41
Bootstrap results: κ

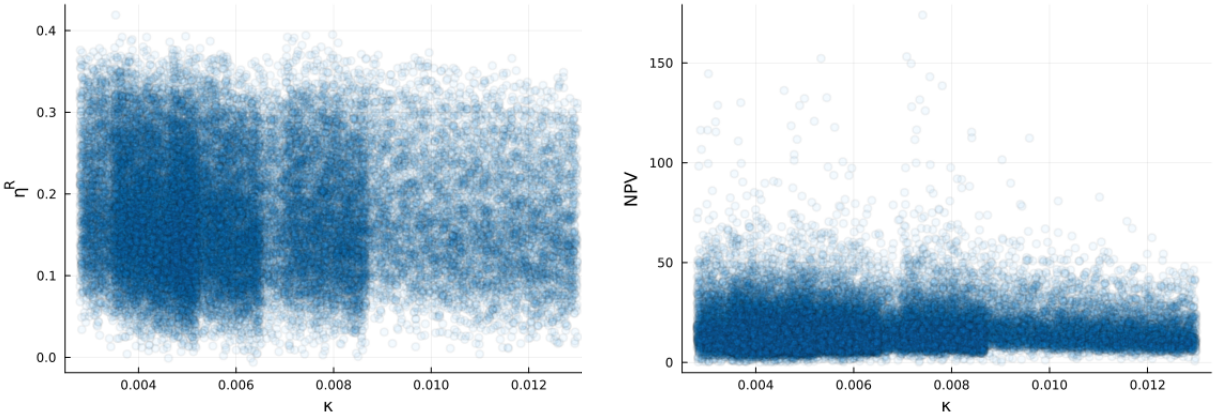

(a) Residential agglomeration forces (η^R) **(b)** Economic impact factor of the PC

Notes: These figures show the correlation of κ with: residential agglomeration forces in Panel (a), and economic impact factor of the PC removal in Panel (b), from a bootstrap procedure of $40,000$ random draws of $\{\epsilon, \alpha_H, \alpha_T, \alpha_S, \kappa, \tau, \beta_H^S, \beta_L^S, \beta_M^S, \beta_H^T, \beta_L^T, \beta_M^T, \mu\}$.

Figure A.42
Bootstrap results: α^H

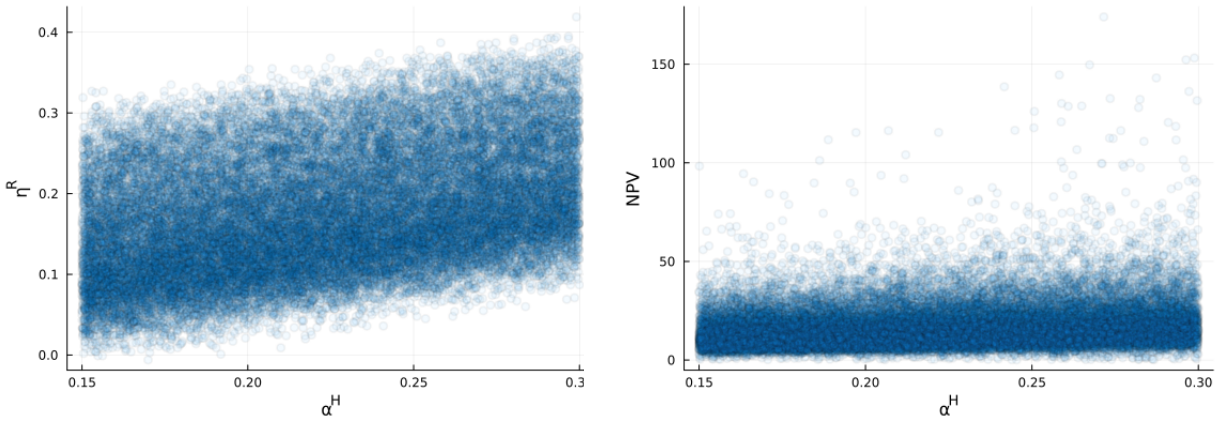

(a) Residential agglomeration forces (η^R) **(b)** Economic impact factor of the PC

Notes: These figures show the correlation of α^H with: residential agglomeration forces in Panel (a), and economic impact factor of the PC removal in Panel (b), from a bootstrap procedure of 40,000 random draws of $\{\epsilon, \alpha_H, \alpha_T, \alpha_S, \kappa, \tau, \beta_H^S, \beta_L^S, \beta_M^S, \beta_H^T, \beta_L^T, \beta_M^T, \mu\}$.

Figure A.43
Bootstrap results: β_L^T

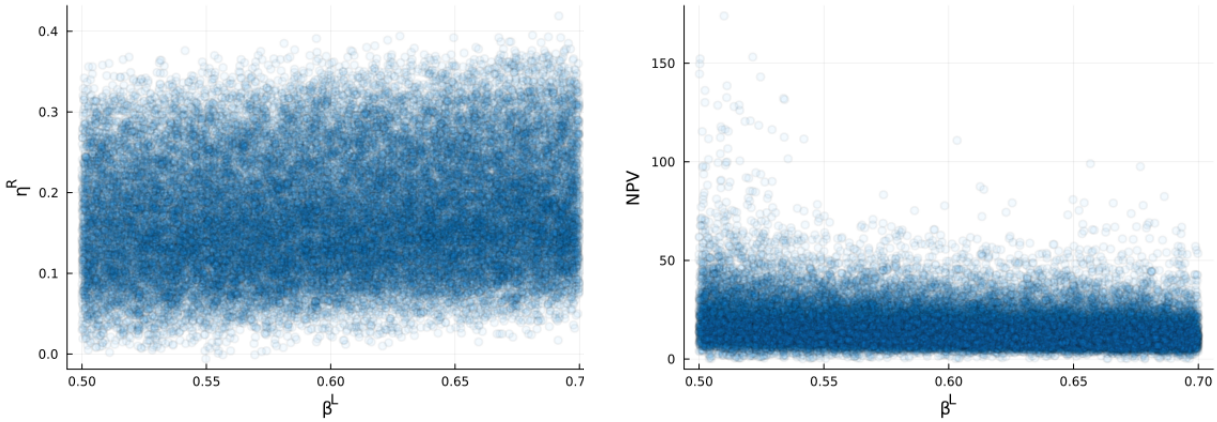

(a) Residential agglomeration forces (η^R) **(b)** Economic impact factor of the PC

Notes: These figures show the correlation of β_L^T with: residential agglomeration forces in Panel (a), and economic impact factor of the PC removal in Panel (b), from a bootstrap procedure of 40,000 random draws of $\{\epsilon, \alpha_H, \alpha_T, \alpha_S, \kappa, \tau, \beta_H^S, \beta_L^S, \beta_M^S, \beta_H^T, \beta_L^T, \beta_M^T, \mu\}$.

A.8.2 Decomposition

Table A.18
Bootstrap - decomposition of η^R

	η^R					
	(1)	(2)	(3)	(4)	(5)	(6)
ϵ	-0.052***					-0.035***
	(0.0002)					(0.0002)
ν		-1.94***				-0.857***
		(0.008)				(0.007)
κ			-1.72***			0.920***
			(0.140)			(0.050)
α^S				0.577***		0.582***
				(0.008)		(0.003)
β_L^T					0.185***	0.179***
					(0.006)	(0.002)
Observations	40,000	40,000	40,000	40,000	40,000	40,000
R^2	0.713	0.626	0.004	0.120	0.022	0.895

Notes: Each column reports estimates from a separate regression. Regressions use results from 40,000 bootstrap draws. Dependent variable is the residential agglomeration forces parameter estimated within each draw. Standard errors are in parentheses and ***, **, * indicate significance at the 1%, 5% and 10% level, respectively.

Table A.19
Bootstrap - decomposition of NPV

	η^R							
	(1)	(2)	(3)	(4)	(5)	(6)	(7)	(8)
ϵ	-0.236***							-0.352***
	(0.002)							(0.004)
ν		-9.79***						-14.3***
		(0.092)						(0.134)
η^R			3.11***					-7.15***
			(0.039)					(0.079)
μ				1.00***				1.07***
				(0.010)				(0.007)
κ					9.38***			39.9***
					(1.20)			(0.786)
α^S						2.84***		6.35***
						(0.070)		(0.062)
β_L^T							-2.19***	-0.436***
							(0.053)	(0.035)
Observations	36,301	36,301	36,301	36,301	36,301	36,301	36,301	36,301
R^2	0.213	0.236	0.148	0.204	0.002	0.043	0.045	0.650

Notes: Each column reports estimates from a separate regression. Regressions use results from 40,000 bootstrap draws. Dependent variable is the NPV estimated within each draw, and failed convergence or negative NPV are drop from the sample. Standard errors are in parentheses and ***, **, * indicate significance at the 1%, 5% and 10% level, respectively.

A.9 Model extension: Dynamic Quantitative Spatial Model

A.9.1 Workers

I consider a homogeneous mass of workers within a closed city of J discrete locations. An individual ν derives a utility flow from living in n and working in i, which takes the form of

$$ln\ u_{ni,t} + \epsilon_{ni,t}(\nu),$$

with first term being a deterministic component and last term being a idiosyncratic shock with $\epsilon_{ni,t} \backsim T1EV(1)$.

More precisely, individuals are interested in amenities, wages, rents and commuting costs when choosing their live-work pair location. Therefore, preferences take the form of

$$u_{ni,t} = \frac{B_n w_i}{d_{ni} P_n^{1-\phi} Q_n^{\phi}},$$

where B_n is the amenity, w_i the wage, d_{ni} the bilateral commuting cost, Q_n the rent, and ϕ is the share of consumption dedicated to the housing and consumption good is taken as numeraire ($P_n = 1$ for all n).

Moreover, they also take into account the possibility of changing pair of residence-work locations in the future. Therefore, the value function of an individual ν living in n and working in i at time t can be represented as follow,

$$U_{ni,t} = ln\ u_{ni,t} + \epsilon_{ni,t}(\nu) + \beta\theta U_{ni,t+1} + \beta(1-\theta)V_{t+1},$$

where, β is a discount factor, and θ represents an exogenous mobility friction as in Heblich et al. (2021). This exogenous migration frictions parameter is going to capture stickiness in the location choices of workers. Even if workers want to relocate, they are subject to immobility constraint. Finally, V_{t+1} is the value function for a household with the opportunity to relocate, taking the form of,

$$V_{t+1} = \max_{kl}\{ln\ u_{kl,t+1} + \epsilon_{kl,t+1} + \beta\theta U_{kl,t+2} + \beta(1-\theta)V_{t+2}\}.$$

Because idiosyncratic shocks follow a standardised T1EV distribution and are independent

in time and across workers, it is possible to express the probability that a worker chooses the pair n and i at time t as follow,

$$n^*_{ni,t} = \frac{e^{ln\ u_{ni,t}+\beta\theta U_{ni,t+1}+\beta(1-\theta)V_{t+1}}}{\sum_k \sum_l e^{ln\ u_{kl,t}+\beta\theta U_{kl,t+1}+\beta(1-\theta)V_{t+1}}} \tag{A.15}$$

where k and l represent all residence and workplace, respectively. Using forwards iteration, $n^*_{ni,t}$ can be rearranged and simplified to obtain the following expression,

$$n^*_{ni,t} = \frac{u_{ni,t}\Pi^{\infty}_{\tau=1} u^{(\beta\theta)^\tau}_{ni,t+\tau}}{\sum_k \sum_l u_{kl,t}\Pi^{\infty}_{\tau=1} u^{(\beta\theta)^\tau}_{kl,t+\tau}}. \tag{A.16}$$

In this setting, if there is friction mobility ($\theta > 0$) workers care about the future path of residence-workplace pair when making their commuting choices in t. If not ($\theta = 0$), we retrieve the static framework developed in Ahlfeldt et al. (2015).

A.9.2 Firms

The freely traded final good is produced by a representative myopic firm under constant returns to scale. For simplicity, its production function in location i takes the form of a Cobb–Douglas,

$$y_{i,t} = A_{i,t}\left(\frac{L_{i,t}}{\alpha_L}\right)^{\alpha_L}\left(\frac{F_{i,t}}{\alpha_F}\right)^{\alpha_F}\left(\frac{M_{i,t}}{\alpha_M}\right)^{\alpha_M},$$

with $A_{i,t}$ being the TFP in i, $L_{i,t}$ being the total labor supply in i, $F_{i,t}$ being the floorspace used commercially in i, and finally $M_{i,t}$ being the machinery capital used in i. The shares of labor, machinery and floorspace dedicated in the production function are respectively α_L, α_M and α_F.

A.9.3 Law of motions

Commuters Using the notation N_{ni} for the total numbers of commuters from n to i, with N being the total population, law of motions,

$$\begin{cases} N_{ni,t} = (1-\theta)N^*_{ni,t} + \theta N_{ni,t-1}, & \text{for commuters} \\ R_{n,t} = (1-\theta)R^*_{n,t} + \theta R_{n,t-1}, & \text{for residence employment} \\ L_{i,t} = (1-\theta)L^*_{i,t} + \theta L_{i,t-1}, & \text{for worplace employment} \end{cases} \tag{A.17}$$

need to be respected. In other words, equation A.17 implies that current bilateral flows ($N_{ni,t}$), residence employment ($R_{n,t}$), and workplace employment ($L_{i,t}$) are the sum of (i) locations choices in t weighted by the probability of moving $(1-\theta)$, and previous employment in $t-1$ weighted by the probability of staying (θ).

Housing stock The housing stock law of motion can be written as,

$$H_{n,t} = (1-\mu)H_{n,t-1} + S_{n,t}, \tag{A.18}$$

where $H_{n,t}$ represents the housing stock at time t within location n, μ is the depreciation rate of previous housing stock, and $S_{n,t}$ is the housing supply. The later is function of rents ($Q_{n,t}$), housing supply elasticity (h) and land area available (K_n), $S_{n,t} = Q_{n,t}^{h} K_n$.

A.9.4 Model Inversion

Using these following option values notations, for amenities $\Omega_{n,t} \equiv B_{n,t}\Pi_{\tau=1}^{\infty} B_{n,t+\tau}^{(\beta\theta)^\tau}$; for commuting cost $D_{ni,t} \equiv d_{ni,t}\Pi_{\tau=1}^{\infty} d_{ni,t+\tau}^{(\beta\theta)^\tau}$; for wages $\omega_{i,t} \equiv w_{i,t}\Pi_{\tau=1}^{\infty} w_{i,t+\tau}^{(\beta\theta)^\tau}$; for rents $\Upsilon_{n,t} \equiv Q_{n,t}^{\phi}\Pi_{\tau=1}^{\infty}(Q_{n,t+\tau}^{\phi})^{(\beta\theta)^\tau}$, we can express equation A.16 as follow,

$$n_{ni,t}^{*} = \frac{\Omega_{n,t}\omega_{i,t}(D_{ni,t}\Upsilon_{n,t})^{-1}}{\underbrace{\sum_k \sum_l \Omega_{k,t}\omega_{l,t}(D_{kl,t}\Upsilon_{k,t})^{-1}}_{=\Phi_{kl}}}.$$

Summing across workplace we get the probability that a worker lives in residence n,

$$n_{n,t}^{*,R} = \frac{\sum_l \Omega_{n,t}\omega_{l,t}(D_{nl,t}\Upsilon_{n,t})^{-1}}{\Phi_{kl}} = \frac{\Omega_{n,t}(\Upsilon_{n,t})^{-1}\sum_l \omega_{l,t}(D_{nl,t})^{-1}}{\Phi_{kl}},$$

and, summing across residence we obtain the probability that a worker is employed in workplace i,

$$n_{i,t}^{*,L} = \frac{\sum_k \Omega_{k,t}\omega_{i,t}(D_{ki,t}\Upsilon_{k,t})^{-1}}{\Phi_{kl}} = \frac{\omega_{i,t}\sum_k \Omega_{k,t}(D_{ki,t}\Upsilon_{k,t})^{-1}}{\Phi_{kl}}.$$

Then, the conditional probability that a worker commutes to workplace i conditional on living in residence n can be expressed,

$$n_{ni|n,t}^{*,R} = \frac{n_{ni,t}^{*}}{n_{n,t}^{*,R}} = \frac{\omega_{i,t}/D_{ni,t}}{\sum_l \omega_{l,t}/D_{nl,t}},$$

and the conditional probability that a worker commutes from residence n conditional on working in workplace i is

$$n^{*,L}_{ni|i,t} = \frac{\Omega_{n,t}/(D_{ni,t}\Upsilon_{n,t})}{\sum_{k\in J}\Omega_{k,t}/(D_{ki,t}\Upsilon_{k,t})}$$

Step 1: recover wages options values The commuting market clearing condition on movers can be written as follow,

$$(1-\theta)L^*_{i,t} = \sum_{n\in J} n^{*,R}_{ni|n,t}(1-\theta)R^*_{n,t}.$$

Using the conditional probability and the law of motions, we can rewrite the commuting market clearing conditions on movers,

$$(L_{i,t} - \theta L_{i,t-1}) = \sum_{n\in J}\frac{\omega_{i,t}/D_{ni,t}}{\sum_l \omega_{l,t}/D_{nl,t}}(R_{n,t} - \theta R_{n,t-1}). \tag{A.19}$$

Proposition 2 *Given the parameters $\{\beta, \theta\}$, the observed data on employment ($L_{i,t}$) and residents ($R_{n,t}$), and commuting costs option values ($D_{ni,t}$), there exists a unique vector of wages option values $\omega_{i,t}$ that solve the commuters market clearing condition.*

Proposition 3 *Given the recursive structure of option values, it is possible to retrieve static wages by progressing backward from the final year T to the initial year t.*

Step 2: recover amenities options values Symmetrically, the same methodology can be used to estimate amenities value options and statics amenities. Using law of motions and conditional probability,

$$(R_{n,t} - \theta R_{n,t-1}) = \sum_{i\in J}\frac{\Omega_{n,t}/(D_{ni,t}\Upsilon_{n,t})}{\sum_{k\in J}\Omega_{k,t}/(D_{ki,t}\Upsilon_{k,t})}(L_{i,t} - \theta L_{i,t-1}). \tag{A.20}$$

Step 3: recover productivity Through the classic application of the First-Order Condition (FOC) and the zero profit condition, it becomes feasible to derive unobservable productivity along with the solutions for wage rates and the observed price of floorspace,

$$A_{i,t} = w^{\alpha_L}_{i,t} Q^{\alpha_F}_{i,t} r^{\alpha_M}_{i,t}. \tag{A.21}$$

I make the assumption that machinery capital is freely traded in the city, and normalize the price of the machinery capital $r_{i,t} = 1, \forall$ workplace l.[3]

Step 4 : recover density of development Turning into the final step, the land market clearing condition needs to satisfy,

$$H_{n,t} = F^R_{n,t} + F^F_{n,t},$$

where $F^R_{n,t}$ and $F^F_{n,t}$ are respectively the residential and commercial floorspace demand, and $H_{n,t}$ is the stock of housing.

By making the assumption that stayers do not choose another workplace between two periods, it is possible to express the land market clearing condition as follow,

$$\begin{aligned}\varphi_{n,t} K_{n,t} =& \phi \left(\frac{\sum_{i \in J} n^{*,R}_{ni|n,t} w_{i,t} (1-\theta) R^*_{n,t} + \sum_{i \in J} n^R_{ni|n,t-1} w_{i,t} \theta R_{n,t-1}}{Q_{n,t}} \right) \\ &+ \left(\left(\frac{\alpha_F}{\alpha_L} \right) w_{n,t} \left(\frac{(1-\theta) L^*_{n,t} + \theta L_{n,t-1}}{Q_{n,t}} \right) \right)\end{aligned} \tag{A.22}$$

Dynamic Spatial Equilibrium Definition: *Given an initial distribution* $\{L_{i,0}, R_{n,0}\}$, *the economic parameters* $\{\beta, \theta, \kappa, \alpha, \phi\}$, *and a commuting cost parametrization* $\{t_{ni,t}\}$, *a dynamic spatial equilibrium is defined with a sequence of observed vectors* $\{R_{n,t}, L_{i,t}, K_{n,t}, Q_{n,t}\}$, *and a sequence of unobserved vectors* $\{w_{i,t}, A_{i,t}, B_n, \varphi_{n,t}\}$ *such that: i) labor markets clear (A.19),(A.20); ii) FOC of the firm clears (A.21) and iii) floorspace markets clear (A.22).*

[3] According to the industrial survey of 1872, machinery capital was provided by the public authorities of Paris. They offered industrial enterprises the option to rent motorized resources. Hence, this assumption seems plausible.

B Appendix to Optimal Urban Transport Design in a Quantitative Spatial Model

B.1 Additional Figures

B.1.1 Map of omnibus and tramways

Figure B.1
Omnibus and tramways in 1896

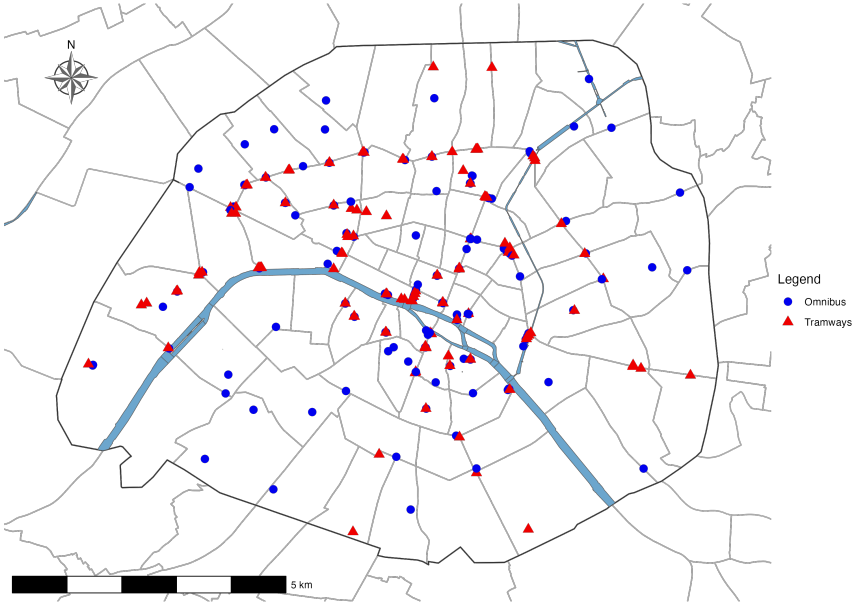

B.1.2 Map of residential sorting by skill

Figure B.2
Spatial sorting of residents by skill in 1896

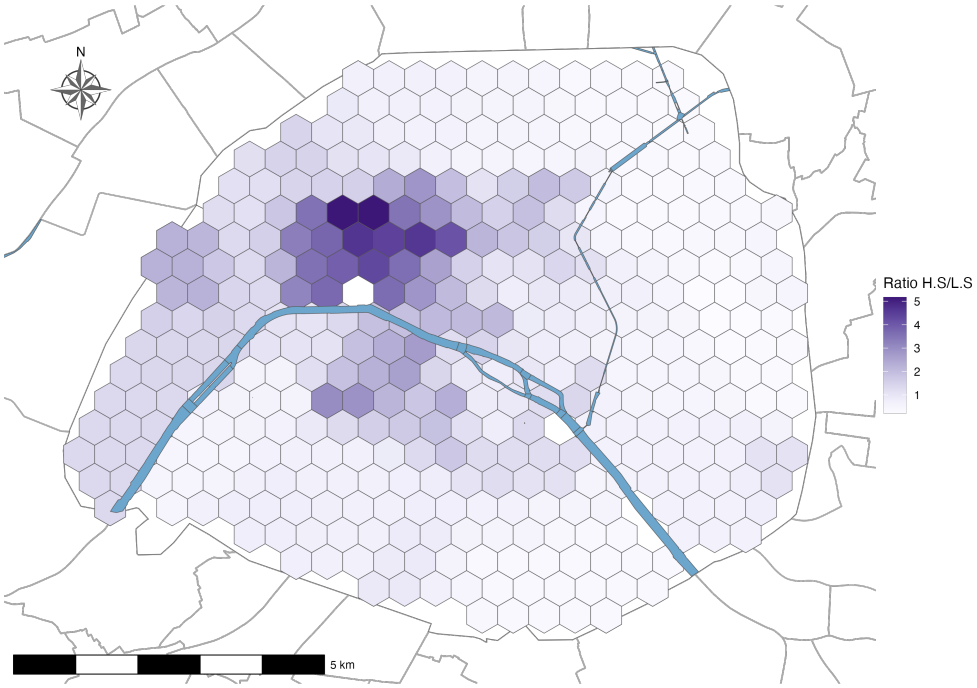

Notes: This figure illustrates the spatial residential sorting by skill level in 1896 by showing the ratio of the high-skilled residence employment with respect to the low-skilled residence employment. The darker shades indicate relatively higher concentrations of high-skilled residents.

B.2 Theoretical Appendix

B.2.1 Canonical Quantitative Urban Model

Housing supply The supply of housing is determined by a competitive construction sector with a Cobb-Douglas technology following Combes et al. (2021),

$$H_i = K_i^{\mu} \Lambda_i^{1-\mu}, \tag{B.1}$$

where H_i is the housing supplied in location i, K_i is the land in location i, and Λ_i is the capital in location i. Finally, μ is the share of land within the construction technology, and the capital is assumed to be supplied without any cost in the wider economy at a price $\mathbb{P} = 1$. Therefore, the maximization of the firm's profit in the construction sector gives,

$$(1-\mu)^{1/\mu} Q_i^{1/\mu} K_i = \Lambda_i. \tag{B.2}$$

Plugging equation (B.2) into equation (B.1) gives,

$$H_i = K_i (1-\mu)^{\frac{1-\mu}{\mu}} Q_i^{\frac{1-\mu}{\mu}}, \tag{B.3}$$

which is equal to equation (2.9) in the main paper.

Iterative algorithm to solve a spatial equilibrium Table B.1 shows the iterative procedure to solve for a spatial equilibrium given the exogenous characteristics $\{A_i, B_n, d_{ni}, H_n^S, R_{\mathbb{N}}\}$, the structural parameters $\{\alpha, \beta, \kappa, \epsilon\}$ and a canonical quantitative urban model and a closed city setting. It starts with an initial guess for the variables $\{L_i^0, R_n^0, w_i^0, Q_n^0\}$, and progressively updates them with the housing market equilibrium condition.

Table B.1
Algorithm for solving spatial equilibrium

Line	Code	Description/Comment
0	$\{L_i^0, R_n^0, w_i^0, Q_n^0\}$	Initial guess
1	`while er > tol`	
2	$w_i = A_i^{\frac{1}{\alpha}} Q_i^{\frac{\alpha-1}{\alpha}}$	Compute location wages
3	$U_{ni} = \frac{B_n w_i}{d_{ni} Q_n^{\beta}}$	Compute pair locations utility
4	$\Phi_{ni} = \left(U_{ni}\right)^{\epsilon}$	——
5	$\Phi = \sum_{k \in N} \sum_{l \in N} \Phi_{kl}$	——
6	$\lambda_{ni} = \frac{\Phi_{ni}}{\Phi}$	Compute commuting flows probability
7	$R_n = \sum_{i \in N} \lambda_{ni} \; R_{\mathbb{N}}$	Compute residential choices
8	$L_i = \sum_{n \in N} \lambda_{ni} \; R_{\mathbb{N}}$	Compute working choices
9	$\lambda^R_{ni\|n} = \frac{\lambda_{ni}}{\sum_{i \in N} \lambda_{ni}}$	Compute conditional commuting probability
10	$H_n^R = \beta \; \frac{\sum_{i \in N} \lambda^R_{ni\|n} w_i R_n}{Q_n}$	Compute residential floorspace demand
11	$H_n^F = \frac{1-\alpha}{\alpha} \; \frac{w_n L_n}{Q_n}$	Compute commercial housing demand
12	$H_n = H_n^R + H_n^F$	Compute total housing demand
13	$Q_n^1 = Q_n \left(\frac{H_n}{H_n^S}\right)$	Update rent with housing market clearing condition
14	$\text{er} = \max\left(\left\|(Q_n^1 - Q_n)\right\|\right)$	Compute error based on previous and updated rents
15	$Q_n = 0.1 \times Q_n^1 + 0.9 \times Q_n$	Update rent
16	`end`	

B.2.2 Extension of the Canonical QUM

Residential-workplace choices Following the type-specific indirect utility equation (2.17), the type-specific commuting probability can be expressed as,

$$\lambda_{ni,g} = \frac{L_{ni,g}}{R_{\mathbb{N}_g}} = \frac{(B_{n,g}w_{i,g})^{\epsilon_g}(d_{ni}Q_n^{\beta_g})^{-\epsilon_g}}{\sum_{k\in\mathbb{N}}\sum_{l\in\mathbb{N}}(B_{k,g}w_{l,g})^{\epsilon_g}(d_{kl}Q_l^{\beta_g})^{-\epsilon_g}} = \frac{\Phi_{ni,g}}{\sum_{k\in\mathbb{N}}\sum_{l\in\mathbb{N}}\Phi_{kl,g}}, \tag{B.4}$$

where only amenities ($B_{n,g}$), the wage ($w_{i,g}$), the share of income spend on housing (β_g), and the Fréchet parameter (ϵ_g) differ from equation (2.2) since they are type-specific.

By summing across workplaces, I get the probability that a worker of type g lives in n,

$$\lambda^R_{n,g} = \frac{R_{n,g}}{R_{\mathbb{N}_g}} = \frac{\sum_{i\in\mathbb{N}}\Phi_{ni,g}}{\sum_{k\in\mathbb{N}}\sum_{l\in\mathbb{N}}\Phi_{kl,g}}, \tag{B.5}$$

and by summing across residence places, I get the probability that a worker of type g works in i,

$$\lambda^L_{i,g} = \frac{L_{i,g}}{R_{\mathbb{N}_g}} = \frac{\sum_{n\in\mathbb{N}}\Phi_{ni,g}}{\sum_{k\in\mathbb{N}}\sum_{l\in\mathbb{N}}\Phi_{kl,g}}. \tag{B.6}$$

Using the types-specific commuting probability, and the type-specific residential probability, the type-specific conditional commuting probability can be expressed as,

$$\lambda^R_{ni|n,g} = \frac{\lambda_{ni,g}}{\lambda^R_{n,g}} = \frac{(w_{i,g}/d_{ni})^{\epsilon_g}}{\sum_{l\in N}(w_{l,g}/d_{nl})^{\epsilon_g}}. \tag{B.7}$$

where only wage ($w_{i,g}$) differs from equation (2.10).

Finally, population mobility for a given type g ensures that everyone derives the same expected utility in the city,

$$\overline{U}_g = \delta_g\Big[\sum_{k\in\mathbb{N}}\sum_{l\in\mathbb{N}}\Phi_{kl,g}\Big]^{1/\epsilon_g}, \tag{B.8}$$

with $\delta_g \equiv \Gamma\Big(\frac{(\epsilon_g-1)}{\epsilon_g}\Big)$, $\Gamma(.)$ the gamma function.

Wage cost index Using the firm profit $\pi = Y_i - W_iL_i - r_iM_i - Q_iH_i^L$, the total firm labor payments $W_iL_i = \sum_g w_{i,g}L_{i,g}$, the FOC of firm with respect to the type-specific labor supply equation (2.21), and the FOC of firm with respect to the total labor supply

$W_i = \alpha_L^{(1-\alpha_L)} A_i L_i^{\alpha-1} \left(\frac{H_i^L}{\alpha_F}\right)^{\alpha_F} \left(\frac{M_i}{\alpha_M}\right)^{\alpha_M}$, it is possible to express the aggregate wages as,

$$W_i = \left(\sum_g w_{i,g}^{\frac{\rho}{\rho-1}} a_{i,g}^{\frac{1}{1-\rho}}\right)^{\frac{\rho-1}{\rho}}. \tag{B.9}$$

Housing and Machinery demands The respective ratios of the first-order conditions (FOCs) from the housing equation (2.22) and the machinery equation (2.23) to the FOC of the labor supply equation (2.21) are given by,

$$M_i = \frac{\alpha_M}{\alpha_L} \frac{L_{i,g}^{1-\rho} L_i^{\rho}}{a_{i,g}} w_{i,g}, \tag{B.10}$$

$$H_i^L = \frac{\alpha_F}{\alpha_L} \frac{L_{i,g}^{1-\rho} L_i^{\rho}}{a_{i,g}} \frac{w_{i,g}}{Q_i}. \tag{B.11}$$

Exact-hat algebra Using "hat" expression with $\widehat{x} = \frac{x'}{x}$, every equation can be expressed in terms of change relative to the baseline equilibrium.

The relative change in type-specific amenities can be expressed as,

$$\widehat{B}_{n,g} = \widehat{R}_n^{\eta^R}, \tag{B.12}$$

which includes only changes in residential employment ($\widehat{R}_n$) since land is fixed.

Similarly, the relative change in productivity can be expressed as,

$$\widehat{A}_i = \widehat{L}_i^{\eta^L}, \tag{B.13}$$

which includes only changes in workplace employment ($\widehat{L}_i$) since land is fixed.

The relative change in location choices can be expressed as,

$$\widehat{\lambda}_{ni,g} = \frac{\left(\widehat{B}_{n,g}\widehat{w}_{i,g}\right)^{\epsilon_g}\left(\widehat{d}_{ni}\widehat{Q}_n^{\beta_g}\right)^{-\epsilon_g}}{\sum_k \sum_l \lambda_{kl,g}\left(\widehat{B}_{k,g}\widehat{w}_{l,g}\right)^{\epsilon_g}\left(\widehat{d}_{kl}\widehat{Q}_k^{\beta_g}\right)^{-\epsilon_g}}, \tag{B.14}$$

which is function of changes in living cost ($\widehat{Q}_n$), changes in commuting costs ($\widehat{d}_{ni}$), changes in type-specific amenities ($\widehat{B}_{n,g}$), and changes in type-specific wages ($\widehat{w}_{i,g}$).

The relative change in type-specifc Parisian total population can be expressed as,

$$\left(\widehat{R}_{\mathbb{N}_g}\right)^{1/\epsilon_g} = \Big[\sum_k \sum_l \lambda_{kl}\Big(\widehat{B}_{k,g}\widehat{w}_{l,g}\Big)^{\epsilon}\Big(\widehat{d}_{kl}\widehat{Q}_k^{\beta_g}\Big)^{-\epsilon_g}\Big]^{1/\epsilon_g}, \tag{B.15}$$

which is function of changes in living cost ($\widehat{Q}_n$), changes in commuting costs ($\widehat{d}_{ni}$), changes in type-specific amenities ($\widehat{B}_{n,g}$), and changes in type-specific wages ($\widehat{w}_{i,g}$).

The relative change in commercial housing demand can be expressed as,

$$\widehat{H}_n^L = \widehat{L}_n^{\rho}\ \widehat{L}_{n,g}^{1-\rho}\ \frac{\widehat{w}_{n,g}}{\widehat{Q}_n}, \tag{B.16}$$

and the relative change in machinery demand can be expressed as,

$$\widehat{M}_n = \widehat{L}_n^{\rho}\ \widehat{L}_{n,g}^{1-\rho}\ \widehat{w}_{n,g}. \tag{B.17}$$

The change in type-specific residential housing demand can be expressed as,

$$\widehat{H}_{n,g}^R H_{n,g}^R = \beta_g\left[\sum_{i\in\mathbb{N}}\left(\frac{\lambda_{ni|n,g}^R\big(\frac{\widehat{w}_{i,g}}{\widehat{d}_{ni}}\big)^{\epsilon_g}}{\sum_{l\in\mathbb{N}}\lambda_{nl|n,g}^R\big(\frac{\widehat{w}_{i,g}}{\widehat{d}_{nl}}\big)^{\epsilon_g}}\right)\right]\frac{\widehat{\lambda}_{n,g}^R\lambda_{n,g}^R\widehat{R}_{\mathbb{N}_g}R_{\mathbb{N}_g}}{\widehat{Q}_n Q_n}, \tag{B.18}$$

and the change in commercial housing demand can be expressed as,

$$\widehat{H}_n^L H_n^L = \frac{\alpha_F}{\alpha_L}\ \widehat{L}_n^{\rho}L_n^{\rho}\ \widehat{L}_{n,g}^{1-\rho}L_{n,g}^{1-\rho}\ \frac{\widehat{w}_{n,g}w_{n,g}}{\widehat{Q}_n Q_n}. \tag{B.19}$$

The relative change in total production can be expressed as,

$$\widehat{Y}_i = \widehat{A}_i\ \left(\widehat{L}_i\right)^{\alpha_L}\ \left(\widehat{H}_i^L\right)^{\alpha_F}\ \left(\widehat{M}_i\right)^{\alpha_M}. \tag{B.20}$$

The relative change in type-specific wages can be expressed as,

$$\widehat{w}_{i,g} = \widehat{A}_i^{1/\alpha_L}\ \widehat{L}_{i,g}^{\rho-1}\ \widehat{L}_i^{1-\rho}\ \widehat{Q}_i^{-\alpha_F/\alpha_L}. \tag{B.21}$$

Finally, the change in rateable values can be expressed as,

$$\widehat{\mathbb{Q}}_n\mathbb{Q}_n = \widehat{Q}_n^{1+\mu}\mathbb{Q}_n. \tag{B.22}$$

B.3 Simulated Annealing Algorithm and Additional Results

B.3.1 Calibration of construction cost

As detailed in the main paper, the metro construction costs are defined based on estimates from Heblich et al. (2020). Specifically, the costs are £330,000 per mile for "cut-and-cover" and £500,000 per mile for "bored-tube" as of 1921. Using an exchange rate of 25, these costs are converted to francs. Employing the "cut-and-cover" estimates, the total metro construction cost is calibrated to 5,126,325 francs per kilometer.

To deduce the construction cost parameters ϑ, the total length of the Fulgence Bienvenüe metro project, which is 60 kilometers, is used. This results in a total budget of 307,579,500 francs. Within this total budget, it is assumed that 15% is allocated to technology acquisition and other fixed costs, yielding $\vartheta_0 = 307,579,500 \text{ francs} \times 0.15 = 46,136,926$ francs.

Furthermore, it is assumed that 30% of the total metro construction costs per kilometer is dedicated to stations. Given that, on average, three stations are built per kilometer (since the average distance between each station is 500 meters), the cost per station $\vartheta_1 = 5,126,325 \text{ francs} \times \frac{0.3}{3} = 512,632.5$ francs is calculated. The tunneling costs are then derived from the remaining budget, resulting in a tunneling cost per kilometer $\vartheta_2 = 5,126,325 \text{ francs} \times (1 - 0.3 - 0.15) = 2,819,479$ francs.

B.3.2 Metro stations and economic impact - whole iterations

Figure B.3
Metro size and economic impact for all iterations

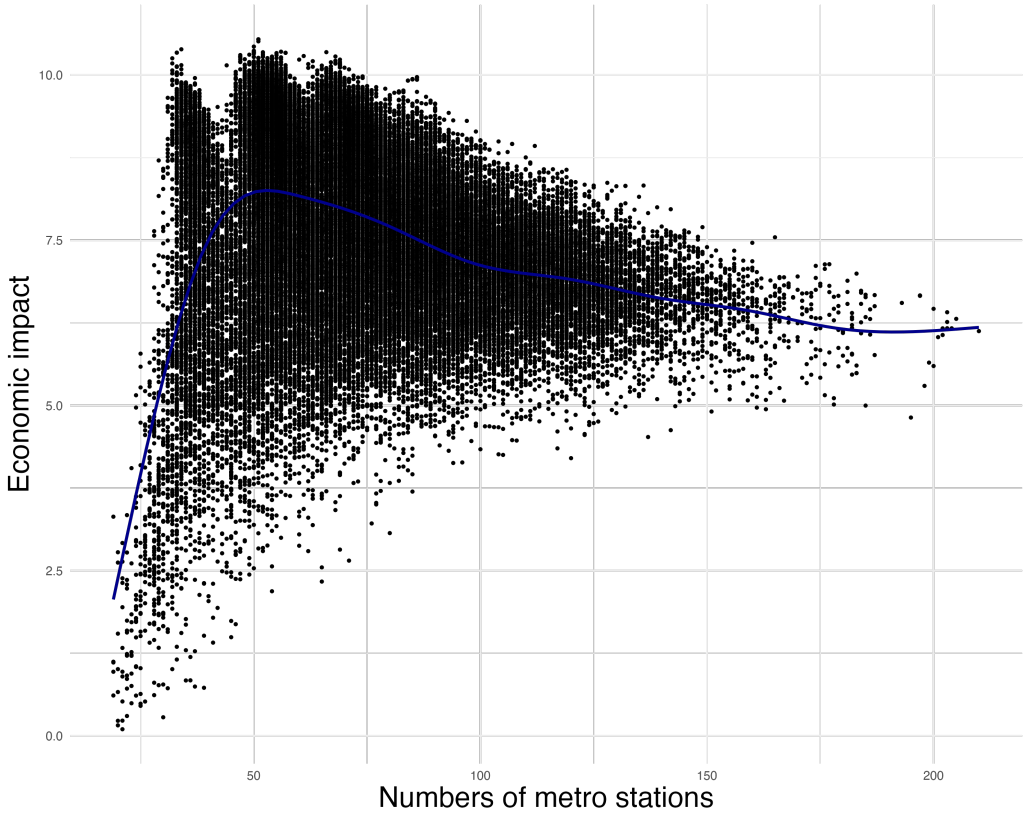

B.3.3 Baseline results - change in economic activities

Figure B.4
Change in economic activities

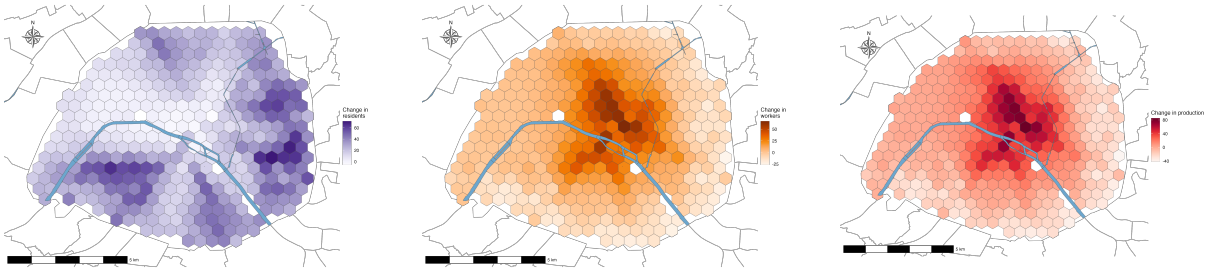

(a) Residence employment **(b)** Workplace employment **(c)** Production

Notes: This figure shows changes in percentage points of location economic activities with respect to the initial. Panel (a) depicts the change in residence employment. Panel (b) shows the change in workplace employment. Panel (c) illustrates the change in production. Darker shades indicate areas with higher positive changes with respect to the baseline.

B.3.4 Targeting specific population

Figure B.5
Difference between $z = 0$ and $z = 1$ sampled metro networks

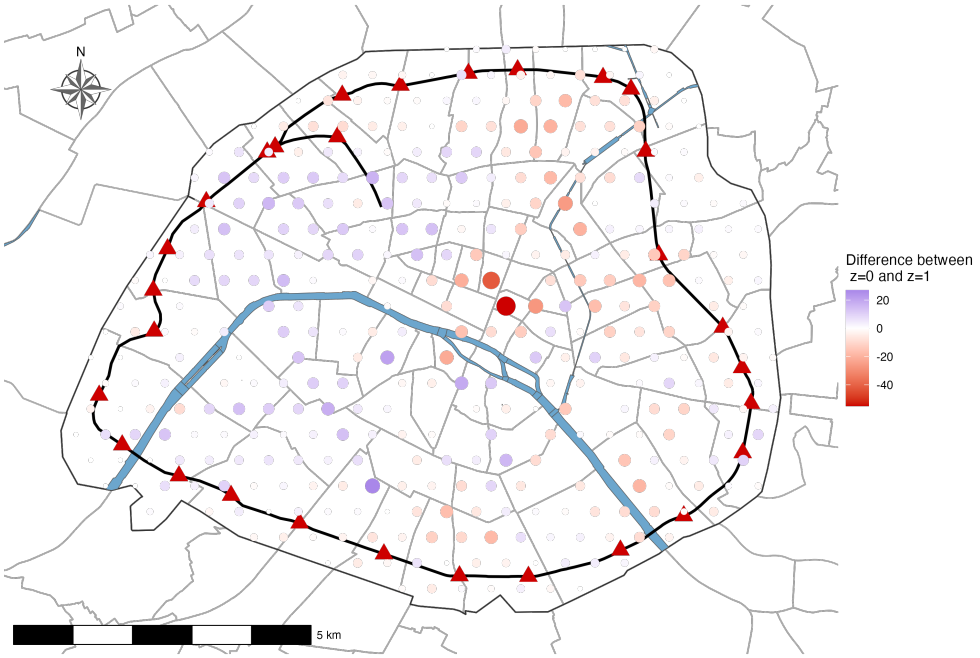

Notes: This figure shows the change in frequency of metro stations occurring in the simulated annealing runs between the $z = 0$ (targeting high-skilled workers) and the $z = 1$ scenarios (targeting low-skilled workers). The economic objective is

$\max: \ (1 - z) \times \widehat{U}_H(M; \theta) + z \times \widehat{U}_L(M; \theta)$. Blue indicates a positive change in frequency, while red indicates a negative change. The size of the dots is proportional to the absolute value of the frequency change.

C Appendix to Racial Preferences and Local Public Goods

C.1 Stylized facts

C.1.1 White share by natural amenities within-city

Figure C.1

Within-city racial sorting by natural amenities status 1880-2010

Notes: This figure shows the average difference in the white share at the neighborhood level by natural amenities status within the same city over the 1880-2010 period. Considered natural amenities include coastline, lake, river, or hill (average slope above 15°). The grey area represents the 95% confidence interval.

C.1.2 Confederate monuments over time

Figure C.2

Numbers of Confederate monuments within the U.S over 1880-2010 period

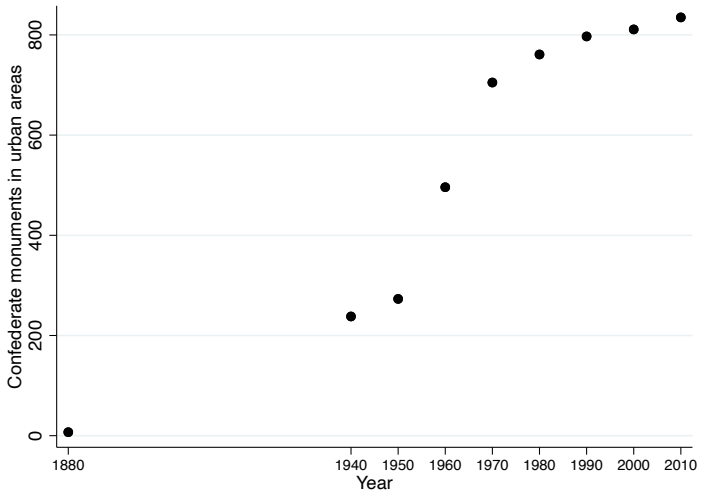

Notes: This figure shows the number of Confederate monuments within the U.S. over the 1880-2010 period. Only Confederate monuments within 2010 Core-Based Statistical Areas (CBSAs) are considered.

C.1.3 Confederate monuments location

To investigate whether there is a strategy behind the location of Confederate monuments, I run the following linear probability model,

$$\mathbb{1}^{\text{CM}}_{n(m),t} = \beta \text{ Log distance to CBD}_n + \Gamma^{NA}_n \gamma + \delta_{m,t} + \epsilon_{n(m),t}, \tag{C.1}$$

where $\mathbb{1}^{\text{CM}}_{n(m),t}$ is a dummy variable indicating whether neighborhood n has a Confederate monument at time t. Γ^{NA}_n is a set of natural features proximity variables: coast, lakes, hills, rivers (see the racial sorting empirical specification in Section III for more details on the variable definitions). $\delta_{m,t}$ represents city-year fixed effects, and $\epsilon_{n(m),t}$ are the standard errors clustered at the metropolitan area-year level.

Table C.1
Location of Confederate monuments within the city

	Confederate monument					
	(1)	(2)	(3)	(4)	(5)	(6)
Log. distance to CBD	-0.0038***					-0.0037***
	(0.0004)					(0.0004)
Coast		0.0038***				0.0028***
		(0.0007)				(0.0007)
Rivers			0.0000			0.0003
			(0.0005)			(0.0006)
Lakes				-0.0092***		-0.0088***
				(0.0011)		(0.0012)
Hill					-0.0023***	-0.0015**
					(0.0006)	(0.0006)
R^2	0.038	0.038	0.038	0.038	0.038	0.038
Observations	362,886	364,617	364,617	364,617	364,617	362,886
MSA-years FE	1,638	1,697	1,697	1,697	1,697	1,638

Notes: This table presents the regression results for the location of Confederate monuments within cities. Each column represents a separate regression. All regressions include city-year fixed effects. The dependent variable is the presence of Confederate monuments within a neighborhood. Controls include the log distance to CBD, proximity to coasts, rivers, lakes, and hills (average slope above 15°). Standard errors are clustered by city-year, and ***, **, * indicate significance at the 1%, 5%, and 10% levels, respectively.

C.1.4 Confederate monuments and neighborhood white share

To investigate whether the dedication of Confederate monuments impacted the white share growth in U.S. neighborhoods, taking into account the staggered timing of the treatment, I rely on the estimator proposed by De Chaisemartin and d'Haultfoeuille (2024) and run the following differences-in-differences event-study specification:

$$s_{n(m),t} = \psi_m + \eta_t + \sum_{\tau \neq -1} \beta_\tau \mathbb{1}\{t - E_n = \tau\} + \epsilon_{n(m),t}, \tag{C.2}$$

where $s_{n(m),t}$ is the white share of neighborhood n at time t, ψ_m and η_t are city and year fixed effects, respectively, E_n is the time when neighborhood n initially receives the treatment, and $\mathbb{1}$ corresponds to the binary treatment indicator for whether a Confederate monument is dedicated within the neighborhood.

I employ a large period window (1940-2010) with data observed every 10 years to analyze pre-trends and dynamic treatment effects estimated by the coefficients β_τ associated with indicators for being τ periods relative to the treatment. The city fixed effects capture inherent characteristics such as topography, altitude, and city-level exogenous amenities. This ensures that the comparison between neighborhoods receiving a Confederate monument and other neighborhoods is made within the same city. The standard errors are clustered at the neighborhood level to allow for serial correlations. Figures C.3(a) and C.3(b) show the event-study plots and suggest that the dedication of a Confederate monument within a neighborhood increases, on average, the white share by 0.05 percentage points. Figures C.3(c) and C.3(d) conduct pre-trends sensitivity analysis using the honestdid package developed by Rambachan and Roth (2023). I use the second differences (SD) approach to create robust confidence intervals for the last three lags using deviations from a linear extrapolation of the pre-trend information and find that it is possible to rule out a null effect when considering a linear trend.

Figure C.3
Event-study plots: Confederate monuments and neighborhood white share

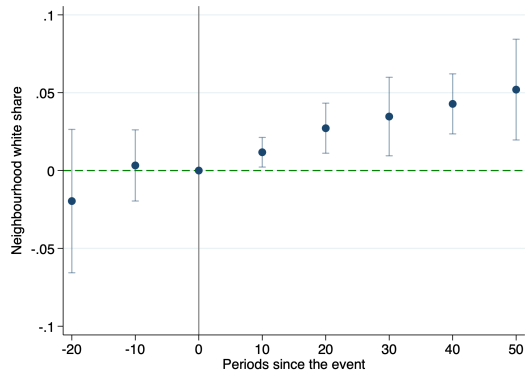

(a) Event-study with linear trends

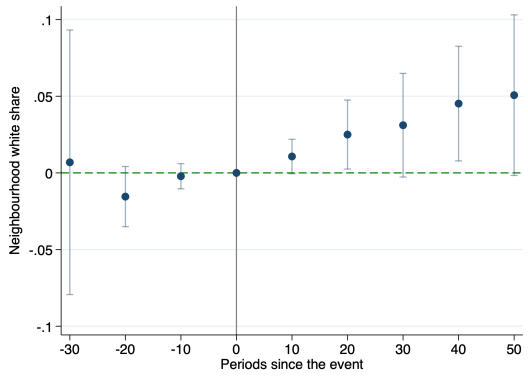

(b) Event-study without linear trends

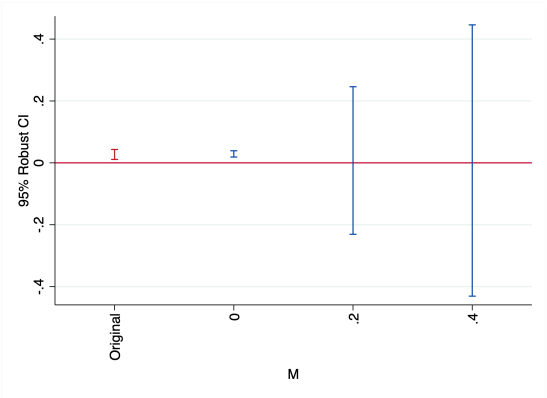

(c) Sensitivity test with linear trends

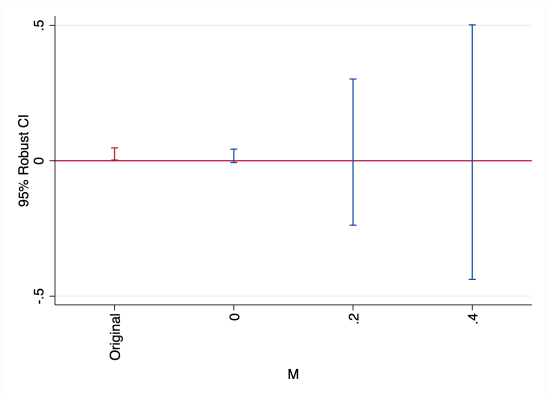

(d) Sensitivity test without linear trends

Notes: This figure presents event-study plots examining the impact of Confederate monument dedications on neighborhood white share in U.S. cities. Panels (a) and (b) show event-study plots with and without linear trends, respectively. Panels (c) and (d) provide sensitivity tests using robust confidence intervals for pre-trends analysis.

C.2 Additional results

C.2.1 Heterogeneity by year: coastal status and racial segregation

To investigate whether the effect of natural amenities on racial segregation changes over time, I run the following specification,

$$D_{m,t} = \alpha_m + \theta_t + \sum_{\tau \neq 0}^{\tau=60} \beta_\tau (\mathbb{1}_m^{Coast} \times \mathbb{I}_\tau) + X_{m,t}\gamma + \epsilon_{m,t}, \tag{C.3}$$

where $D_{m,t}$ is the racial segregation index between blacks and whites within city m at time t (either the dissimilarity index equation (3.1), or the distance index equation (3.2)), $\mathbb{1}_m^{Coast}$ is a variable indicating the coastal status of city m, $\mathbb{I}_\tau$ is an indicator variable that equals 1 in treatment year τ (the excluded category being $\tau = 0$), $X_{m,t}$ is a vector of time-varying controls at the city level, and finally α_m and θ_t represent city and time fixed effects, respectively. The standard errors $\epsilon_{m,t}$ are clustered at the city

Figure C.4
Coastal status and racial segregation by year

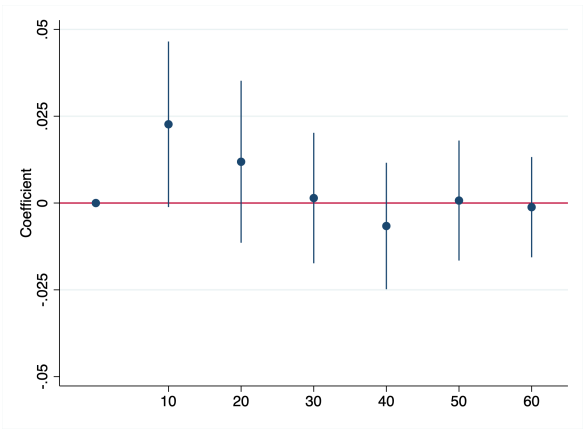

(a) Dissimilarity index - controls

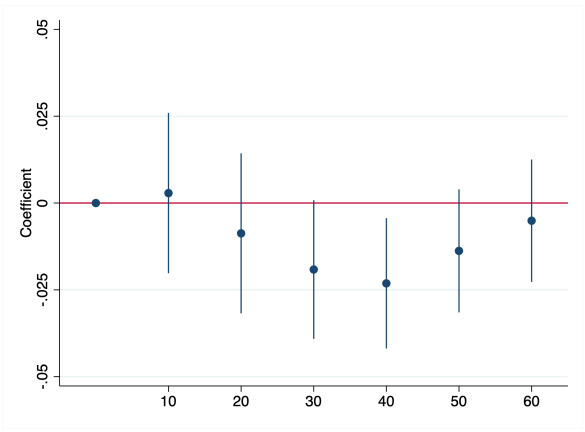

(b) Dissimilarity index - without controls

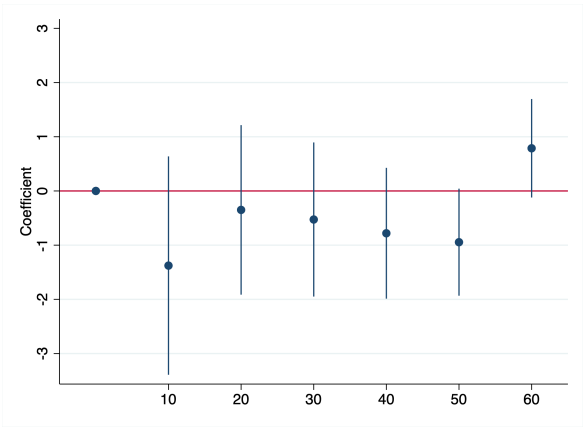

(c) Distance index - controls

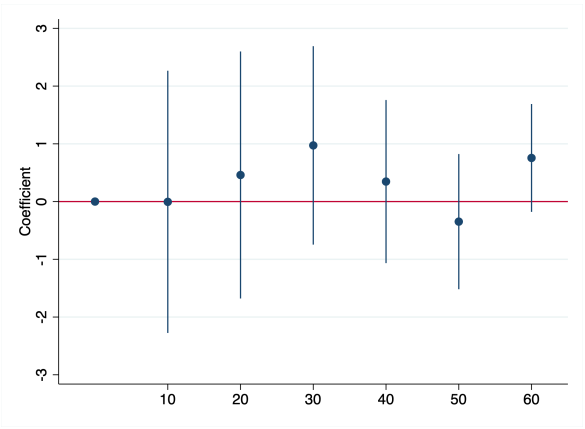

(d) Distance index - without controls

Notes: This figure examines the relationship between coastal status and racial segregation over time. Panels (a) and (b) display the dissimilarity segregation index with and without controls, respectively. Panels (c) and (d) show the distance segregation index with and without controls, respectively.

C.2.2 Heterogeneity by region: market effect

Figure C.5

Market effect of natural amenities by region 1880-2010

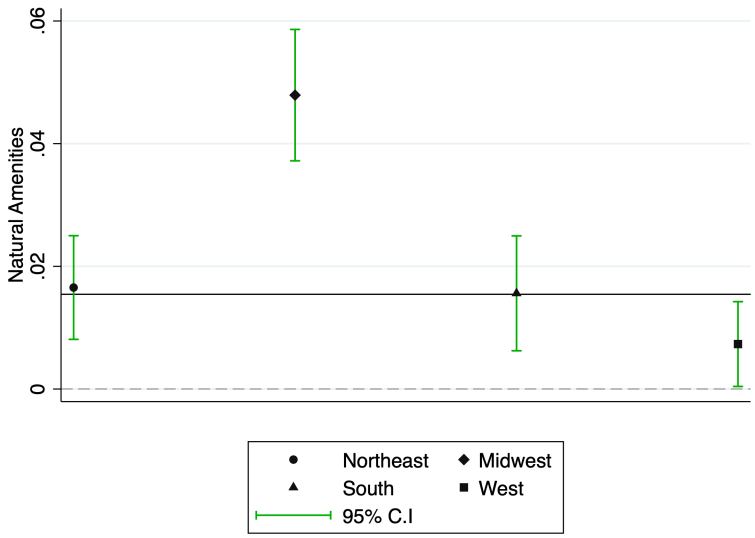

Notes: This figure displays the market effect of natural amenities from separate regression by region, referring to column (3) in Table 3.4, and the added controls are the percentile income rank, the log distance to seaport, the log distance to CBD, and the log population density.

C.2.3 Heterogeneity by region: exclusion effect

Figure C.6

Exclusion effect of natural amenities by region 1880-2010

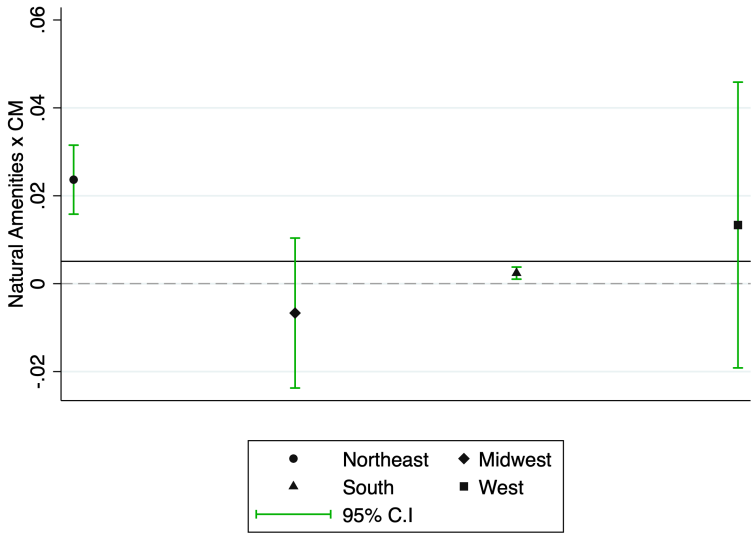

Notes: This figure displays the exclusion effect of natural amenities from separate regression by region, referring to column (4) in Table 3.4, and the added controls are the percentile income rank and the log population density.

C.2.4 Long-differences

To test whether the market and exclusion effects hold with another empirical strategy, I run the following long-differences specification:

$$\Delta s_{n(m),2010-t} = \beta_1 \mathbb{1}^{NA}_{n(m)} + \beta_2 \mathbb{1}^{NA}_{n(m)} \times \Delta \text{CM}_{m,2010-t} + X_{n(m),t}\gamma + \delta_m + \epsilon_{n(m),t}, \qquad \text{(C.4)}$$

where the dependent variable $\Delta s_{n(m),2010-t}$ is the variation in white share between the starting period t and 2010 of neighborhood n in city m, the dummy variable $\mathbb{1}^{NA}_{n(m)}$ indicates whether neighborhood n within city m has access to a coastline, a lake, a river, or is over a hill.[1] The term $\Delta \text{CM}_{m,2010-t} \equiv \ln\left(\frac{\text{CM}_{m,2010}}{\text{CM}_{m,t}}\right)$ is the growth of Confederate monuments within city m between t and 2010, which is used as a proxy for city-level anti-black attitudes. The city fixed effect δ_m ensures that the identification comes from within the city, and the vector $X_{n(m),t}$ controls for initial and growth of neighborhood characteristics. The standard errors $\epsilon_{n(m),t}$ are clustered at the city level.

Table C.2
Long-differences 2010: market and exclusion effects of natural amenities

	1940		1950		1960		1970	
	(1)	(2)	(3)	(4)	(5)	(6)	(7)	(8)
Natural amenities	0.091***	0.059***	0.088***	0.044***	0.074***	0.025***	0.060***	0.028***
	(0.011)	(0.009)	(0.010)	(0.008)	(0.009)	(0.004)	(0.008)	(0.003)
NA × Conf. monu	0.014	0.017	0.012	0.029**	-0.029	0.031**	-0.057**	-0.021
	(0.011)	(0.015)	(0.012)	(0.013)	(0.021)	(0.015)	(0.023)	(0.019)
Set of Controls	○	✓	○	✓	○	✓	○	✓
R^2	0.213	0.275	0.195	0.264	0.218	0.339	0.261	0.390
Observations	7,522	7,522	9,712	9,712	22,297	22,297	29,577	29,539

Notes: This table presents the long-differences regression results for the market and exclusion effects of natural amenities on neighborhood white share from 1940 to 2010. Each column represents a separate regression for different decades. Standard errors are clustered at the city level, and ***, **, * indicate significance at the 1%, 5%, and 10% levels, respectively. The dependent variable is the variation in white share between the starting period and 2010. Controls include initial and growth characteristics of neighborhoods. The independent variables are natural amenities and the interaction between natural amenities and the growth of Confederate monuments.

[1] The neighborhood is within 500 meters of a natural feature such as an ocean, the Gulf of Mexico, a lake, a major river, or has an average slope greater than 15°.

C.3 Structural analysis

C.3.1 Full-table of quantification

Table C.3
Structural Estimation

	B_n^b			B_n^w		
	(1)	(2)	(3)	(4)	(5)	(6)
η^w	-0.202***	-0.268***	-0.258***	0.619***	0.516***	0.504***
	(0.028)	(0.041)	(0.039)	(0.030)	(0.022)	(0.019)
Natural amenities		-0.004	0.192***		0.023**	-0.201***
		(0.005)	(0.041)		(0.010)	(0.054)
Log distance to seaport		0.007	0.011		0.025*	0.030**
		(0.012)	(0.013)		(0.012)	(0.014)
Log housing age		-0.124***	-0.139***		-0.024	-0.051*
		(0.017)	(0.015)		(0.037)	(0.028)
Log distance to CBD		0.063***	0.085***		0.145***	0.173***
		(0.014)	(0.011)		(0.020)	(0.022)
η^c			-0.201***			0.279***
			(0.043)			(0.069)
η^r			0.032***			0.044***
			(0.006)			(0.014)
City FE	✓	✓	✓	✓	✓	✓
Observations	16,590	16,590	16,590	16,642	16,642	16,642
R^2	0.106	0.273	0.301	0.381	0.527	0.546

Notes: This table displays structural parameters estimations from group-specific separated regressions of amenities equation (3.25). Dependant variables are group-specific amenities. Each regressions control for a city fixed-effect and ***, **, * indicate significance at the 1%, 5% and 10% level, respectively.

C.3.2 Counterfactuals: racial sorting and natural amenities

Table C.4

Counterfactuals: racial sorting and natural amenities

	Baseline: $s_n(m)$	Counterfactuals: $\Delta s_n(m)$	
	(1)	(2)	(3)
Natural amenities	0.024***	-0.144***	-0.188***
	(0.006)	(0.007)	(0.019)
Log. distance to CBD	0.057***	-0.003***	-0.035***
	(0.013)	(0.0005)	(0.010)
Scenario	∘	$\eta^c = 0$	$\eta^c = \eta^w = 0$
City FE	✓	✓	✓
Observations	16,642	16,642	16,642
R^2	0.195	0.757	0.208

Notes: Each column reports estimates from separate regressions. The dependent variable is the white share within a neighborhood. Each regressions control for city fixed-effects. Column (1) shows the result considering the initial equilibrium, while columns (2) and (3) show the change following counterfactual exercices. ***, **, * indicate significance at the 1%, 5% and 10% level, respectively.

C.3.3 Model fit

Table C.5

Full result: validity of estimated density of development

CBSA	R-squared	Slope
Houston, TX	0.83	0.87
Philadelphia, PA	0.87	0.92
Dallas, TX	0.84	0.90
San Jose, CA	0.84	0.92
Chicago, IL	0.88	0.95
Los Angeles, CA	0.84	0.92
Austin, TX	0.89	0.90
Charlotte, NC	0.78	0.76
Columbus, OH	0.88	0.89
Denver, CO	0.87	0.93
Indianapolis, IN	0.90	0.88
Seattle, WA	0.88	0.85
Jacksonville, FL	0.85	0.86
Phoenix, AZ	0.83	0.94
San Antonio, TX	0.90	0.90
San Diego, CA	0.84	0.91

Notes: This table presents the model fit of the land market by comparing the log of estimated residential housing demand with the log of actual housing density for all cities.

Résumé de la thèse

I La ville comme objet de recherche

La ville constitue un objet de recherche singulier en raison de leur croissance et de leur influence significative sur nos conditions de vie. Actuellement, 55% de la population mondiale vit dans des zones urbaines, et les projections indiquent que cette proportion atteindra 68% d'ici 2050. Cette tendance est particulièrement marquée dans les pays en développement, où l'urbanisation augmente rapidement. Par conséquent, les villes reflètent un choix collectif, les individus s'y concentrant pour y résider, y exercer des activités économiques et y interagir socialement.

L'urbanisation est étroitement liée à la croissance et au développement économiques. Les études empiriques démontrent une forte corrélation entre les niveaux d'urbanisation et le PIB par habitant (Bryan et al., 2025). Les villes sont essentielles pour accroître l'activité économique et réduire la pauvreté, car la densité crée des économies d'agglomération, des opportunités de mobilité économique et de progrès social.

L'importance des villes continuera de croître, façonnant les conditions de vie de milliards d'individus et définissant la trajectoire du progrès humain. Ainsi, l'étude des villes apparait comme nécessaire et permet une meilleure compréhension des dynamiques urbaines. Ces recherches sont essentielles pour aider les décideurs politiques à concevoir des stratégies efficaces pour le développement durable, la planification des infrastructures et l'équité sociale.

L'émergence de l'économie urbaine en tant que champ de recherche indépendant

Les économistes urbains se concentrent sur les villes, qui sont par nature définies par la proximité des activités économiques, une caractéristique clé qui crée des économies d'agglomération. Les micro-fondations de ces économies d'agglomération ont été introduites pour la première fois par Marshall (1890). Bien que les fondements théoriques soient anciens, l'économie urbaine en tant que champ distinct au sein de l'économie est relativement récente. A titre d'exemple, le *Journal of Urban Economics* a été créé en 1974, et il a fallu plusieurs décennies pour voir une augmentation significative du nombre d'articles en économie urbaine publiés dans les principales revues économiques (Henderson and

Thisse, 2024). Le champ a connu un essor substantiel suite au prix Nobel de 2008 décerné à Krugman pour ses contributions à la géographie économique, bien que l'économie urbaine reste distincte dans la mesure où elle se concentre spécifiquement sur les activités intra-urbaines. Cette distinction mène à une division classique entre les phénomènes intra-urbains et inter-urbains, même si ces domaines de recherche se chevauchent souvent en pratique. Plus récemment, Jonathan Dingel a documenté au sein de son blog une augmentation du nombre total de papiers dits de «*Job Market* »se présentant comme de l'économie spatiale. Avec l'essor de la recherche basée sur les données et le développement des méthodes économétriques, les économistes urbains ont quantifié l'ampleur des économies d'agglomération et étudié leurs mécanismes sous-jacents. Par exemple, des recherches pionnières sur la taille des villes, la densité de l'emploi et la productivité ont été initiées par Ciccone and Hall (1996) et ont été considérablement étendues au cours des deux dernières décennies (voir Rosenthal and Strange (2004); Combes and Gobillon (2015) à ce propos). Plus récemment, une méta-analyse de Ahlfeldt and Pietrostefani (2019) montre une élasticité des salaires par rapport à la densité de population égale à 4%, mais elle cache une hétérogénéité substantielle selon les différents contextes.

Plus récemment, l'intersection entre l'histoire économique et l'économie urbaine connaît un élan significatif, comme le soulignent Hanlon and Heblich (2022). Cette tendance croissante reflète à la fois les avancées méthodologiques et les nouvelles directions de recherche en économie urbaine (voir la section II pour plus de détails). Les progrès technologiques en matière de numérisation et de calcul ont considérablement élargi la portée des données historiques disponibles pour l'économie urbaine, surmontant les limitations précédentes qui contraignaient autrefois une telle recherche. Une direction centrale de la recherche en économie urbaine étudie comment les développements passés façonnent encore les structures urbaines contemporaines, en examinant les effets à long terme des grands investissements en infrastructure tels que les réseaux de transport et les systèmes d'assainissement sur l'organisation urbaine actuelle et les schémas de ségrégation spatiale. Cette perspective historique offre des informations précieuses sur les déterminants gouvernant la distribution d'équilibre des résidents, des travailleurs et des valeurs foncières à travers les espaces urbains.

Cette thèse de doctorat s'inscrit dans cette tendance émergente à travers trois chapitres en économie urbaine, chacun s'appuyant sur des études de cas historiques. Les deux premiers chapitres examinent la distribution spatiale de l'activité économique au sein de Paris au 19ème siècle et les effets sur le bien-être résultant du développement d'infrastructures publiques. Le dernier chapitre étudie comment les aménités naturelles influencent le tri

racial dans les villes américaines tout au long du 20ème siècle. À travers ces analyses, cette thèse de doctorat vise à élargir les recherches en économie urbaine utilisant des expériences naturelles historiques.

Cadre théorique de la structure intra-urbaine

Le modèle monocentrique canonique, développé par Alonso (1964), Muth (1969) et Mills (1967) et souvent nommé modèle AMM, vise à comprendre la structure au sein d'une ville. Ce cadre théorique a été conçu pour correspondre aux gradients observés et comprendre, en particulier comment la densité de population, les prix du logement et les prix du foncier diminuent à mesure que l'on s'éloigne du centre-ville. Dans le modèle canonique d'AMM, on suppose que tous les emplois sont concentrés dans un quartier central des affaires (dit CBD). Les travailleurs font face à des coûts de transport lorsqu'ils se rendent au travail, ce qui rend les endroits à proximité du CBD plus attractifs que ceux éloignés. Par conséquent, les travailleurs arbitrent entre des prix du foncier plus bas plus loin du CBD et des coûts de transport plus élevés. Cela entraîne une structure monocentrique des prix du foncier, avec un pic de prix du foncier au CBD et un gradient de prix du foncier qui diminue de manière monotone avec la distance par rapport au CBD. Empiriquement, Liotta et al. (2022) testent le modèle AMM avec un ensemble de données contenant des informations sur les densités de population, les loyers, l'offre de logement et les transports dans 192 villes du monde entier. Ils trouvent que 100% et 87% des villes présentent respectivement les gradients de densité de population et de loyers négatifs attendus, conformément au modèle AMM. Par conséquent, le modèle de ville monocentrique amène à des prédictions très pertinentes, et permet de décrite un pattern retrouvé dans les données.

Cependant, même s'il correspond à des faits stylisés, le modèle AMM ne permet pas de prendre en compte toute l'hétérogénéité au sein des villes. Par exemple, il existe des différences marquées dans les prix des logements entre des quartiers proches. Certains endroits d'une ville peuvent avoir accès à des zones d'eau, et ainsi être mieux adaptés à un usage industriel (Heblich et al., 2021), tandis que d'autres endroits peuvent avoir accès à des espaces ouverts, les rendant bien adaptés à un usage résidentiel (Lee and Lin, 2018). D'autres parties de la ville peuvent avoir de bonnes connexions de transport et être accessibles pour l'activité de détail (You, 2021; Miyauchi et al., 2025). Au sein des villes, l'on observe de grandes différences entre les lieux en termes de prix du foncier et des riches motifs d'utilisation des sols (Duranton and Puga, 2015). Certaines localités sont utilisées pour les lieux de travail, tandis que d'autres sont utilisées pour les résidences. Au sein de la même ville, certains lieux résidentiels sont prospères (comme le 16ème arrondisse-

ment à Paris), tandis que d'autres sont pauvres (comme Aubervilliers à la frontière de Paris). L'essor des modèles spatiaux quantitatifs (QSM) au cours de la dernière décennie a permis l'intégration de ces éléments, tout en abordant les réponses d'équilibre, en rendant possible des prédictions sur les futures politiques et en fournissant de meilleures mesures du bien-être (voir Redding (2022) à ce propos). Une distinction classique au sein des QSM est faite entre (i) les modèles de villes (modèles régionaux quantitatifs) qui se concentrent sur les interactions entre les villes, et (ii) les modèles intra-urbains (modèles urbains quantitatifs) qui se concentrent sur les interactions au sein d'une ville. En outre, cette classe de modèles n'impose aucune structure spécifique à la ville, telle qu'un cadre monocentrique. Ainsi, ces modèles permettent un meilleure appréhension de la réalité, où des quartiers relativement proches peuvent successivement alterner entre résidentiel et commercial. Cependant, il est encore possible de combiner une structure monocentrique avec le modèle urbain quantitatif, comme le démontre Bagagli (2023). Par conséquent, ces modèles sont nécessaires pour rationaliser l'équilibre spatial et comprendre les impacts des politiques publiques urbaines, telles que les changements d'infrastructure sur la distribution de la population, des entreprises, ainsi que des effets d'agglomération.

Cette thèse de doctorat s'aligne sur cette littérature émergente des QSM, dans la mesure où chaque chapitre utilise un modèle quantitatif urbain (QUM) spécifique à leur question de recherche, mais partage des similitudes. La tractabilité de ces cadres théoriques permet d'aligner les questions de recherche avec les données correspondantes et fournit des informations sur les équilibres spatiaux alternatifs. Dans ce résumé, la section IV est dédiée à la description plus détaillée des avantages de ces modèles.

II Nouvelles données, nouvelles opportunités

L'expansion des données historiques offre de nouvelles perspectives de recherche en permettant l'utilisation d'expériences naturelles et en offrant des informations précédemment inaccessibles. Plusieurs approches méthodologiques facilitent cette avancée dans la recherche en économie urbaine (voir par exemple Abramitzky et al. (2025) à ce propos).

La fusion de données entre différents recensements historiques, comme démontré par Abramitzky et al. (2021), représente une avancée significative. Cette méthodologie offre aux chercheurs la possibilité de suivre les individus au fil du temps, permettant ainsi des études sur les impacts à long terme des chocs économiques sur les schémas de mobilité professionnelle, les décisions de migration et divers résultats socio-économiques. La numérisation des cartes historiques est apparue comme une autre méthode importante

pour définir l'exposition aux événements historiques. Les chercheurs peuvent utiliser des outils de système d'information géographique (SIG) pour reconstruire manuellement divers objets urbains, tels que les réseaux de transport historiques entre les villes (Atack, 2013; Thevenin et al., 2016; Ciccarelli and Groote, 2018) et au sein des zones urbaines (Brooks and Lutz, 2019; Heblich et al., 2020), ainsi que les routes de communication historiques (Wang, 2025; Skoglund, 2025). Cependant, les techniques dites de *machine learning* ont gagné en importance dans ce processus de numérisation, particulièrement pour l'analyse des cartes d'utilisation des sols et des empreintes des bâtiments (Heblich et al., 2023; Lin et al., 2023; Combes et al., 2025a,b). L'analyse de Combes et al. (2022) offre un panorama de ces applications de *machine learning* dans la recherche en économie urbaine. D'autre part, la technologie de reconnaissance optique de caractères (dit «*optical character recognition* ») s'est avérée précieuse pour extraire des informations de vastes documents d'archives, en particulier les annuaires, ou Pages jaunes (You, 2021; Albers and Kappner, 2023; Ellen et al., 2025). Cette approche offre une alternative intéressante aux données de recensement traditionnelles car les annuaires permettent un géo-référencement des entreprises et des ménages sur plusieurs périodes et à des résolutions spatiales plus fines.

Bien que les données administratives restent la principale source d'information en économie urbaine, la recherche intègre de plus en plus des sources de données alternatives. Ces ensembles de données émergents offrent de nouvelles perspectives sur diverses dimensions de la recherche en économie urbaine. Les images satellites, par exemple, fournissent des mesures détaillées d'illumination nocturne (Henderson et al., 2012; Martinez, 2022) et des empreintes des bâtiments (Harari, 2020; Henderson et al., 2021a; Gechter and Tsivanidis, 2023). Les données de téléphone mobile représentent également une autre source important, notamment pour analyser les déplacements des individus, les comportements de consommation et les tendances de mobilité de manière plus large (Barwick et al., 2023; Kreindler and Miyauchi, 2023). De plus, les données de transaction par carte de paiement sont devenues attractives car elles permettent de mesurer des dépenses à un niveau local (Allen et al., 2020).

Cette thèse de doctorat contribue à ces tendances émergentes de données en économie urbaine en utilisant des données historiques numérisées de Paris. Les premier et deuxième chapitres utilisent de nouveaux ensembles de données comprenant des informations au niveau des entreprises provenant d'annuaires historiques (Pages jaunes), des recensements de population et fiscaux provenant des archives municipales, et des reconstructions détaillées des systèmes de transport historiques de Paris et des empreintes urbaines, cou-

vrant tout le 19ème siècle. Le troisième chapitre adopte une approche mixte en intégrant à la fois des données historiques sur les emplacements des monuments confédérés à travers les États-Unis au cours du 20ème siècle et des données de recensement contemporaines et des statistiques d'emploi Origine-Destination LEHD. En exploitant ces divers ensembles de données, cette recherche contribue à la littérature croissante qui utilise des informations historiques détaillées pour identifier des expériences naturelles et améliorer notre compréhension théorique et empirique des processus économiques urbains.

III Ce qui caractérise la ville

Dans cette thèse de doctorat, je me concentre sur trois caractéristiques clés parmi les nombreux aspects qui définissent les villes. Plus précisément, cette thèse examine : (i) les infrastructures de transport qui réduisent les temps de trajet et augmentent la proximité entre les individus, les entreprises et les lieux; (ii) le bien-être associé au déploiement d'infrastructures publiques; et (iii) le tri spatial des individus au sein des villes, caractérisé par la ségrégation et l'accès inégal aux biens publics locaux. En analysant ces trois caractéristiques urbaines fondamentales, cette thèse vise à approfondir l'appréhension des villes et de leurs dynamiques complexes.

Infrastructure de transport urbain

L'émergence des villes au cours du 19ème siècle et l'accélération de l'urbanisation ont été accompagnées par une diminution des coûts de transport et de déplacement, ainsi que par le renouvellement urbain et le développement des infrastructures publiques. D'une part, ces facteurs ont pu accélérer la concentration des individus au sein des villes, tandis que d'autre part, ils ont pu atténuer les effets négatifs de l'urbanisation. Par exemple, les capitales européennes ont été confrontées à des défis urbains tels que des crises sanitaires, des pénuries de logement dues à la croissance rapide de la population et des besoins de déplacement résultant de réseaux de transport médiocres à l'époque. Ainsi, les planificateurs ont mis en place des infrastructures afin de restructurer les villes.

Le premier chapitre, constituant le travail principal de cette thèse, étudie l'impact d'un chemin de fer circulaire nommé "Petite Ceinture" (PC) à Paris en 1854 sur la distribution spatiale des résidents et des entreprises, les schémas de déplacement, la consommation et le bien-être. Étant donné que l'objectif initial était de réduire les coûts de transport des marchandises en détournant le trafic du centre-ville de Paris, ce chemin de fer possède une caractéristique unique avec sa forme circulaire, en faisant le premier système de transit

circulaire pour passagers au monde.

Pour mener mon analyse, j'harmonise la géographie de Paris au fil du temps et combine plusieurs nouvelles sources de données. Tout d'abord, j'ai numérisé des données sur les quartiers parisiens et les tendances de population des municipalités environnantes pour étudier les dynamiques des choix résidentiels sur 150 ans au sein de Paris[1]. Ensuite, j'utilise les annuaires de la ville de Paris de 1799 à 1908 pour suivre l'évolution de l'activité économique au fil du temps et à travers les quartiers. Cette base de données unique géolocalise les entreprises par activité et me permet de suivre leur localisation sur une longue période et à une petite échelle spatiale. Cette riche source de données micro-géographiques est encore très peu utilisée en économie urbaine comme le documente Albers and Kappner (2023). Troisièmement, j'ai reconstruit le réseau de transport parisien en utilisant de nouvelles données sur le chemin de fer de PC, les omnibus, les tramways et les rues afin de calculer les changements de temps de trajet bilatéraux entre les quartiers sur la période. Enfin, j'ai numérisé les données fiscales des quartiers afin de capturer les variations des niveaux de loyer à travers les emplacements. Dans l'ensemble, cette base de données unique me permet de mesurer précisément l'évolution des activités économiques des quartiers parisiens et des municipalités suburbaines pour une période s'étendant de 1801 à 1954 afin d'évaluer quantitativement l'impact d'une nouvelle infrastructure de transport urbain.

Ce premier chapitre de thèse apporte des preuves sur les effets à court et à long terme du chemin de fer de PC sur la distribution spatiale de l'activité économique parisienne. En ce qui concerne les effets à court terme, je construis des mesures d'accès de marché des entreprises et des résidents et j'exploite les changements spatiaux entre 1861 et 1896[2]. En contrôlant pour la part initiale des bâtiments ainsi que la proximité aux rénovations haussmanniennes, et en employant une stratégie de variable instrumentale pour exploiter uniquement les variations des coûts de transports, les résultats montrent qu'une augmentation de 10% de l'accès au marché des résidents conduit à une augmentation de 2,2% de la population et de 4,7% des loyers au sein d'un quartier. De plus, une augmentation de 10% de l'accès au marché des entreprises entraîne une augmentation de 3,9% du nombre d'usines et de 6,9% des établissements de détail dans des carreaux de 200m×200m. Par

[1] La géographie de Paris en 1860 est divisée en 20 arrondissements, et chaque arrondissement est divisé en 4 quartiers administratifs. Il y a un total de 80 quartiers dans la zone de Paris.

[2] Pour un lieu d'origine donné, l'accès au marché des entreprises est défini comme la somme pondérée des populations à travers tous les lieux, avec des poids déterminés par les coûts de transports associés. Inversement, l'accès au marché résidentiel est défini comme la somme pondérée des entreprises à travers tous les lieux, avec des poids déterminés par les coûts de transports associés.

ailleurs, les résultats précédents sont confirmés en utilisant des spécifications alternatives et en mettant en œuvre une méthode de doubles différences. En testant les mécanismes, je ne trouve aucun effet de la réduction du temps de trajet sur la densité des rues. Par conséquent, les résultats semblent être principalement dus à des réductions du temps de trajet, et non à l'urbanisation (c'est-à-dire le développement du réseau de rues et du tissu urbain) près des gares du chemin de fer de PC. Cela implique que le chemin de fer de PC a poussé l'industrie parisienne et les résidents hors du centre-ville, créant finalement une décentralisation de l'activité économique en périphérie. Motivé par ces résultats, je développe et calibre un modèle spatial quantitatif avec un secteur de biens échangeables et un secteur de services non échangeables afin de rationaliser l'équilibre spatial intra-urbain, et d'estimer structurellement l'impact du chemin de fer de PC sur les choix de localisation des travailleurs et des entreprises, ainsi que sur les prix des biens échangeables. Je documente un aplatissement de la relation des salaires spécifiques au secteur estimés par rapport à la distance du centre-ville au fil du temps, indiquant un éloignement du modèle de ville monocentrique. En d'autres termes, les quartiers proches du centre-ville deviennent moins spécialisés dans les lieux de travail, et l'emploi devient plus uniformément distribué à travers les quartiers. Concernant les paramètres du modèle structurel, j'estime une élasticité des forces d'agglomération des aménités de 0,168 (dans la lignée de Heblich et al. (2020)) en utilisant ma variation quasi-expérimentale des coûts de transports. De plus, j'estime l'élasticité de l'offre de logement en exploitant les variations spatiales et temporelles des valeurs locatives et du nombre de logement. En contrôlant pour les rénovations haussmanniennes, je trouve une élasticité de l'offre de logement de 0,517, qui est relativement faible par rapport aux estimations précédentes dans la littérature. Cela confirme que le développement du logement pendant cette période était principalement influencé par les politiques urbaines, et moins par les variations de loyer. Ensuite, j'utilise mon modèle spatial quantitatif combiné avec de l'«*exact-hat algebra* »pour estimer structurellement l'impact du chemin de fer de PC sur l'équilibre spatial de Paris. Dans un exercice contrefactuel considérant un cadre de ville ouverte, je trouve que la fermeture de la PC diminue la population totale et les valeurs locatives, respectivement de 10,0% et 10,1%, et crée une redistribution de l'activité économique vers le centre-ville. Je trouve également qu'il y a des effets considérables sur le prix des biens échangeables, augmentant de 1,6% à 8,0% dans les quartiers proches de la périphérie. Cela met en évidence les effets duaux du chemin de fer de PC sur le bien-être des travailleurs parisiens, avec une réduction des coûts de déplacement et de fret, permettant un meilleur accès au marché et à la consommation. Enfin, l'exercice contrefactuel étudiant l'impact du *design* des transports fournit des preuves que le chemin de fer radial, comme à Londres, est plus efficace en

termes de bien-être qu'un système de transport circulaire comme la PC, et crée une plus grande séparation entre le lieu de travail et la résidence. Cependant, la combinaison des deux infrastructures de transport permet des gains de bien-être supplémentaires, indiquant qu'elles sont complémentaires dans la réduction des coûts de transports. Ainsi, ce premier chapitre de thèse contribue de manière significative à la littérature sur les transports urbains en introduisant un cadre historique unique avec un système de transport circulaire qui évite de traverser le centre-ville, rendant les déplacements dans les quartiers périphériques plus accessibles pour les marchandises et les passagers. Cela contraste avec les systèmes de transit historiques dans des villes comme Berlin, Boston, Chicago et Londres, qui présentent un modèle radial. Cependant, les villes modernes ont rapidement adopté des lignes circulaires. De plus, mon cadre théorique s'appuie sur le modèle urbain canonique de Heblich et al. (2020), qui modélise les choix de déplacement dans une ville ouverte, et intègre (i) un composant Armingtonien pour considérer un secteur de biens échangeables (Armington, 1969) et (ii) un composant de nouvelle géographie économique (Krugman, 1991b; Helpman et al., 1995) pour considérer un secteur de services non échangeables. Par conséquent, le modèle spatial développé accommode la double fonction du chemin de fer circulaire en modélisant à la fois le commerce des marchandises et les déplacements des passagers. En ce qui concerne les effets à long terme, j'utilise les différences à long terme entre les populations de 1906 et 1954 pour éclairer la persistance de l'impact de la PC. La période de départ correspond à l'année marquant le déclin du trafic de la PC dû à la concurrence croissante avec le métro à Paris. En contrôlant pour la distance par rapport au centre-ville, pour traiter de l'émigration du centre-ville, et la croissance de l'accessibilité de la ville par le métro, je trouve que les quartiers qui étaient à moins de 500 mètres d'une gare de la PC ont connu une croissance de la population de 22% sur 48 ans supérieure à celle des autres quartiers. Ainsi, cette analyse contribue à la littérature sur la persistance et la dépendance au sentier en fournissant des preuves supplémentaires que l'histoire joue un rôle significatif dans l'explication de la croissance inégale au sein d'une ville.

Le premier chapitre de cette thèse se concentre sur un élément crucial des villes : la proximité des individus, des entreprises, et des localités, obtenue en réduisant les coûts de déplacement et de fret. Il quantifie l'effet d'un design de chemin de fer circulaire sur la distribution spatiale des activités économiques et du bien-être en utilisant une expérience naturelle historique et nous aide à comprendre la distribution spatiale actuelle de l'activité économique et à planifier les futures infrastructures de transport urbain.

Bien-être et fourniture optimale d'infrastructure

Au sein des villes, les décideurs peuvent mettre en œuvre des politiques publiques, y compris des infrastructures, pour améliorer la qualité de vie des résidents et travailleurs. Cette mise en place de biens publics est une caractéristique supplémentaire des villes. Étant donné le large éventail d'options disponibles pour le planificateur, les interactions au sein de la ville et l'hétérogénéité des localités, une question clé se pose : comment concevoir, de manière optimale, l'infrastructure publique ? Plus précisément, le deuxième chapitre de cette thèse examine comment concevoir un système de transport pour maximiser le bien-être au sein d'une ville.

Dans ce chapitre, je crée un cadre pour identifier la conception optimale d'infrastructure de transport urbain. Le cadre intègre les effets d'équilibre général, qui apparaissent lorsque les travailleurs se ré-allouent vers différentes résidences et lieux de travail au sein de la ville en réponse aux interventions des politiques publiques, influençant ainsi le marché foncier où les travailleurs et les entreprises sont en concurrence pour le logement. De plus, il prend en compte plusieurs modes de transport et tient compte de l'hétérogénéité des quartiers en termes d'aménités, de productivité et d'offre de logement. Il permet également de considérer des forces d'agglomération de production et résidentielles. La prise en compte de ces éléments est cruciale pour améliorer l'efficacité des systèmes de transport urbain. Dans ce cadre, le problème du planificateur consiste à choisir un réseau de métro M basé sur un objectif économique $W(M;\theta)$, qui dépend des paramètres structurels θ. De plus, les préférences du planificateur sont influencées par des facteurs au-delà de l'objectif économique, tels que des préférences non observées pour des caractéristiques spécifiques du réseau de métro. Je modélise cela comme un choc idiosyncratique, noté ι_M. Par conséquent, le planificateur est confronté à un problème de choix discret dans l'espace de tous les réseaux de métro possibles. Bien qu'il soit impossible de trouver un réseau de métro global unique en raison du problème d'optimisation de haute dimension, un algorithme de recuit simulé est utilisé pour échantillonner des réseaux de métro (sous-)optimaux.

J'applique ma méthodologie pour répondre à la question suivante : comment le métro parisien aurait-il dû être planifié à la fin du 19ème siècle ? Je combine les mêmes données historiques que dans le premier chapitre et divise l'espace parisien en une grille de carreaux 500m×500m pour créer des emplacements et des stations de métro potentielles. Dans cette application, je développe et calibre un modèle urbain quantitatif (QUM) avec des travailleurs hétérogènes pour rationaliser l'équilibre spatial intra-urbain. Dans le scé-

nario initial, je définis un objectif économique $W(M;\theta)$ comme les gains en valeur locative dans un cadre de ville ouverte, suivant le théorème de Henry George (George, 1879)[3]. De plus, j'estime le coût de construction du métro M en fonction des coûts fixes, du nombre de stations et de lignes. Je trouve que les emplacements stratégiques des stations sont déterminés par les équipements et la productivité. De plus, la centralité de la station dans le réseau est également un déterminant important dans le choix du réseau de métro par le planificateur. Ce résultat est en accord avec Borusyak and Hull (2023), qui soulignent que les stations centrales sont plus susceptibles d'être choisies pour augmenter le potentiel du marché. Sur les réseaux de métro échantillonnés, le facteur d'impact économique moyen est d'environ 9,71, en accord avec les résultats de Heblich et al. (2020). Cela signifie que les bénéfices économiques sont 9,71 fois supérieurs aux coûts de construction du métro. Le nombre moyen de stations de métro est d'environ 55, ce qui conduit à une distance moyenne d'environ 913 mètres par rapport à une station de métro[4]. Les augmentations moyennes de la production totale et de la population au sein de la ville sont respectivement de 32,0% et 23,7%. De plus, la diminution moyenne du temps total de trajet au sein de la ville est de 20,4%, avec des disparités significatives et des améliorations plus importantes dans les emplacements plus proches du centre-ville. Ensuite, je mène plusieurs expériences de statiques comparatives pour évaluer le rôle des paramètres structurels et des paramètres de coût de construction du métro. Le cadre développé réagit à ceux-ci, se traduisant par des *designs* de métro différents. Ainsi, ce deuxième chapitre de thèse contribue à la littérature de conception optimale des réseaux de transport. Des travaux récents ont étudié la fourniture d'infrastructures de transport entre les villes en utilisant une perspective commerciale, ou d'infrastructures de transport intra-urbaines sans effets d'équilibre général. Je contribue à cette littérature sur la conception optimale des transports en m'appuyant sur Kreindler et al. (2024) pour fournir un cadre intra-urbain qui intègre les effets d'équilibre général, lorsque les travailleurs se ré-allouent vers différentes résidences et lieux de travail suite à des améliorations des infrastructures de transport urbain. Ce cadre permet de prendre en compte les forces d'agglomération et considère plusieurs modes de transport. De plus, il permet aux planificateurs de fixer les paramètres

[3] Dans l'approche classique pour évaluer les biens publics, les propriétaires fonciers bénéficient des gains de bien-être liés à la nouvelle technologie de transport à travers les changements de valeur des terrains et des bâtiments (George, 1879). Cette méthodologie a également été utilisée dans Heblich et al. (2020) pour évaluer le métro à Londres.

[4] La superficie potentielle totale se compose de 367 cellules de grille. Chaque cellule de grille couvre 0,25 km^2, résultant en une superficie totale de 91,75 km^2. Avec 55 stations, chaque station couvre environ 1,668 km^2. En supposant une superficie carrée par station, la longueur du côté est $\sqrt{1,668\ \text{km}^2} \approx 1,292$ km. La diagonale de ce carré est $1,292\ \text{km} \times \sqrt{2} \approx 1,826$ km, donc la distance moyenne est la moitié de la diagonale : $1,826\ \text{km}/2 \approx 0,913$ km.

de coût de construction du métro et le nombre minimum de lignes à construire.

Le deuxième chapitre de cette thèse fournit aux planificateurs urbains des solutions pour la conception optimale d'infrastructures publiques. Cela vise à améliorer le bien-être des résidents de la ville en garantissant que l'infrastructure publique est efficace et également accessible en fonction de l'objectif du planificateur.

Tri et ségrégation spatiale

Les villes sont également caractérisées par le tri des individus dans l'espace. Celui-ci peut être soit un tri par revenu, où il existe une forte séparation spatiale entre riches et pauvres, soit un tri racial avec une forte séparation spatiale entre les minorités raciales et le reste de la population. Le dernier chapitre étudie comment les biens publics locaux peuvent façonner le tri racial entre individus Noirs et Blancs, augmentant ainsi la ségrégation raciale dans le contexte des États-Unis. Je considère les aménités naturelles comme des biens publics locaux puisqu'elles fournissent des loisirs, ancrent les quartiers à un niveau de revenu élevé (Lee and Lin, 2018), et les individus peuvent coopérer pour améliorer leur qualité ou leur accès.

Dans le troisième chapitre de cette thèse, j'explore deux mécanismes qui pourraient expliquer le tri racial créé par les aménités naturelles : (i) un effet de marché reflété dans des loyers plus élevés, résultant d'une demande accrue pour les quartiers proches de ces biens publics locaux ; (ii) un effet d'exclusion apparaissant lorsque les individus coopèrent pour restreindre l'accès aux biens publics locaux au sein de leur propre groupe ethnique (Albouy et al., 2020). J'utilise la variation des monuments confédérés à travers la ville au fil du temps et entre les villes comme un proxy pour les attitudes anti-Noirs (Henderson et al., 2021b; Ferlenga, 2023) pour éclairer l'effet d'exclusion. Ils devraient capturer une hostilité raciale plus élevée des Blancs envers les Noirs, dans la mesure où ils représentent des symboles d'oppression.

Tout d'abord, je fournis des preuves dits de "forme réduite" montrant que les deux mécanismes des aménités naturelles sont en jeu. Je trouve que les quartiers ayant accès aux aménités naturelles sont, en moyenne, plus Blancs par rapport à d'autres quartiers au sein d'une ville sur la période 1880-2010. De plus, les quartiers proches des aménités naturelles connaissent une augmentation de leur part de Blancs suite à une augmentation des monuments confédérés dans toute la ville. En faisant cela, je fais le lien entre la littérature sur le tri par revenu et le tri racial, en étendant Lee and Lin (2018) en examinant le rôle des aménités naturelles dans le tri racial au-delà du revenu, et en étudiant le

rôle des préférences raciales dans le choix résidentiel. Contrairement aux travaux précédents, cet article inverse la relation entre l'impact de la diversité sur les biens publics, et étudie comment la proximité des aménités naturelles influence la composition raciale des quartiers.

Ensuite, j'utilise un modèle urbain quantitatif (QUM) d'agents hétérogènes pour récupérer les aménités spécifiques à l'ethnie, et je trouve des paramètres de homophilie forts et significatifs pour les Blancs et les Noirs, avec un paramètre plus élevé pour les Blancs (Krysan and Farley, 2002; Ihlanfeldt and Scafidi, 2002), lors des choix résidentiels des deux groupes de résidents. De plus, je trouve un effet positif de la proximité des aménités naturelles (telles que les côtes, les lacs, les rivières et les collines) sur les aménités retrouvées par le modèle structurel, et un effet de complémentarité par rapport à la composition raciale. Plus précisément, la présence de leur propre groupe racial dans un quartier renforce la valeur de l'accès aux aménités naturelles pour les résidents Noirs et Blancs. Ces résultats soulignent le rôle de la composition raciale dans le déverrouillage des biens publics locaux (Albouy et al., 2020). Ensuite, je montre dans un exercice contrefactuel que la suppression de toutes les préférences raciales diminue, en moyenne, la ségrégation raciale de 11,6 points de pourcentage. En m'appuyant sur des modèles spatiaux intra-urbains récents, cette étude estime les préférences raciales en utilisant des données contemporaines et une variation intra-urbaine, tout en examinant comment les aménités naturelles affectent ces forces endogènes.

Le chapitre final se concentre sur la manière dont les aménités naturelles façonnent le tri racial, visant à fournir une meilleure compréhension de la ségrégation raciale durable. Ces éléments sont importants puisque les aménités naturelles sont fixes et continueront d'influencer le tri des individus au sein des villes américaines.

IV Modèle Urbain Quantitatif

Pourquoi ?

Le modèle urbain quantitatif (QUM) standard a été développé par Ahlfeldt et al. (2015), s'inspirant de la littérature sur le commerce (Eaton and Kortum, 2002) et macroéconomique. Ce cadre nécessite un petit nombre de paramètres structurels (élasticités) et permet aux chercheurs de rationaliser l'équilibre spatial intra-urbain avec les caractéristiques observées des données. Contrairement au modèle monocentrique, il accommode de nombreux emplacements qui diffèrent en termes de productivité, d'équipements, de superficie, d'offre

de surface de plancher et de connexions de transport au sein d'une ville. Ces modèles permettent aux chercheurs de faire la distinction entre la géographie de première nature (typiquement des avantages naturels) et la géographie de seconde nature (typiquement des forces d'agglomération). La géographie de première nature correspond à des avantages naturels exogènes ou à des fondamentaux de localisation, tels que l'accès à l'eau naturelle ou un emplacement en bord de mer dans un port naturel. La géographie de seconde nature correspond à la localisation des agents économiques les uns par rapport aux autres dans l'espace géographique.

Le QUM standard est caractérisé par trois agents dans la ville : (i) une entreprise unique utilisant des locaux commerciaux et du travail pour produire un bien final librement échangé au sein de la ville, (ii) des travailleurs qui vivent et travaillent, et (iii) des promoteurs fournissant des logements résidentiels et commerciaux.

Dans chaque emplacement, ces agents interagissent ensemble à travers plusieurs marchés. Les entreprises et les travailleurs se rencontrent sur le marché du travail (le QUM standard suppose le plein emploi), mais ils sont en concurrence les uns avec les autres sur le marché du logement. Ces interactions permettent aux chercheurs de considérer les effets d'équilibre général : à mesure que les travailleurs se localisent près des entreprises pour éviter les coûts de déplacement, cela fait monter les prix du logement, créant des forces de dispersion. Ces effets d'équilibre général sont cruciaux pour évaluer les réponses contrefactuelles des politiques publiques (par exemple, la mise en place d'un chemin de fer au sein de la ville).

Comment ?

Seules quelques données sont nécessaires pour résoudre un QUM puisque le modèle reste tractable. La méthode classique consiste à obtenir des données sur les résidents (où vivent les travailleurs), l'emploi (où travaillent les travailleurs), les prix du logement par emplacement et le temps de trajet entre tous les emplacements. Bien que l'accès à ces informations puisse être relativement facile grâce aux données administratives (par exemple, les données LODES fournissent les flux de déplacement entre quartiers aux États-Unis, et le temps de trajet peut être obtenu avec Google Maps (Akbar, 2024)), des méthodes alternatives existent dans les environnements où les données sont rares (typiquement les pays en développement). Par exemple, les flux de déplacement des travailleurs peuvent être estimés grâce aux données téléphoniques (Kreindler and Miyauchi, 2023; Miyauchi et al., 2025) ou aux enquêtes (Balboni et al., 2020; Franklin et al., 2024). Pour les infor-

mations sur les prix du logement, elles peuvent être estimées en extrayant des données des sites immobiliers (Liotta et al., 2022). Cependant, Sturm et al. (2023) n'observent pas les loyers et procèdent différemment : ils utilisent de nouvelles données satellitaires sur les zones bâties et les hauteurs des bâtiments pour estimer les données de loyer.

Une fois ces données obtenues, les équations d'équilibre du QUM permettent de retrouver les caractéristiques non observées des emplacements (salaires, équipements, productivité et densité de développement) en inversant le modèle, et correspondent exactement aux caractéristiques observées dans les données. De plus, la distinction entre les avantages naturels et les forces d'agglomération peut être faite en utilisant les hypothèses du modèle. Un test de sur-identification peut être effectué en comparant les données observées avec les caractéristiques estimées des localités, en utilisant, par exemple, des données disponibles sur les salaires ou le développement du logement pour valider les prédictions du QUM.

Une autre propriété de cette classe de QUM est que des statistiques suffisantes peuvent être calculées sur la base de mesures d'accès au marché, comme le montre Tsivanidis (2024), pour capturer les effets d'équilibre général. Cependant, cela ne peut être fait qu'en ignorant les changements dans l'offre de logement, les équipements et la productivité. Redding (2025) montre que les prédictions basées uniquement sur l'accès au marché peuvent diverger substantiellement des véritables changements contrefactuels en raison de ces hypothèses fortes, et que le modèle doit être entièrement résolu afin d'évaluer correctement l'effet d'une politique publique.

Depuis le QUM fondamental de Ahlfeldt et al. (2015), un nombre croissant de travaux a étendu ce cadre, démontrant sa flexibilité à travers diverses applications, telles que l'étude des améliorations des transports (Heblich et al., 2020; Allen and Arkolakis, 2022; Balboni et al., 2020; Severen, 2021), la congestion (Herzog, 2024), l'accès à la consommation (Miyauchi et al., 2025; Lee and Tan, 2024), le commerce de biens (Monte et al., 2018), le tri de groupes hétérogènes de travailleurs (Tsivanidis, 2024; Loumeau, 2024; Weiwu, 2024; Redding and Sturm, 2024; Bagagli, 2023), le zonage et les réglementations d'utilisation des sols (Allen et al., 2015; Parkhomenko, 2023; Chen et al., 2024), les choix d'écoles (Loumeau, 2023; Pietrabissa, 2023), les choix de modes de transport (Koster, 2024), les désaménités liées aux infrastructures de transport (Brinkman and Lin, 2022; Champalaune and Cosentino, 2025), la revitalisation urbaine (Owens III et al., 2020; Gechter and Tsivanidis, 2023), et le télétravail (Delventhal et al., 2022; Monte et al., 2023; Delventhal and Parkhomenko, 2024).

Les trois chapitres de cette thèse de doctorat utilisent un QUM, s'appuyant sur les travaux

fondateurs de Ahlfeldt et al. (2015). Une caractéristique commune à tous les chapitres est le marché du logement partagé, qui est caractérisé par une offre de logement dérivée d'une technologie Cobb-Douglas utilisant du sol ainsi que du capital, comme détaillé dans Combes et al. (2021). Cette façon de modéliser le marché du logement afin d'obtenir une élasticité du logement par rapport au loyer est couramment utilisée dans la littérature. Cependant, les chapitres divergent dans leurs spécifications des fonctions d'utilité des travailleurs et des fonctions de production des entreprises. Dans le premier chapitre, le QUM est étendu pour incorporer à la fois des services non échangeables et des biens échangeables au sein d'une ville, contribuant ainsi à la littérature sur le commerce des biens et l'accès à la consommation. Par conséquent, dans le premier chapitre, un prix des biens échangeables et un prix des services non échangeables entrent dans les préférences d'utilité des travailleurs, tandis que les deux autres chapitres considèrent un prix pour les biens finaux librement échangés dans la ville (c'est-à-dire pris comme numéraire). Les autres chapitres, en revanche, se concentrent sur l'intégration de deux groupes distincts de travailleurs (hautement qualifiés et peu qualifiés dans le deuxième chapitre, ou Noirs et Blancs dans le troisième chapitre) avec des préférences non homothétiques, contribuant aux applications de tri de groupes hétérogènes de travailleurs. Par exemple, les deux groupes de travailleurs diffèrent dans la part du revenu consacrée au logement. Concernant les fonctions de production, tous les chapitres utilisent une spécification Cobb-Douglas pour les biens échangeables. Les premier et deuxième chapitres, contrairement au troisième, incorporent du capital de machine en plus du travail et du logement pour refléter l'environnement de production du 19ème siècle Heblich et al. (2020). Les deux derniers chapitres emploient plutôt une offre de travail imbriquée avec une élasticité de substitution constante entre les groupes de travailleurs (Herzog, 2024; Tsivanidis, 2024; Redding and Sturm, 2024; Weiwu, 2024; Champalaune and Cosentino, 2025), permettant l'intégration de différents types de travailleurs au sein d'un cadre de production unifié plutôt que de supposer une production séparée de biens finaux comme dans Loumeau (2024). Dans l'ensemble, les QUM varient à travers les trois chapitres pour s'aligner sur le contexte spécifique à chaque question de recherche. Cependant, ils partagent une structure similaire, basée sur une classe de modèles urbains pour tirer des conclusions généralisables.

Quoi de neuf dans la littérature sur les QUM ?

Dynamiques

Une avancée récente dans la littérature sur les QUM est la modélisation des dynamiques. Celles-ci sont essentielles pour prendre en compte les externalités dynamiques d'agglomération (Allen and Donaldson, 2020), les choix de localisation prévisionnels (Artuç et al., 2010), l'accumulation de capital (Kleinman et al., 2023), et l'évolution de la richesse à travers l'espace (Brunetti et al., 2025). Deux caractéristiques clés sont intéressantes dans les contextes dynamiques suite à un choc économique. Premièrement, ces cadres calculent les dynamiques de transition et la vitesse de convergence vers un nouvel équilibre. En revanche, les modèles statiques ne parviennent pas à rendre compte de cela puisqu'ils résolvent un équilibre spatial à l'état stationnaire. Deuxièmement, les effets distributionnels peuvent différer le long des dynamiques de transition. En présence de frictions de migration, la valeur d'option des décisions futures dépend des choix que les agents font aujourd'hui. Par conséquent, la décision de localisation optimale pour un agent aujourd'hui pourrait être de rester, même si les gains actuels sont plus élevés ailleurs, si l'agent anticipe que les gains futurs seront plus grands à cet endroit. Par conséquent, les effets distributionnels peuvent différer largement entre les contextes dynamiques et statiques. Bien que les dynamiques aient été largement étudiées dans la littérature macroéconomique, les considérer au sein d'une ville avec de nombreuses localités conduit à des problèmes de dimensionnalité et à des défis techniques. Des méthodes récentes ont été développées pour surmonter ces problèmes et modéliser les frictions de mobilité. Une première façon de modéliser les frictions de mobilité est à la manière de Calvo (Heblich et al., 2021; Takeda and Yamagishi, 2023), où les travailleurs tirent l'opportunité de se déplacer d'une probabilité exogène. Le premier chapitre s'aligne avec ce cadre et propose une extension en annexe du QUM standard en dynamique en partant du cadre de Heblich et al. (2021). Il intègre les choix de lieu de travail, les coûts de déplacement et les forces d'agglomération. Dans ce cadre étendu, les individus sont modélisés comme faisant des prédictions précises sur les trajectoires futures des quartiers, les entreprises sont myopes et les promoteurs fournissent des logements qui se déprécient entre deux périodes. Une autre façon de considérer les frictions de mobilité est de les faire dépendre des coûts de migration entre les emplacements, et le modèle peut être résolu en algèbre dynamique *exact-hat* (Caliendo et al., 2019; Warnes, 2021). Cependant, dans les deux cas, la rigidité des décisions de migration est due aux frictions de mobilité calibrées, et cela peut totalement influencer les dynamiques de transition. Plus récemment, Greaney et al. (2024) innove en proposant

un QUM dynamique qui considère les décisions de consommation-épargne, permettant l'accumulation de richesse et les décisions de migration qui sont coûteuses. Cela permet aux chercheurs de prendre en compte des changements de dynamiques de transition plus riches et des chocs et politiques spatialement hétérogènes.

Politiques optimales

Un autre progrès dans l'utilisation des QUM est la mise en œuvre de politiques optimales (voir Fajgelbaum and Gaubert (2025) à ce propos), en particulier pour les réseaux de transport. Cela est important car les réseaux actuels sont souvent inefficaces et pourraient être reconfigurés pour améliorer le bien-être. La sous-optimalité de ces réseaux peut être attribuée à plusieurs facteurs, notamment la dépendance au sentier, où les investissements passés contraignent les développements futurs, et le désalignement entre les objectifs des planificateurs et le but de maximiser le bien-être global. De plus, la nature dynamique des fondamentaux économiques signifie que les réseaux conçus pour être efficaces à un moment donné peuvent devenir moins efficaces à mesure que les conditions changent. Le problème d'identification des réseaux de transport optimaux est complexe en raison de sa haute dimensionnalité et de sa non-convexité. Les réseaux de transport se composent de nœuds et de liens, et les améliorations d'une partie peuvent affecter l'ensemble du système, rendant l'optimisation difficile. La littérature explore deux principaux types d'investissement dans les transports : l'investissement continu dans les liens, qui se concentre sur l'intensité de l'investissement dans les infrastructures, et les approches d'investissement binaires, qui considèrent les investissements comme des choix discrets. Les applications de ces modèles, telles que celles de Fajgelbaum and Schaal (2020), fournissent des conditions dans lesquelles le problème peut être globalement convexe, assurant une tractabilité numérique. Santamaria (2020) étudie les problèmes non convexes en incorporant les conditions de marché comme restrictions supplémentaires dans le problème de le planificateur, mais cela ne garantit pas un investissement dans le réseau globalement optimal. Lorsque les investissements sont considérés comme binaires, des algorithmes heuristiques (Alder, 2016; Loumeau, 2023; Kreindler et al., 2024) peuvent être utilisés pour étudier l'efficacité d'un réseau de transport, mais cela ne garantit pas un réseau globalement optimal. Le troisième chapitre s'aligne sur cette littérature émergente en utilisant un algorithme heuristique pour résoudre un réseau de transport urbain sous-optimal et en considérant les effets d'équilibre général à travers un QUM.

Bibliography

Aaronson, D., Hartley, D., Mazumder, B., 2021. The effects of the 1930s holc" redlining" maps. American Economic Journal: Economic Policy 13, 355–92.

Abramitzky, R., Boustan, L., Eriksson, K., Feigenbaum, J., Pérez, S., 2021. Automated linking of historical data. Journal of Economic Literature 59, 865–918.

Abramitzky, R., Boustan, L.P., Storeygard, A., 2025. New data and insights in regional and urban economics .

Ahlfeldt, G.M., Pietrostefani, E., 2019. The economic effects of density: A synthesis. Journal of Urban Economics 111, 93–107.

Ahlfeldt, G.M., Redding, S.J., Sturm, D.M., Wolf, N., 2015. The economics of density: Evidence from the berlin wall. Econometrica 83, 2127–2189.

Akbar, P., 2024. Who benefits from faster public transit? Available at SSRN 4979194 .

Albers, T.N., Kappner, K., 2023. Perks and pitfalls of city directories as a micro-geographic data source. Explorations in Economic History 87, 101476.

Albouy, D., Christensen, P., Sarmiento-Barbieri, I., 2020. Unlocking amenities: Estimating public good complementarity. Journal of Public Economics 182, 104110.

Alder, S., 2016. Chinese roads in india: The effect of transport infrastructure on economic development. Available at SSRN 2856050 .

Alesina, A., Baqir, R., Easterly, W., 1999. Public goods and ethnic divisions. The Quarterly Journal of Economics 114, 1243–1284.

Alesina, A., Devleeschauwer, A., Easterly, W., Kurlat, S., Wacziarg, R., 2003. Fractionalization. Journal of Economic growth 8, 155–194.

Alesina, A., Gennaioli, C., Lovo, S., 2019. Public goods and ethnic diversity: Evidence from deforestation in indonesia. Economica 86, 32–66.

Alesina, A., Murard, E., Rapoport, H., 2021. Immigration and preferences for redistribution in europe. Journal of Economic Geography 21, 925–954.

Algan, Y., Hémet, C., Laitin, D.D., 2016. The social effects of ethnic diversity at the local level:

A natural experiment with exogenous residential allocation. Journal of Political Economy 124, 696–733.

Aliprantis, D., Carroll, D.R., Young, E.R., 2022. What explains neighborhood sorting by income and race? Journal of Urban Economics , 103508.

Allen, T., Arkolakis, C., 2022. The welfare effects of transportation infrastructure improvements. Review of Economic Studies 89, 2911–2957.

Allen, T., Arkolakis, C., Li, X., 2015. Optimal city structure. Yale University, mimeograph .

Allen, T., Donaldson, D., 2020. Persistence and path dependence in the spatial economy. Technical Report. National Bureau of Economic Research.

Allen, T., Fuchs, S., Ganapati, S., Graziano, A., Madera, R., Montoriol-Garriga, J., 2020. Is tourism good for locals? evidence from barcelona. Dartmouth College, Mimeograph .

Almagro, M., Chyn, E., Stuart, B.A., 2023. Urban Renewal and Inequality: Evidence from Chicago's Public Housing Demolitions. Technical Report. National Bureau of Economic Research.

Alonso, W., 1964. Location and land use: Toward a general theory of land rent. Harvard University Press google schola 2, 16–22.

Althoff, L., Reichardt, H., 2022. Jim crow and black economic progress after slavery. Manuscript, Princeton University .

Armington, P.S., 1969. A theory of demand for products distinguished by place of production. Staff Papers-International Monetary Fund , 159–178.

Artuç, E., Chaudhuri, S., McLaren, J., 2010. Trade shocks and labor adjustment: A structural empirical approach. American Economic Review 100, 1008–1045.

Atack, J., 2013. On the use of geographic information systems in economic history: The american transportation revolution revisited. The Journal of Economic History 73, 313–338.

Azoulay, B., de Courson, B., 2021. Gallicagram: un outil de lexicométrie pour la recherche .

Baerlocher, D., Silva, D.F.C.d., Lambais, G., Reis, E., Veras, H., 2023. Old but gold: Historical pathways and path dependence. Available at SSRN 4513384 .

Bagagli, S., 2023. The (Express)Way to Segregation: Evidence from Chicago. Technical Report. Department of Economics, Harvard University. Job Market Paper.

Balboni, C., Bryan, G., Morten, M., Siddiqi, B., 2020. Transportation, gentrification, and urban mobility: The inequality effects of place-based policies. Preliminary Draft .

Balboni, C.A., 2019. In harm's way? infrastructure investments and the persistence of coastal cities. Ph.D. thesis. London School of Economics and Political Science.

Barwick, P.J., Liu, Y., Patacchini, E., Wu, Q., 2023. Information, mobile communication, and referral effects. American Economic Review 113, 1170–1207.

Baum-Snow, N., 2007. Did highways cause suburbanization? The Quarterly Journal of Economics 122, 775–805.

Baum-Snow, N., 2020. Urban transport expansions and changes in the spatial structure of us cities: Implications for productivity and welfare. Review of Economics and Statistics 102, 929–945.

Baum-Snow, N., Hartley, D., 2020. Accounting for central neighborhood change, 1980–2010. Journal of Urban Economics 117, 103228.

Bayer, P., Casey, M.D., McCartney, W.B., Orellana-Li, J., Zhang, C.S., 2022. Distinguishing Causes of Neighborhood Racial Change: A Nearest Neighbor Design. Technical Report. National Bureau of Economic Research.

Bayer, P., Charles, K.K., Park, J., 2021. Separate and unequal: Race and the geography of the american housing market. Unpublished manuscript .

Bleakley, H., Lin, J., 2012. Portage and path dependence. The Quarterly Journal of Economics 127, 587–644.

Borusyak, K., Hull, P., 2023. Nonrandom exposure to exogenous shocks. Econometrica 91, 2155–2185.

Boustan, L.P., 2010. Was postwar suburbanization "white flight"? evidence from the black migration. The Quarterly Journal of Economics 125, 417–443.

Brinkman, J., Lin, J., 2022. Freeway revolts! the quality of life effects of highways. Review of Economics and Statistics , 1–45.

Brooks, L., Lutz, B., 2019. Vestiges of transit: Urban persistence at a microscale. Review of Economics and Statistics 101, 385–399.

Brueckner, J.K., Rosenthal, S.S., 2009. Gentrification and neighborhood housing cycles: will america's future downtowns be rich? Review of Economics and Statistics 91, 725–743.

Brueckner, J.K., Thisse, J.F., Zenou, Y., 1999. Why is central paris rich and downtown detroit poor?: An amenity-based theory. European economic review 43, 91–107.

Brunetti, R., Gaigné, C., Moizeau, F., 2025. Land, wealth, and taxation. Working Paper.

Bryan, G.T., Frye, K., Morten, M., 2025. Spatial economics for low-and middle-income countries. Technical Report. National Bureau of Economic Research.

Caliendo, L., Dvorkin, M., Parro, F., 2019. Trade and labor market dynamics: General equilibrium analysis of the china trade shock. Econometrica 87, 741–835.

Card, D., 2009. Immigration and inequality. American Economic Review 99, 1–21.

Card, D., Mas, A., Rothstein, J., 2008. Tipping and the dynamics of segregation. The Quarterly Journal of Economics 123, 177–218.

Champalaune, P., Cosentino, P., 2025. Commuting, air quality, and welfare. Work in Progress.

Chen, L., Hasan, R., Jiang, Y., Parkhomenko, A., 2024. Faster, taller, better: Transit improvements and land use policies. Journal of Development Economics 171, 103322.

Ciccarelli, C., Groote, P., 2018. The spread of railroads in italian provinces: a gis approach. Scienze Regionali 17, 189–224.

Ciccone, A., Hall, R.E., 1996. Productivity and the density of economic activity. American Economic Review 86, 54–70.

Combes, P.P., Duranton, G., Gobillon, L., 2021. The production function for housing: Evidence from france. Journal of Political Economy 129, 2766–2816.

Combes, P.P., Duranton, G., Gobillon, L., Gorin, C., 2025a. Measuring land use changes by (machine) learning from historical maps. Working Paper.

Combes, P.P., Duranton, G., Gorin, C., Gobillon, L., Robert-Nicoud, F., 2025b. Urbanisation and urban divergence: France 1760-2020. Work in Progress.

Combes, P.P., Gobillon, L., 2015. The empirics of agglomeration economies, in: Handbook of regional and urban economics. Elsevier. volume 5, pp. 247–348.

Combes, P.P., Gobillon, L., Zylberberg, Y., 2022. Urban economics in a historical perspective: Recovering data with machine learning. Regional Science and Urban Economics 94, 103711.

Cosentino, P., 2025. Circular railroad: Evidence from the Parisian Parisian *Petite Ceinture*. Technical Report. Work in Progress.

Cottereau, A., 2004. Les batailles pour la création du métro: un choix de mode de vie, un succès pour la démocratie locale. Revue d'histoire du XIXe siècle. Société d'histoire de la révolution de 1848 et des révolutions du XIXe siècle , 89–151.

Couture, V., Handbury, J., 2020. Urban revival in america. Journal of Urban Economics 119, 103267.

Cutler, D.M., Glaeser, E.L., Vigdor, J.L., 1999. The rise and decline of the american ghetto. Journal of Political Economy 107, 455–506.

Davis, D.R., Weinstein, D.E., 2002. Bones, bombs, and break points: the geography of economic activity. American economic review 92, 1269–1289.

De Chaisemartin, C., d'Haultfoeuille, X., 2024. Difference-in-differences estimators of intertemporal treatment effects. Review of Economics and Statistics , 1–45.

Dekle, R., Eaton, J., Kortum, S., 2007. Unbalanced trade. American Economic Review 97, 351–355.

Delventhal, M., Parkhomenko, A., 2024. Spatial implications of telecommuting. Available at SSRN 3746555 .

Delventhal, M.J., Kwon, E., Parkhomenko, A., 2022. Jue insight: How do cities change when we work from home? Journal of Urban Economics 127, 103331.

Derenoncourt, E., Kim, C.H., Kuhn, M., Schularick, M., 2024. Wealth of two nations: The us racial wealth gap, 1860–2020. The Quarterly Journal of Economics 139, 693–750.

Desmet, K., Nagy, D.K., Rossi-Hansberg, E., 2018. The geography of development. Journal of Political Economy 126, 903–983.

Donaldson, D., Hornbeck, R., 2016. Railroads and american economic growth: A "market access" approach. The Quarterly Journal of Economics 131, 799–858.

Duncan, O.D., Duncan, B., 1955. Residential distribution and occupational stratification. American journal of sociology 60, 493–503.

Duranton, G., Puga, D., 2015. Urban land use, in: Handbook of regional and urban economics. Elsevier. volume 5, pp. 467–560.

Easterly, W., Levine, R., 1997. Africa's growth tragedy: policies and ethnic divisions. The Quarterly Journal of Economics , 1203–1250.

Eaton, J., Kortum, S., 2002. Technology, geography, and trade. Econometrica 70, 1741–1779.

Egorov, G., Enikolopov, R., Makarin, A., Petrova, M., 2021. Divided we stay home: Social distancing and ethnic diversity. Journal of Public Economics 194, 104328.

Ellen, I.G., Hartley, D.A., Lin, J., You, W., 2025. The bronx is burning: Urban disinvestment effects of the fair access to insurance requirements. Working Paper.

Fajgelbaum, P.D., Gaubert, C., 2025. Optimal spatial policies. Technical Report. National Bureau of Economic Research.

Fajgelbaum, P.D., Gaubert, C., Gorton, N., Morales, E., Schaal, E., 2023. Political Preferences and Transport Infrastructure: Evidence from California's High-Speed Rail. Technical Report. National Bureau of Economic Research.

Fajgelbaum, P.D., Schaal, E., 2020. Optimal transport networks in spatial equilibrium. Econometrica 88, 1411–1452.

Faure, A., 2010. Emploi industriel à paris et résidence ouvrière (1860-1914): Pluralité des distances, diversité des modes de vie, in: Feiertag, O., Lespinet-Moret, I. (Eds.), L'économie faite homme: Hommage à Alain Plessis. Librairie Droz, pp. 63–76.

Faure, A., Jaillet, M.C., 2008. "La ségrégation, ou les métamorphoses historiographiques du baron Haussmann", in: Diversité sociale, ségrégation urbaine, mixité. Plan urbanisme construction et architecture -PUCA (Paris), pp. 51–64.

Ferlenga, F., 2023. Symbols of oppression. the role of confederate monuments in the great migration .

Francke, M., Korevaar, M., 2021. Housing markets in a pandemic: Evidence from historical outbreaks. Journal of Urban Economics 123, 103333.

Franklin, S., Imbert, C., Abebe, G., Mejia-Mantilla, C., 2024. Urban public works in spatial equilibrium: Experimental evidence from ethiopia. American Economic Review 114, 1382–1414.

Gaigné, C., Koster, H.R., Moizeau, F., Thisse, J.F., 2022. Who lives where in the city? amenities, commuting and income sorting. Journal of Urban Economics 128, 103394.

Garcia-López, M.À., Hémet, C., Viladecans-Marsal, E., 2017. Next train to the polycentric city: The effect of railroads on subcenter formation. Regional Science and Urban Economics 67, 50–63.

Gechter, M., Tsivanidis, N., 2023. Spatial spillovers from high-rise developments: Evidence from the mumbai mills. Unpublished manuscript .

Gendron-Carrier, N., Gonzalez-Navarro, M., Polloni, S., Turner, M.A., 2022. Subways and urban air pollution. American economic journal: Applied economics 14, 164–196.

George, H., 1879. An inquiry into the cause of poverty and progress .

Gonzalez-Navarro, M., Turner, M.A., 2018. Subways and urban growth: Evidence from earth. Journal of Urban Economics 108, 85–106.

Greaney, B., Parkhomenko, A., Van Nieuwerburgh, S., 2024. Dynamic urban economics. Available at SSRN 4897077 .

Hanlon, W.W., Heblich, S., 2022. History and urban economics. Regional Science and Urban Economics 94, 103751.

Harari, M., 2020. Cities in bad shape: Urban geometry in india. American Economic Review 110, 2377–2421.

Harari, M., 2024. Residential Patterns and Local Public Goods in Urban Brazil. Technical Report. Working paper.

Heblich, S., Nagy, D.K., Trew, A., Zylberberg, Y., et al., 2023. The death and life of great British cities. Universitat Pompeu Fabra, Department of Economics and Business.

Heblich, S., Redding, S.J., Sturm, D.M., 2020. The making of the modern metropolis: evidence from london. The Quarterly Journal of Economics 135, 2059–2133.

Heblich, S., Trew, A., Zylberberg, Y., 2021. East-side story: Historical pollution and persistent neighborhood sorting. Journal of Political Economy 129, 1508–1552.

Helpman, E., et al., 1995. The size of regions. Foerder Institute for Economic Research.

Henderson, J.V., Regan, T., Venables, A.J., 2021a. Building the city: from slums to a modern metropolis. Review of Economic Studies 88, 1157–1192.

Henderson, J.V., Storeygard, A., Weil, D.N., 2012. Measuring economic growth from outer space. American Economic Review 102, 994–1028.

Henderson, J.V., Thisse, J.F., 2024. Urban and spatial economics after 50 years. Journal of Urban Economics 144, 103711.

Henderson, K., Powers, S., Claibourn, M., Brown-Iannuzzi, J.L., Trawalter, S., 2021b. Confederate monuments and the history of lynching in the american south: An empirical examination. Proceedings of the National Academy of Sciences 118, e2103519118.

Hennig, J., 2021. Neighborhood quality and opposition to immigration: Evidence from german refugee shelters. Journal of Development Economics 150, 102604.

Herzog, I., 2024. The city-wide effects of tolling downtown drivers: Evidence from london's congestion charge. Journal of Urban Economics 144, 103714.

Ihlanfeldt, K.R., Scafidi, B., 2002. Black self-segregation as a cause of housing segregation: Evidence from the multi-city study of urban inequality. Journal of Urban Economics 51, 366–390.

Kahrl, A.W., 2018. Free the beaches: The story of Ned Coll and the battle for America's most exclusive shoreline. Yale University Press.

Kleinman, B., Liu, E., Redding, S.J., 2023. Dynamic spatial general equilibrium. Econometrica 91, 385–424.

Kline, P., Moretti, E., 2014. Local economic development, agglomeration economies, and the big push: 100 years of evidence from the tennessee valley authority. The Quarterly Journal of Economics 129, 275–331.

Koster, H.R., 2024. The welfare effects of greenbelt policy: Evidence from england. The Economic Journal 134, 363–401.

Kreindler, G., Gaduh, A., Graff, T., Hanna, R., Olken, B.A., 2024. Optimal public transportation networks: Evidence from the world's largest bus rapid transit system in jakarta. conditionally accepted, American Economic Review .

Kreindler, G.E., Miyauchi, Y., 2023. Measuring commuting and economic activity inside cities with cell phone records. Review of Economics and Statistics 105, 899–909.

Krugman, P., 1991a. History versus expectations. The Quarterly Journal of Economics 106, 651–667.

Krugman, P., 1991b. Increasing returns and economic geography. Journal of Political Economy 99, 483–499.

Krysan, M., Farley, R., 2002. The residential preferences of blacks: Do they explain persistent segregation? Social forces 80, 937–980.

Lee, K.H., Tan, B.J., 2024. Urban transit infrastructure and inequality. Review of Economics and Statistics , 1–46.

Lee, S., Lin, J., 2018. Natural amenities, neighbourhood dynamics, and persistence in the spatial distribution of income. Review of Economic Studies 85, 663–694.

LeRoy, S.F., Sonstelie, J., 1983. Paradise lost and regained: Transportation innovation, income, and residential location. Journal of Urban economics 13, 67–89.

Lin, J., Rauch, F., 2022. What future for history dependence in spatial economics? Regional Science and Urban Economics 94, 103628.

Lin, Y., Li, J., Porr, A., Logan, G., Xiao, N., Miller, H.J., 2023. Creating building-level, three-dimensional digital models of historic urban neighborhoods from sanborn fire insurance maps using machine learning. Plos one 18, e0286340.

Liotta, C., Viguié, V., Lepetit, Q., 2022. Testing the monocentric standard urban model in a global sample of cities. Regional Science and Urban Economics 97, 103832.

Loumeau, G., 2023. Locating public facilities: Theory and micro evidence from paris. Journal of Urban Economics 135, 103544.

Loumeau, G., 2024. Accommodating the rise in urbanisation: Are new towns a good solution? The Economic Journal 134, 2530–2557.

Mahajan, A., 2024. Highways and segregation. Journal of Urban Economics 141, 103574.

Marshall, A., 1890. Principles of economics.

Martin, A., 1894. Etude historique et statistique sur les moyens de transport dans Paris, avec plans, diagrammes et cartogrammes. Imprimerie nationale.

Martinez, L.R., 2022. How much should we trust the dictator's gdp growth estimates? Journal of Political Economy 130, 2731–2769.

McFadden, D., 1974. The measurement of urban travel demand. Journal of public economics 3, 303–328.

Miguel, E., Gugerty, M.K., 2005. Ethnic diversity, social sanctions, and public goods in kenya. Journal of public Economics 89, 2325–2368.

Mills, E.S., 1967. An aggregative model of resource allocation in a metropolitan area. American Economic Review 57, 197–210.

Miyauchi, Y., Nakajima, K., Redding, S.J., 2025. The economics of spatial mobility: Theory and evidence using smartphone data. Technical Report. National Bureau of Economic Research.

Monte, F., Porcher, C., Rossi-Hansberg, E., 2023. Remote work and city structure. Technical Report. National Bureau of Economic Research.

Monte, F., Redding, S.J., Rossi-Hansberg, E., 2018. Commuting, migration, and local employment elasticities. American Economic Review 108, 3855–3890.

Muth, R.F., 1969. Cities and housing; the spatial pattern of urban residential land use. .

Nagy, D.K., 2022. Quantitative economic geography meets history: Questions, answers and challenges. Regional Science and Urban Economics 94, 103675.

Oster, E., 2019. Unobservable selection and coefficient stability: Theory and evidence. Journal of Business & Economic Statistics 37, 187–204.

Ottaviano, G., Tabuchi, T., Thisse, J.F., 2002. Agglomeration and trade revisited. International economic review , 409–435.

Ottaviano, G.I., Peri, G., 2006. The economic value of cultural diversity: evidence from us cities. Journal of Economic geography 6, 9–44.

Owens III, R., Rossi-Hansberg, E., Sarte, P.D., 2020. Rethinking detroit. American Economic Journal: Economic Policy 12, 258–305.

Papayanis, N., Sanconie, M., 1998. Urbanisme du paris souterrain: premiers projets de chemin de fer urbain et naissance de l'urbanisme des cités modernes. Histoire, économie et société , 745–770.

Parkhomenko, A., 2023. Local causes and aggregate implications of land use regulation. Journal of Urban Economics 138, 103605.

Passalacqua, A., 2012. La vitesse ferroviaire comme point de mire: le monde des transports parisiens et le rail. Revue d'histoire des chemins de fer , 155–173.

Peri, G., 2012. The effect of immigration on productivity: Evidence from us states. Review of Economics and Statistics 94, 348–358.

Pietrabissa, G., 2023. School access and city structure. Unpublished manuscript .

Rambachan, A., Roth, J., 2023. A more credible approach to parallel trends. Review of Economic Studies 90, 2555–2591.

Redding, S., Venables, A.J., 2004. Economic geography and international inequality. Journal of international Economics 62, 53–82.

Redding, S.J., 2022. Trade and geography. Handbook of International Economics 5, 147–217.

Redding, S.J., 2025. Evaluating transport improvements in spatial equilibrium .

Redding, S.J., Sturm, D.M., 2024. Neighborhood effects: Evidence from wartime destruction in london. Working Paper.

Redding, S.J., Sturm, D.M., Wolf, N., 2011. History and industry location: evidence from german airports. Review of Economics and Statistics 93, 814–831.

Redding, S.J., Turner, M.A., 2015. Transportation costs and the spatial organization of economic activity. Handbook of regional and urban economics 5, 1339–1398.

Rosenthal, S.S., Strange, W.C., 2004. Evidence on the nature and sources of agglomeration economies, in: Handbook of regional and urban economics. Elsevier. volume 4, pp. 2119–2171.

Saiz, A., 2010. The geographic determinants of housing supply. The Quarterly Journal of Economics 125, 1253–1296.

Santamaria, M., 2020. Reshaping infrastructure: Evidence from the division of germany .

Severen, C., 2021. Commuting, labor, and housing market effects of mass transportation: Welfare and identification. Review of Economics and Statistics , 1–99.

Skoglund, L.L., 2025. The revolution will not be telegraphed. Working Paper.

Sood, A., Speagle, W., Ehrman-Solberg, K., 2019. Long shadow of racial discrimination: Evidence from housing covenants of minneapolis. Available at SSRN 3468520 .

Sturm, D.M., Takeda, K., Venables, A.J., 2023. How useful are quantitative urban models for cities in developing countries? evidence from dhaka. Unpublished manuscript .

Takeda, K., Yamagishi, A., 2023. History versus expectations in the spatial economy: Lessons from hiroshima. Available at SSRN 4339170 .

Thevenin, T., Mimeur, C., Schwartz, R., Sapet, L., 2016. Measuring one century of railway accessibility and population change in france. a historical gis approach. Journal of Transport Geography 56, 62–76.

Tsivanidis, N., 2024. Evaluating the impact of urban transit infrastructure: Evidence from bogota's transmilenio. American Economic Review .

Wang, T., 2025. The electric telegraph, news coverage, and political participation. The Journal of Economic History 85, 1–32.

Warnes, P.E., 2021. Transport infrastructure improvements and spatial sorting: Evidence from buenos aires. Unpublished manuscript .

Weiwu, L., 2024. Unequal Access: Racial Segregation and the Distributional Impacts of Interstate Highways in Cities. Technical Report. MIT. Job Market Paper.

White, M.J., 1983. The measurement of spatial segregation. American journal of sociology 88, 1008–1018.

You, W., 2021. The economics of speed: the electrification of the streetcar system and the decline of mom-and-pop stores in boston, 1885–1905. American Economic Journal: Applied Economics 13, 285–324.